

SRI-MME-93-261-7244.02

CGF CARTRIDGE DEVELOPMENT
VOLUME I

Final Report To:

NASA MARSHALL SPACE FLIGHT CENTER
Marshall Space Flight Center, AL 35812

Contract Number NAS8-39026

By:

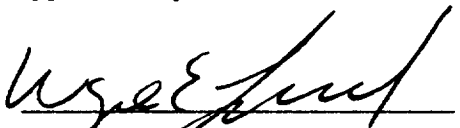
SOUTHERN RESEARCH INSTITUTE
2000 Ninth Avenue South
Birmingham, AL 35205

Written By:

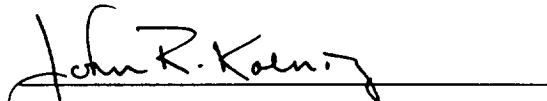


Carl A. Dixon
Assistant Engineer

Approved By:



Wayne E. Lundblad
Head, Applied Thermal Section



John R. Koenig
Research Director
Thermophysical Research Department

March 1993

TABLE OF CONTENTS

	<u>Page</u>
1.0 INTRODUCTION	1
2.0 INVESTIGATION OF WELDING/BRAZING MOLYBDENUM AND TZM ALLOY	2
2.1 EVALUATION OF TZM AS A POTENTIAL SOLUTION	12
2.2 CONCLUSIONS OF THE WELDING/BRAZING INVESTIGATION	31
2.3 REFERENCES FOR RECRYSTALLIZATION STUDY	33
3.0 EVALUATION OF TZM AS A CARTRIDGE MATERIAL	34
3.1 CONCLUSIONS	35
4.0 EVALUATION OF WC-103 AS AN ALTERNATE TO TZM	39
4.1 CONCLUSIONS	39
5.0 SURVEY OF OXIDATION RESISTANT COATINGS FOR TZM AND WC-103	40
5.1 CONCLUSIONS	41
6.0 CHEMICAL COMPATIBILITY STUDIES	42
7.0 FINAL DESIGN OF CGF CARTRIDGE	43
8.0 SUPPORT WORK	45
9.0 FUTURE IMPROVEMENTS	46
9.1 LITERATURE SEARCH FOR ALTERNATE CARTRIDGE MATERIALS	46
9.2 IMPROVED AMPOULE DESIGN	54
9.3 COMPUTERIZED MATERIALS DATABASE DEVELOPMENT	60
LIST OF APPENDICES	61

LIST OF ILLUSTRATIONS

<u>Figure</u>	<u>Page</u>
2.0.1 Cross-Section of Crystal Growth Cartridge Showing Placement of Adjustment Block and End Cap	4
2.0.2 Photomicrograph (25x) of a Cross-Section of Molybdenum Tube	5
2.0.3 Photomicrograph (25x) of a Cross-Section of Molybdenum Tube Heat Treated at 1065°C for One Hour	6
2.0.4 Photomicrograph (25x) of Adjustment Block Brazed to Molybdenum Tube	7
2.0.5 Quartz Dilatometer for Measuring Thermal Expansion to 1500°F	8
2.0.6 Thermal Expansion of PM-TZM (Same as Literature Values for Molybdenum)	9
2.0.7 Thermal Expansion of 304L Stainless Steel (from TPRL Handbook)	10
2.0.8 Photomicrograph (25x) of Electron Beam Weld Area of Molybdenum Tube	11
2.1.1 Photomicrograph (25x) of a Bar Section of Arc-Cast TZM Alloy	14
2.1.2 Photomicrograph (25x) of a Bar Section of PM-TZM	15
2.1.3 Typical Hot Zone Cavities Available	16
2.1.4 Standard Char Cycle	17
2.1.5 Photomicrograph (25x) of a Bar Section of Arc-Cast TZM Alloy Heat Soaked at 1370°C for 50 Hours	18
2.1.6 Photomicrograph (25x) of a Bar Section of PM-TZM Heat Treated at 1370°C for 50 Hours	19
2.1.7 Photomicrograph (25x) of Virgin PM-TZM in Longitudinal Direction of Bar	20
2.1.8 Photomicrograph (100x) of an Actual PM-TZM Cartridge Run in the CGF for 90 Hours at 1260°C	21
2.1.9 Photomicrograph (100x) of Virgin PM-TZM Showing Microhardness Indentations	22
2.1.10 Photomicrograph (100x) of PM-TZM Bar Heat Treated at 1370°C for One Hour Showing Hard Outside Coating	23
2.1.11 Schematic of Ring-Flex Test	24

LIST OF ILLUSTRATIONS (Continued)

<u>Figure</u>	<u>Page</u>
2.1.12 Load-Deflection of Arc-Cast Molybdenum Cartridge Rings	25
2.1.13 Load-Deflection of PM-TZM Cartridge Rings	26
2.1.14 Photomicrograph (100x) of Hardness Indentation in 80 Hours 1370°C Heat Soaked PM-TZM	27
3.0.1 Graphite Dilatometer for Measuring Thermal Expansion to 5500°F	36
3.0.2 Unit Thermal Expansion of FBD Zirconia Insulation from CGF	37
3.0.3 Molybdenum Oxide Test Facility	38
7.0.1 CGF Cartridge Schematic	44
9.2.1 Prototype Ampoule	56
9.2.2 Alternate Sealing Technique for Re-designed Ampoule	57
9.2.3 Ampoule Failure Sensing Mechanism for Non-conductive Ampoules	58
9.2.4 Ampoule Failure Sensing Mechanism for Conductive Ampoules	59

LIST OF TABLES

<u>Table</u>		<u>Page</u>
2.1.1	PM-TZM Micro-Hardness, 100 Gram Load	28
2.1.2	Arc-Cast Micro-Hardness, 100 Gram Load	29
2.1.3	PM-TZM NASA CGF Cartridge Micro-Hardness (100 gm Load)	30
2.2.1	Brazes for Molybdenum and TZM	32
9.1.1	Candidate Materials Considered for CGF Tube	49
9.1.2	Immediate Minimum Goals (Refractory Metals)	50
9.1.3	Immediate Minimum Goals (Ceramics)	51
9.1.4	Long Term Preferred Goals (Refractory Metals)	52
9.1.5	Long Term Preferred Goals (Ceramics)	53

1.0 INTRODUCTION

This is Volume I of a final report for work performed by the Southern Research Institute (SRI) for the NASA Marshall Space Flight Center (NASA/MSFC) under contract number NAS8-39026. This report will present a summary of SRI's research efforts in the development of crystal growth cartridges for the Crystal Growth Furnace (CGF) used for experiments aboard USML-1.

2.0 INVESTIGATION OF WELDING/BRAZING MOLYBDENUM AND TZM ALLOY

SRI's initial efforts on the CGF cartridge development program involved investigating the welding and brazing techniques of molybdenum tubes. NASA/MSFC's initial cartridge design is shown in Figure 2.0.1. A molybdenum tube, fabricated by rolling, was fitted with a spherical end cap (electron-beam welded) and a 304L stainless steel adjustment block (vacuum brazed). During the welding and brazing operations, however, the molybdenum tube recrystallized and became extremely brittle. Hoop stresses generated by both the welding and brazing operations caused failures of the cartridge.

Figure 2.0.2 is a photomicrograph of a section of a NASA/MSFC supplied molybdenum cartridge. This cartridge had not been heat treated. As can be seen, the molybdenum had an aligned grain structure due to the rolling process with which it was formed.

Figure 2.0.3 is a photomicrograph of a sample from the same cartridge but heat treated to 1065°C for one hour. This was the temperature and time at which the cartridge was brazed in a vacuum furnace. As can be seen, the molybdenum had recrystallized. The original grain structure was replaced by randomly oriented large grains yielding a brittle structure.

Figure 2.0.4 is a photomicrograph of a section of the adjustment block brazed to the molybdenum tube. Note the recrystallization of the molybdenum. Also note that the molybdenum tube had crimped slightly and pulled away from the braze and adjustment block. This crimping was due to the large circumferential stresses put on the tube by a thermal expansion mismatch between the stainless steel and the molybdenum.

Figure 2.0.5 is a schematic of one of the quartz dilatometers available at SRI. The quartz dilatometer is capable of measuring thermal expansion up to 980°C with a precision of 10^{-5} cm/cm. Thermal expansion measurements can be performed on solid rods, tubes, and spheres.

Figure 2.0.6 is the thermal expansion of molybdenum measured in SRI's quartz dilatometer. Figure 2.0.7 is the thermal expansion curve for 304L

stainless steel from literature. At 760°C the expansion of the stainless steel is 14.0×10^{-3} cm/cm. The expansion of the molybdenum is about 4.4×10^{-3} cm/cm at the same temperature. The large thermal expansion of the stainless steel caused a gap of about 0.0114 centimeters (at 760°C) between the adjustment block and the tube. This gap then filled with braze. Upon cooling, the braze solidified and the stainless steel adjustment block contracted, placing large hoop compressive and flexural stresses on the tube. Assuming equal compliance between the molybdenum tube and stainless steel adjustment block, the compressive elastic hoop stresses exceed the yield strength of both materials. This stress caused the tube crimping or collapse. The flexural stress where the molybdenum exits the adjustment block was about 2070 MPa (again, elastic analysis). Thus one would also expect collapse of the molybdenum tube due to flexural stress.

Attempts were made by NASA/MSFC to place a 304L stainless steel mandrel in the tube to prevent collapse, but, with the thermal expansion mismatch, the stainless steel mandrel's expansion created extensive stresses and failure of the molybdenum tube during heat up.

Figure 2.0.8 is a photomicrograph of the joint where the spherical end cap was electron beam welded to the tube. The large grain structure is easily visible at the heat affected zone.

In summary, the problems associated with the molybdenum tube/stainless steel adjustment block design were;

- 1] Recrystallization of the molybdenum tube during brazing.
- 2] Compressive hoop and axial stresses from the stainless steel adjustment block.
- 3] Tensile stresses from the stainless steel mandrel.
- 4] Recrystallization of the electron beam welded joint at the spherical end cap.

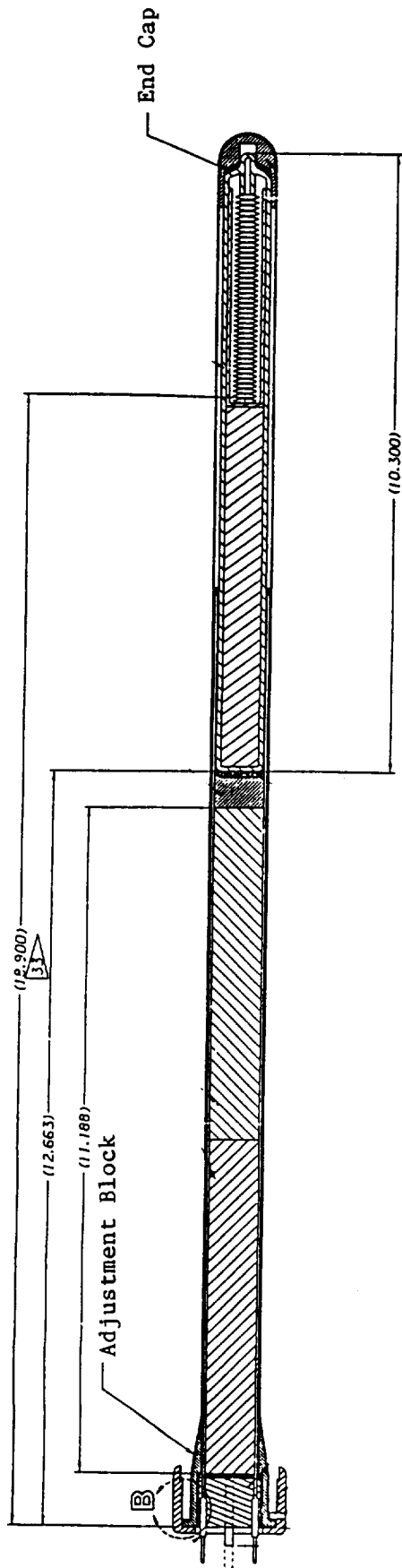


Figure 2.0.1. Cross-Section of Crystal Growth Cartridge Showing Placement of Adjustment Block and End Cap

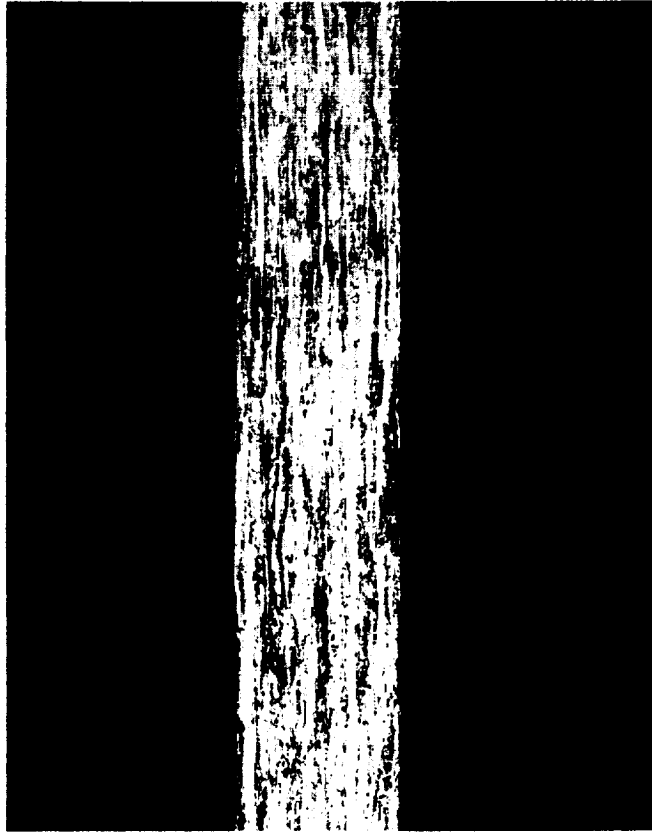


Figure 2.0.0.2. Photomicrograph (25x) of a Cross-Section of Molybdenum Tube



Figure 2.0.3. Photomicrograph (25x) of a Cross-Section of Molybdenum Tube Heat Treated at 1065°C for One Hour



Figure 2.0.4. Photomicrograph (25x) of Adjustment Block Brazed to Molybdenum Tube

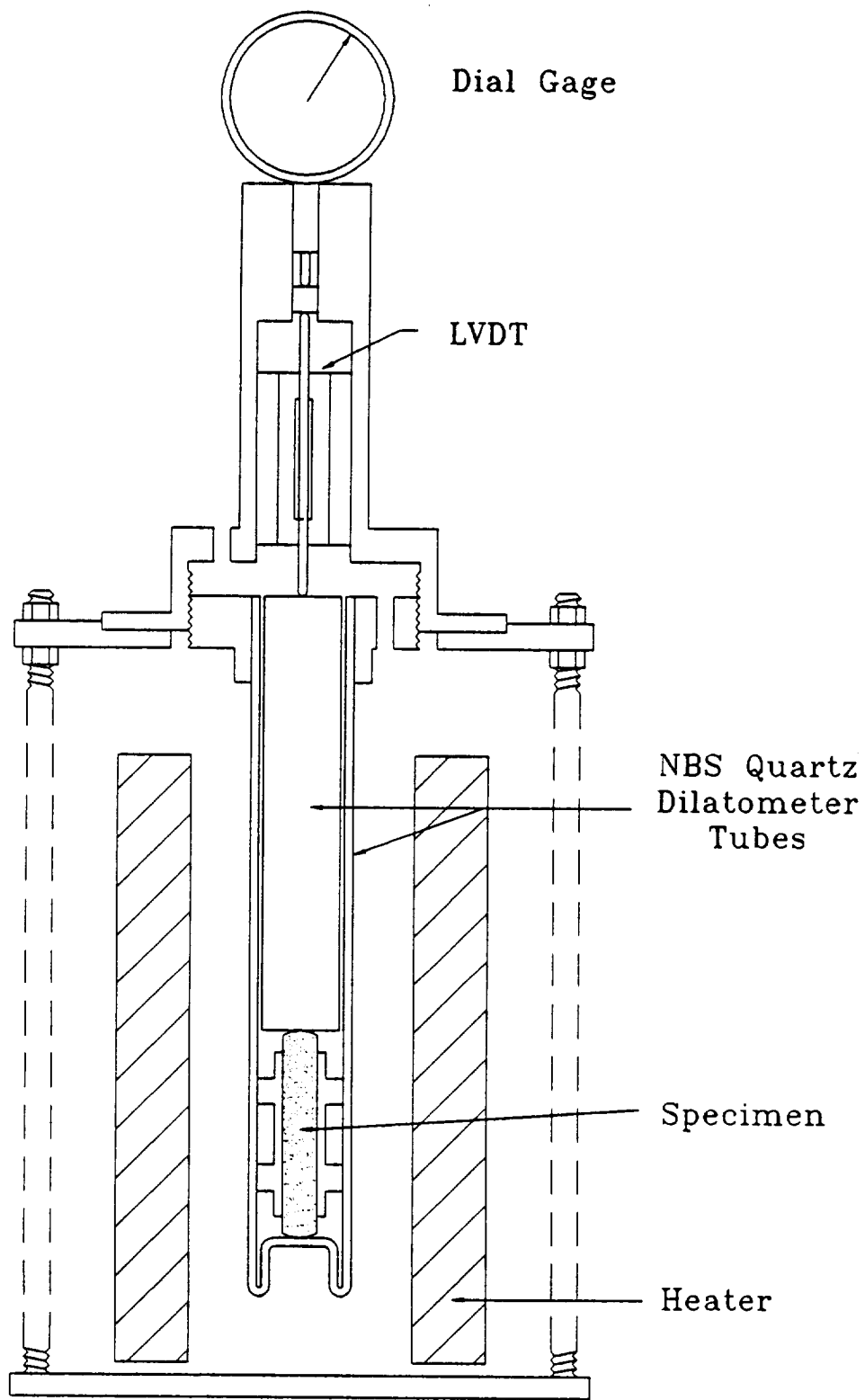


Figure 2.0.5. Quartz Dilatometer for Measuring Thermal Expansion to 1500°F

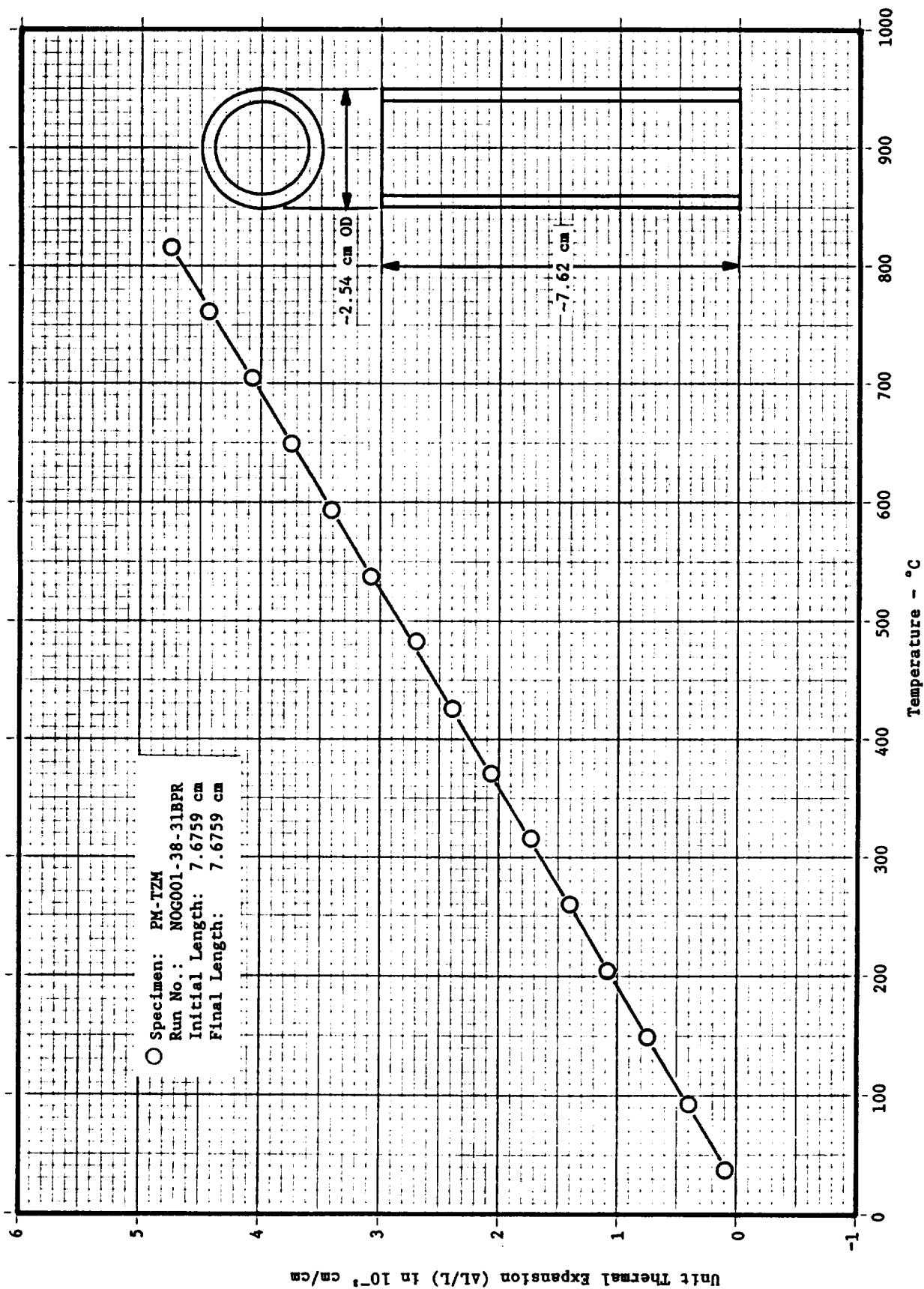


Figure 2.0.6. Thermal Expansion of PM-TZM (Same as Literature Values for Molybdenum)

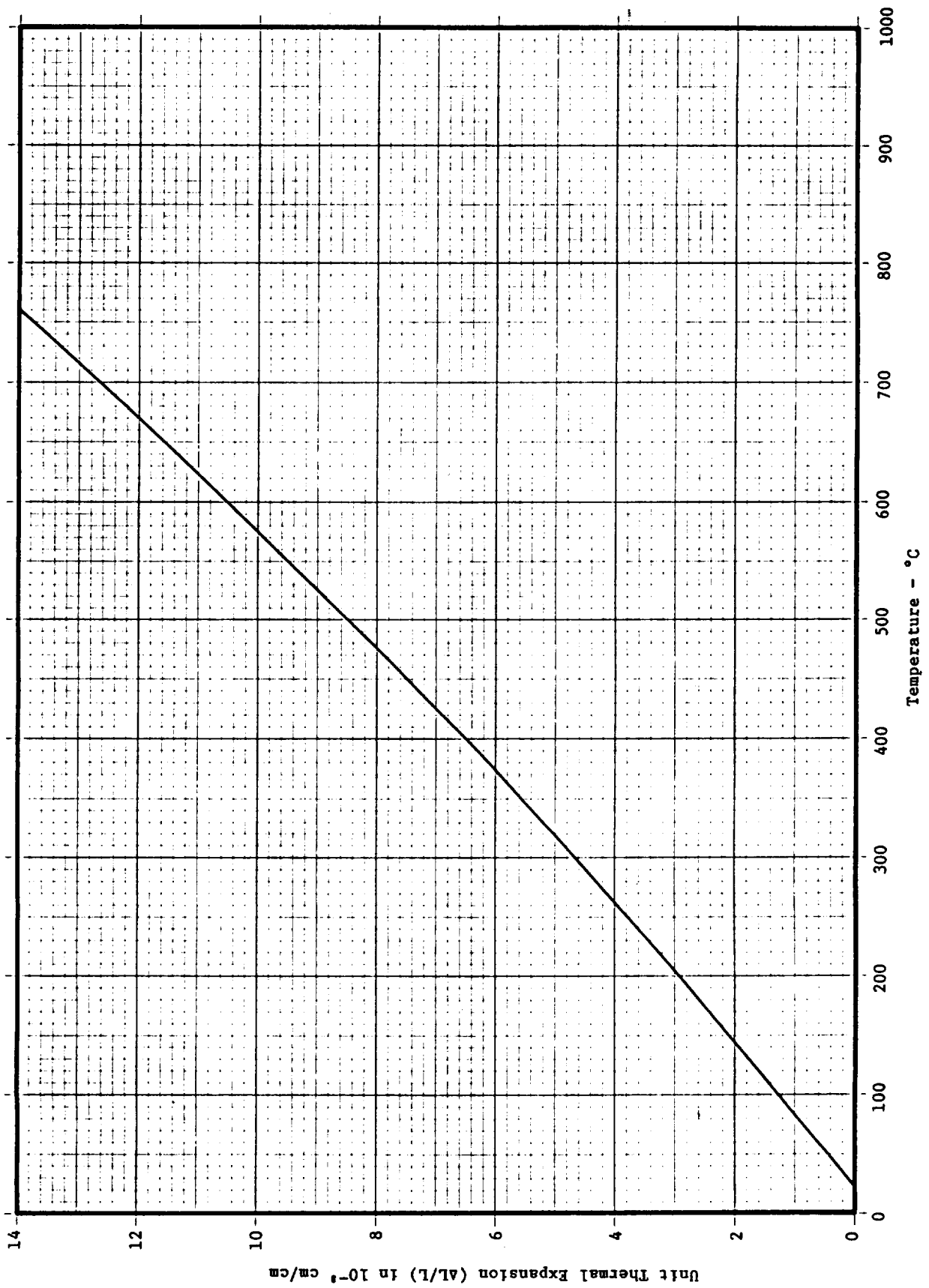


Figure 2.0.7. Thermal Expansion of 304L Stainless Steel (from TPRL Handbook)

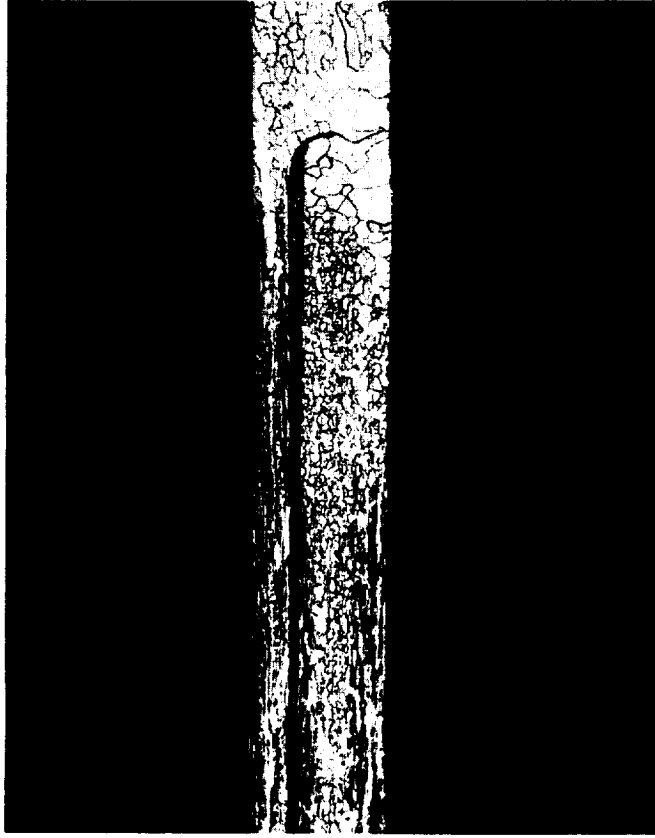


Figure 2.0.0.8. Photomicrograph (25x) of Electron Beam Weld Area of Molybdenum Tube

2.1 EVALUATION OF TZM AS A POTENTIAL SOLUTION

The recrystallization temperature of molybdenum can be increased by alloying it with 0.5% titanium and 0.1% zirconium. The small amounts of titanium and zirconium inhibit grain growth. Recrystallization temperatures^{1,2} for this alloy, known as TZM, become significant around 1370°C.

TZM alloy can be produced by two methods: Arc-cast and powder metallurgy. Historically, powder metallurgy techniques yield TZM with a lower density than arc-cast. However, current technology produces powder metallurgy TZM (PM-TZM) with the same density and approximate mechanical properties as arc-cast TZM^{1,2}. PM-TZM is much more readily available and less expensive than arc-cast TZM.

Figure 2.1.1 is a photomicrograph of a piece of arc-cast TZM alloy taken from a solid rod. The fine grain structure is evident.

Figure 2.1.2 is a photomicrograph of a piece of PM-TZM taken from a solid rod. Note that its grain structure is similar to that of arc-cast TZM. The small voids are created by the powder metallurgy process. The manufacturer claims that these voids have minimal effect on material properties.

Figure 2.1.3 shows the dimensions of the hot zone cavities of the high temperature furnaces available at SRI. SRI's high temperature furnaces use graphite resistance heaters and is capable of reaching temperatures up to 2760°C. Heat soaks can be performed both in air, in an inert gas, or in a prescribed environment (such as the CGF's). Figure 2.1.4 shows the standard cycles used to heat soak specimens.

Figure 2.1.5 is a photomicrograph of a piece of arc-cast TZM that had been heat treated to 1370°C for fifty hours. Slight changes in grain structure were evident but nowhere near as drastic as seen in pure molybdenum.

Figure 2.1.6 is a photomicrograph of a piece of PM-TZM that had also been heat treated to 1370°C for fifty hours. Again, there was only slight recrystallization.

Figure 2.1.7 is a photomicrograph of a piece of PM-TZM in the longitudinal direction of a solid bar. Figure 2.1.8 is a photomicrograph of a section of a PM-TZM cartridge run in the CGF for 90 hours at 1260°C. A comparison of these two figures shows no significant recrystallization.

A series of microhardness tests were run on samples of virgin and heat-soaked TZM. Figure 2.1.9 is a photomicrograph of a section of virgin PM-TZM bar. The hardness indentations are visible. Tables 2.1.1 and 2.1.2 summarize the microhardness readings for PM-TZM and arc-cast TZM. The outside surface of heat-soaked materials apparently had a thin hard coating. This is shown in Figure 2.1.10. The composition of the coating was not known. The data from Tables 2.1.1 and 2.1.2 indicated that continued exposure to high temperatures increases the hardness of the TZM. Microhardness was also run on the PM-TZM tube that was run in the CGF for 90 hours. Hardness readings were taken from areas at both the brazed joint and the end cap. Table 2.1.3 summarizes this data. As expected, there was less change than seen in the 1370°C environment.

Figure 2.1.11 is a schematic of a test technique to qualitatively evaluate ring flexure of samples cut from CGF cartridges. A series of dead weight loads was employed to obtain deformations. Ring samples 0.50 inches wide were cut from an arc-cast molybdenum cartridge and a PM-TZM cartridge. Ring samples from both cartridges were heat treated to 2500°F for six hours. Figure 2.1.12 is the load-deflection curve for the arc-cast molybdenum rings. The effect of heat treating was to lower the strain to failure. Figure 2.1.13 is the load-deflection curve for the PM-TZM rings. Failure could not be obtained with this geometry and facility (load limited).

To evaluate TZM's ductility, SRI's scanning electron microscope was used to photograph the hardness indentations in the 80 hour heat soaked specimen. Figure 2.1.14 is a photomicrograph (3000x) of such an indentation. A brittle material would have cracks propagating from the corners of the indentation. A ductile material would have flow lines around the periphery. Neither of these effects were seen.

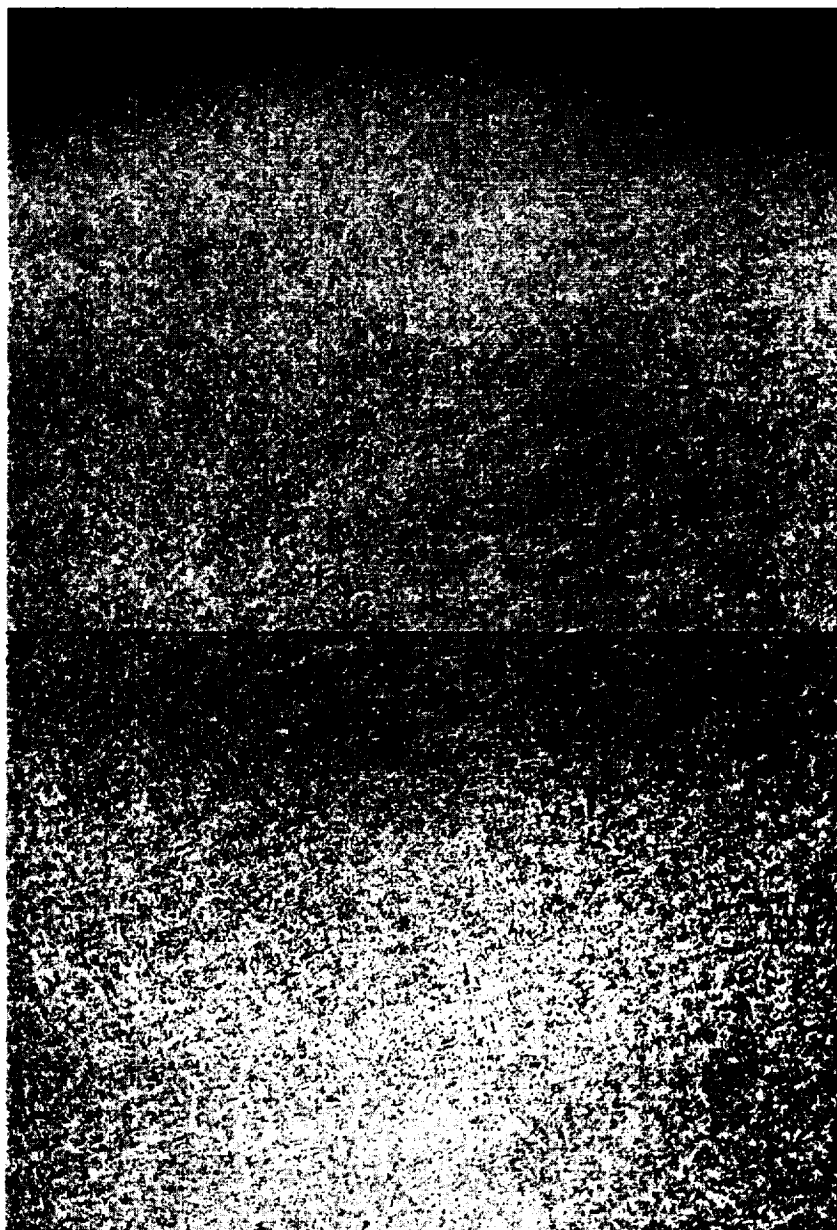
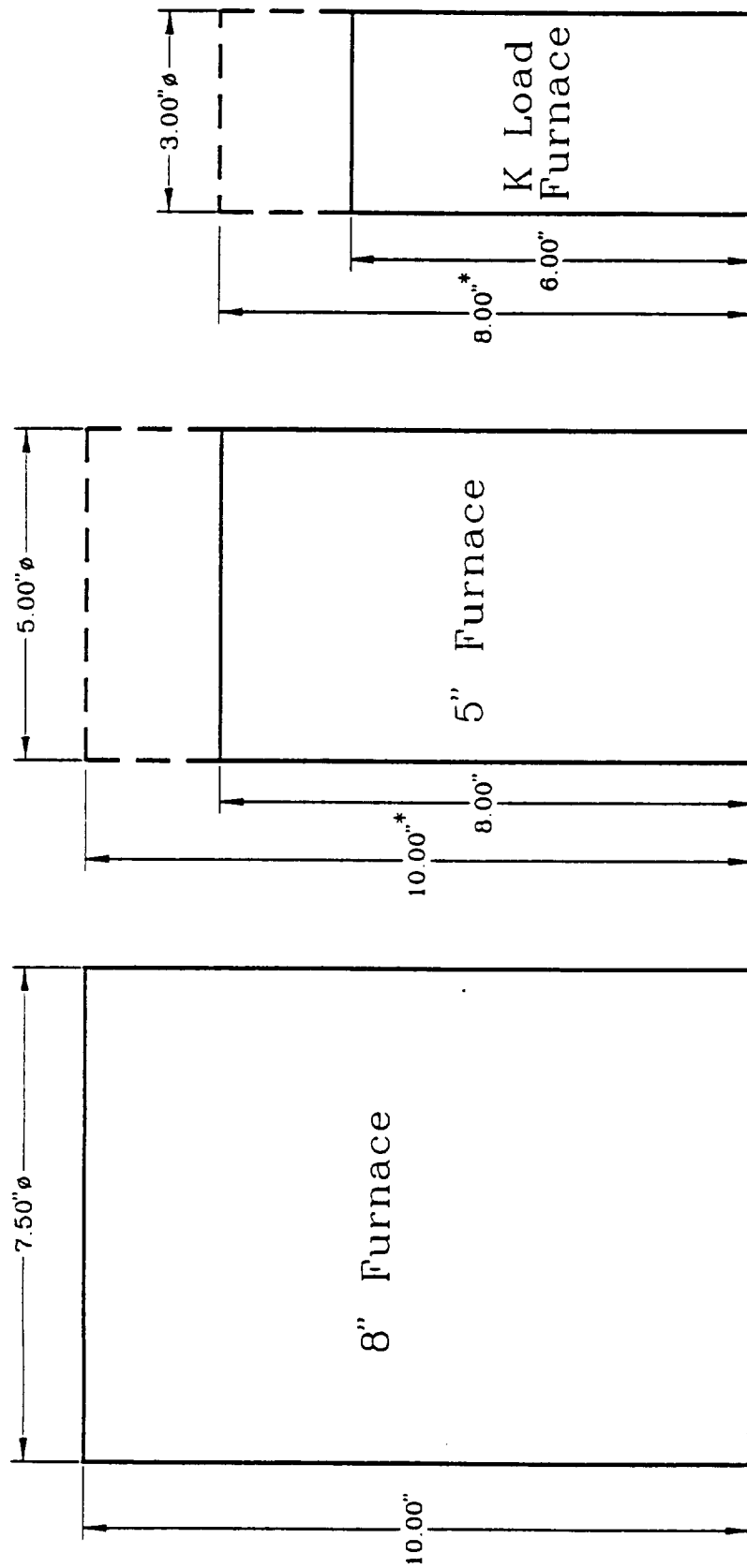


Figure 2.1.1.1. Photomicrograph (25x) of a Bar Section of Arc-Cast TZM Alloy



Figure 2.1.1.2. Photomicrograph (25x) of a Bar Section of PM-TZM



*Special Helix (Not standard)

Figure 2.1.1.3. Typical Hot Zone Cavities Available

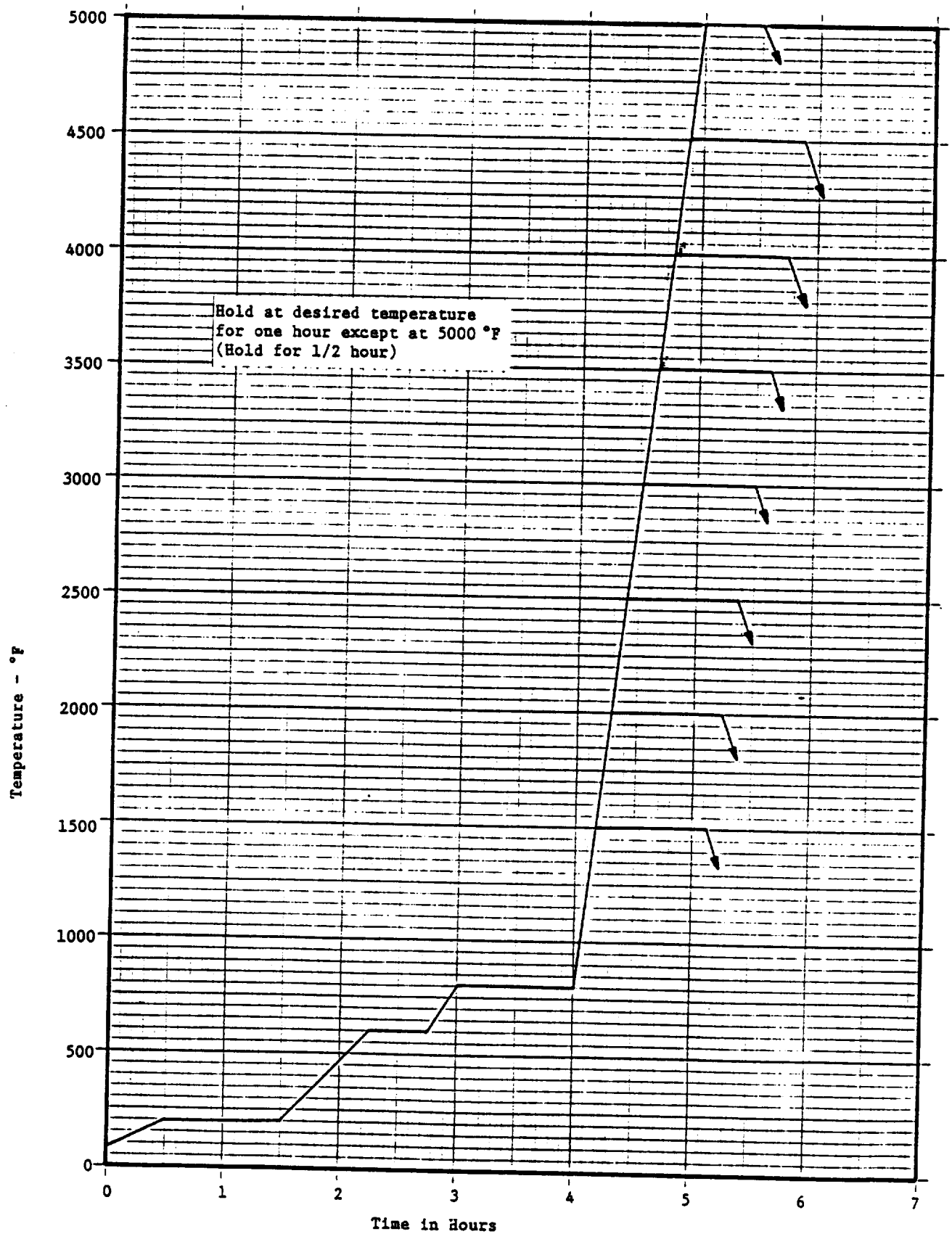


Figure 2.1.4. Standard Char Cycle

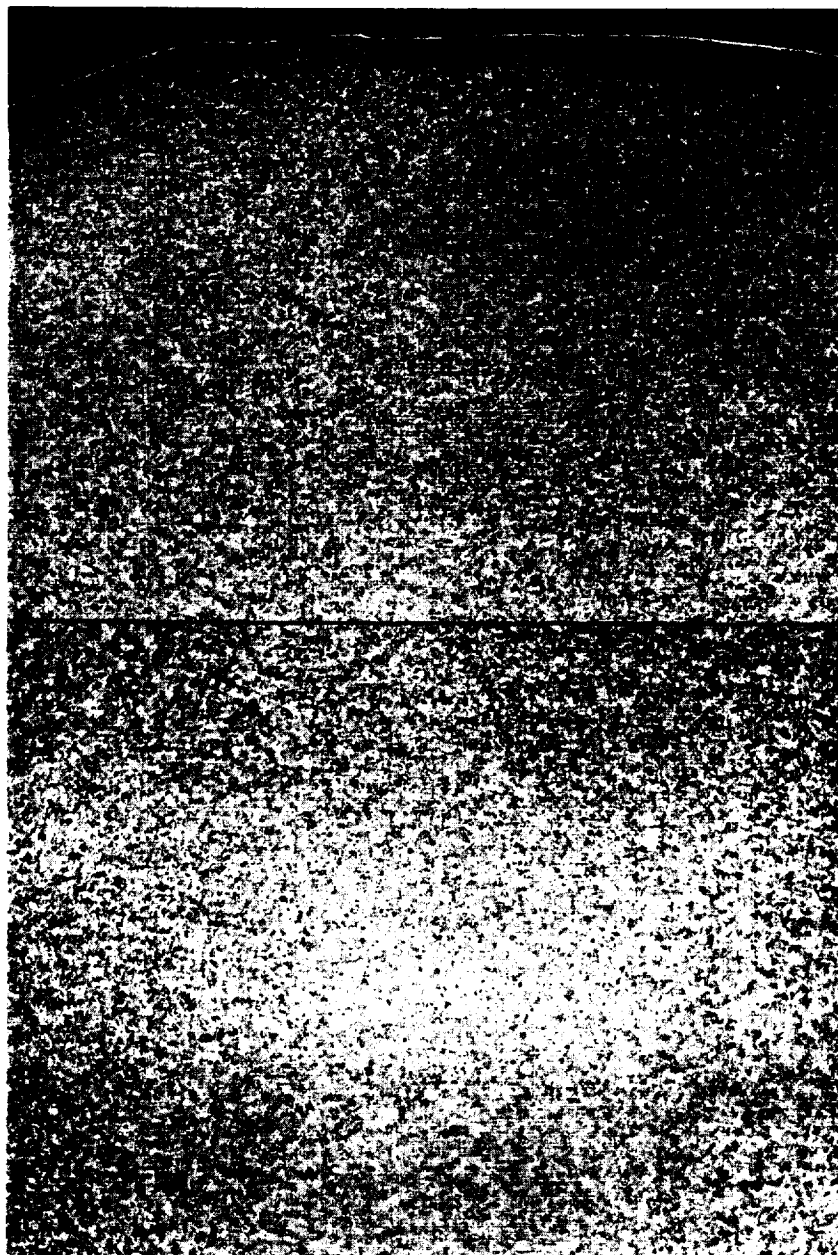


Figure 2.1.1.5. Photomicrograph (25x) of a Bar Section of Arc-Cast TZM Alloy Heat Soaked at 1370°C for 50 Hours

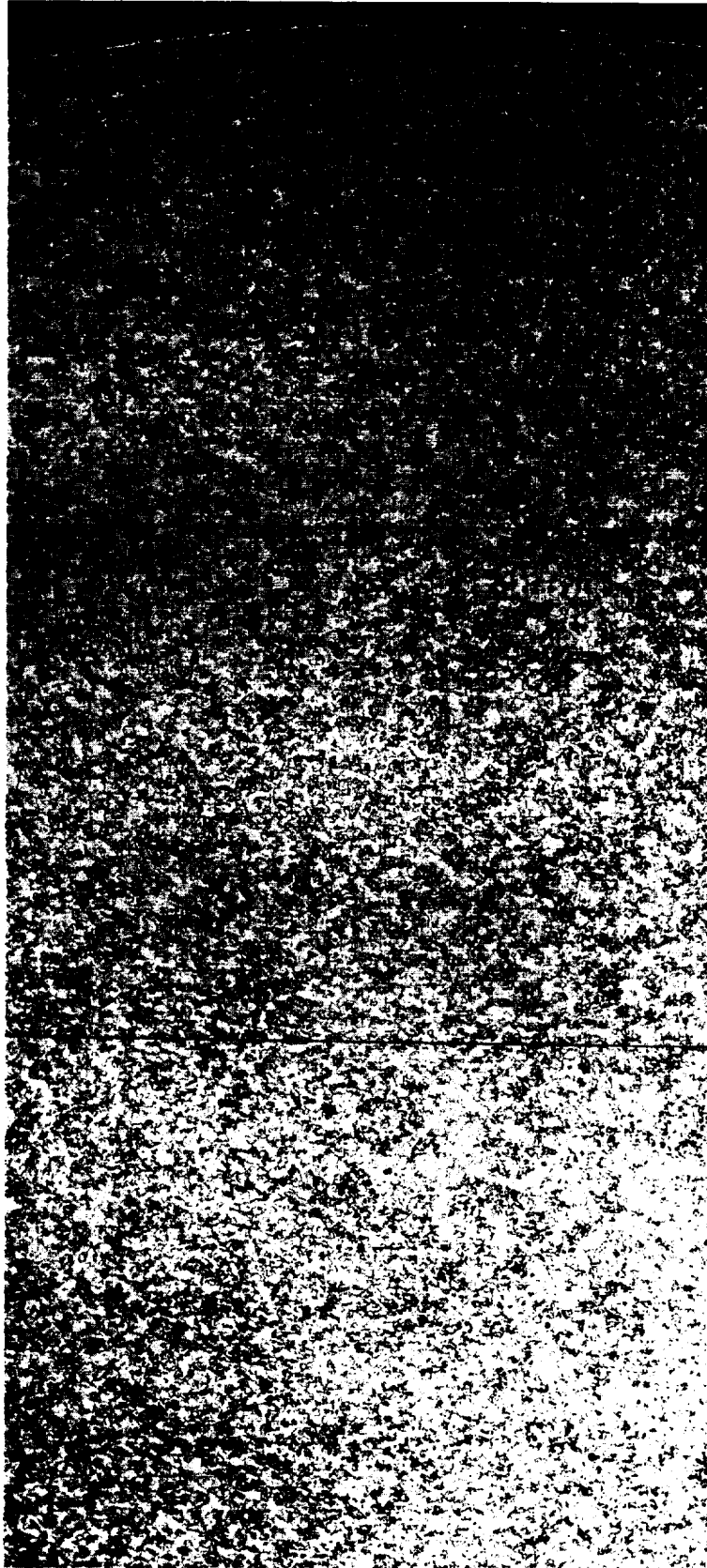


Figure 2.1.1.6. Photomicrograph (25x) of a Bar Section of PM-TZM Heat Treated at 1370°C for 50 Hours

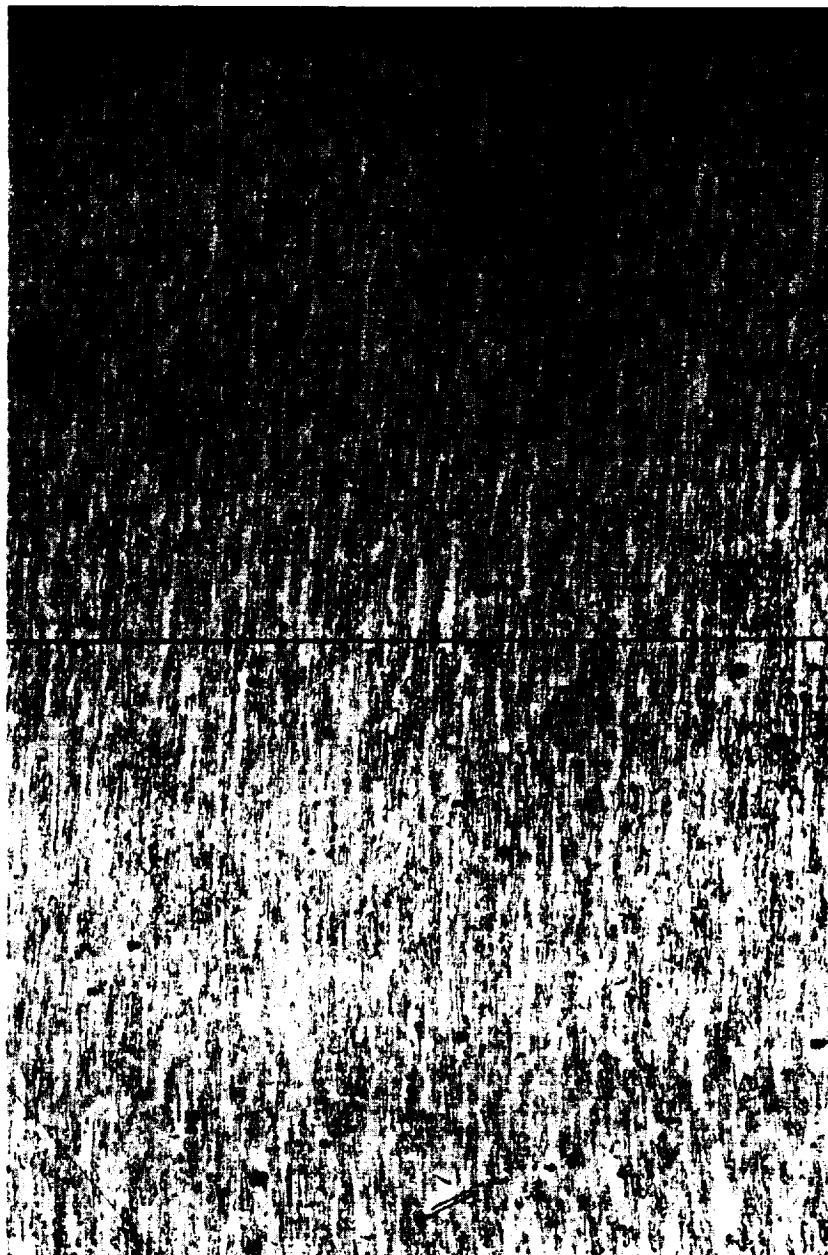


Figure 2.1.1.7. Photomicrograph (25x) of Virgin PM-T2M in Longitudinal Direction of Bar



Figure 2.1.1.8. Photomicrograph (100x) of an Actual PM-TZM Cartridge Run
in the CGF for 90 Hours at 1260°C

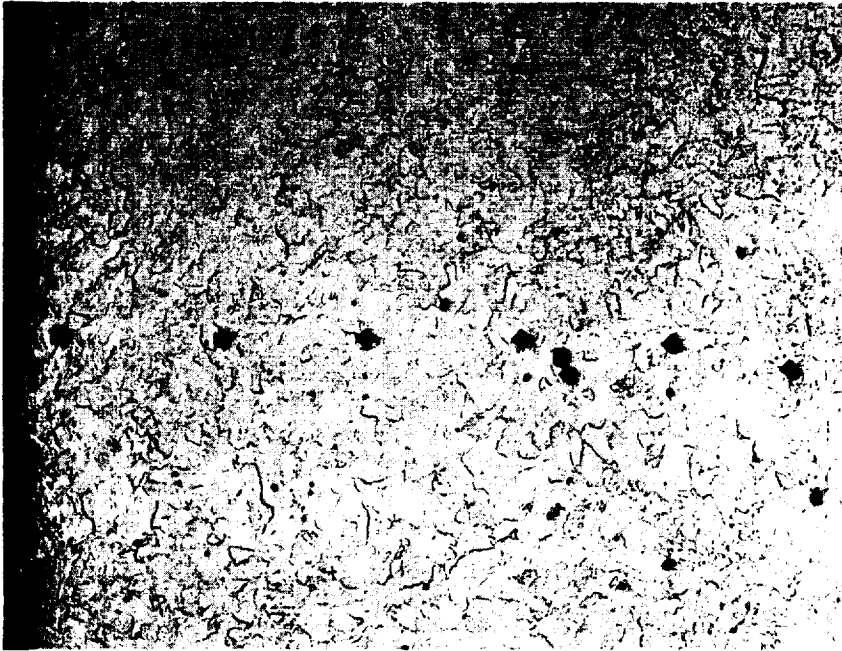


Figure 2.1.1.9. Photomicrograph (100x) of Virgin PM-TZM Showing
Microhardness Indentations



Figure 2.1.10. Photomicrograph (100x) of PM-TZM Bar Heat Treated at 1370°C for One Hour Showing Hard Outside Coating

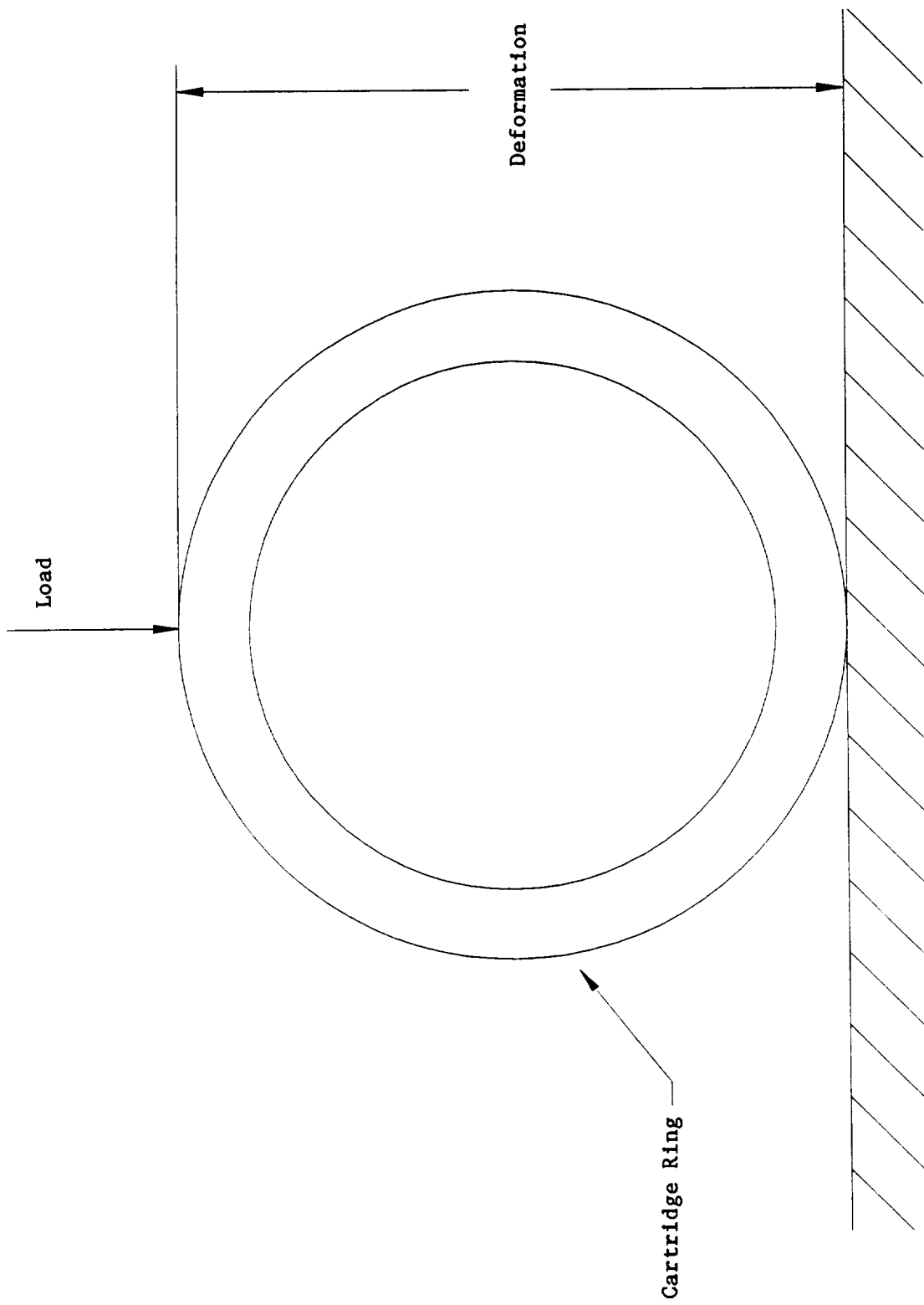
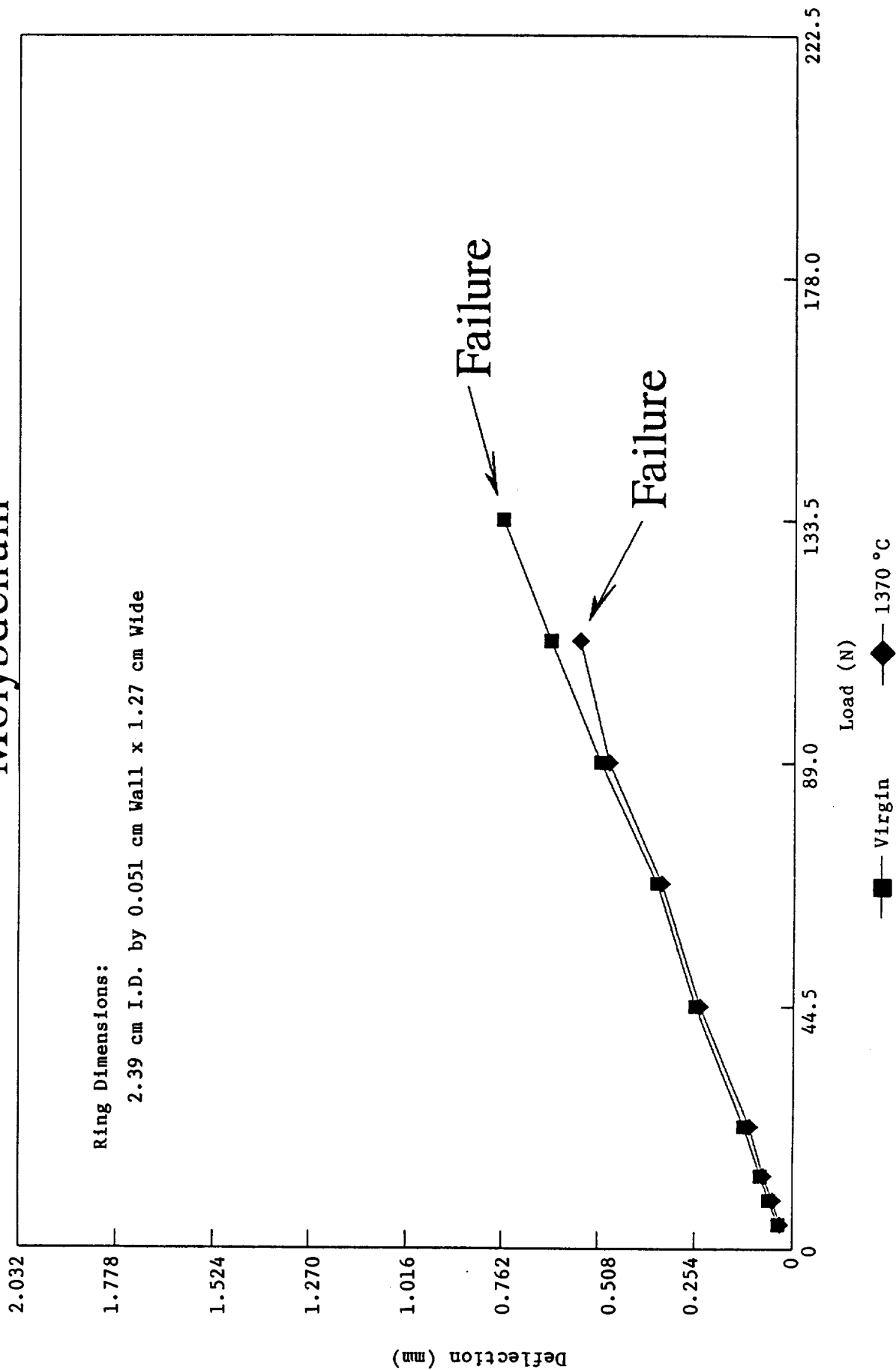


Figure 2.1.11. Schematic of Ring-Flex Test

Molybdenum



PM-TZM

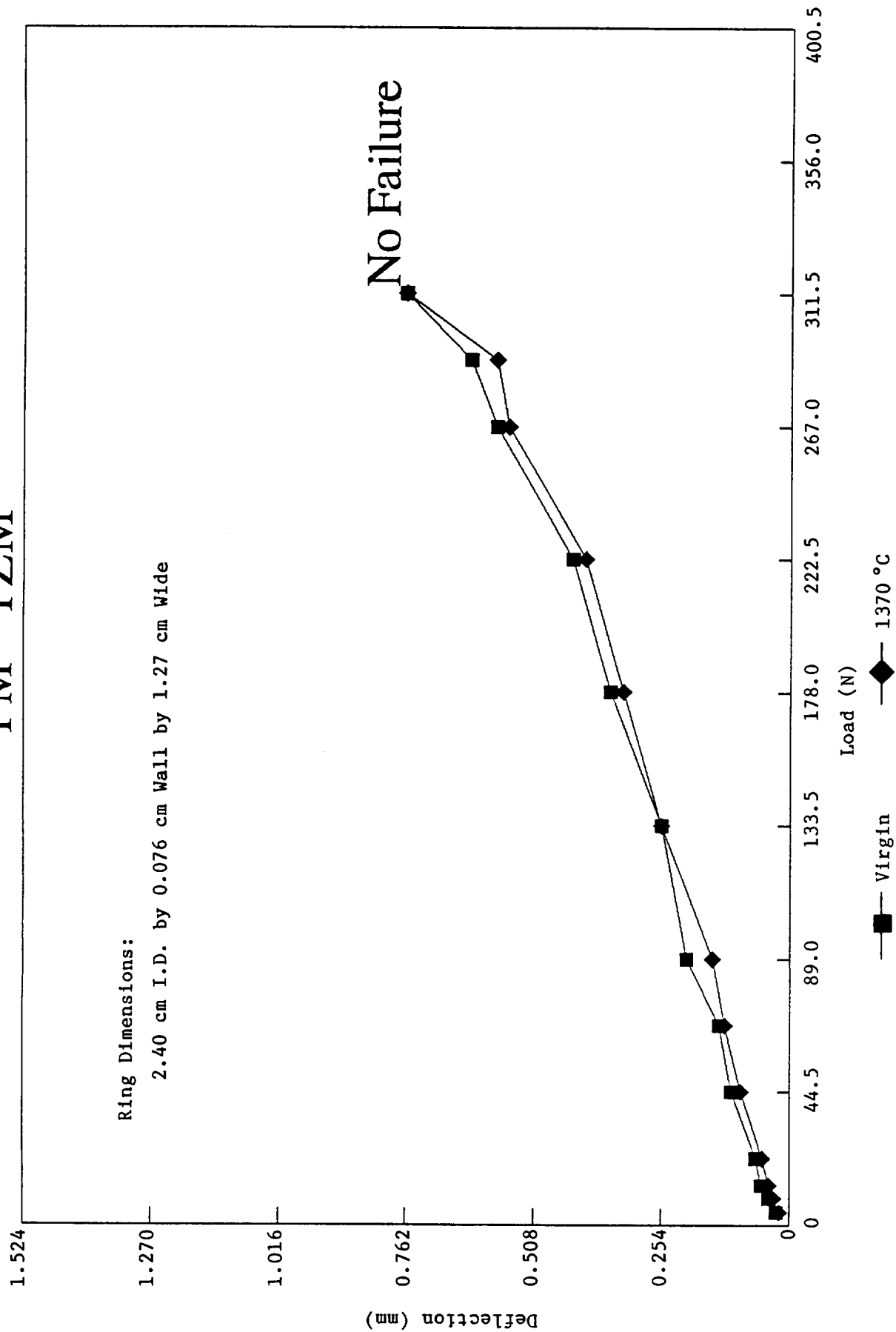


Figure 2.1.13. Load-Deflection of PM-TZM Cartridge Rings

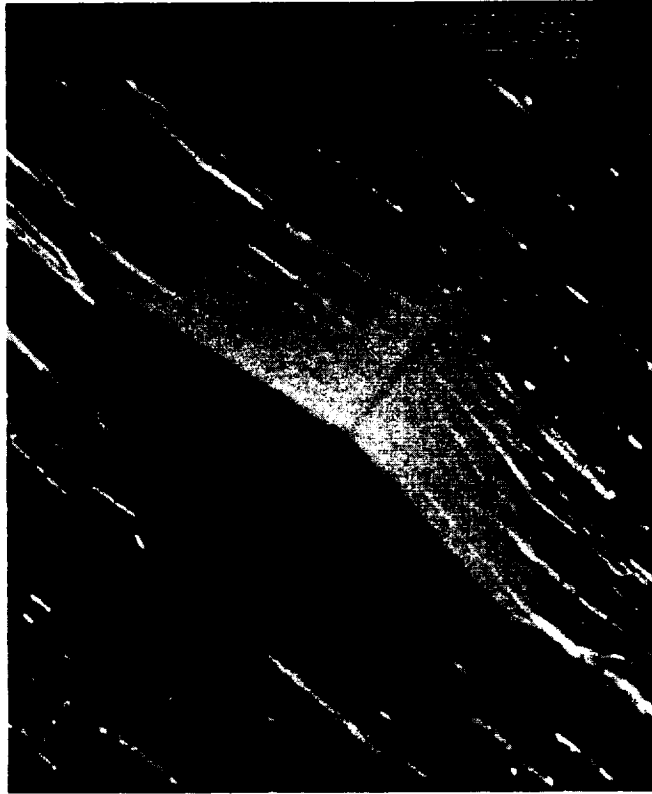


Figure 2.1.1.14. Photomicrograph (3000x) of Hardness Indentation in 80 Hours
1370°C Heat Soaked PM-TZM

Table 2.1.1.1. PM-T2M Micro-Hardness, 100 Gram Load

<u>Position</u>	<u>Virgin</u>	(Time at 1370 °C)					
		<u>1 Hour</u>	<u>6 Hours</u>	<u>12 Hours</u>	<u>24 Hours</u>	<u>50 Hours</u>	<u>78 Hours</u>
1	-	-	71	75	75	71	70
2	26	29	36	26	29	26	32
3	26	23	29	23	29	95	97
4	26	97	23	23	26	95	95
5	29	97	23	23	23	97	95
6	29	97	23	23	23	97	95
7	29	23	23	23	23	97	95
8	26	23	23	23	23	97	95
<u>Rockwell Hardness</u>							

Table 2.1.2. Arc-Cast T2M Micro-Hardness, 100 Gram Load

<u>Position</u>	<u>Virgin</u>	(Time at 1370 °C)					
		<u>1 Hour</u>	<u>6 Hours</u>	<u>12 Hours</u>	<u>24 Hours</u>	<u>50 Hours</u>	<u>78 Hours</u>
1	-	-	-	-	74	72	75
2	29	-	-	-	26	29	32
3	29	-	-	-	97	23	26
4	29	-	-	-	95	97	26
5	32	-	-	-	95	97	26
6	26	-	-	-	95	97	26
7	29	-	-	-	95	97	26
8	29	-	-	-	95	97	23

Rockwell Hardness

Table 2.1.1.3. PM-TZM NASA CGF Cartridge Micro-Hardness (100 gm Load)

(90 Hours at 1260 °C)

<u>Position</u>	<u>Braze Joint</u>	<u>End Cap</u>
1	26	57
2	26	50
3	26	29
4	29	29
5	29	29
6	29	29
7	26	29
8	23	29
Rockwell Hardness		

2.2 CONCLUSIONS OF THE WELDING/BRAZING INVESTIGATION

Based upon the recrystallization study and the simple ring flexure test, PM-TZM was considered to be an acceptable cartridge material. The electron beam welding of the end cap was eliminated by machining the tubes with a closed spherical end from a solid bar of PM-TZM. It was decided that a re-design of the adjustment block was required to eliminate the stresses built up during brazing the adjustment block to the cartridge tube. The new adjustment block configuration was designed by NASA/MSFC and was constructed from PM-TZM to eliminate the thermal expansion mismatch. SRI also researched some brazing alloys recommended^{1,3} for molybdenum and TZM. These alloys are listed in Table 2.2.1 in decreasing order of brazing temperature. Brazing pure molybdenum with these materials would have resulted in some recrystallization. TZM, however, posed no problems.

Table 2.2.1. Brazes for Molybdenum and TZM

<u>Braze</u>	<u>Braze Temperature</u>	<u>Cost</u>	<u>Delivery</u>	<u>Purchased</u>
Gold	1064°C	\$1830./oz	Immediate	.5 oz.
Silver	960°C	\$35./oz	Immediate	5 oz.
82 Au/18 Ni	949°C	\$685./oz*	4 Weeks	2 oz.
80 Au/20 Cu	885°C	\$690./oz*	4 Weeks	2 oz.
72 Ag/28 Cu	835°C	\$485./oz*	4 Weeks	2 oz.
66 Ag/34 Cu-Ni-Ti	815°C	\$84./oz	2 Weeks	2 oz.

*Add \$800.00 initial set-up charge

2.3 REFERENCES FOR RECRYSTALLIZATION STUDY

1. "Fabricating Molybdenum and TZM Alloys", Climax Specialty Metals.
2. "Molybdenum", Metallwerk Plansee GmbH.
3. "Brazing Molybdenum", American Society for Metals (1959).
4. L.H. Stone, A.H. Freedman, and E.B. Mikus, "Recrystallization Behavior and Brazing of the TZM Alloy".

3.0 EVALUATION OF TZM AS A CARTRIDGE MATERIAL

Upon completion of NASA/MSFC's re-design of the adjustment block, SRI arranged to have several test cartridges assembled for ground testing. SRI purchased bar stock of TZM from Climax Specialty Metals in Chicago. Some of this bar stock was subcontracted to a machine shop to be gun-drilled and ground to form the cartridge tube with a closed spherical end. SRI machined the adjustment blocks in-house from the remainder of the TZM bar stock. The adjustment blocks and cartridge tubes were then sent to NASA/MSFC for brazing and ground testing.

The TZM cartridge did not have the problems with recrystallization and brittleness that the previous molybdenum/stainless steel design suffered. However, there were some difficulties with TZM.

The TZM alloy was very difficult to machine. TZM is hard enough that tools wear out very quickly. The tools also required constant cooling with a tapping fluid to machine the alloy. TZM is a fairly brittle material. This brittleness often prevented the material from chipping cleanly and occasionally caused fracture of the part as holes were bored through. Machining the TZM was expensive in both man-hours and tooling.

During high temperature ground tests of the CGF with a TZM cartridge, the low density zirconia insulation in the adiabatic zone of the CGF crumbled and formed a yellow powder. An investigation of the yellow powder by SRI's X-ray diffraction facility showed the presence of large amounts of monoclinic zirconia. Commercial zirconia insulation has a yttria stabilizer added to maintain the zirconia in a stable cubic crystal form. It was apparent from this analysis that something was causing the stable cubic zirconia to break down into the less stable monoclinic form (which is yellow in color).

The transformation from cubic to monoclinic zirconia is accompanied by a three-fold volume change. As a check on the stability of the zirconia insulation supplied by the manufacture to NASA/MSFC, thermal expansion measurements were made on zirconia samples taken from spare parts of the CGF. In order to reach temperatures higher than 980°C, SRI's graphite dilatometer (Figure 3.0.1) was used in conjunction with the quartz dilatometer. The graphite dilatometer is

capable of measuring thermal expansion from about 815°C to 2760°C. Figure 3.0.2 is the thermal expansion curve for the zirconia insulation. The thermal expansion coefficient is uniform, indicating a stable material with no phase changes. Therefore, since the breakdown occurred only when a TZM cartridge was used, it was surmised that the TZM was somehow attacking the zirconia insulation.

A literature search on molybdenum and TZM showed that the volatile oxide formed by molybdenum can act as a catalyst for certain chemical reactions. Since the TZM cartridge readily oxidizes in the CGF, a test was designed to evaluate the effects of molybdenum oxide on zirconia insulation.

Figure 3.0.3 is a schematic of the molybdenum oxide test facility. Shavings of TZM were packed in the forward end of the furnace. A block of zirconia insulation (1 cc) was set in the rear of the furnace. The entire assembly was heated to 1200°C. Air was then purged into the forward end of the furnace through the TZM shavings. The large surface area of the shavings allowed the generation of copious amounts of molybdenum oxide that then passed over the zirconia insulation. The test was run for two hours. By the end of the test, the zirconia insulation had crumbled into a yellow powder. X-ray diffraction showed the powder to be monoclinic zirconia.

The above test showed that the molybdenum oxide generated by the TZM alloy was attacking the zirconia insulation. The chemical mechanism of the attack is not known.

3.1 CONCLUSIONS

There were two possible courses of action in response to the difficulties experienced in using TZM as the CGF cartridge material. Either an alternate material could be selected or a coating of some sort could be applied to the cartridge to prevent oxidation. The adjustment block would require no coating since it operated at only a few hundred degrees centigrade and thus did not oxidize at all.

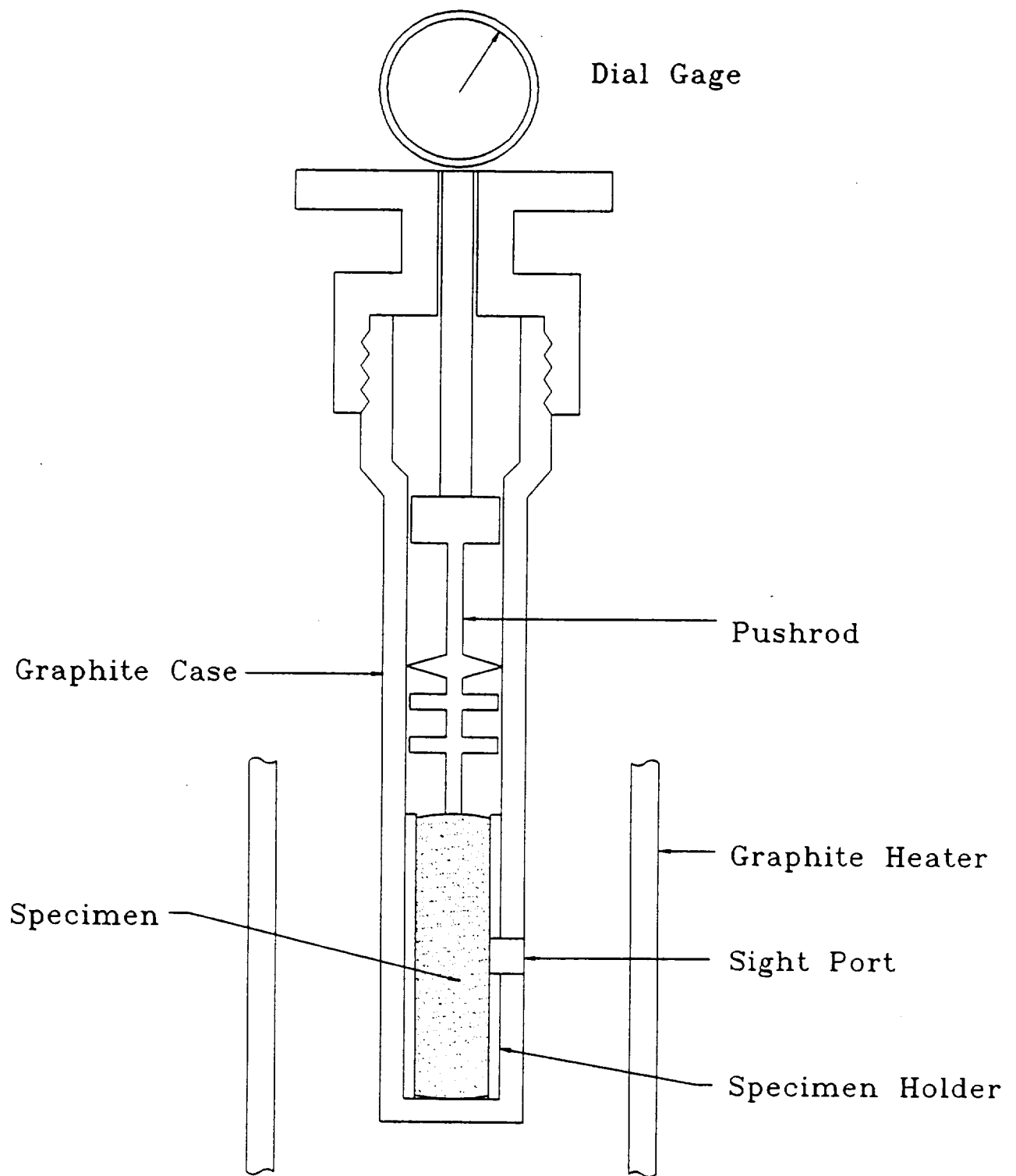


Figure 3.0.1. Graphite Dilatometer for Measuring Thermal Expansion to 5500°F

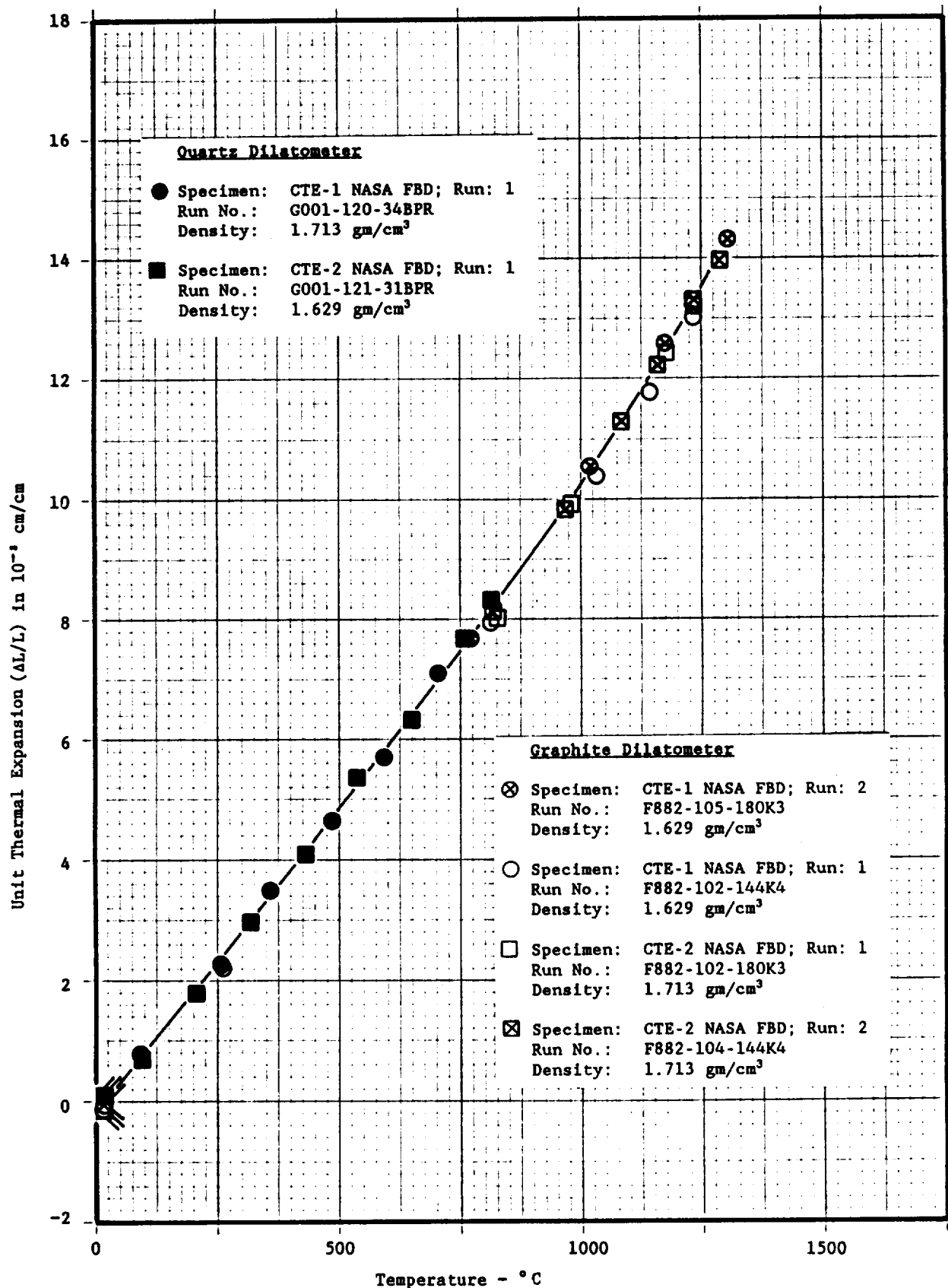


Figure 3.0.2. Unit Thermal Expansion of FBD Zirconia Insulation from CGF

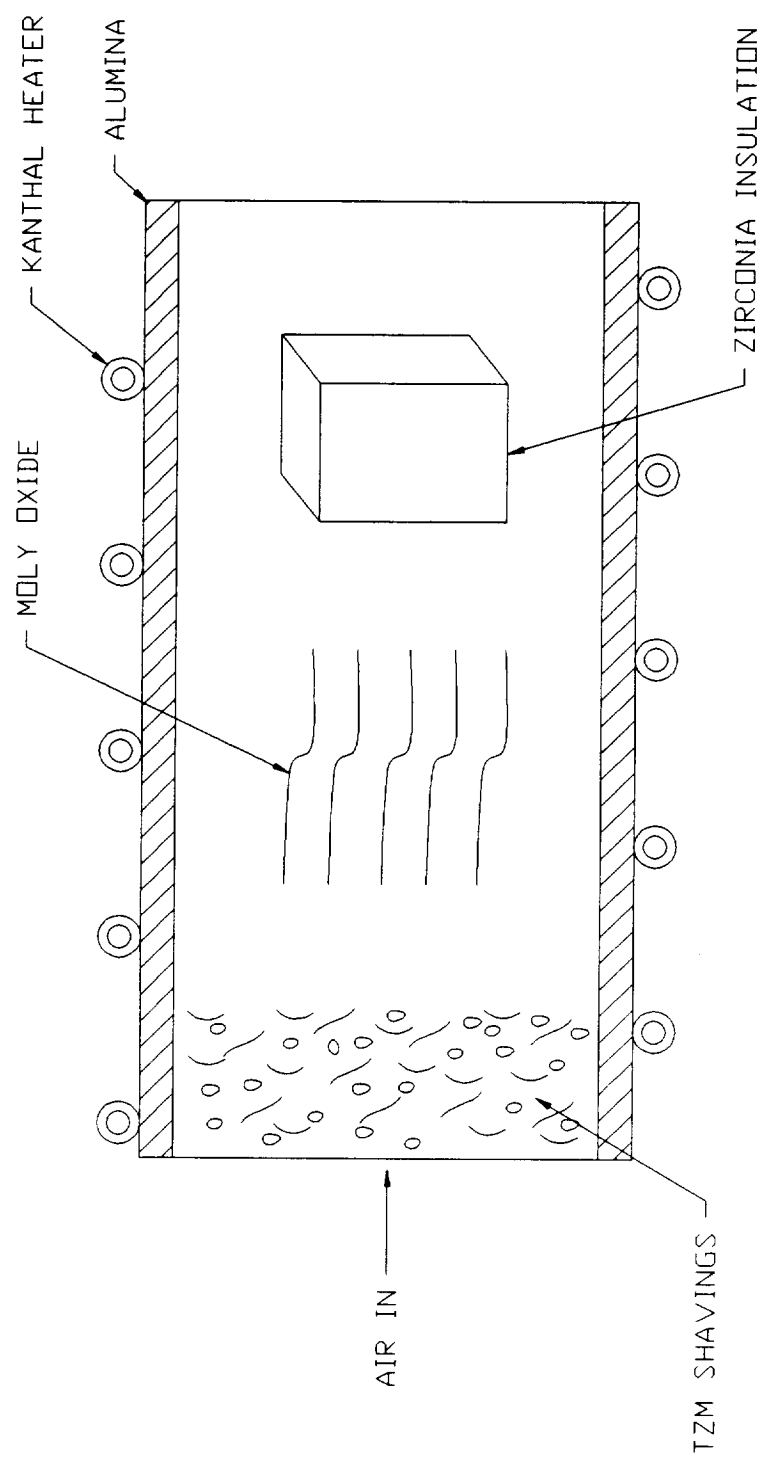


Figure 3.0.3. Molybdenum Oxide Test Facility

4.0 EVALUATION OF WC-103 AS AN ALTERNATE TO TZM

WC-103 is a niobium/hafnium alloy produced by Teledyne Wah-Chang in Albany, Oregon. WC-103 will not recrystallize during electron beam welding or brazing operations. This eliminated the need for machining cartridge tubes from solid rods as with the TZM. Tubes could be bought directly from Teledyne Wah-Chang, then the endcaps could be e-beam welded. This greatly reduced the manufacturing cost of CGF cartridges. Some of that savings was offset, however, by the greater cost of WC-103.

WC-103 is a more ductile alloy than TZM. This made machining the adjustment blocks considerably easier. The greater ductility also meant that the WC-103 cartridges were less susceptible to breakage when jarred than the TZM cartridges.

WC-103 mechanical properties are not as good as TZM (see tables in Section 6.1 for numerical data). However, its properties were deemed sufficient for use in the CGF.

There was only one major drawback to using WC-103 as a CGF cartridge material. The alloy oxidizes extensively at temperatures above about 230°C. In tests run in SRI's high temperature furnace, a WC-103 sample was heated to 1200°C and held for 1 hour in an environment simulating the CGF. The WC-103 broke down completely into a whitish powder. Obviously, such disintegration of the cartridge in the CGF would result in failure of the experiment. However, a coating could be applied to the WC-103 tube to prevent oxidation.

4.1 CONCLUSIONS

The WC-103 appeared to be a viable candidate if the oxidation problem could be solved with some sort of coating. The greater machinability and higher recrystallization temperature of the WC-103 made it desirable over TZM. However, TZM did possess better mechanical properties.

5.0 SURVEY OF OXIDATION RESISTANT COATINGS FOR TZM AND WC-103

Since both the TZM and WC-103 oxidized readily in the CGF environment, a survey was made of oxidation resistant coatings that could be applied to cartridges of these materials. This would allow either of the materials to be successfully used in the CGF.

The survey yielded two types of coatings that could be applied to the cartridges; 1) a silicide coating and 2) a chemical-vapor-deposited (CVD) iridium coating. These two coatings had thermal expansion coefficients that matched those of the base materials. The thermal expansion match was necessary to avoid cracks in the coatings at elevated temperatures.

Plasma sprayed silicide coatings were available from a company called VAC-HYD, based in Los Angeles, California. The silicide coatings were available which had been formulated to have compatible thermal expansion coefficients with both TZM and WC-103. The actual compositions of these coatings were proprietary.

The CVD iridium coating was available from a company called ULTRAMET based in Pacomia, California. Iridium is a high temperature, oxidation resistant metal. The thermal expansion of iridium is compatible with both TZM and WC-103.

Sample coupons of both TZM and WC-103 were sent to VAC-HYD for silicide coatings. A sample coupon of TZM was sent to ULTRAMET for a CVD iridium coating.

The returned samples were then inspected by SRI. It was noted that the silicide coatings were soft and easily rubbed off. The silicide coatings also had a tendency to crack if mishandled. The CVD iridium coating on the TZM, however, did not have any flaws and appeared to be quite rugged.

SRI then performed oxidation testing in the high temperature furnace on all the samples. The coupons were heated to 1200°C in air and held at temperature for eight hours. No oxidation was seen on any of the samples.

Since the silicide coatings were inexpensive and quickly available, a WC-103 cartridge was sent to VAC-HYD for coating. An inspection of the returned

cartridge showed the silicide coating had a tendency to chip off. There were numerous small cracks in the coating. This cartridge was then sent to NASA/MSFC for ground testing.

Since VAC-HYD's silicide coatings were easily damaged, another source of silicide coatings was sought. HITEMCO, based in New York, was able to provide suitable silicide coatings. HITEMCO's coatings were dipped rather than sprayed. The dipped coatings were considerably more rugged than the VAC-HYD's sprayed coatings. HITEMCO's coatings were also much less expensive than VAC-HYD's sprayed coatings (\$250 per tube vs. \$500 per tube). The dipped coatings provided adequate oxidation protection of the cartridges in the CGF.

A TZM cartridge was sent to ULTRAMET for an iridium coating. Upon inspection of the returned cartridge, the coating was durable and without defects. Testing at NASA/MSFC indicating that the iridium coating protected the TZM from oxidation. The zirconia insulation was not attacked.

5.1 CONCLUSIONS

Both the silicide and iridium coatings provided adequate protection from oxidation for both TZM and WC-103. The iridium is much more durable than the silicide coatings which require careful handling to avoid damage. However, the iridium coating's cost is prohibitive. The single TZM tube that was iridium coated cost around \$25,000. This cost was broken into two parts; a \$15,000 setup charge, then \$10,000 per tube for the iridium coating. HITEMCO's silicide coatings, on the other hand, cost only around \$250 per tube. This savings in cost of coating was deemed sufficient to offset the extra care required in handling the silicide coated tubes.

6.0 CHEMICAL COMPATIBILITY STUDIES

Two semiconductor materials were scheduled to be run aboard USML-1. They were gallium arsenide (GaAs) and cadmium zinc telluride (CdZnTe). Chemical compatibility between these semiconductors and the CGF cartridge material is of importance in the event of an ampoule failure during the experiment. Such a failure would result in direct contact of the molten semiconductor and cartridge. If the metal were attacked too extensively the cartridge would fail releasing molten semiconductor into the CGF, ruining the facility. Also the molten semiconductor could possibly escape the CGF entirely, posing a threat to shuttle personnel. The investigation of chemical compatibility was subcontracted by SRI to Dr. Rosalia Andrews of the Department of Materials Science and Engineering at the University of Alabama at Birmingham. Chemical compatibility studies were conducted as shown in the following matrix;

	<u>WC-103</u>	<u>WC-103</u>	<u>WC-103</u>	<u>TZM</u>	Silicide Coated <u>WC-103</u>	Hot Pressed Boron <u>Nitride</u>
GaAs @ 1260°C	24 hours	12 hours	6 hours	---	24 hours	24 hours
CdZnTe @ 1170°C	90 hours	24 hours	12 hours	90 hours	90 hours	---

All compatibility test reports are contained in Appendix A.

7.0 FINAL DESIGN OF CGF CARTRIDGE

The final design of the CGF cartridge is shown in Figure 7.0.1. The selected materials were WC-103 for both the cartridge and the adjustment block. The cartridge was coated inside and out with a silicide coating by HITEMCO. The WC-103 end cap was e-beam welded and the adjustment block was brazed.

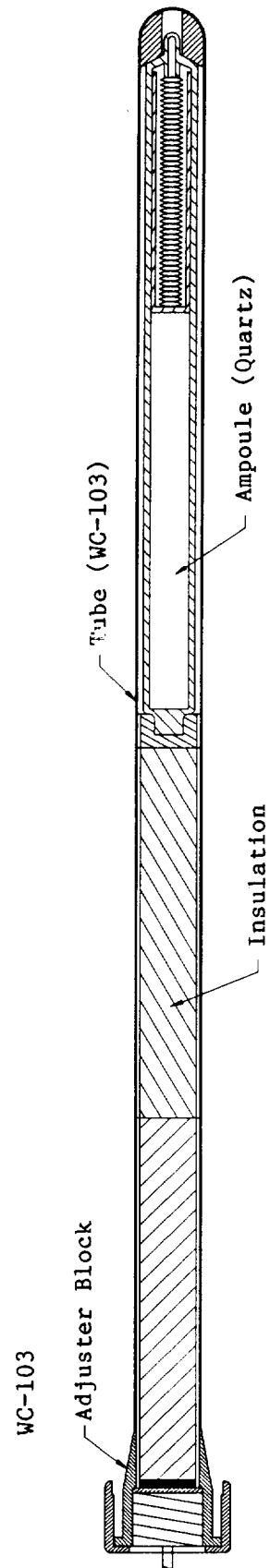


Figure 7.0.1. CGF Cartridge Schematic

8.0 SUPPORT WORK

In addition to the extensive research effort performed under this contract, SRI also carried out support work for NASA/MSFC. This support work consisted mainly of machine shop time to fabricate test articles and flight hardware in support of the USML-1 schedule.

9.0 FUTURE IMPROVEMENTS

The following sections are some efforts directed toward improving the current CGF cartridge design for future USML missions.

9.1 LITERATURE SEARCH FOR ALTERNATE CARTRIDGE MATERIALS

WC-103 proved to be a workable material for use as a CGF cartridge when protected by a silicide coating. However, the silicide coating was easily damaged. It was decided to begin to conduct a survey of alternate cartridge materials for use in later USML flights. Table 9.1.1 is a preliminary list of candidate materials selected by NASA/MSFC and SRI as being most likely to qualify as cartridge materials. These materials were selected primarily for their high operating temperatures.

As a preliminary step in selecting alternate cartridge materials, a literature search for thermal, mechanical, oxidative, and chemical properties was performed on the materials listed in Table 9.1.1. Appendix B of this report contains all available data on the candidate metals and metal alloys. Appendix C lists all data on the candidate ceramic materials. Blank spaces were left where data was not available. Data is presented in both International System (SI) and British Gravitational (BG) units. No information on chemical compatibility with semiconductor crystal compounds was found for any of the candidate materials. Appendix D summarizes thermal and mechanical properties for the candidate materials both at room temperature and at elevated temperatures. Appendix E lists the references used in the literature search.

Table 9.1.2 lists the candidate metals and metal alloys subject to a preliminary screening based upon the following conditions;

- 1) The material must survive at 1350°C in a mildly oxidizing environment. The CGF environment has about one-half percent oxygen.
- 2) The material must withstand thermal shock. The translating hot zone of the CGF subjects the cartridge to large thermal gradients.

- 3) The material must be commercially available.
- 4) The material must be machinable.
- 5) The material must be able to be formed into a sealed tube.
The tube must maintain its shape (not be too malleable).

As can be seen in Table 9.1.2, only one metal survives the preliminary screening. The downfall of many of the metals is the oxidation requirement. Most of the metals and metal alloys oxidize at elevated temperatures.

Table 9.1.3 presents the candidate ceramic materials subject to the same screening conditions. Only two materials survived. The downfall of the ceramics is the thermal gradient requirement. Most ceramics are very susceptible to thermal shock and cracking at elevated temperatures. The final two selections, silicon carbide and silicon nitride, present a problem in that they can only be formed into tubes with about a six millimeter wall thickness. This is a much thicker wall than the current design allows.

Tables 9.1.4 and 9.1.5 contain the metal and ceramic candidates (respectively) subjected to a higher temperature requirement (1575°C) in anticipation of future USML flights that will require greater temperatures. As can be seen, the results of the second screening are the same as the first.

It is evident from this preliminary study and experience with TZM and WC-103 that candidate metals and metal alloys must have some form of oxidation protection if they are to survive at high temperatures in the CGF environment. Iridium, though not subject to oxidation, is too expensive to be a feasible cartridge material. Many of the metals rejected in the preliminary screening could become viable candidates with an oxidation resistant coating. However, a more durable coating than the silicide coatings used with WC-103 would be desired.

Silicon nitride and silicon carbide seem to be two good potential ceramic cartridge materials. These materials are oxidation resistant, have high operating temperatures, and are not susceptible to thermal shock. However, the thick-wall requirement would necessitate the redesign of the ampoule and

thermocouple assembly currently used in the CGF. A silicon nitride tube was ordered and fabricated by Ceradyne Inc. in Costa Mesa, California, under this contract for future evaluation as a CGF cartridge.

TABLE 9.1.1
CANDIDATE MATERIALS CONSIDERED FOR CGF TUBE

METALS	CERAMICS
Iridium	Aluminum Oxide
Niobium	Aluminum Oxide/SiC Whiskers
Niobium (WC-103)	Beryllium Oxide (Isopressed)
Platinum	Boron Nitride (HP Grade)
Platinum/20% Iridium	Chromium Bonded Aluminum Oxide
Platinum/20% Rhodium	Quartz (Fused Silica)
Rhenium	Silicon Carbide (Sintered Alpha)
Rhodium	Silicon Nitride (Hot Pressed)
Tantalum	Zirconium Oxide (Sintered; MgO Stabilized)
Tantalum/10% Tungsten	
Tantalum/Rhenium	
Tungsten	
Tungsten/25% Rhenium	
TZM	

TABLE 9.1.2
IMMEDIATE MINIMUM GOALS (REFRACTORY METALS)

MATERIAL	1350°C and above operating temperature in an oxidizing environment	Survives high thermal gradient?	Availability	Machinability	Ability to form tube to NASA requirements
Niobium					
WC - 103 (Niobium Alloy)					
Iridium	Iridium	Iridium	Iridium *	Iridium	Iridium
Platinum	Platinum	Platinum	Platinum *	Platinum	
Platinum/20% Iridium	Platinum/20% Iridium	Platinum/20% Iridium			
Platinum/20% Rhodium	Platinum/20% Rhodium	Platinum/20% Rhodium			
Rhenium					
Rhodium	Rhodium	Rhodium	Rhodium *	Rhodium	
Tantalum					
Tantalum/10% Tungsten					
Tantalum/Rhenium					
Tungsten					
Tungsten/25% Rhenium					
TZM					

*Extremely costly.

TABLE 9.1.3
IMMEDIATE MINIMUM GOALS (CERAMICS)

MATERIAL	1350°C and above operating temperature in an oxidizing environment	Survives high thermal gradient?	Availability	Machinability	Ability to form tube
Aluminum Oxide	Aluminum Oxide				
Aluminum Oxide/SiC	Aluminum Oxide/SiC				
Beryllium Oxide	Beryllium Oxide	Beryllium Oxide	Beryllium Oxide		
Boron Nitride					
Chromium bonded AlO	Chromium bonded AlO				
Quartz					
Silicon Carbide	Silicon Carbide	Silicon Carbide	Silicon Carbide	Silicon Carbide	Silicon Carbide
Silicon Nitride	Silicon Nitride	Silicon Nitride	Silicon Nitride	Silicon Nitride	Silicon Nitride
Zirconium Oxide	Zirconium Oxide				

TABLE 9.1.4
LONG TERM PREFERRED GOALS (REFRACTORY METALS)

MATERIAL	1575°C and above operating temperature in an oxidizing environment	Survives high thermal gradient?	Availability	Machinability	Ability to form tube
Niobium					
WC-103 (Niobium Alloy)					
Iridium	Iridium	Iridium	Iridium *	Iridium	Iridium
Platinum	Platinum	Platinum	Platinum *	Platinum	
Platinum/20% Iridium	Platinum/20% Iridium	Platinum/20% Iridium			
Platinum/20% Rhodium	Platinum/20% Rhodium	Platinum/20% Rhodium			
Rhenium					
Rhodium	Rhodium	Rhodium	Rhodium *	Rhodium	
Tantalum					
Tantalum/10% Tungsten					
Tantalum/Rhenium					
Tungsten					
Tungsten/25% Rhenium					
TZM					

*Extremely costly.

TABLE 9.1.5
LONG TERM PREFERRED GOALS (CERAMICS)

MATERIAL	1575°C and above operating temperature in an oxidizing environment	Survives high thermal gradient?	Availability	Machinability	Ability to form tube
Aluminum	Aluminum Oxide				
Aluminum Oxide/SiC	Aluminum Oxide/SiC				
Beryllium Oxide	Beryllium Oxide	Beryllium Oxide	Beryllium Oxide		
Boron Nitride					
Chromium bonded AlO					
Quartz					
Silicon Carbide	Silicon Carbide	Silicon Carbide	Silicon Carbide	Silicon Carbide	Silicon Carbide
Silicon Nitride	Silicon Nitride	Silicon Nitride	Silicon Nitride	Silicon Nitride	Silicon Nitride
Zirconium Oxide	Zirconium Oxide				

9.2 IMPROVED AMPOULE DESIGN

The semiconductor crystals are contained in a sealed quartz ampoule in the current CGF design. However, quartz becomes soft at around 1260°C, enabling the vapor pressure of the crystal material to "balloon" the ampoule. This difficulty was overcome by pressurizing the CGF cartridge to prevent the ampoule's ballooning. Another problem with the quartz ampoule was its chemical incompatibility with gallium arsenide (GaAs) at elevated temperatures. The GaAs attacked the quartz severely leading to failure of the ampoule. To prevent failure, a pyrolytic boron nitride sleeve was inserted into the ampoule. Pyrolytic boron nitride does not react with GaAs and the sleeve prevented the attack of the quartz. An effort was made to improve the ampoule design for future USML missions which will require higher temperatures.

The redesigned CGF ampoule must meet three requirements. First, the material must survive the CGF operating temperature and be chemically inert with the semiconductor crystals it contains. Second, the ampoule must be sealable. An added improvement would be to include a failure sensing device that would alert the operator of an ampoule failure during the experiment. These three requirements were addressed by SRI.

Only ceramic materials were considered as candidate ampoules due to the oxidation problems experienced with most metals and metal alloys. Pyrolytic boron nitride was successfully used with GaAs in ground testing of the CGF for USML-1. However, pyrolytic boron nitride is not available in pieces large enough to construct an ampoule. Hot pressed boron nitride is available but the chemical compatibility with semiconductor crystals must be determined. SRI had an ampoule constructed from boron nitride for evaluation under this contract. This ampoule is shown in Figure 9.2.1. Testing is ongoing. Also, from the literature search described in Section 8.1 of this report, silicon carbide and silicon nitride seem to be viable candidates as well.

Future experiments may require consideration of other ceramics to ensure chemical compatibility with other semiconductor crystals. SRI possesses a complex finite-element analysis computer program (NISA) that can be used to

ensure the ampoule configuration (wall thickness) and material properties are sufficient to contain various semiconductors during the CGF experiments.

Ceramics are not as easily sealed as quartz. The prototype ampoule was designed with a threaded cap and a small crushable platinum seal (chemically inert with most semiconductors) equipped with nodes that would penetrate the ampoule material upon tightening the cap (Figure 9.2.1) thus sealing the ampoule. Another proposed technique would be to machine a slightly oversized plug, cool it to cryogenic temperature, then insert it into a slightly heated ampoule. Upon reaching thermal equilibrium, the plug would tightly seal the ampoule (Figure 9.2.2).

The failure sensing device devised by SRI consisted of a metallic circuit etched on the outside of the ampoule (Figure 9.2.3). Upon failure of the ampoule, the circuit would either be broken by cracks or attacked by the escaping semiconductor. Either case would result in a broken circuit that would alert the operator of ampoule failure. For conductive ampoule materials, such as silicon carbide, the metal circuit could be placed inside a permeable insulator and placed near the ampoule (Figure 9.2.4). Again, if the ampoule fails, the semiconductor would attack the circuit and break it, signalling an alert. SRI has completed the preliminary design work on such a circuit but no prototypes have been constructed.

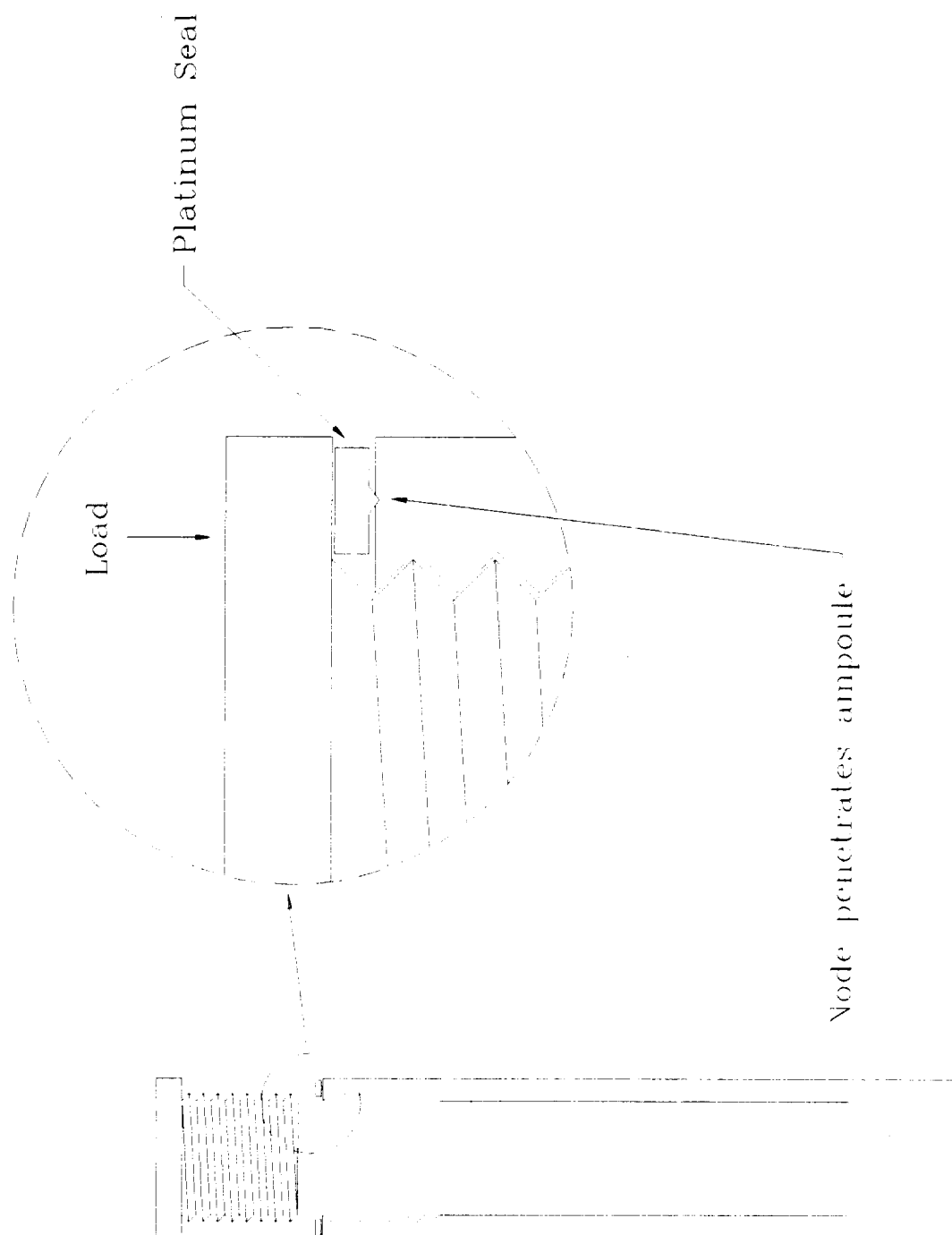


Figure 9.2.1. Prototype Ampoule

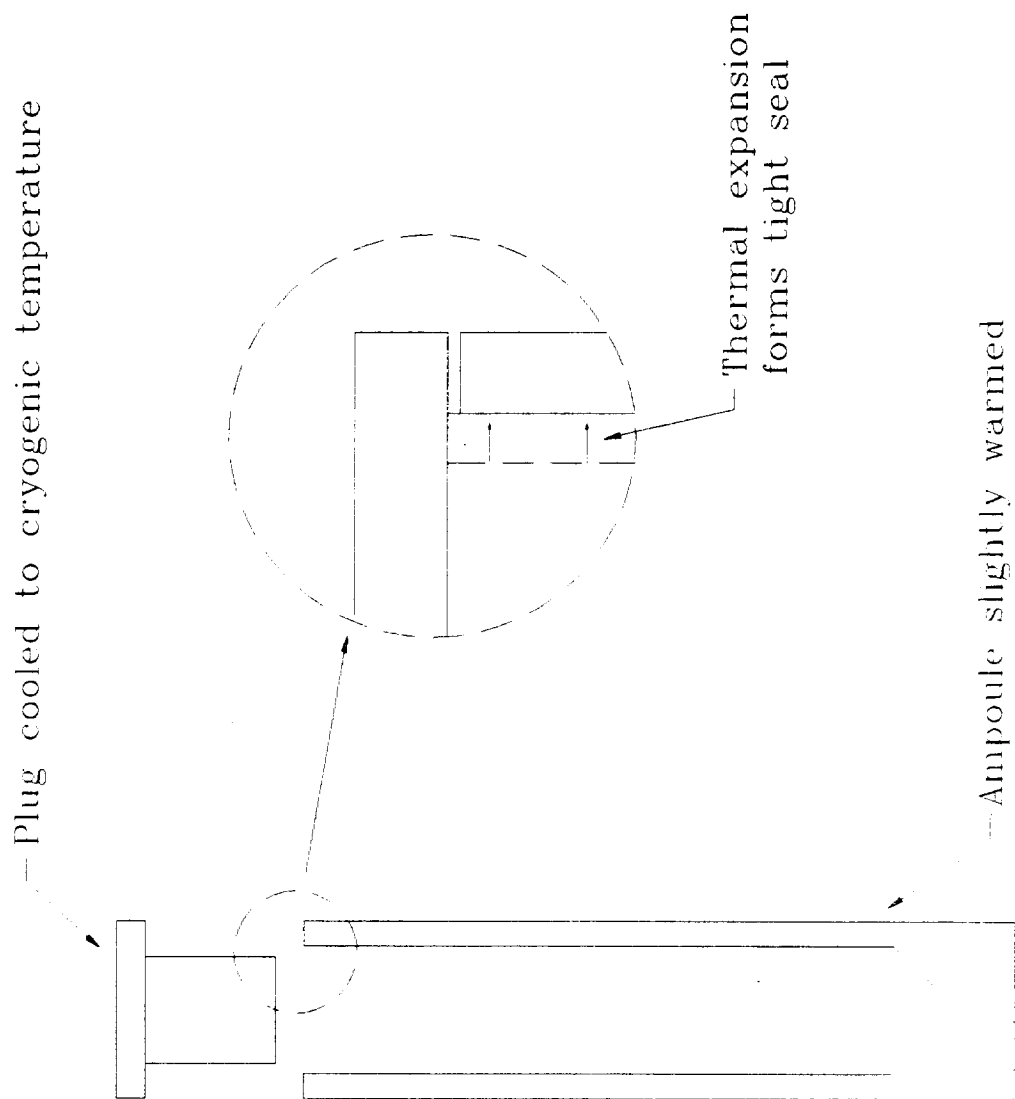


Figure 9.2.2. Alternate Sealing Technique for Re-designed Ampoule

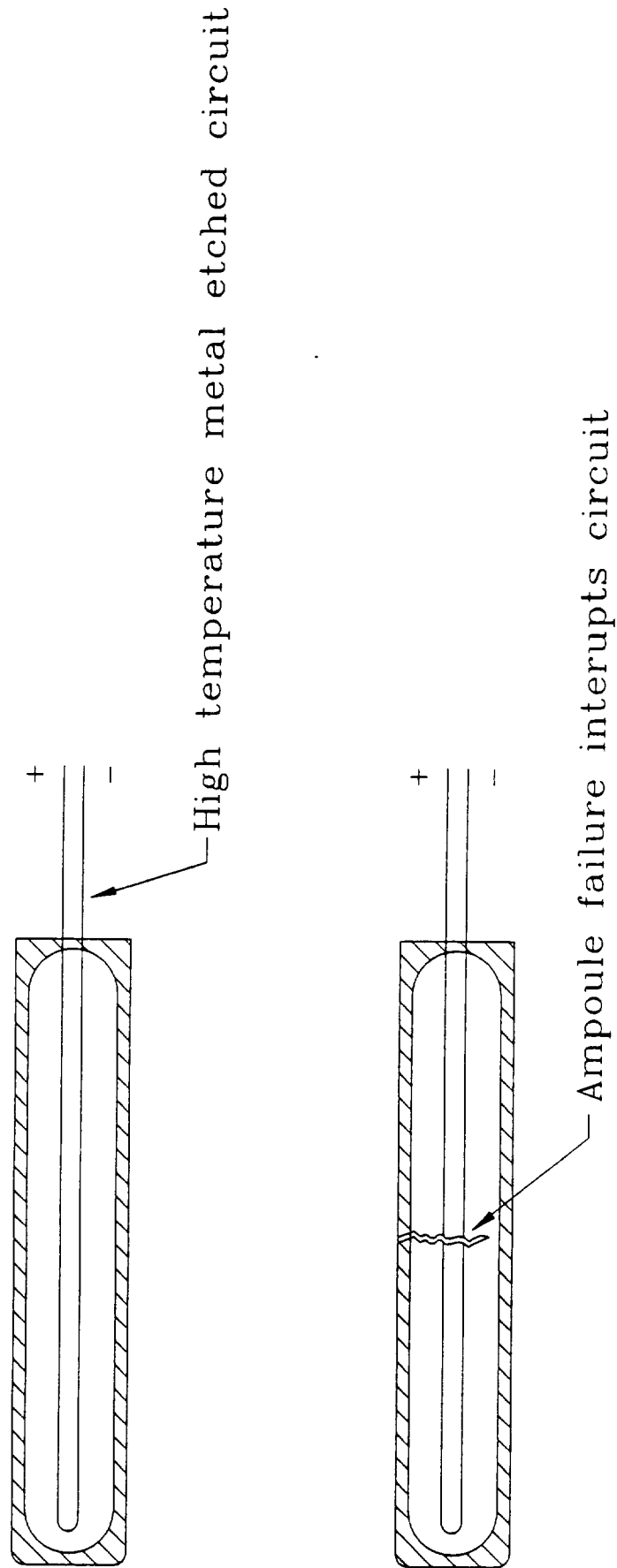


Figure 9.2.3. Ampoule Failure Sensing Mechanism for Non-conductive Ampoules

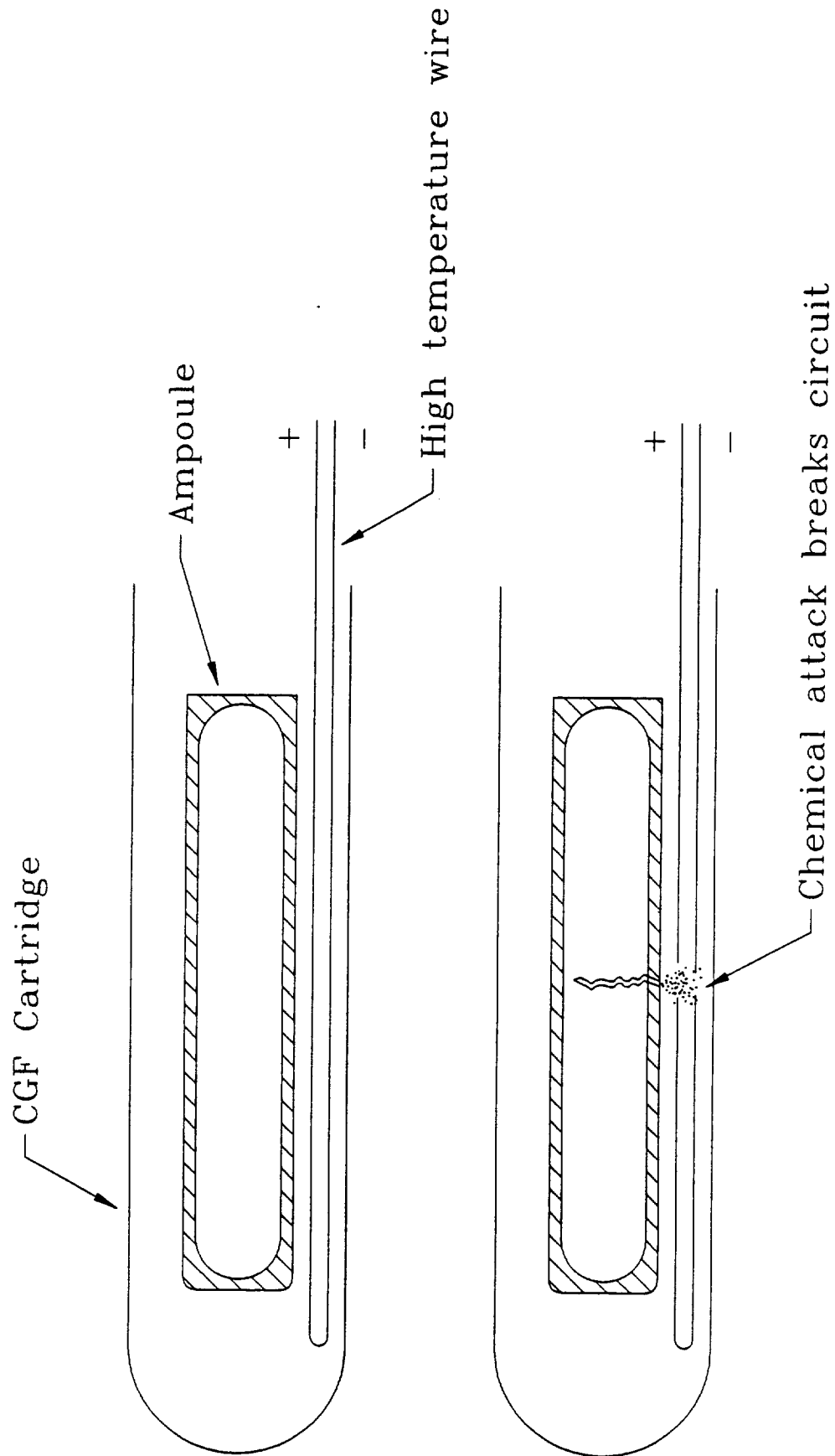


Figure 9.2.4. Ampoule Failure Sensing Mechanism for Conductive Ampoules

9.3 COMPUTERIZED MATERIALS DATABASE DEVELOPMENT

SRI has developed a computer program that maintains a database on mechanical and thermal properties of candidate cartridge and ampoule materials. The database currently contains all of the information listed in Appendixes B and C. The program is capable of switching between SI and BG units. Provisions for adding candidate materials to the database have been made. The program will be especially useful in selecting appropriate ampoule materials for specific semiconductor crystals since chemical compatibility information can be maintained.

LIST OF APPENDICES

APPENDIX A	CHEMICAL COMPATIBILITY STUDIES
APPENDIX B	CGF CARTRIDGE CANDIDATE METALS AND METAL ALLOYS
APPENDIX C	CGF CARTRIDGE CANDIDATE CERAMIC MATERIALS
APPENDIX D	CANDIDATE CARTRIDGE MATERIALS SUMMARY TABLES
APPENDIX E	LITERATURE SEARCH REFERENCES

APPENDIX A

CHEMICAL COMPATIBILITY STUDIES

Progress Report

Chemical Compatibility Studies of GaAs and CdZnTe with WC-103 and TZM

by:

Rosalia N. Andrews, Ph.D., P.E.
Department of Materials Science and Engineering
University of Alabama at Birmingham
Birmingham, Alabama 35294

February 10, 1992

Introduction

The purpose of this investigation was to evaluate the chemical compatibility of both GaAs and CdZnTe with the alloys WC-103 and TZM. These two alloys are candidate cartridge materials for use in the Crystal Growth Furnace (CGF) during crystal growth experiments aboard USML-1. WC-103 is an 89%Nb - 10%Hf - 1%Ti alloy and TZM is a Mo - 0.5%Ti - 0.19%Zr alloy.

The chemical compatibility issue is of critical importance in the event of an ampule failure during crystal growth experiments. Such a failure, would result in the metal and molten semiconductor being in direct contact, possibly over an extended period of time at high temperatures. The extent of any semiconductor/metal reaction is thus a critical safety issue question. This investigation was undertaken to determine the occurrence of any reactions or metal loss at the molten semiconductor/metal interface during long term contact. This study fully evaluated the chemical compatibility of GaAs and CdZnTe with WC-103 at 1260°C and 1170°C, respectively and also provides preliminary data for the chemical compatibility of CdZnTe with TZM.

Experimental Procedure

The metal-semiconductor reaction couple was loaded into the appropriate crucible (Pyrolytic Boron Nitride (PBN) for GaAs and Quartz for CdZnTe), then covered and sealed in an evacuated quartz ampule. The design of the test configuration is shown in Figure #1. This configuration simulates very closely the actual conditions that would occur in the event of an unexpected ampule failure at elevated temperatures. Namely, the metal would be exposed to a

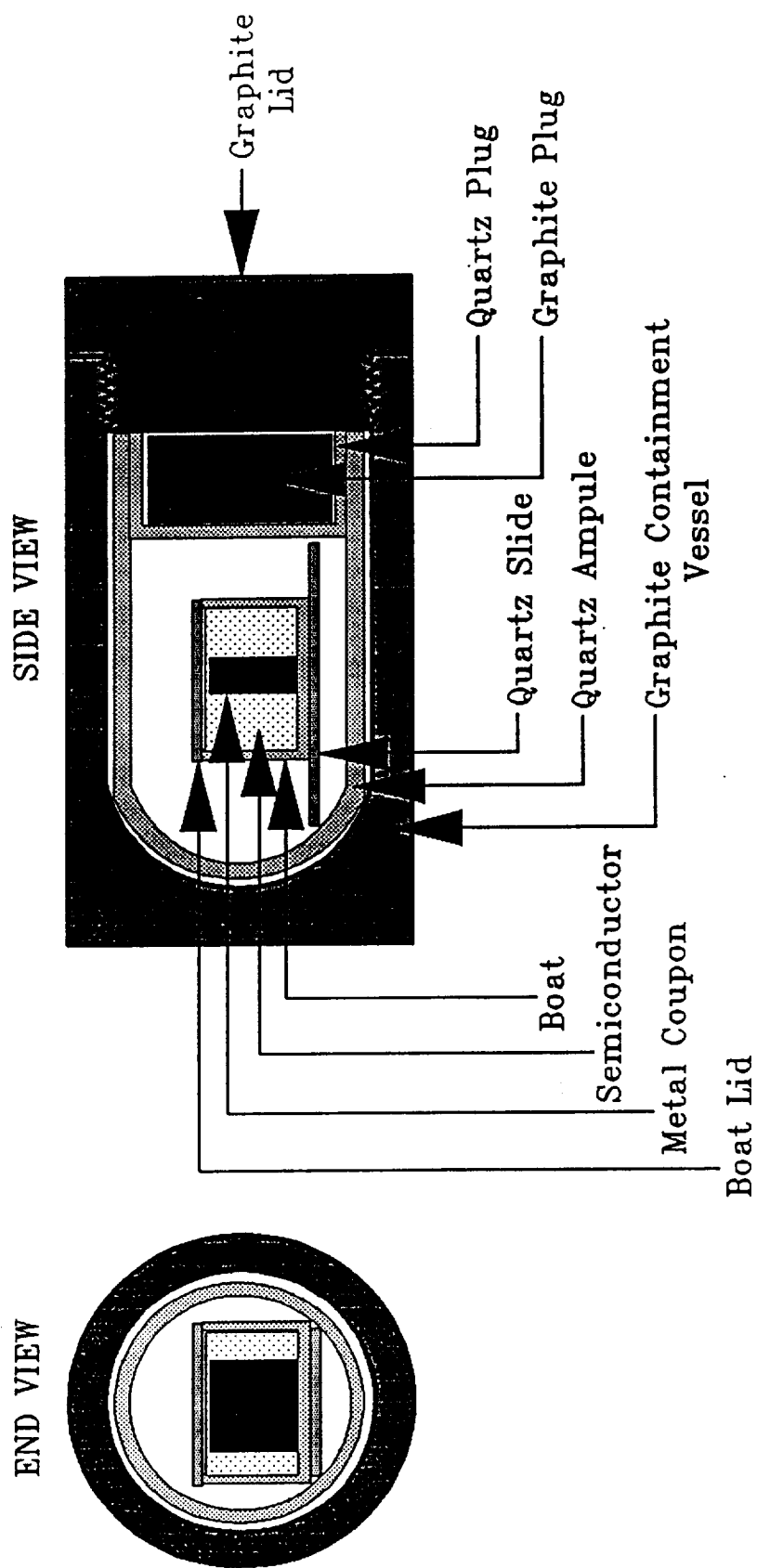


Figure 1. Schematic of experimental set-up including graphite containment vessel.

semi-infinite supply of molten semiconductor for the duration of the growth experiment at an elevated temperature. The longest duration for the CdZnTe experiment would be 90 hours and that for the GaAs would be 24 hours at temperature. The test matrix utilized in this study is shown in Table #1 and was selected to determine the progressive semiconductor/metal attack as a function of time.

Table I

	WC-103	WC-103	WC-103	TZM
GaAs 1260°	24 Hours	12 Hours	6 Hours	-
CdZnTe 1170°	90 Hours	24 Hours	12 Hours	90 Hours

All GaAs compatibility tests were performed at 1260°C and all CdZnTe compatibility tests were performed at 1170°C. The heating and cooling profiles followed for both GaAs and CdZnTe couples are shown in Figures 2 and 3, respectively. After processing, all semiconductor/metal reaction couples were examined both optically and with Scanning Electron Microscopy (SEM) and Energy Dispersive Spectroscopy (EDS) to determine both the extent of metal loss, the presence of any semiconductor/metal reaction zone, and the resultant chemical compatibility of the couple.

Details of the sample preparation, ampule loading and characterization techniques used in this study are given below.

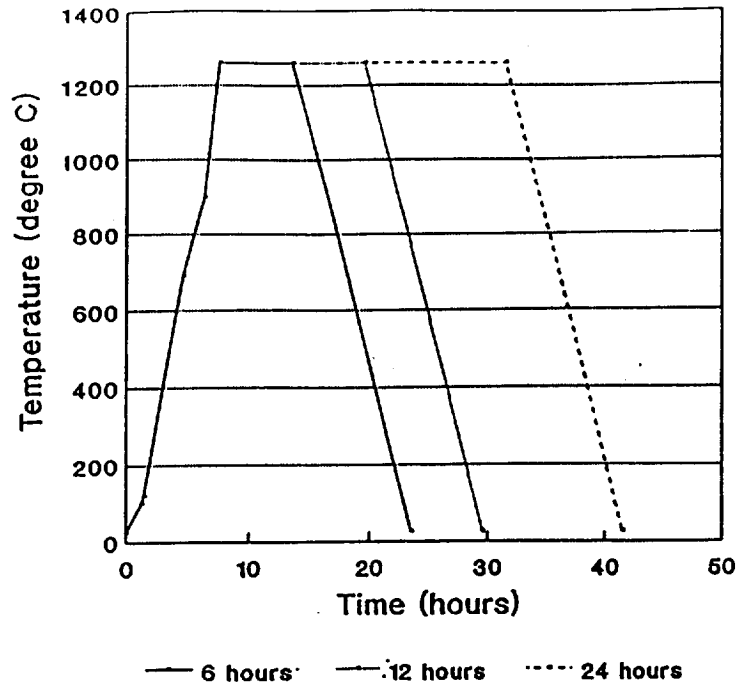


Figure 2.

Furnace Heating Schedule for GaAs Compatibility Tests; 6, 12, and 24 hour runs at 1260°C.

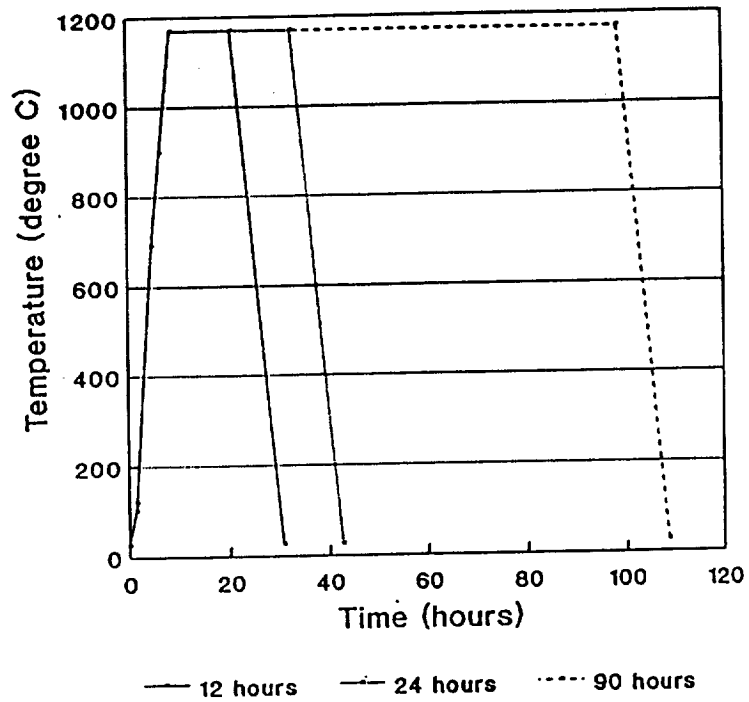


Figure 3.

Furnace Heating Schedule for CdZnTe Compatibility Tests; 12, 24, and 90 hour runs at 1170°C.

Semiconductor/Metal Couple Preparation

Metal coupons of approximately 10mm x 10mm x 5mm were cut from a slab of WC-103 or TZM and were ground and polished using successively, 240, 400 and 600 grit SiC, followed by 9.5 μ m, 5.0 μ m and 1.0 μ m alumina polish. The coupons were then cleaned with distilled water and methanol. A schematic of the metal coupon is shown in Figure 4.

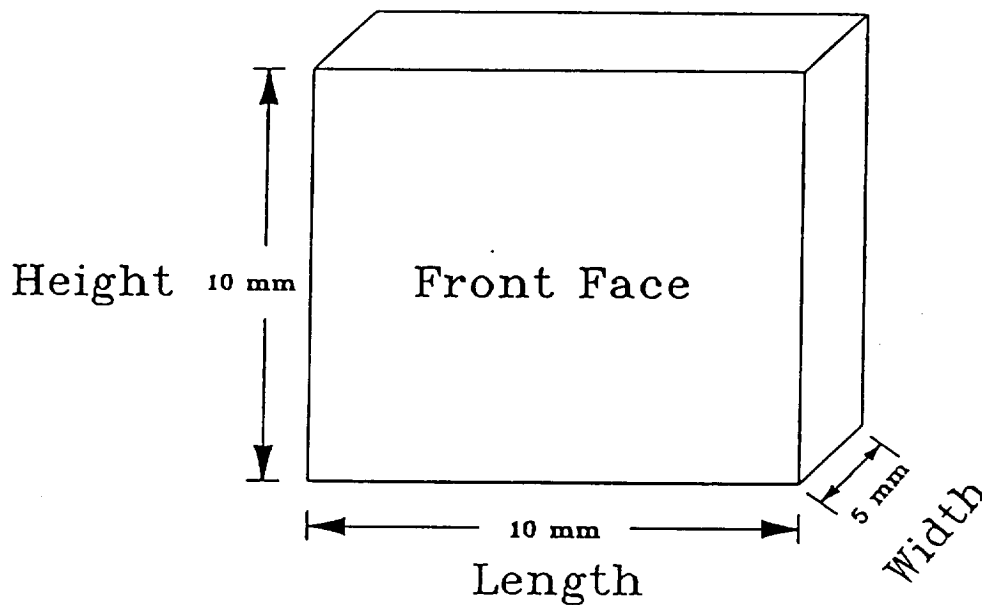


Figure 4. Schematic of metal coupon used in compatibility studies.

For the GaAs experiments, pyrolytic boron nitride boats and lids were used to contain the metal/semiconductor couple. The boats and lids were rinsed in distilled water and then soaked in aqua regia (3 parts concentrated HCl and 1 part concentrated HNO₃) overnight. Upon removing the pyrolytic boron nitride from the aqua regia, the pieces were rinsed several times

in warm distilled water and subsequently placed in a furnace and heated in air at 700°C for 3 hours.

The GaAs was cleaned in a solution consisting of 2 parts H₂SO₄, 1 part peroxide, and 1 part distilled H₂O. After soaking for 2 minutes, the GaAs was removed and thoroughly rinsed with distilled water, with a final rinse in methanol. The CdZnTe was used in the as-received condition. Both semiconductor materials were stored in a vacuum desiccator.

The quartz ampule, plug, and support slide used in all experiments were initially cleaned in distilled water and methanol. They were then rinsed in hydrofluoric acid for 30 seconds followed by thorough rinsing in distilled water. A final methanol rinse was used. The quartz boats and lids used for the CdZnTe experiments were also cleaned using the above procedure.

The weight of the empty boats as well as the weight and dimensions of the metal coupon were recorded prior to each compatibility run. To load the boats, the metal coupon was first placed into the boat on edge so that the front and back faces did not touch any portion of the boat. The boat was then filled with crushed semiconductor. The boat was then repeatedly tapped and filled until the semiconductor was level with the top of the boat. The filled boat was then weighed.

The filled boat was covered using the appropriate lid and secured to a support slide using quartz yarn. After the boat was secured to the slide, the boat and slide were placed in the ampule and positioned at the very end of the ampule. Once the boat was in place, the quartz plug was slid to the end of the ampule so that it was in contact with the square end of the support slide. The loaded ampule was then slowly evacuated down to 3×10^{-6} Torr. Argon gas was used to back fill the ampule to atmospheric pressure. The ampule was again evacuated and

backfilled two more times. A final vacuum of 3×10^{-7} Torr was achieved prior to the actual sealing of the ampule.

An oxygen-hydrogen torch was used to seal the ampule. The quartz ampule was heated so that it collapsed onto the quartz plug and formed a seal between the two surfaces. The sealing was done in several steps so that the end of the ampule containing the boat could be cooled. Distilled water was used to cool the end of the ampule. To avoid thermally shocking the quartz, the water was not applied directly to the region being sealed. The cooling of the ampule helped to prevent vaporization of the semiconductor during the sealing procedure.

A diamond wire saw was then used to cut the excess length off of the ampule and the ampule was then cleaned with methanol to remove any residue. A graphite plug was ground to fit into the quartz plug, and the ampule (with the graphite plug in place) was then loaded into a graphite containment vessel. This graphite container was used to hold the sealed quartz ampule to minimize any ballooning effect of the quartz which may occur at high temperatures. A graphite lid was then screwed into place so that it just touched the end of the quartz ampule, but did not rotate the ampule. Figures 5 and 6 illustrate a loaded boat and ampule, respectively as they are being prepared for placement in the furnace.

The graphite vessel was then loaded into the furnace such that the boat was in the central constant temperature region of the furnace. An external thermocouple was inserted through the end caps on the alumina furnace tube and argon gas at a flow rate of 90 cc/min. was started. The furnace controller was then programmed for the proper heating profile. The heating profile used for the GaAs experiments and for the CdZnTe experiments was shown previously in Figures 2 and 3, respectively.

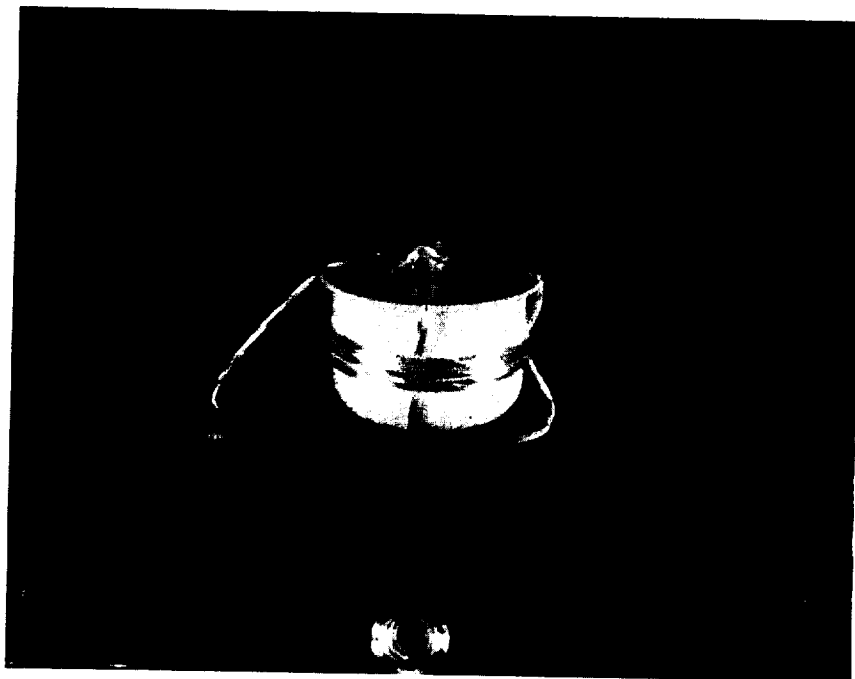


Figure 5. Loaded PBN boat with lid.

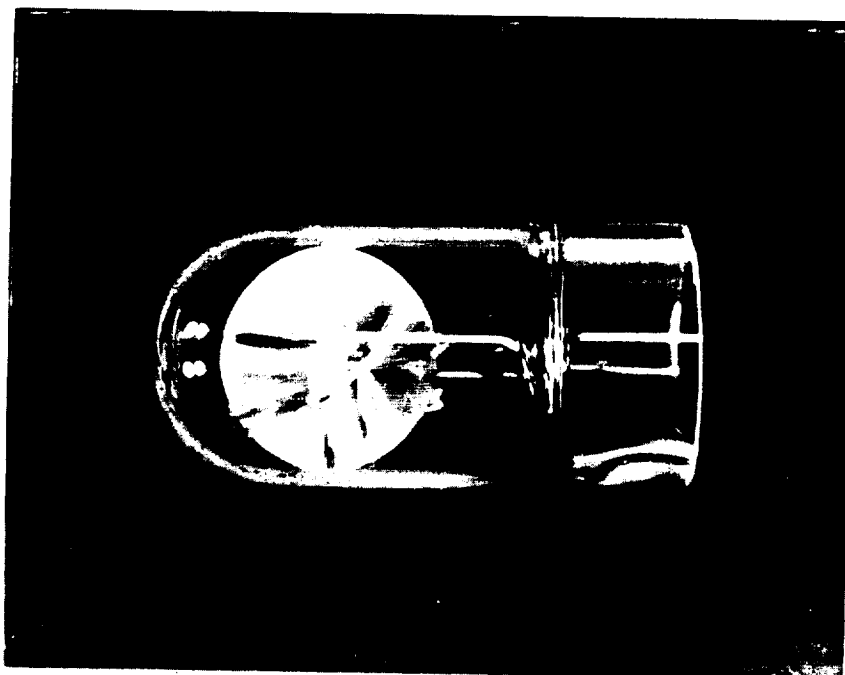


Figure 6. Quartz ampule assembly for compatibility tests.

After the entire heating profile was run and the ampule was again at room temperature, the graphite vessel was removed from the furnace. The quartz ampule was removed and was cut open using a diamond cut off wheel. The boat was removed and a photograph was taken of the boat. The lid was then removed and another photo was taken. Figures 7 and 8 are representative photos of an ampule and boat as they were removed from the furnace. After removing the semiconductor/metal coupon from the boat, the combination was sectioned using a diamond cut off saw and one half of the sample was mounted in an electrically conductive mounting compound. The mounted half was then ground using 240, 400, and 600 grit SiC with final polishing done using 9.5 μm , 5.0 μm , and 1.0 μm alumina polish. The sample was then cleaned in methanol.

A photograph was taken of the mounted sample to show the overall cross section. Optical photographs were then taken of each side of the metal coupon and its bottom to show the microstructure in the region of the metal/semiconductor interface. Optical photographs were taken of all samples at magnifications of 31.25X, 100X, and 200X.

The mounted samples were also examined in the scanning electron microscope, (SEM). Compositional analysis was performed at various locations across the metal semiconductor interface using a KEVEX microanalysis system. All SEM/KEVEX analysis was performed at an accelerating voltage of 16 KeV and a take off angle of 15°. This technique clearly showed any reaction or diffusion zone at the interface between the semiconductor and the metal coupon. Additionally, X-ray maps were taken across the semiconductor/metal interface to more graphically show the reactions taking place.

The final dimensions of the metal coupon were also measured using a micrometer stage and optical microscope so that the amount of metal loss and thickness of any reaction zone could be accurately determined.

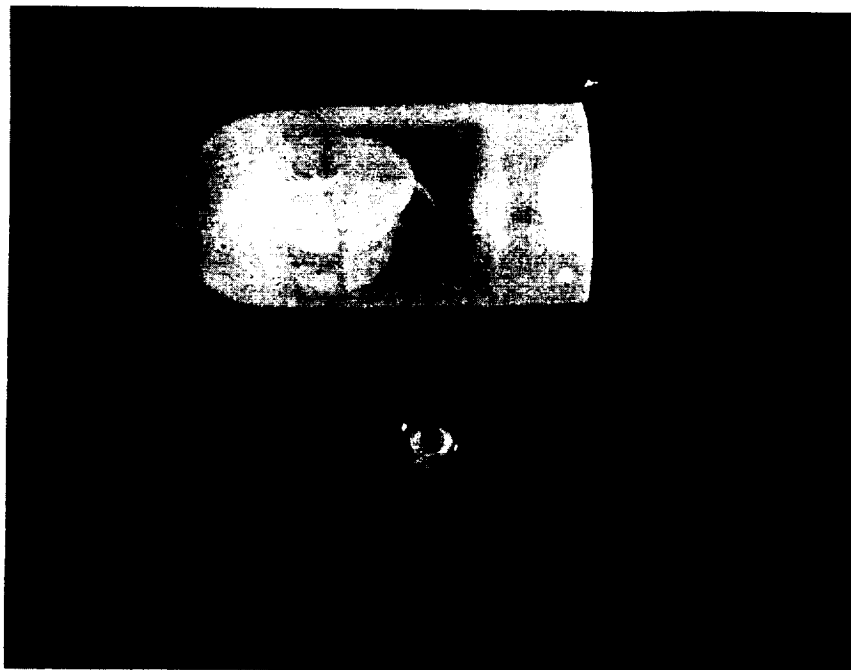


Figure 7. Quartz ampule assemble as removed from furnace after compatibility tests.

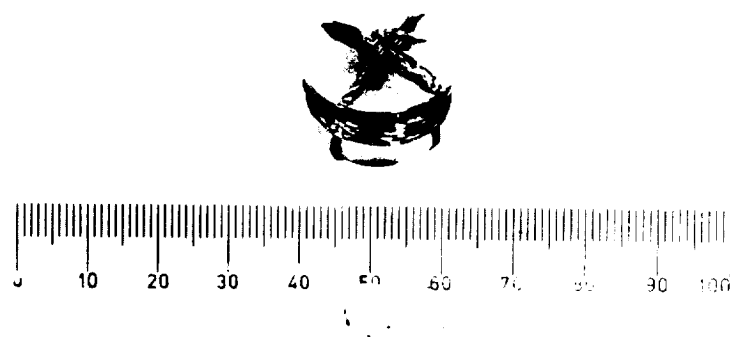


Figure 8. PBN boat removed from ampule after compatibility test.

Results and Discussion

GaAs/WC-103 Compatibility Tests

Three GaAs/WC-103 compatibility tests were conducted to determine the reactivity/compatibility of molten GaAs in contact with WC-103 at 1260°C. Details of the experimental set-up and test procedures were described previously. The three runs conducted and analyzed were for 6, 12, and 24 hours at 1260°C. The results are presented below.

6 hour GaAs/WC-103

An optical micrograph showing a cross-section of the 6 hour GaAs/WC-103 reaction couple is shown in Figure 9. An optical micrograph of the reaction zone at the metal/semiconductor interface is shown in Figure 10. As can be seen in Figure 10, the metal was severely attacked by the semiconductor. It is also apparent that reaction products have formed at the metal/semiconductor interface and that some of these products have begun to break off into the adjacent semiconductor. SEM/EDS analysis across the interface was performed and the compositional results obtained from Figure A1 are shown in Figure A2 (Appendix A).

Points 3, 4, and 5 on Figure A2, (zones 1, 2, 3, on plots) indicate that the reaction products formed are indeed a mixture of semiconductor and metal. In this run, the average thickness of metal lost was 0.7 mm or 2.76 mils. Since the proposed metal cartridge for use in the CGF crystal growth experiments aboard USML-1 is 27 mils thick, the metal loss observed was normalized to this thickness. Thus, for a 27 mil thick metal sample, the amount of metal loss observed for a 6 hour run would amount to a 10% reduction in thickness.

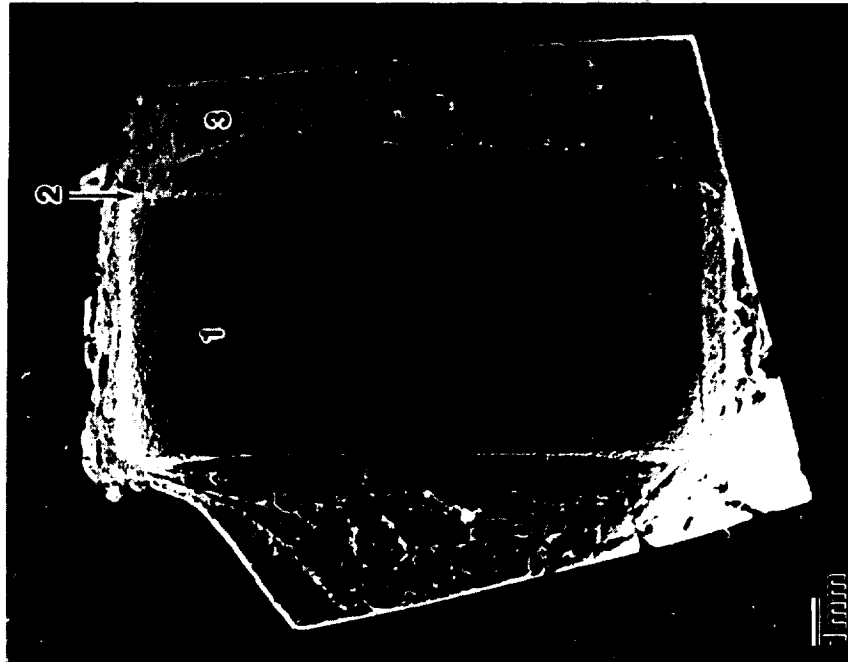


Figure 9. Cross section of a GaAs/WC-103 reaction couple after a 6 hour compatibility run at 1260°C.



Figure 10. Metal/semiconductor interface region in a GaAs/WC-103 compatibility test carried out for 6 hours at 1260°C. 1 = metal, 2 = interface/reaction zone, and 3 = semiconductor.

12 hour GaAs/WC-102

For the 12 hour run, Figure 11 again shows a severe attack present at the metal/semiconductor interface. The reaction products formed at this interface have also spalled off and floated into the adjacent semiconductor. In the compositional analysis performed across the interface (Figures A3 and A4 in Appendix A), it is observed that metal is present a considerable distance away from the metal/semiconductor interface (points 8 and 10 for example) and that reaction products which break off from the reaction zone are a mixture of metal and semiconductor.

In this couple, the average thickness of metal lost was 0.08 mm or 3.15 mils. On a 27 mil thick metal sample, this would correspond to a 12% reduction in thickness.

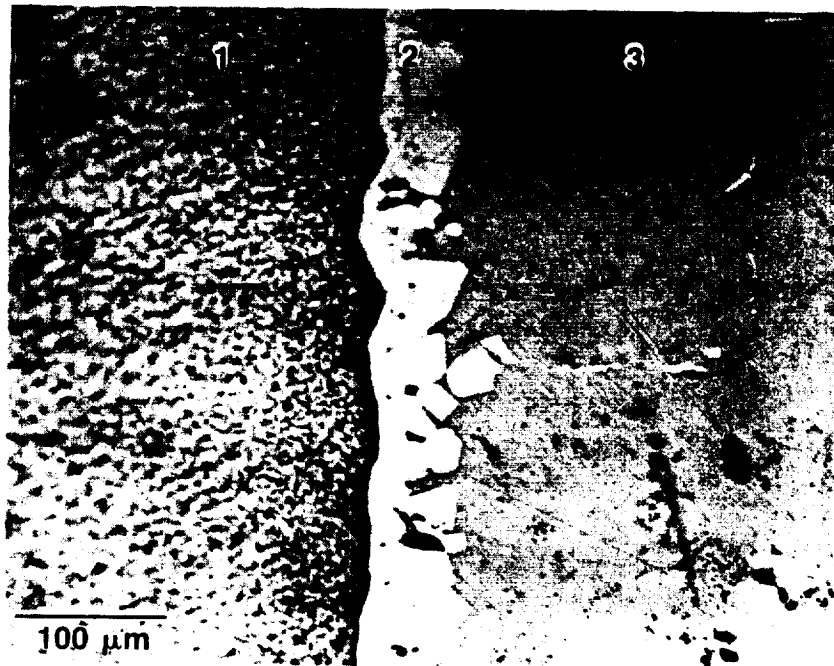


Figure 11. Metal/semiconductor interface region in a GaAs/WC-103 compatibility test carried out for 12 hours at 1260°C. 1 = metal, 2 = interface/reaction zone and 3 = semiconductor.

24 hour GaAs/WC-103

The 24 hour GaAs/WC-103 couple showed a very severe reaction at the metal/semiconductor interface, as can be seen in Figure 12. It is obvious in this micrograph that reaction products formed at the interface between the metal and semiconductor and then broke off and floated into the adjacent molten semiconductor.

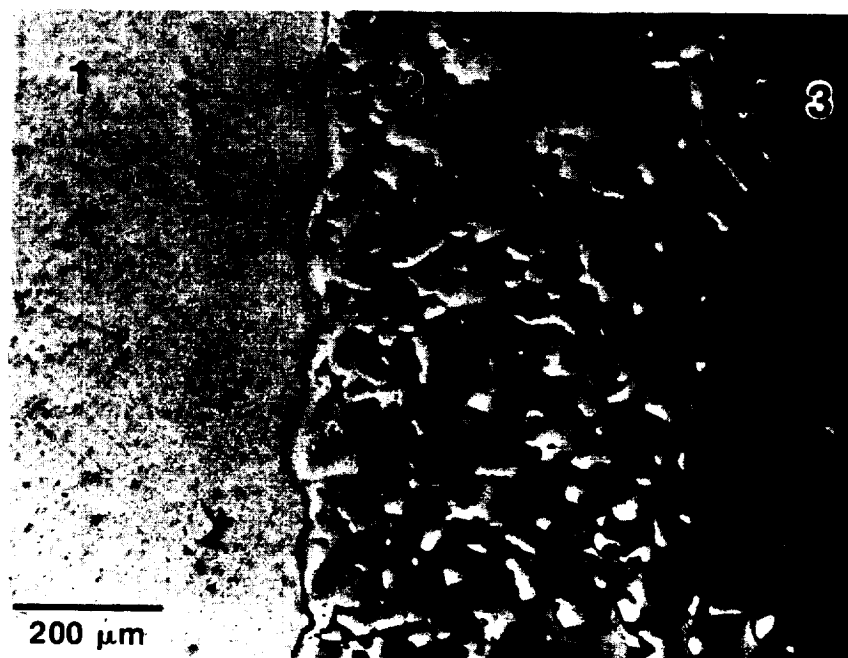


Figure 12. Metal/semiconductor interface region in a GaAs/WC-103 compatibility test carried out for 24 hours at 1260°C. 1 = metal, 2 = interface/reaction zone, and 3 = semiconductor.

The SEM/EDS analysis confirms this observation (Figures A5 and A6 in Appendix A). For example, points 4, 6, and 7 on Figure A6 indicate a mixture of metal and semiconductor in the reaction products which were not adherent to the metal surface.

In this couple, a reduction in metal thickness of 0.17 mm or 6.69 mils. was observed. In a 27 mil thick metal sample, this would result in a 25% reduction in thickness.

Summary - GaAs/WC-103

In all GaAs runs there was a measurable amount of metal loss due to interaction between the metal coupon and semiconductor. The average metal loss for the various times averaged at several locations along the sample are summarized in Table II.

Table II

Time at Temperature	Average Thickness of Metal Lost mm (mils)
6 hours	0.07 (2.76)
12 hours	0.08 (3.15)
24 hours	0.17 (6.69)

Figure 13 shows a plot of the average thickness of metal lost as a function of time at temperature. Metal loss due to the formation of a non adherent reaction layer is expected to exhibit a linear relationship with time. Although there is limited data, there does appear to be a linear relationship between metal lost and time at temperature for this metal/semiconductor combination.

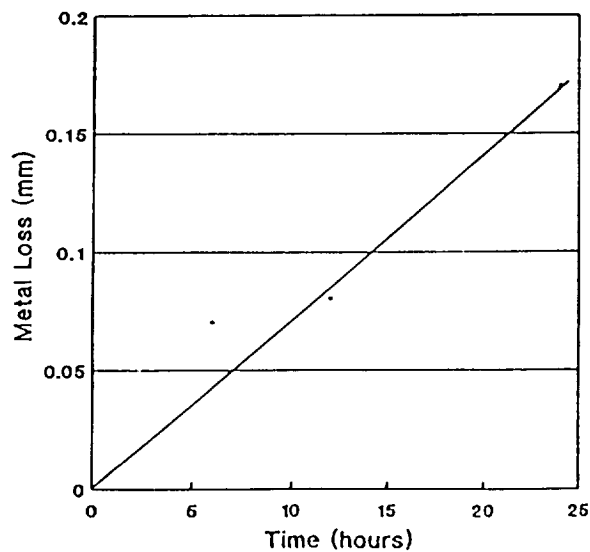


Figure 13. Average thickness of metal lost as a function of time for GaAs/WC-103 couples tested at 1260°C.

In summary, in the region adjacent to the metal surface, an appreciable reaction was observed in all test samples. The metal was severely attacked and the reaction products formed were observed to break off and float into the surrounding semiconductor. Using the 24 hour run as the most severe test, our results indicate that on a 27 mil thick WC-103 sample, an average of 6.69 mils (25% of the thickness) may be lost if the metal and molten semiconductor are held in contact for 24 hours at 1260°C.

CdZnTe/WC-103 Compatibility Tests

Two CdZnTe/WC-103 compatibility tests have been completed. These runs were for 12, 24, and 90 hours at 1170°C. The results of these tests are presented below:

24 hour CdZnTe/WC-103

A cross-section of the 24 hour CdZnTe/WC-103 couple is shown in Figure 14. This macrograph shows the presence of a well defined reaction zone at the metal/semiconductor interface. Figure 15 indicates the presence of an adherent reaction zone.

The SEM/EDS analysis, shown in Figures A7 and A8 in Appendix A, verifies the well defined reaction zone at the metal/semiconductor interface. This reaction zone is a mixture of semiconductor and metal. This reaction zone, as stated above, was adherent and did not appear to break off into the semiconductor as was observed consistently with the GaAs/WC-103 reaction couples.

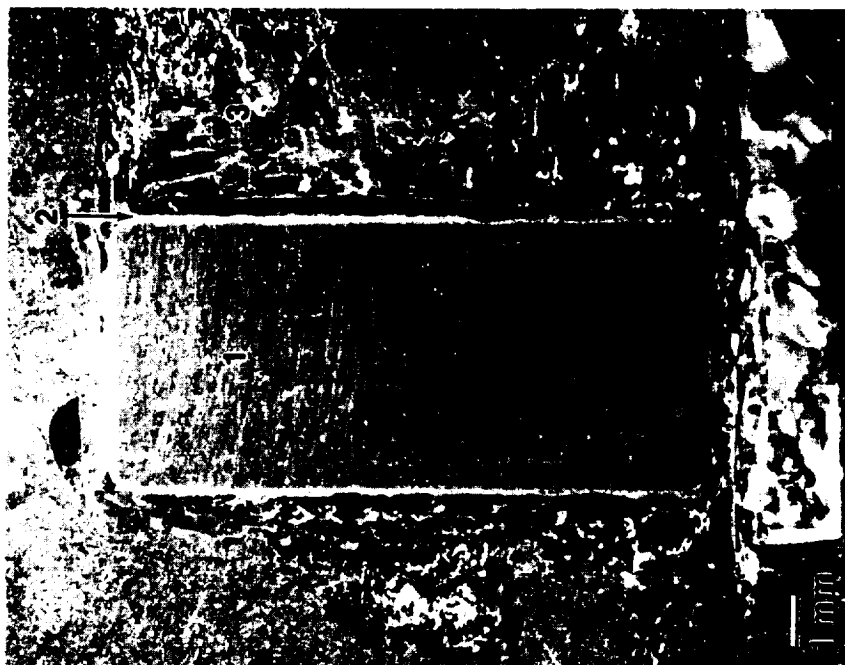


Figure 14. Cross section of a CdZnTe/WC-103 reaction couple after a 24 hour compatibility test at 1170°C.



Figure 15. Metal/semiconductor interface in a CdZnTe/WC-103 compatibility test carried out for 24 hours at 1170°C. 1 = metal, 2 = reaction/diffusion zone, and 3 = semiconductor.

The reaction zone was small, with a measured thickness of 0.062 mm (2.441 mils). This reaction zone did not appear to effect the integrity of the metal. In fact, there was no measurable reduction in the dimensions of the metal coupon.

90 Hour CdZnTe/WC-103

A photograph of a cross section and an optical micrograph of the reaction zone observed in the 90 hour CdZnTe/WC-103 run are shown in Figures 16 and 17, respectively. As seen in Figure 17, a well defined reaction layer was formed. The reaction layer was approximately 0.112 mm or 4.409 mils thick. As in the 24 hour run, the reaction or diffusion layer formed did not affect the integrity of the metal or change its dimensions to any measurable degree. (If anything, it appeared as if the thickness of the metal had increased slightly.) The compositional analysis, which is shown in Figures A9 and A10 in Appendix A, likewise indicates the presence of an adherent reaction zone at the metal/semiconductor interface.

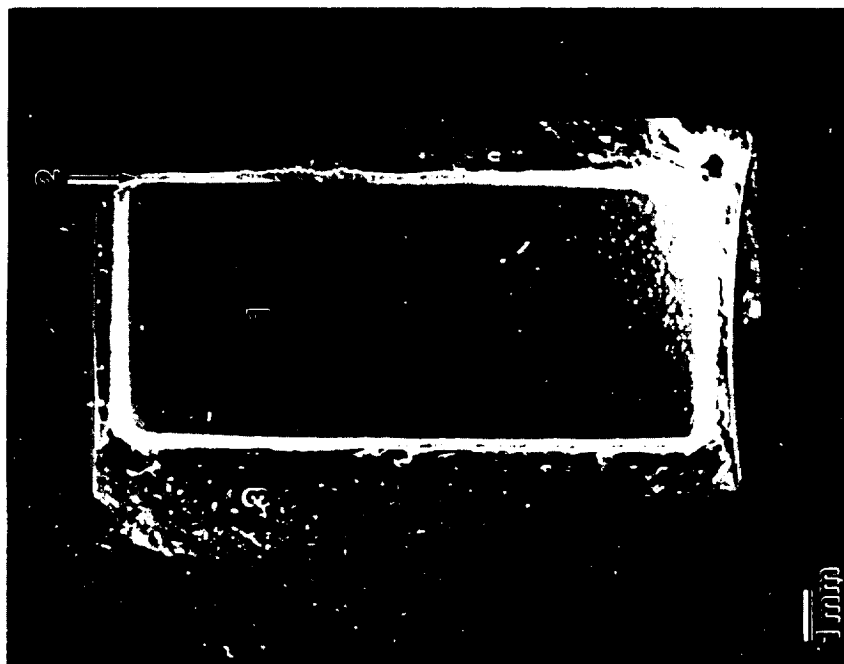


Figure 16. Cross section of a GaAs/WC-103 reaction couple after a 90 hour compatibility test at 1260°C.



Figure 17. Metal/semiconductor interface in a CdZnTe/WC-103 compatibility test carried out for 90 hours at 1170°C. 1 = metal, 2 = reaction/diffusion zone, and 3 = semiconductor.

Summary - CdZnTe/WC-103

Table III summarizes the average reaction zone thickness observed for the CdZnTe/WC-103 runs completed to date.

Table III

Time at Temperature	Average Reaction Zone Thickness mm (mils)
12 hours *	*
24 hours	0.062 (2.441)
90 hours	0.112 (4.409)

*To be completed

As seen in Table III, the reaction layer thickness for the 90 hour run is approximately twice the thickness obtained for the 24 hour run. These results are consistent with the anticipated kinetics for a diffusion controlled process where the reactants must diffuse through the reaction layer in order for the reaction to proceed. A plot of reaction zone thickness as a function of time $^{1/2}$ shows a nearly linear relationship (Figure 18). The composition of the reaction or diffusion zone is clearly seen to be a mixture of semiconductor and metal as evidenced by a compositional analysis in this region (Figure A10). Even though a measurable reaction layer was observed to form with this combination, any loss of metal was undetectable. As a result, the CdZnTe/WC-103 combination appears to be a workable solution to semiconductor containment in the event of an ampule failure.

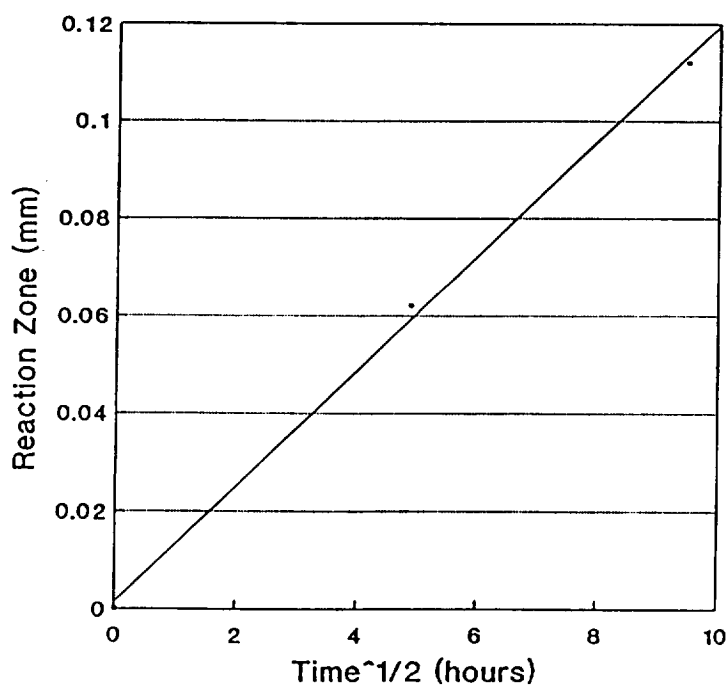


Figure 18. Reaction/diffusion zone thickness as a function of time $^{1/2}$ for CdZnTe/WC-103 reaction couples tested at 1170°C.

CdZnTe/TZM Compatibility Tests

One 90 hour run was completed for the CdZnTe/TZM compatibility tests. A cross section of the metal coupon is shown in Figure 19. From this macrograph, along with the micrograph shown in Figure 20, there does not appear to be any reaction or diffusion zone which is adherent to the semiconductor/metal interface. As seen in the micrographs, a "stringer" is observed in the semiconductor region a short distance from the interface. This stringer is approximately 0.023 mm (0.906 mils) thick and from the SEM/EDS data is seen to be Molybdenum rich. It is postulated that this stringer originated as a reaction layer at the metal/semiconductor interface and over time broke away and floated into the molten semiconductor. The stringer remained in tact and was observed on all sides of the metal coupon. The SEM/EDS analysis across the semiconductor/metal interface is shown in Figures A11 and A12 in Appendix A.

Results of the measurements on the metal coupon indicate no significant effect on the thickness or integrity of the metal.

Summary - CdZnTe/TZM

The CdZnTe/TZM couple, from a semiconductor/metal compatibility standpoint shows minimal reaction for 90 hours at 1170°C. There does not appear to be any significant reaction zone formed or any loss of metal thickness. Thus, from the compatibility tests conducted in this study, the CdZnTe/TZM combination is determined to be a suitable semiconductor/cartridge combination.

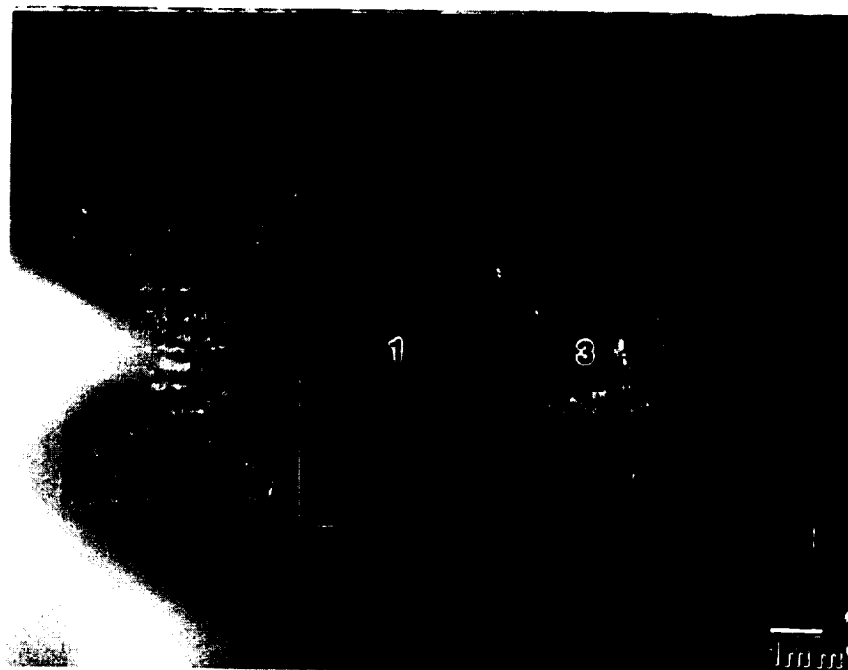


Figure 19. Cross section of a CdZnTe/TZM reaction couple after a 24 hour compatibility test at 1170°C.

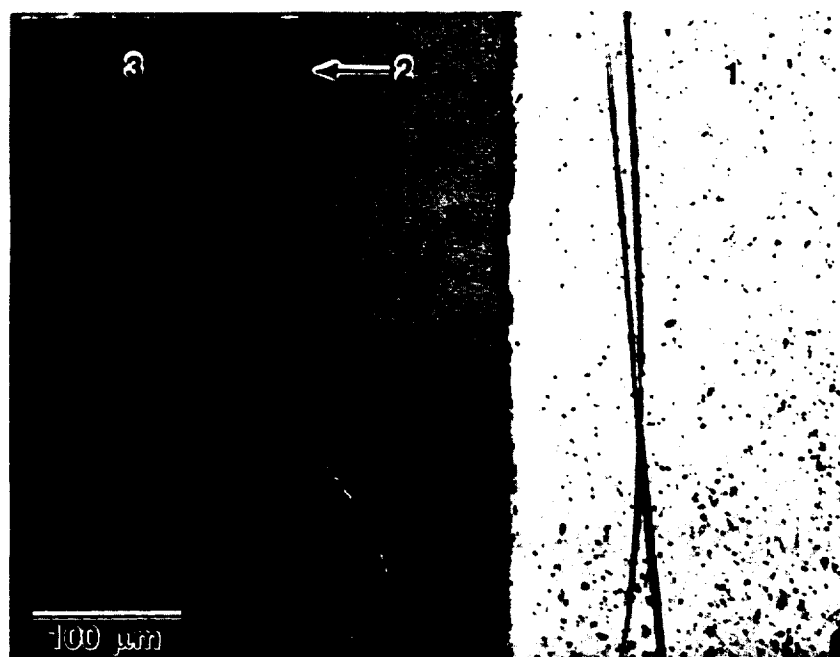


Figure 20. Metal/semiconductor interface in a CdZnTe/TZM compatibility test carried out for 24 hours at 1170°C. 1 = metal, 2 = "stringer", and 3 = semiconductor.

Conclusions

Based upon the results of the experiments conducted in this study, the following conclusions have been made:

1. There was a considerable reaction between the GaAs and the WC-103 couple for all three runs (6 hours, 12 hours, and 24 hours) at 1260°C. Reaction products formed at the metal/semiconductor interface and these products broke off and floated into the molten semiconductor. Metal loss ranged from 0.07 mm (2.76 mils) to 0.17 mm (6.69 mils) for the three runs. In the worst case situation, where the WC-103 was exposed to molten GaAs for 24 hours, it was determined that a 27 mil thick cartridge would undergo a 25% reduction in thickness.
2. In the CdZnTe/WC-103 reaction couples run at 24 and 90 hours at 1170°C, a reaction or diffusion zone was observed to form at the metal/semiconductor interface. This zone was adherent to the metal surface. The average thickness varied from 0.062 mm (2.441 mils) for the 24 hour run to 0.112 mm (4.409 mils) for the 90 hour run. There did not appear to be any significant loss of metal for either reaction couple.
3. The CdZnTe/TZM reaction couple run for 90 hours at 1170°C showed minimal reaction at the metal/semiconductor interface. There did not appear to be any measurable change in the dimensions of the metal in the couple.

Appendix A

**SEM and EDS analysis of GaAs/WC-103, CdZnTe/WC-103,
and CdZnTe/TZM reaction couples.**

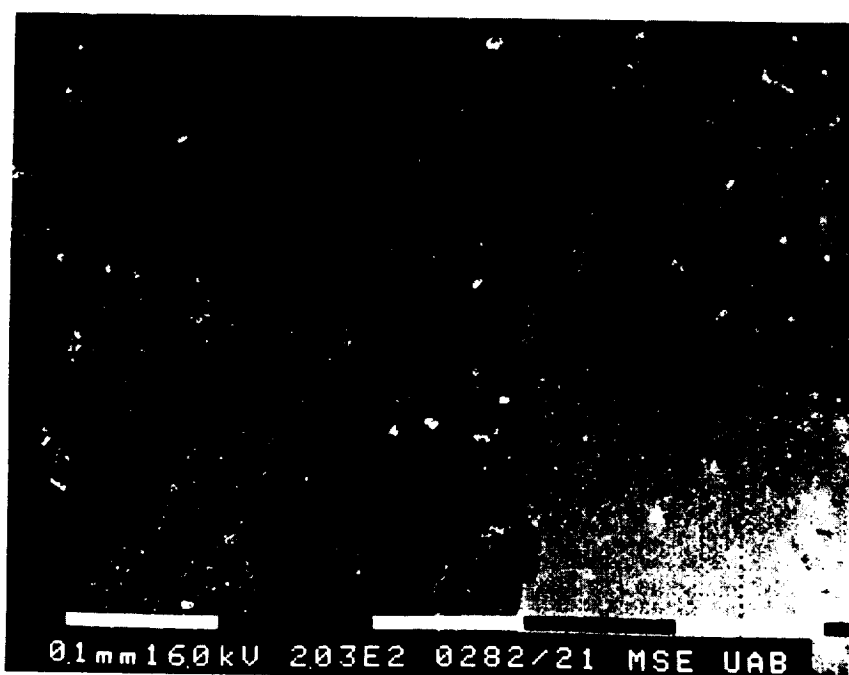
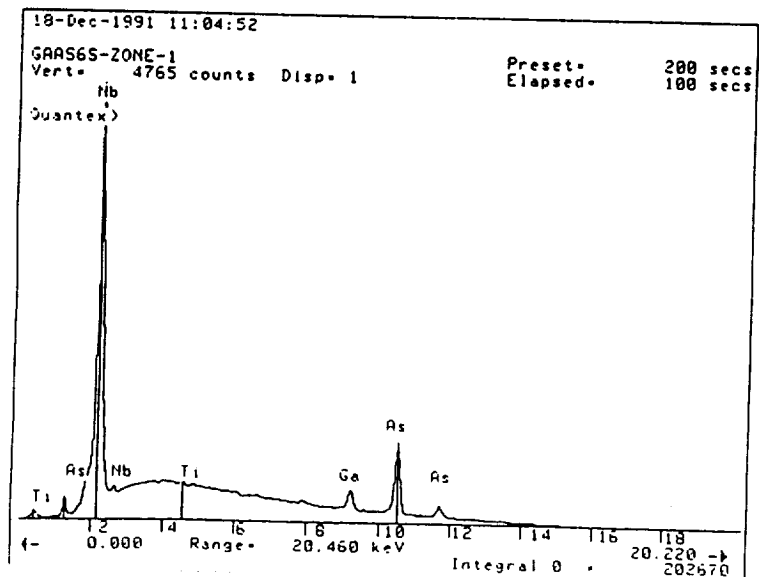
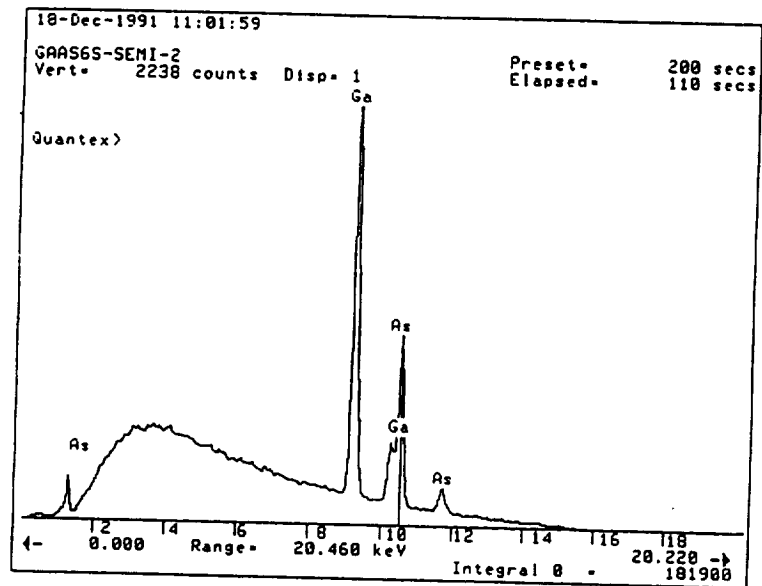
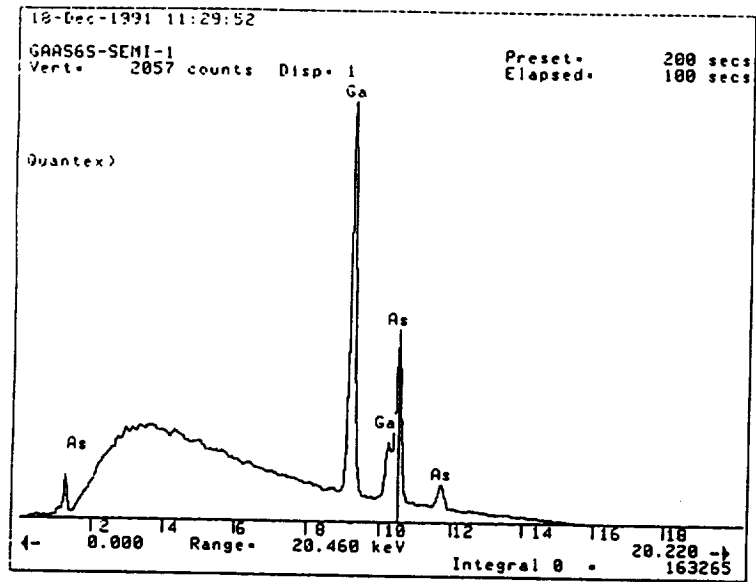
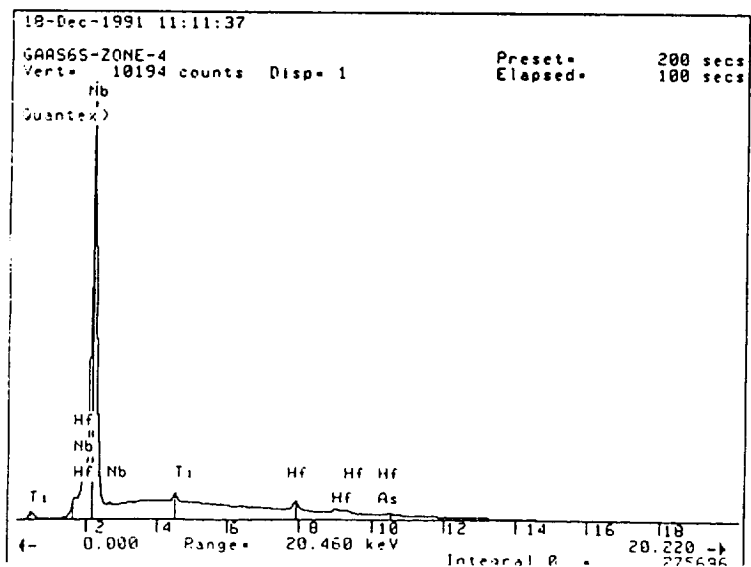
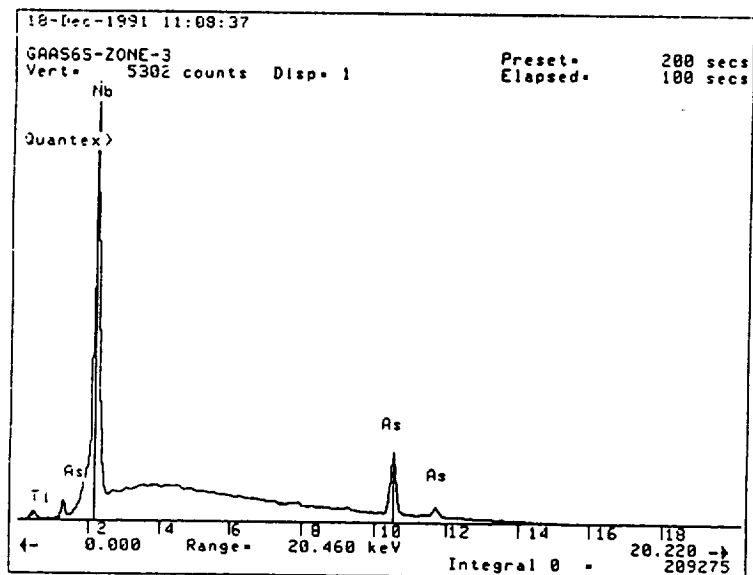
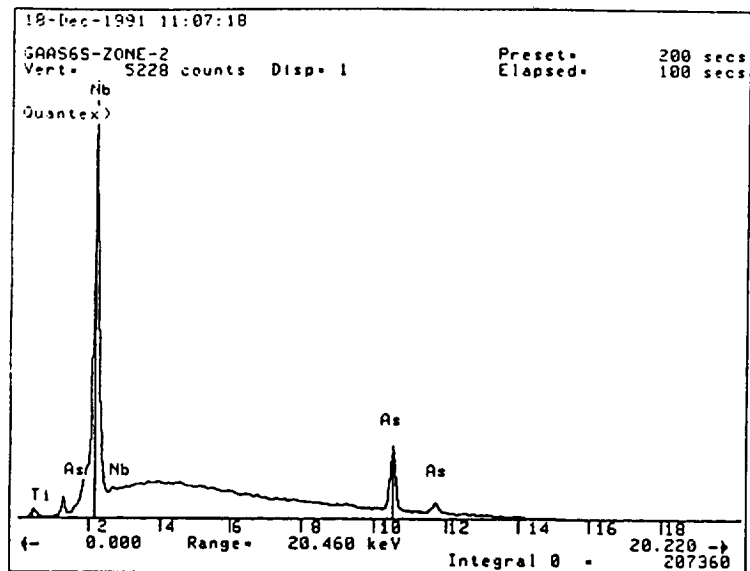


Figure A1. SEM micrograph of GaAs/WC-103 couple tested at 1260°C for 6 hours. Numbers indicate points where compositional analysis was performed.

Figure A2. Compositional spectra across the semiconductor/metal interface of a GaAs/WC-103 reaction couple tested at 1260°C for 6 hours.





C-2.

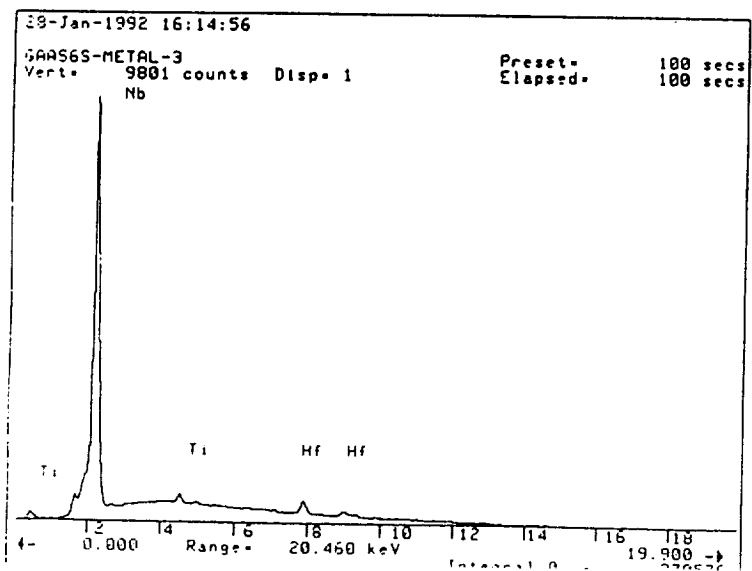
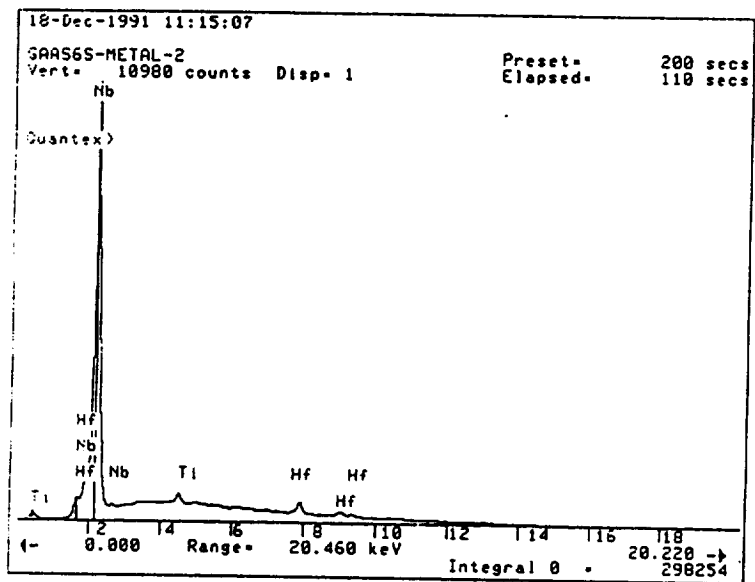
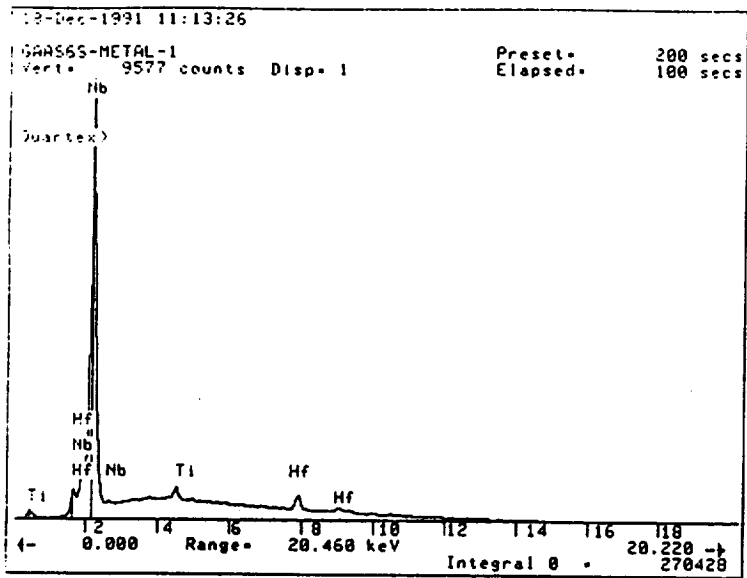
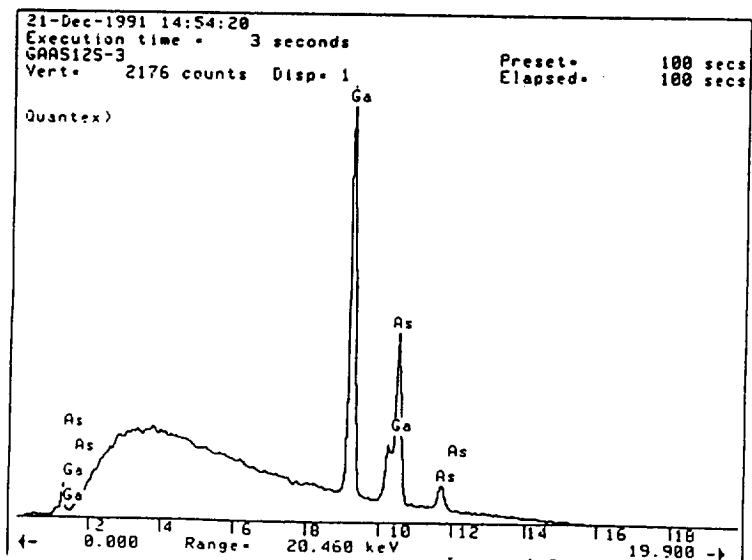
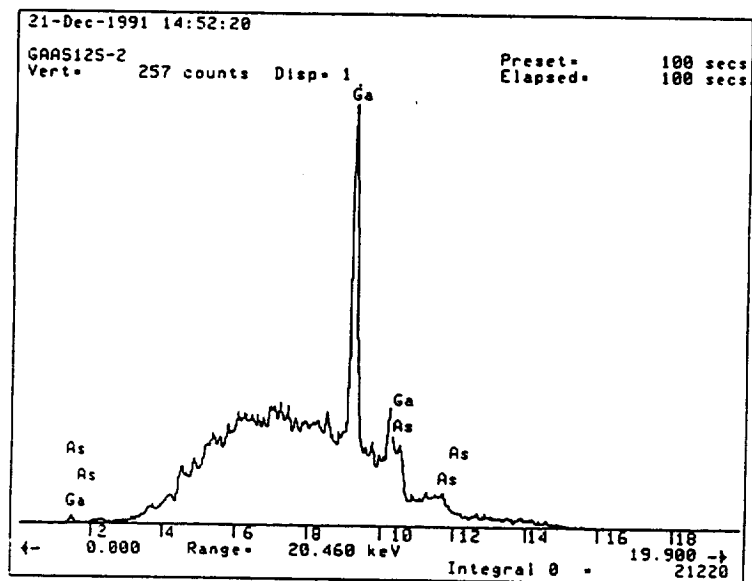
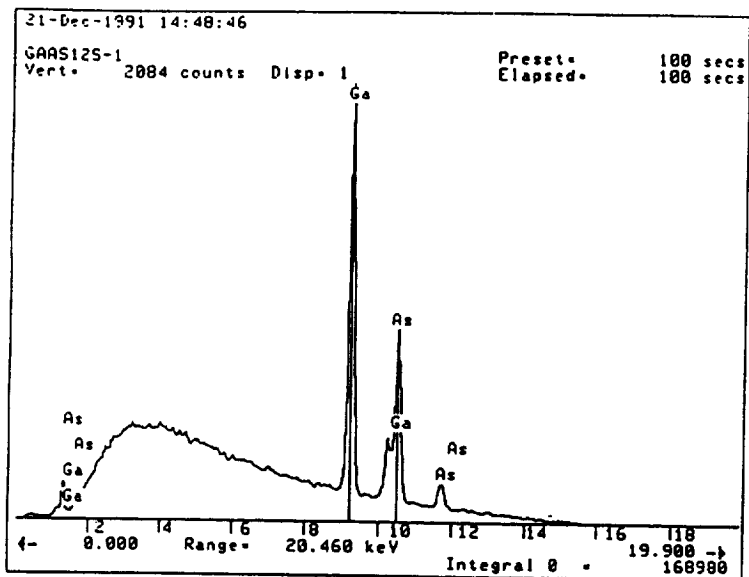
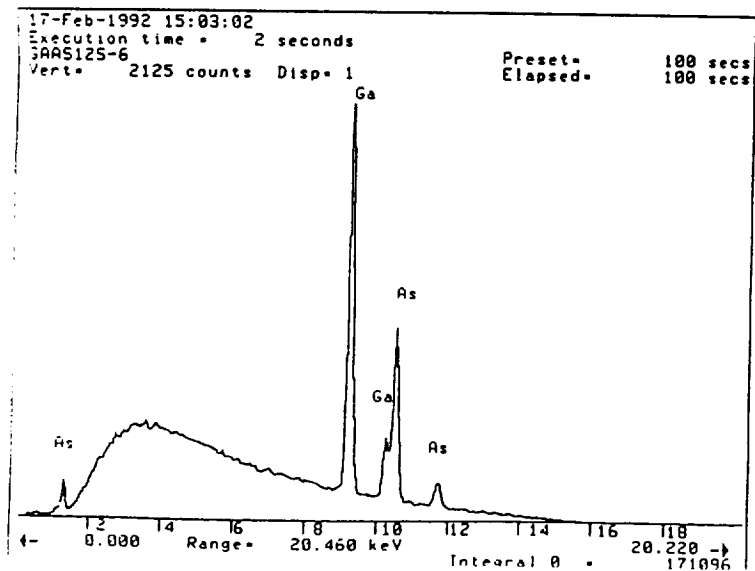
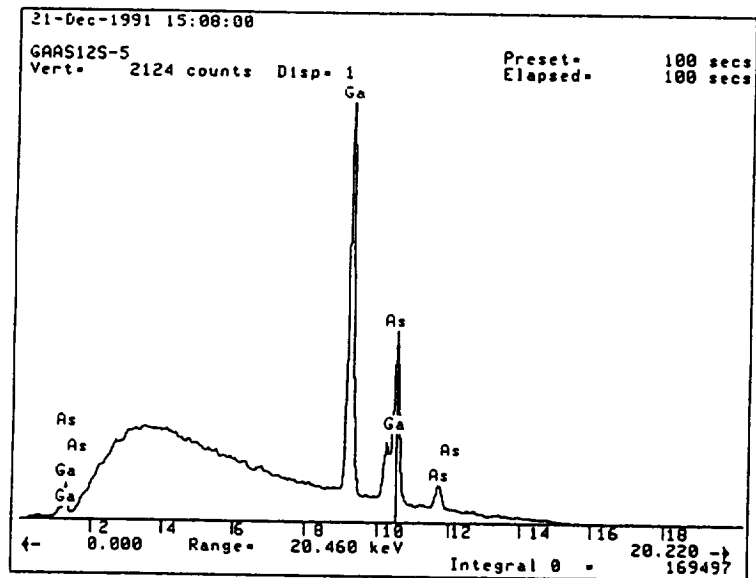
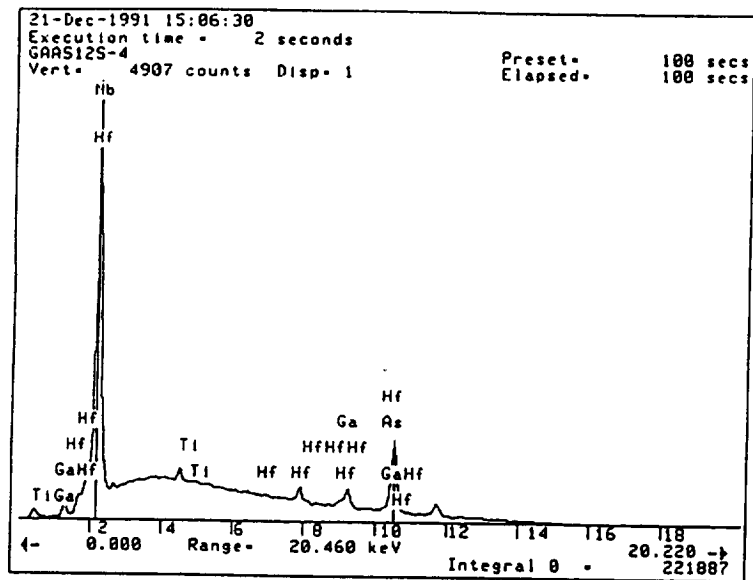


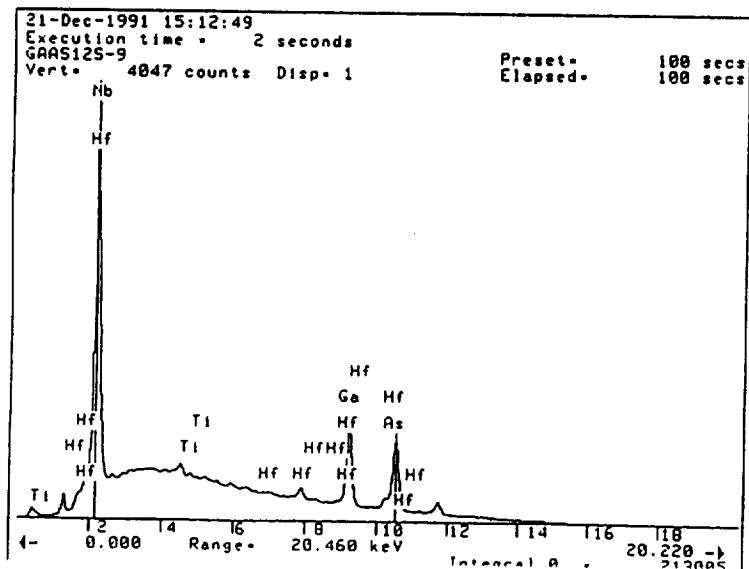
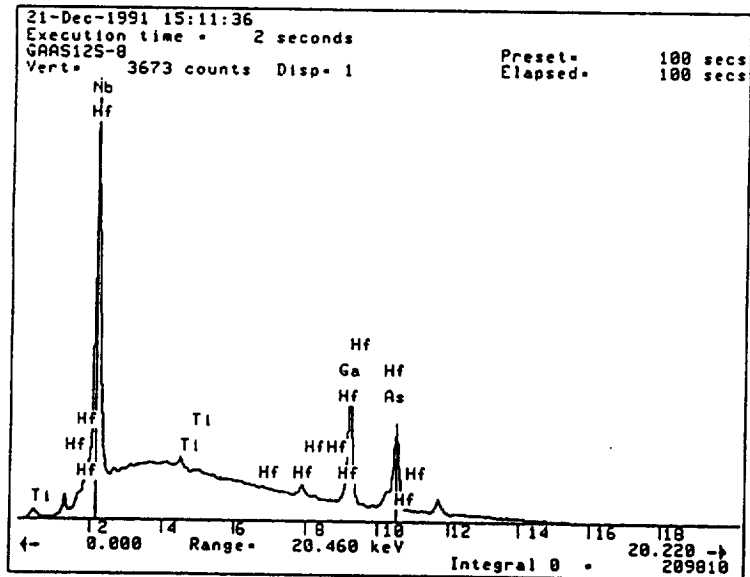
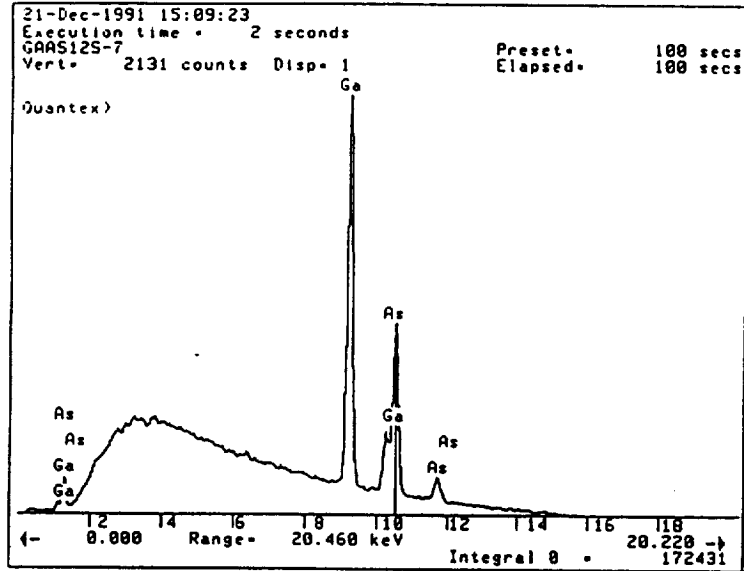


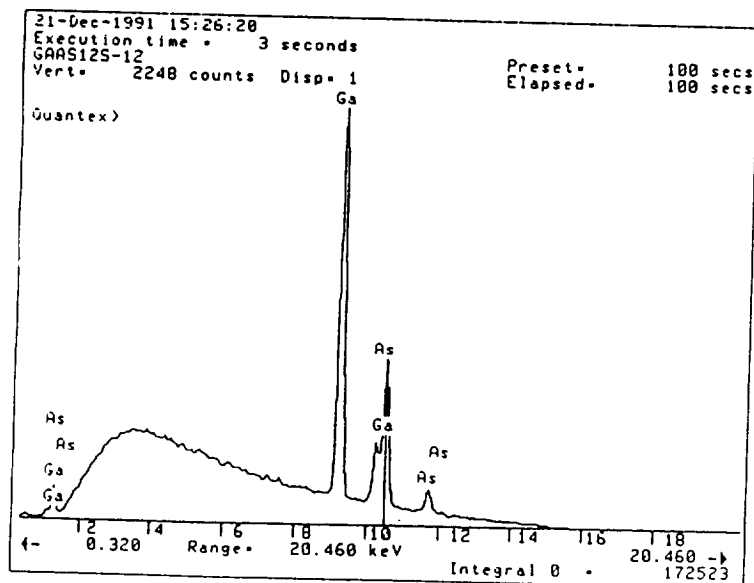
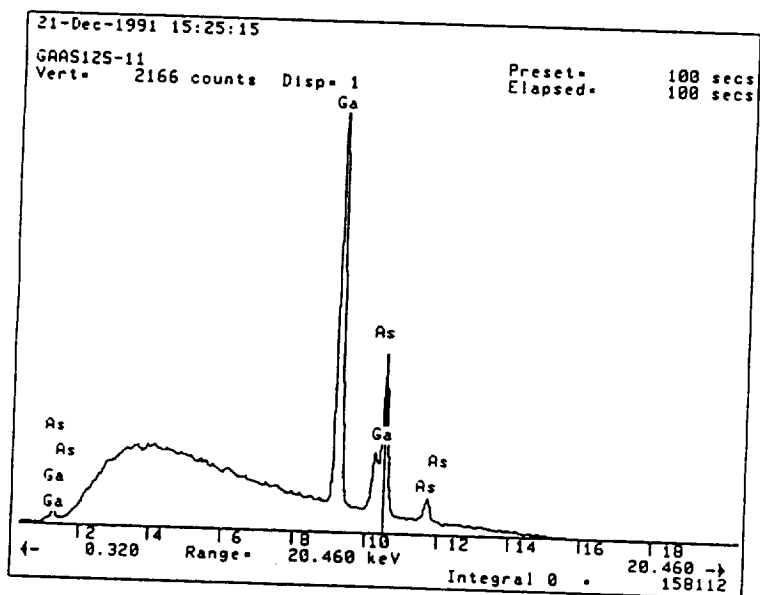
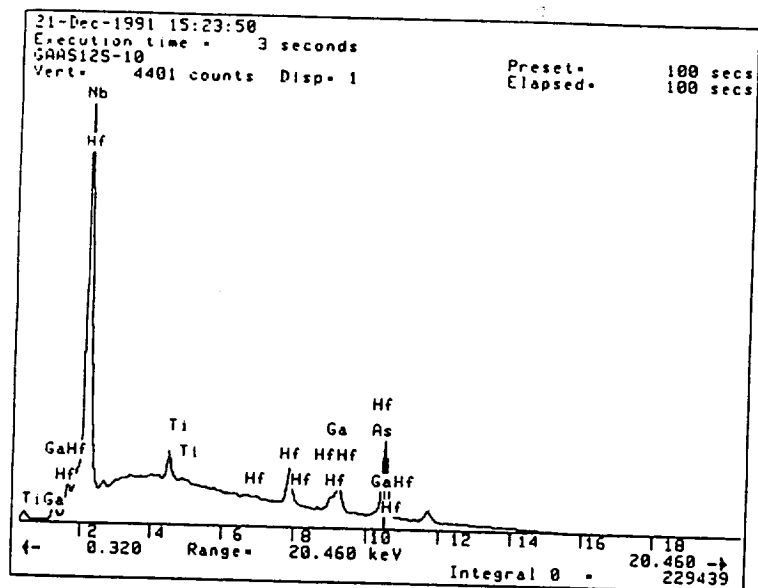
Figure A3. SEM micrograph of GaAs/WC-103 couple tested at 1260°C for 12 hours. Numbers indicate points where compositional analysis was performed.

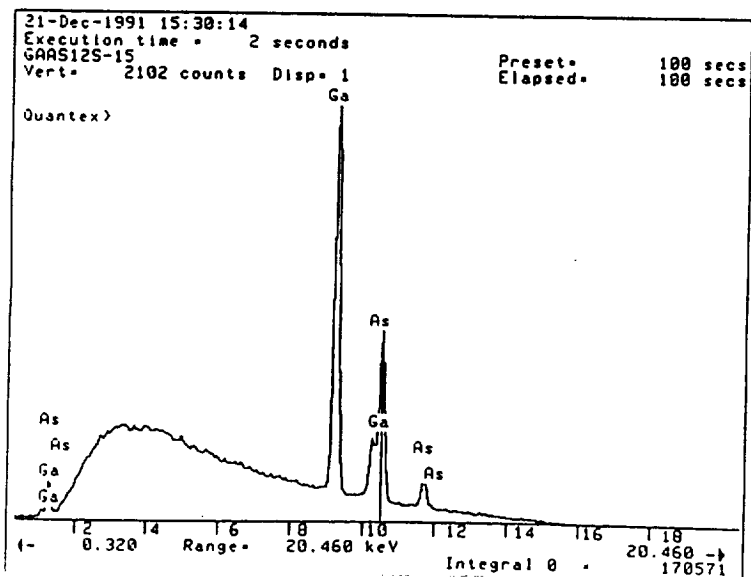
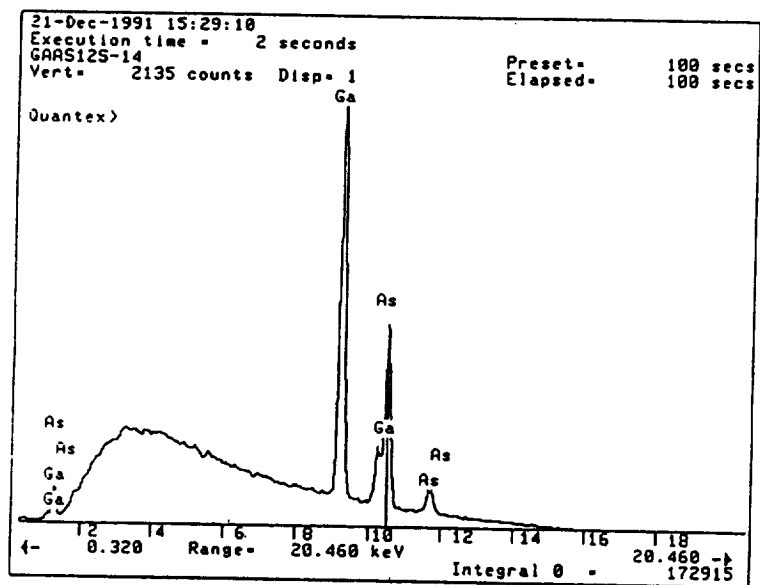
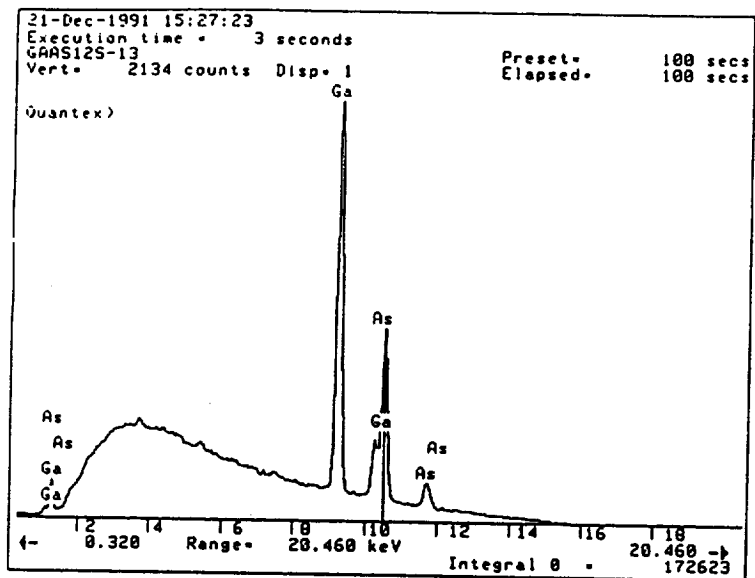
Figure A4. Compositional spectra across the semiconductor/metal interface of a GaAs/WC-103 reaction couple tested at 1260°C for 12 hours.

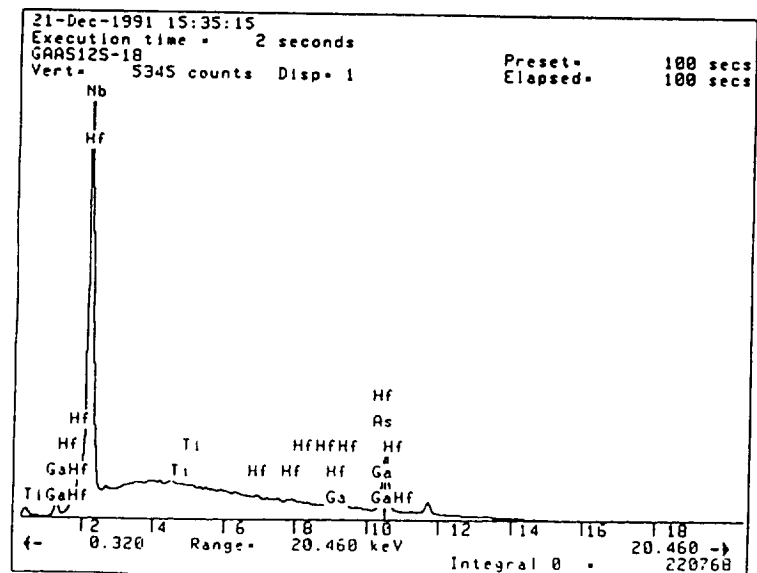
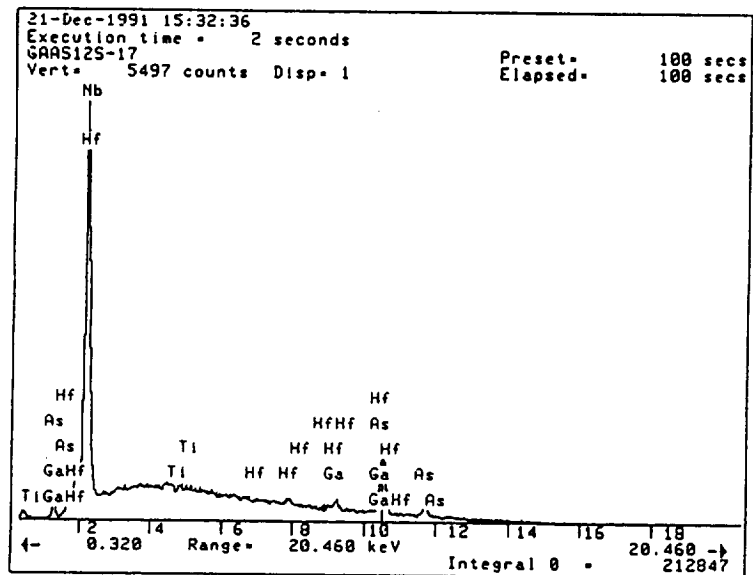
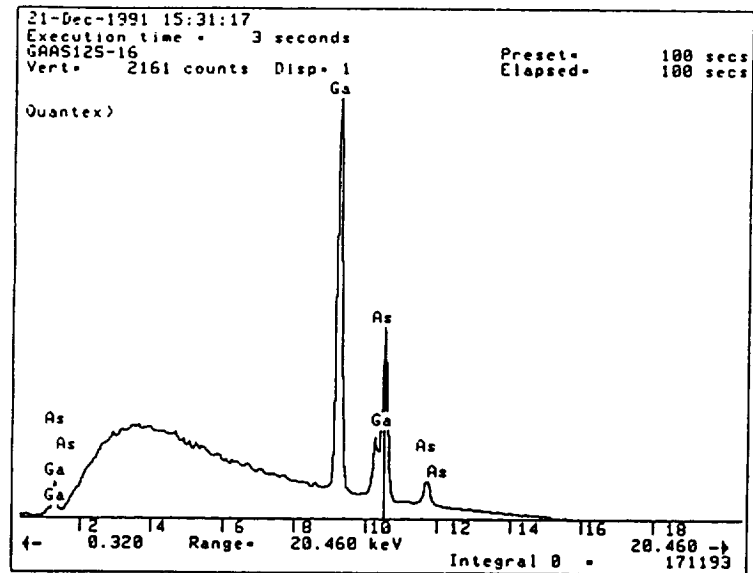


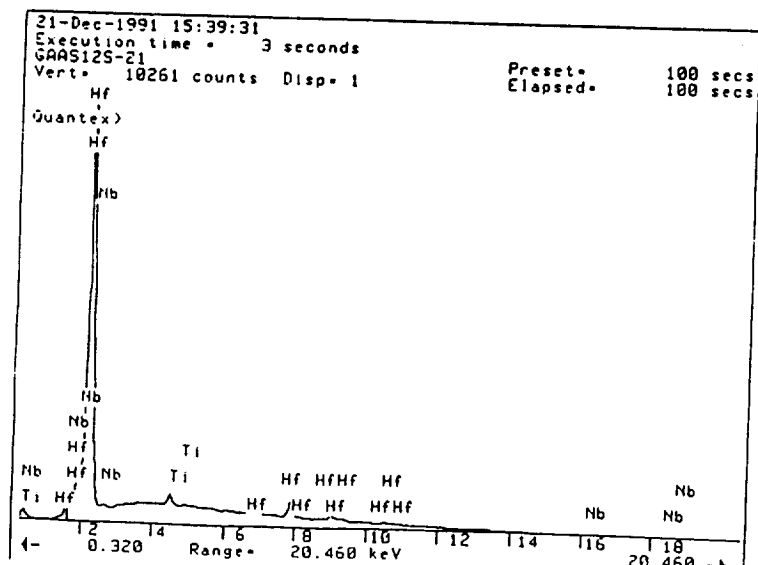
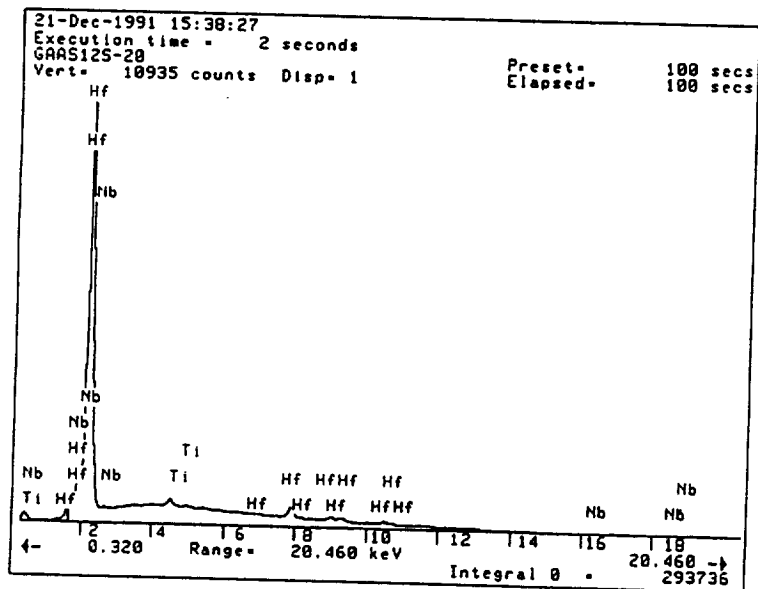
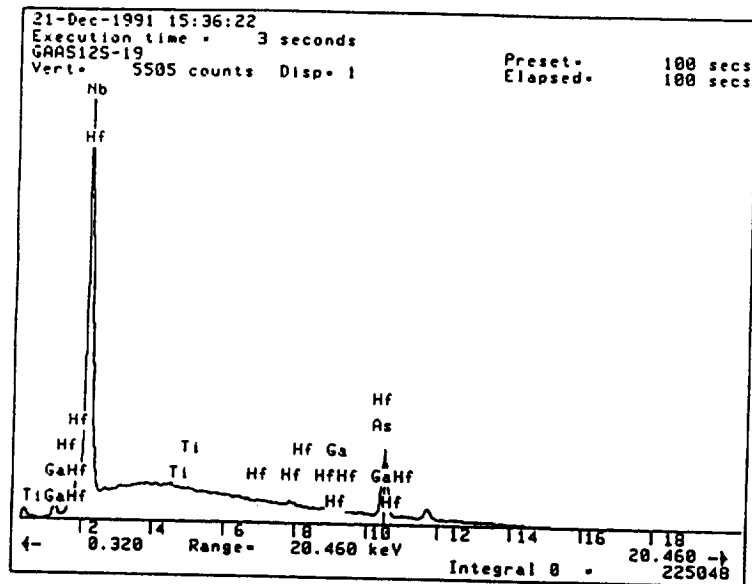












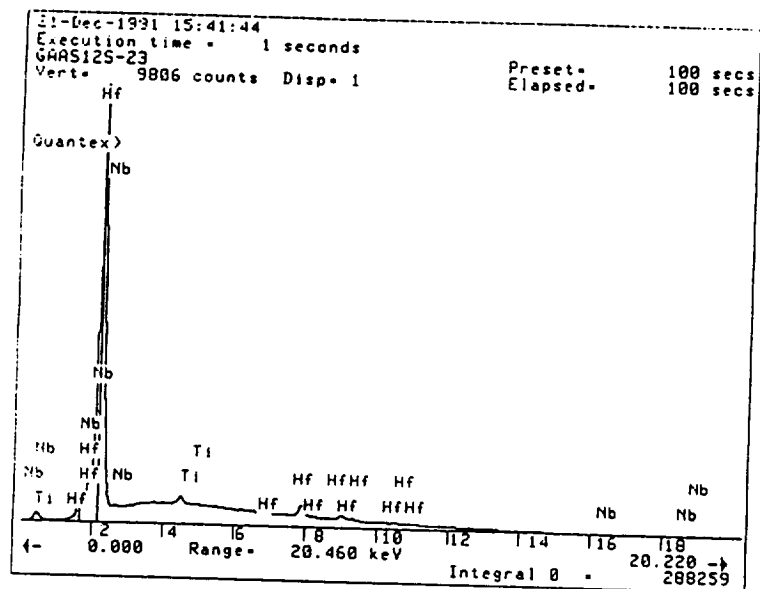
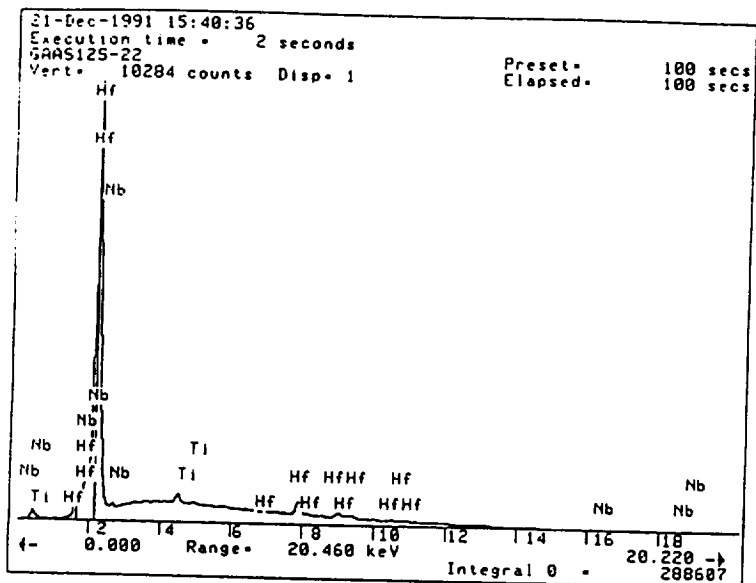
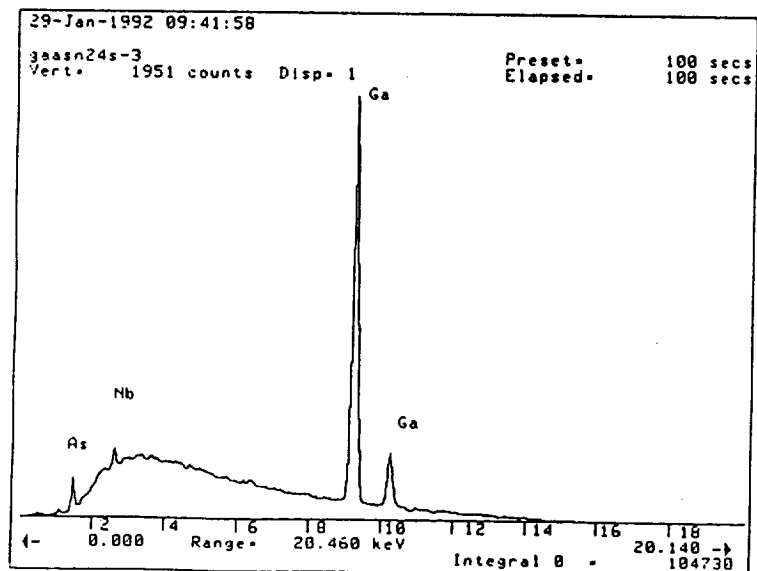
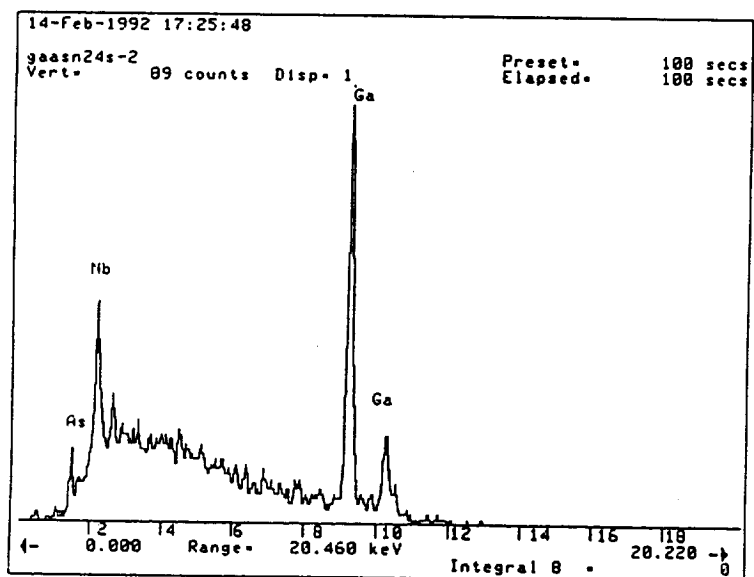
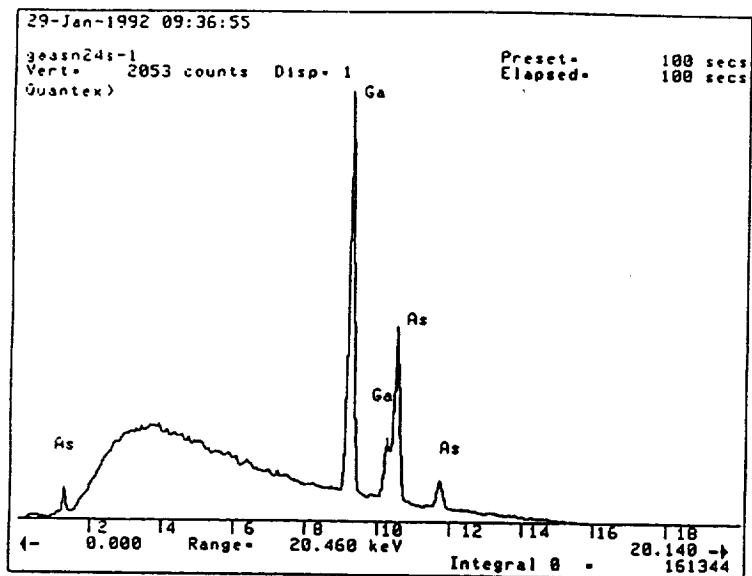
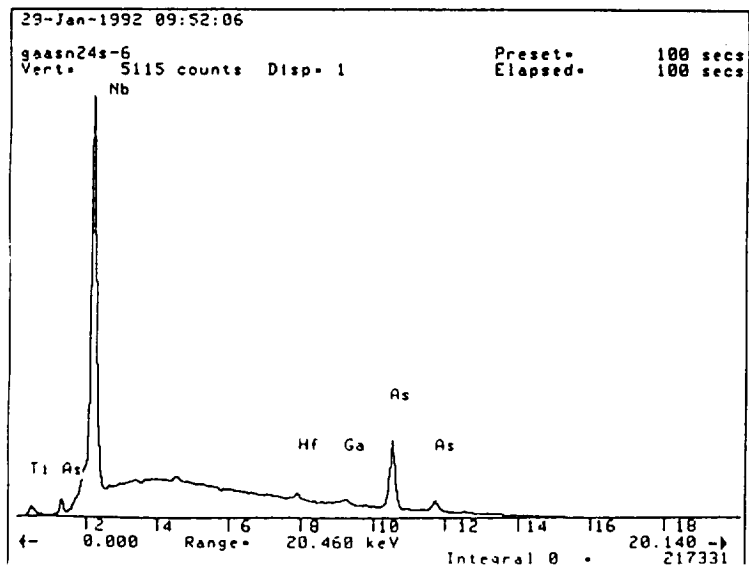
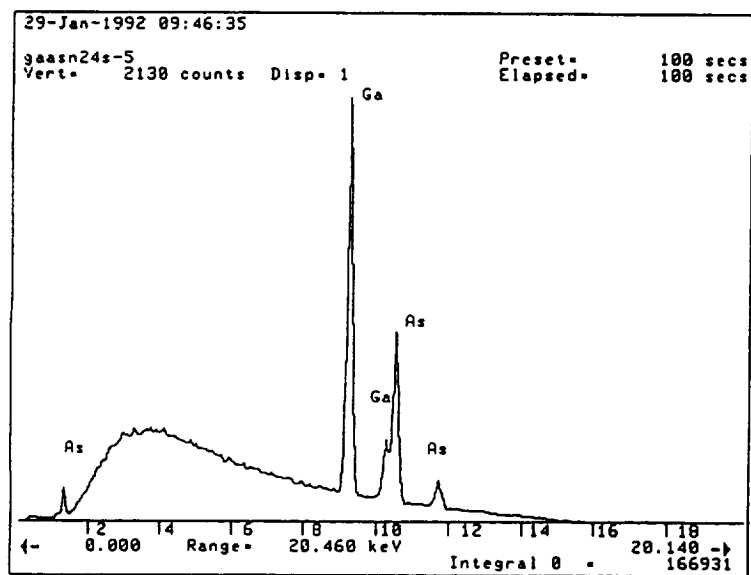
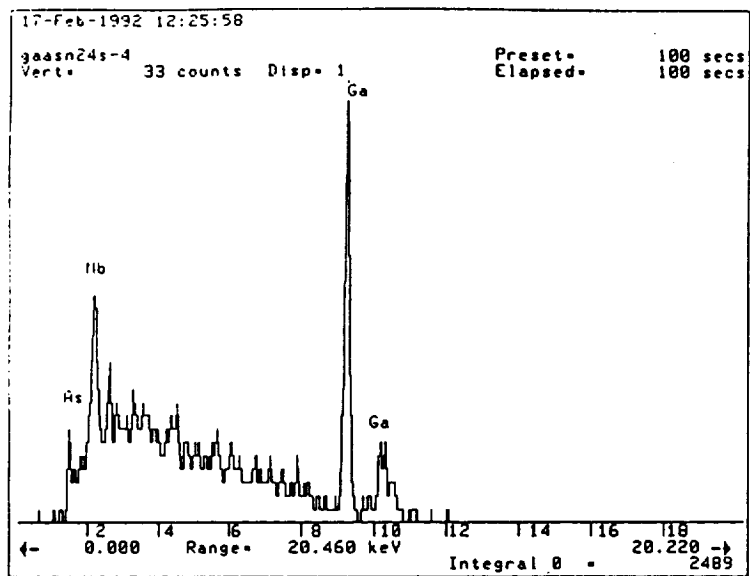


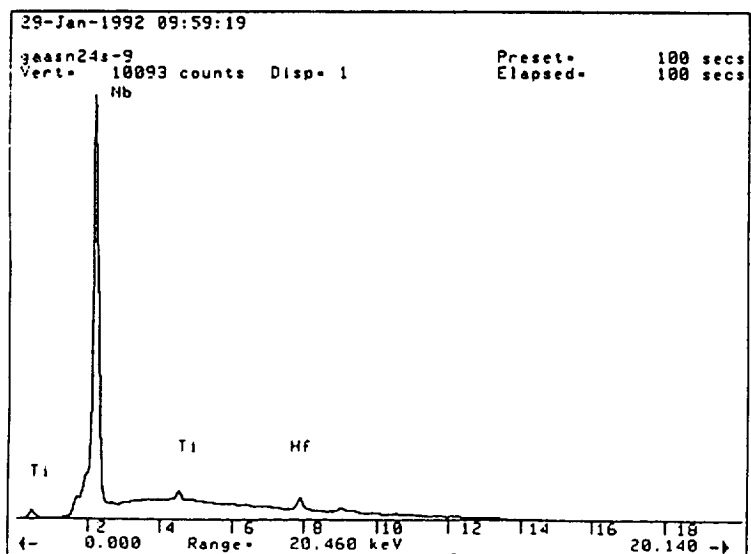
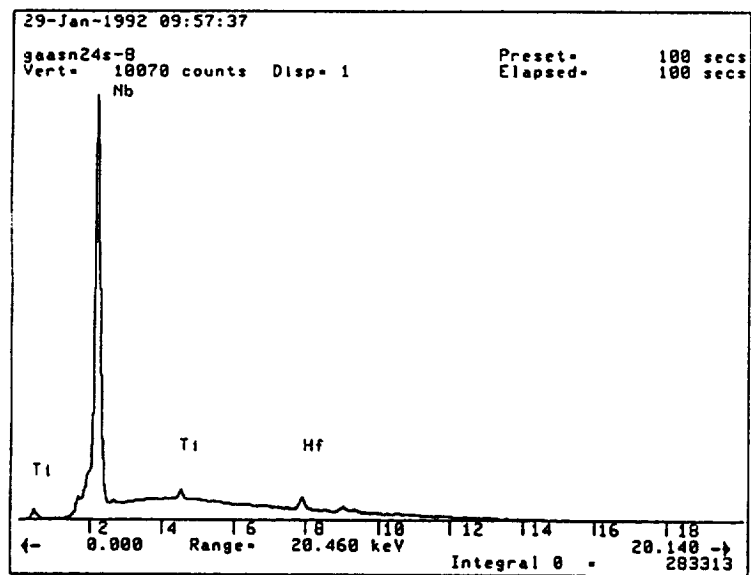
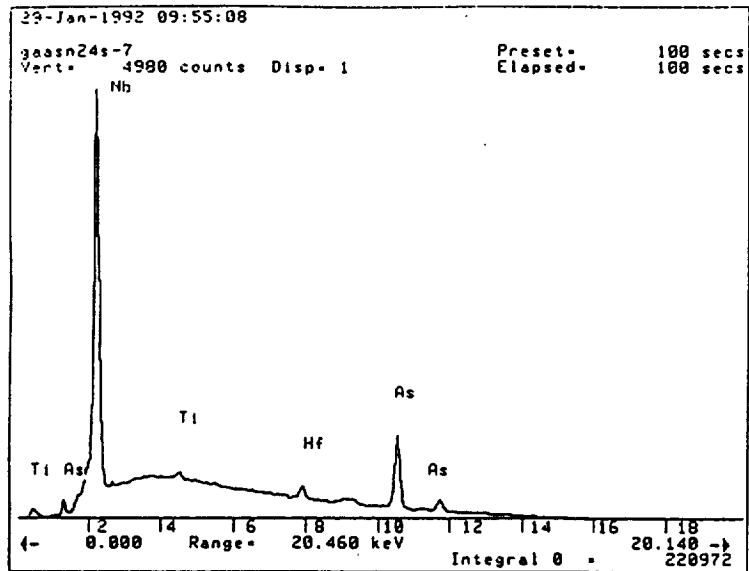


Figure A5. SEM micrograph of GaAs/WC-103 couple tested at 1260°C for 24 hours. Numbers indicate points where compositional analysis was performed.

Figure A6. Compositional spectra across the semiconductor/metal interface of a GaAs/WC-103 reaction couple tested at 1260°C for 24 hours.







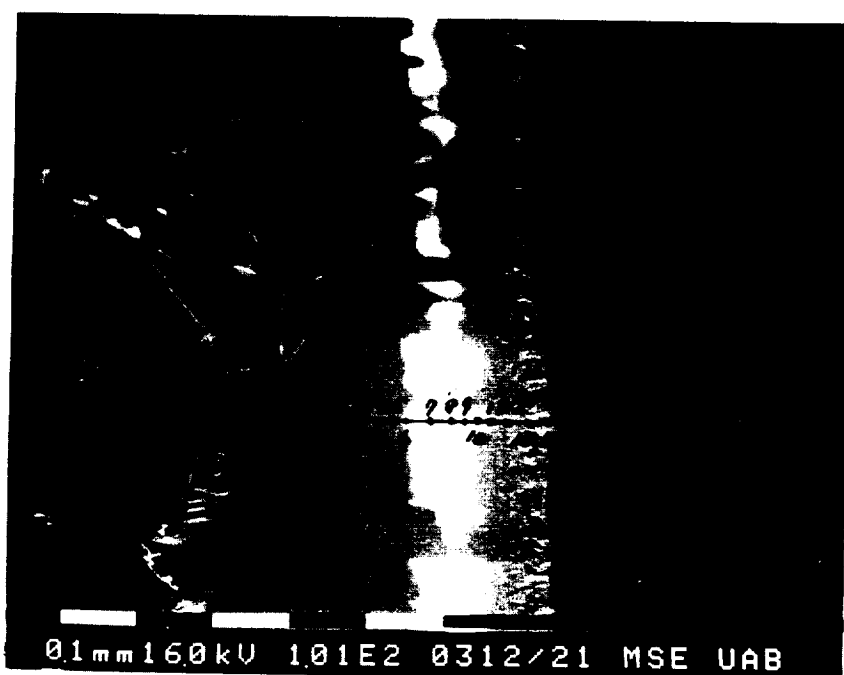
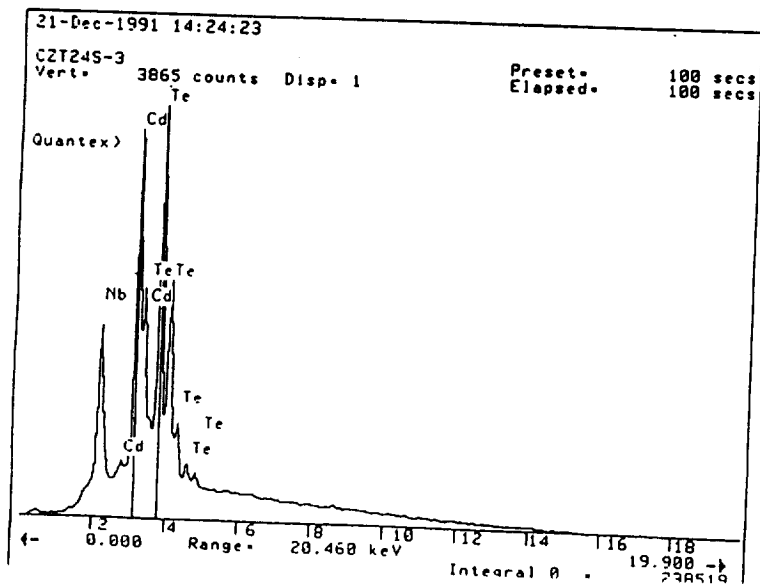
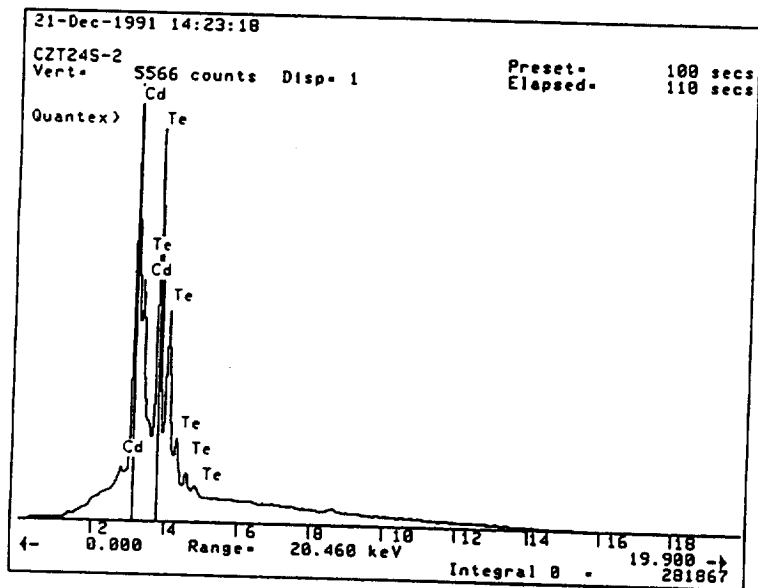
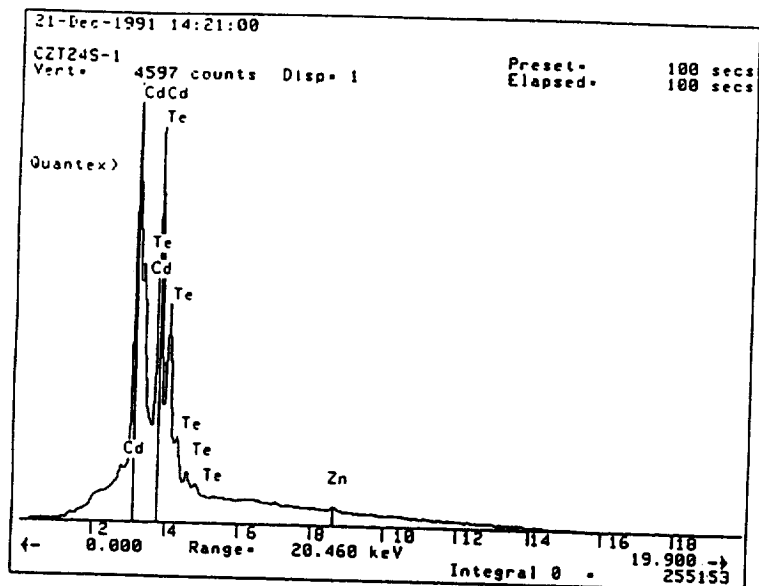
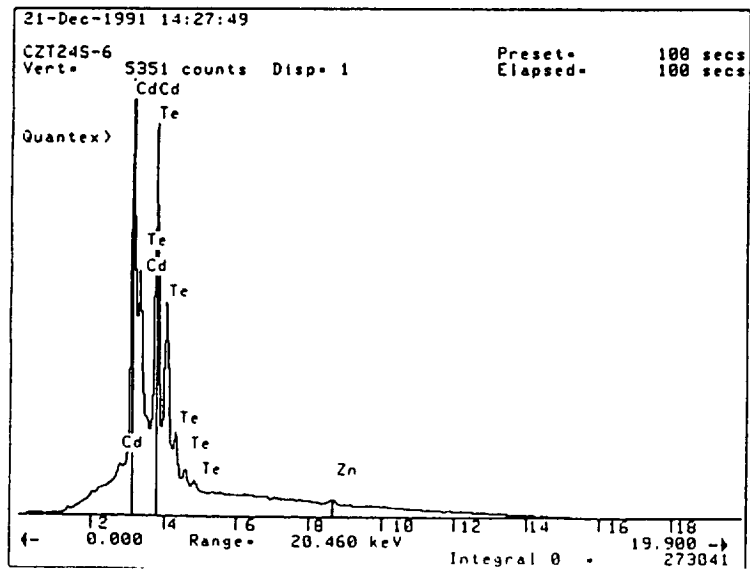
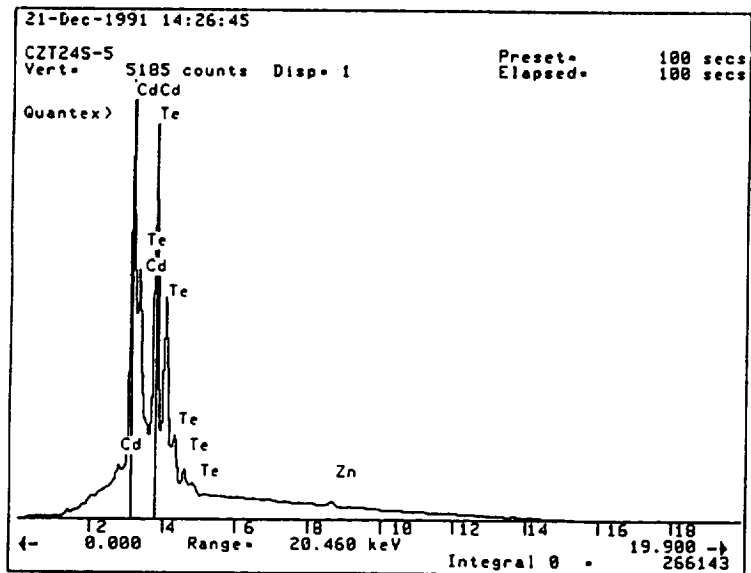
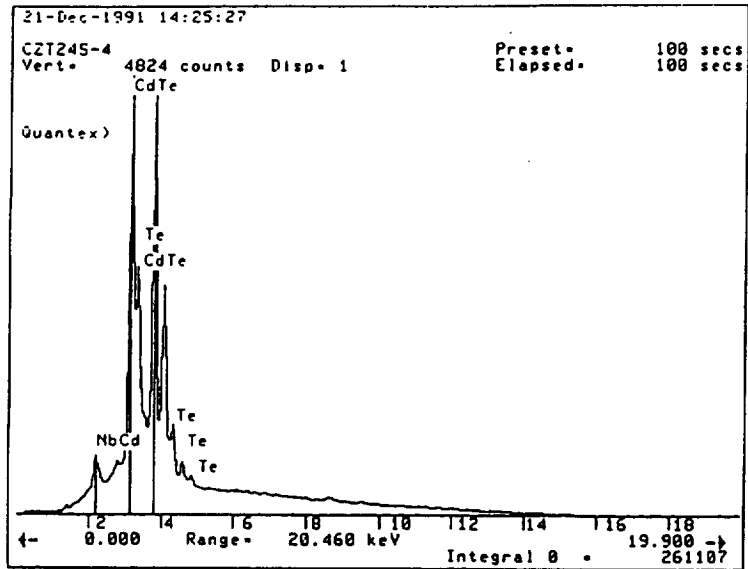
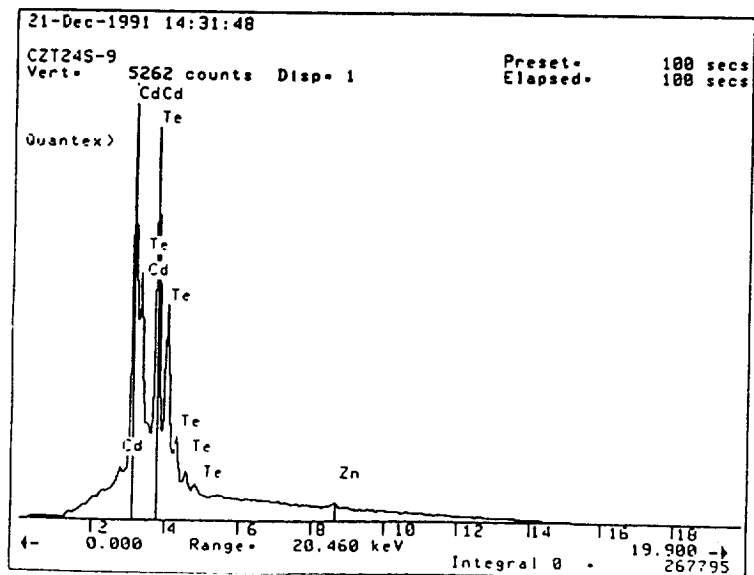
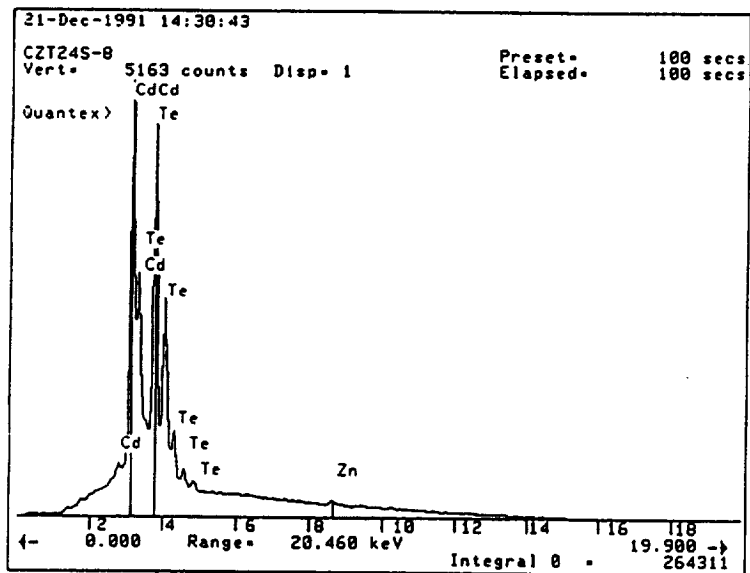
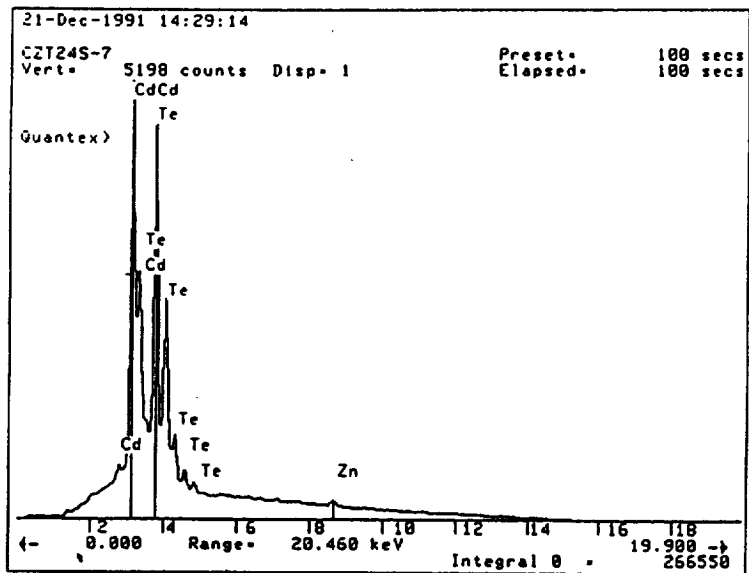


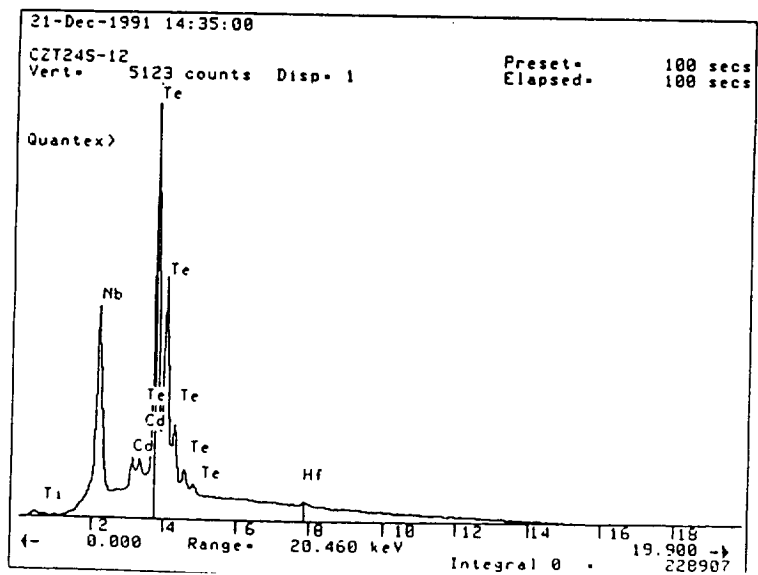
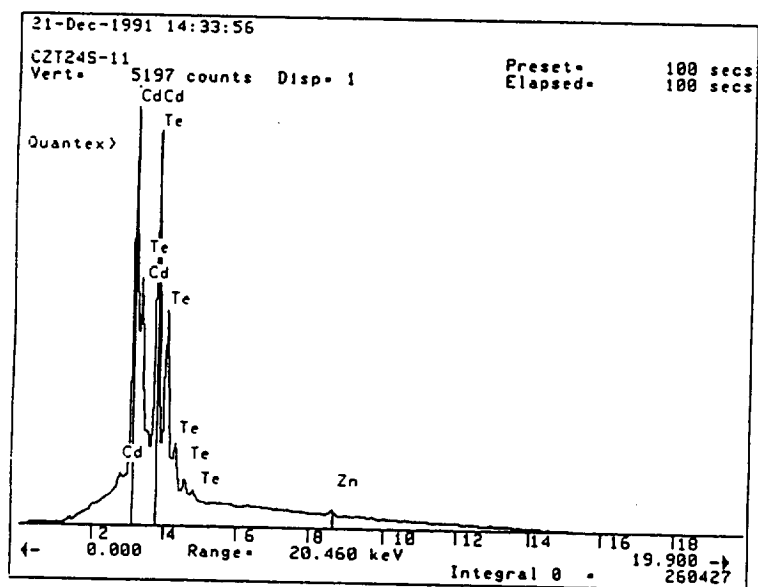
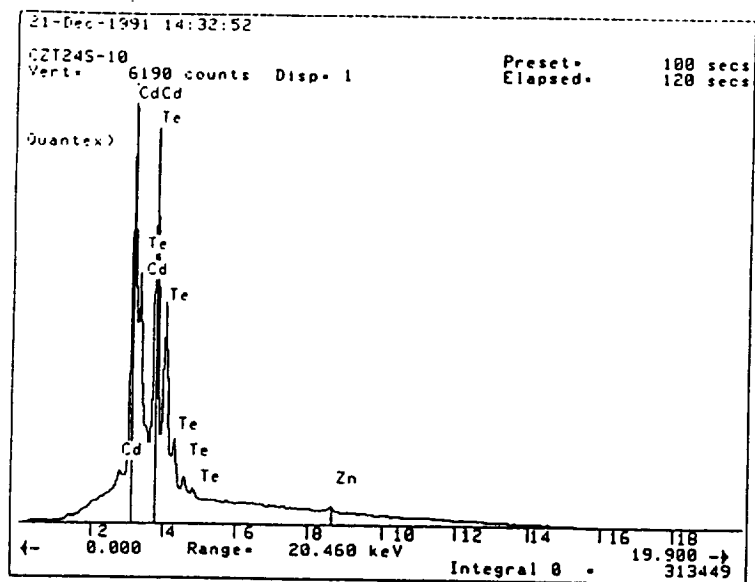
Figure A7. SEM micrograph of CdZnTe/WC-103 couple tested at 1170°C for 24 hours. Numbers indicate points where compositional analysis was performed.

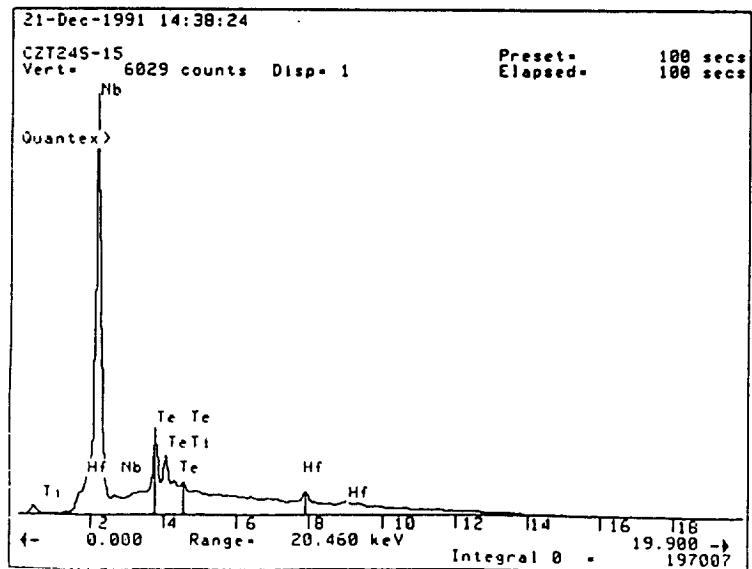
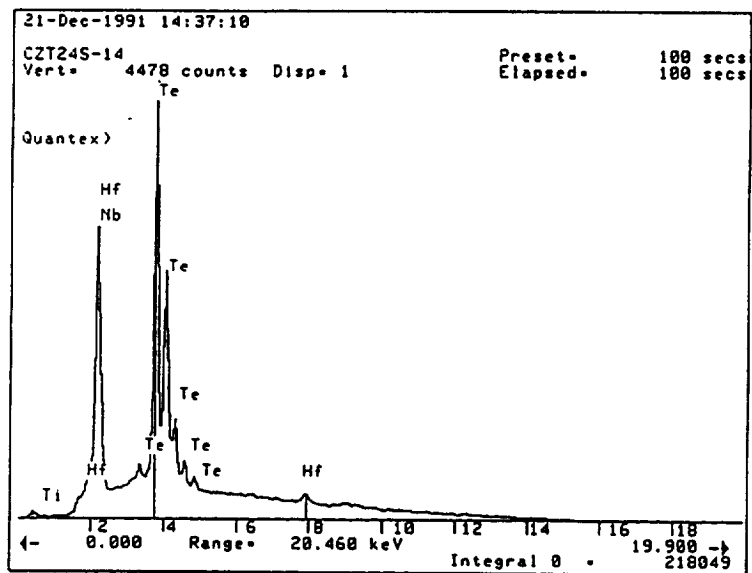
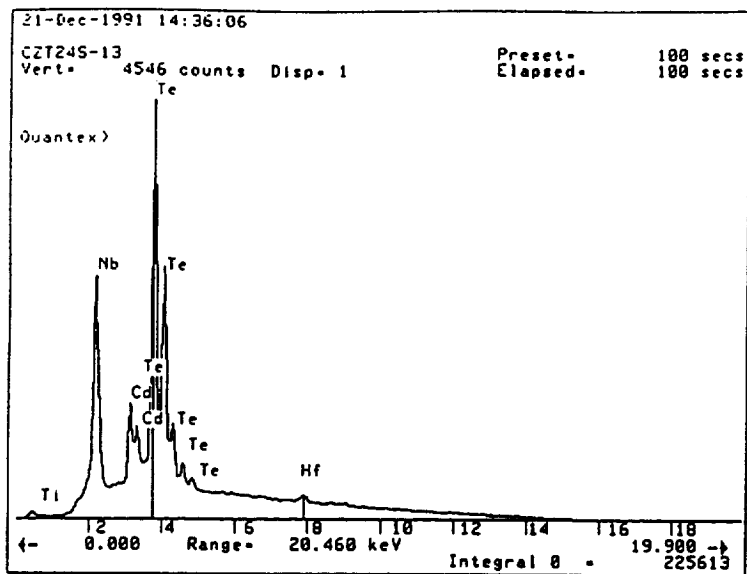
Figure A8. Compositional spectra across the semiconductor/metal interface of a CdZnTe/WC-103 reaction couple tested at 1170°C for 24 hours.

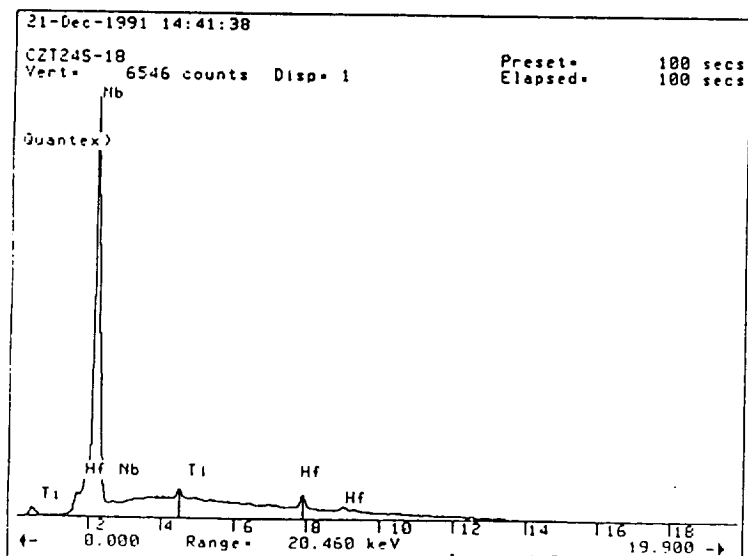
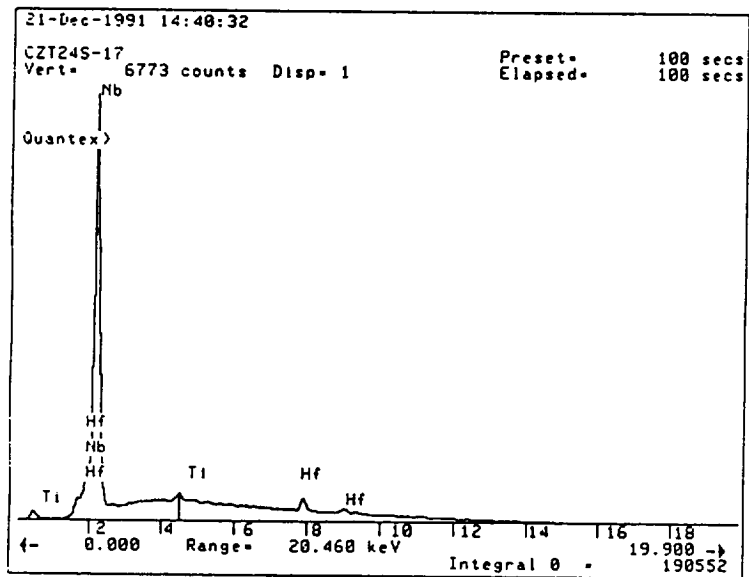
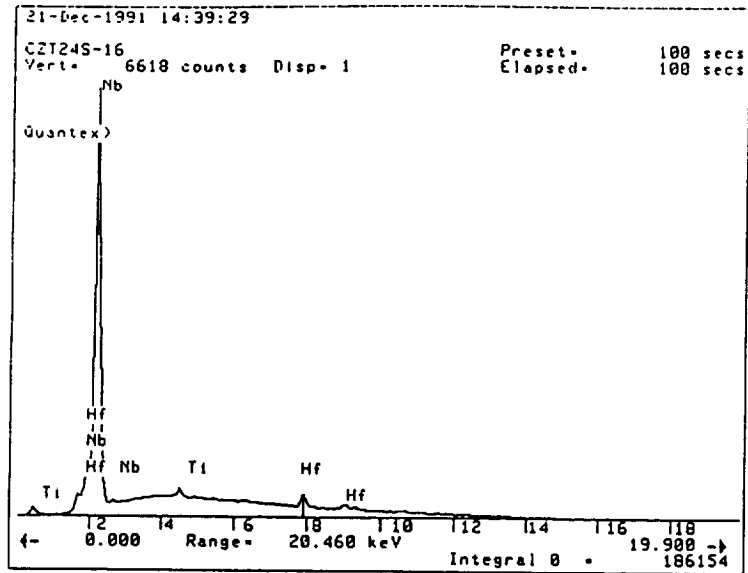












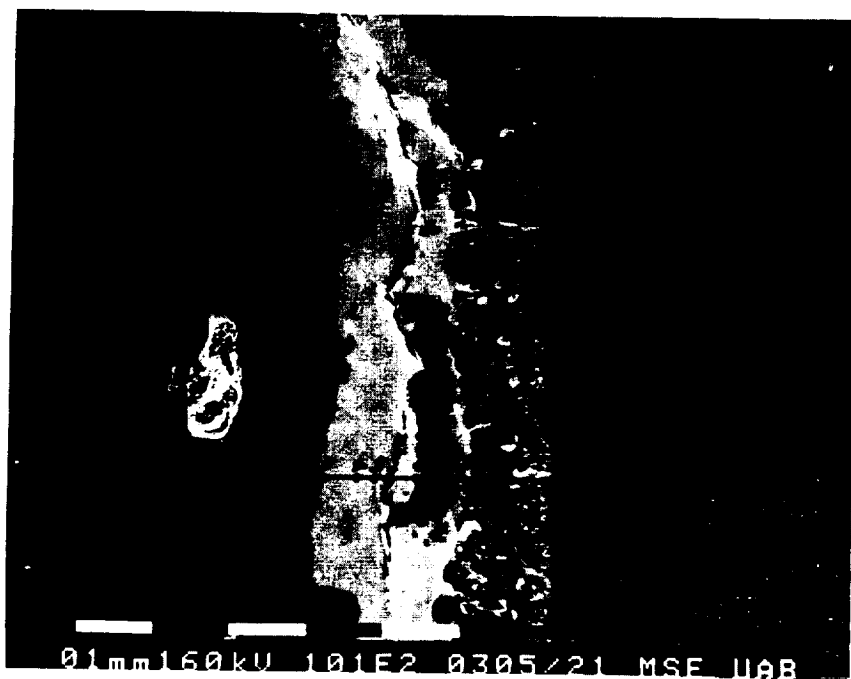
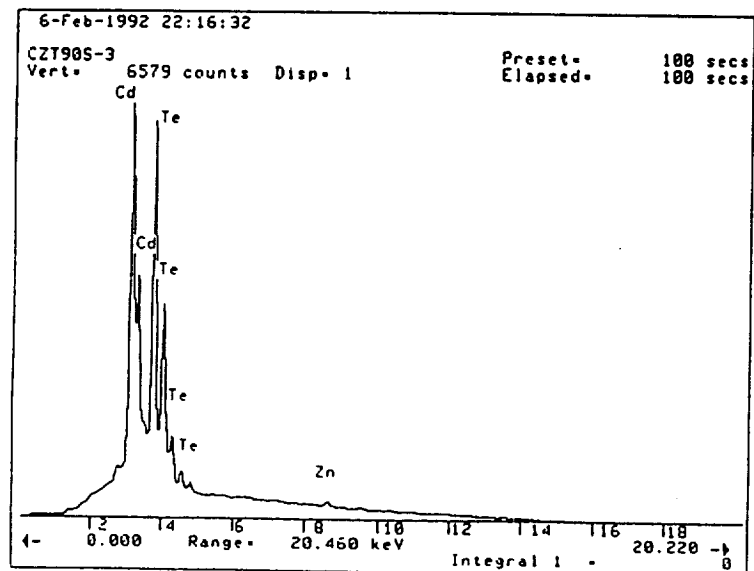
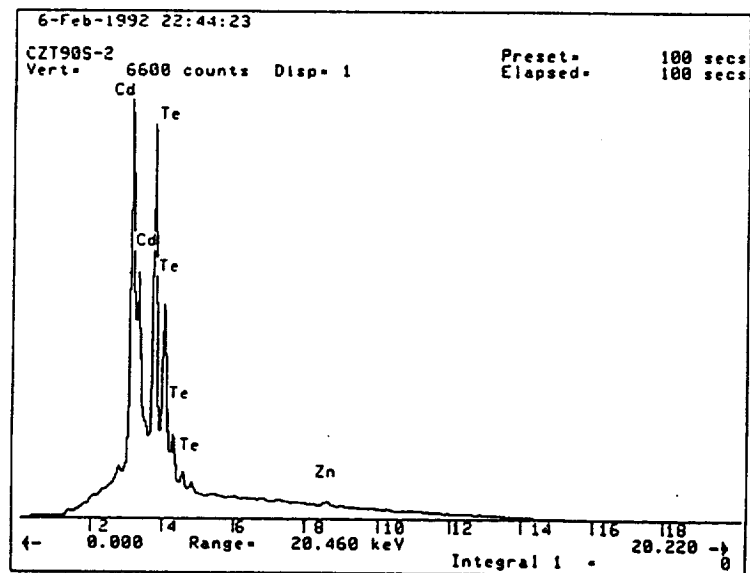
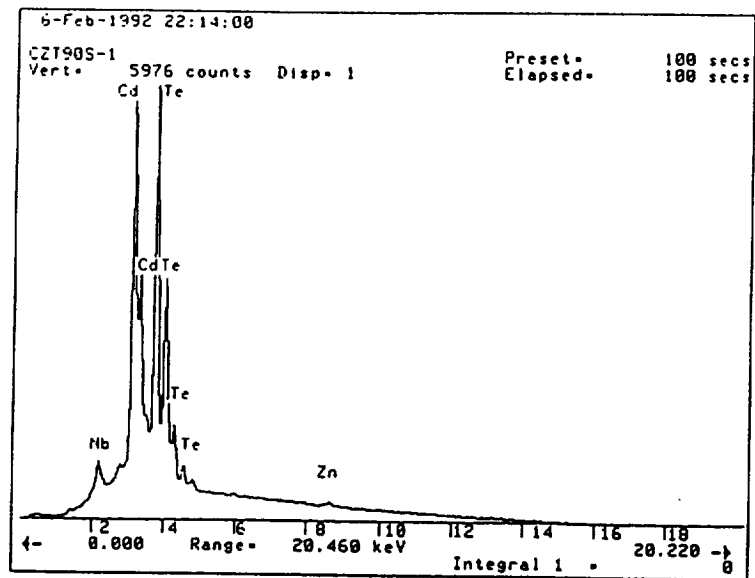
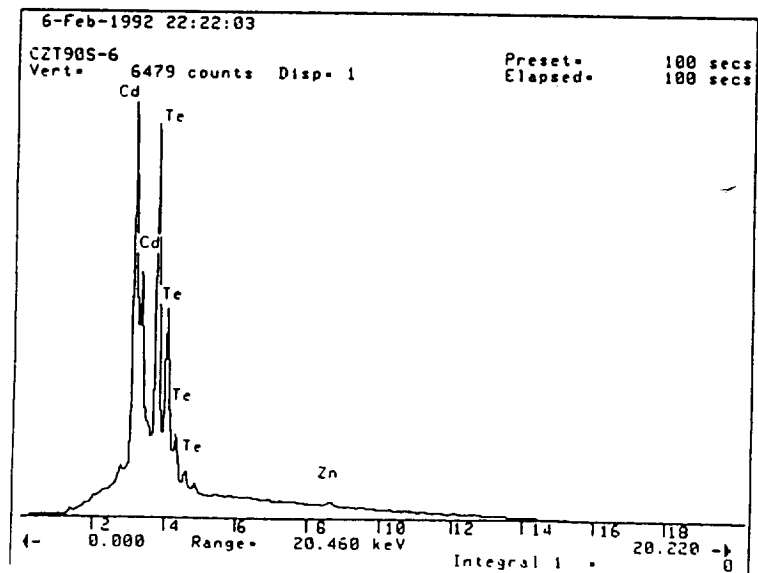
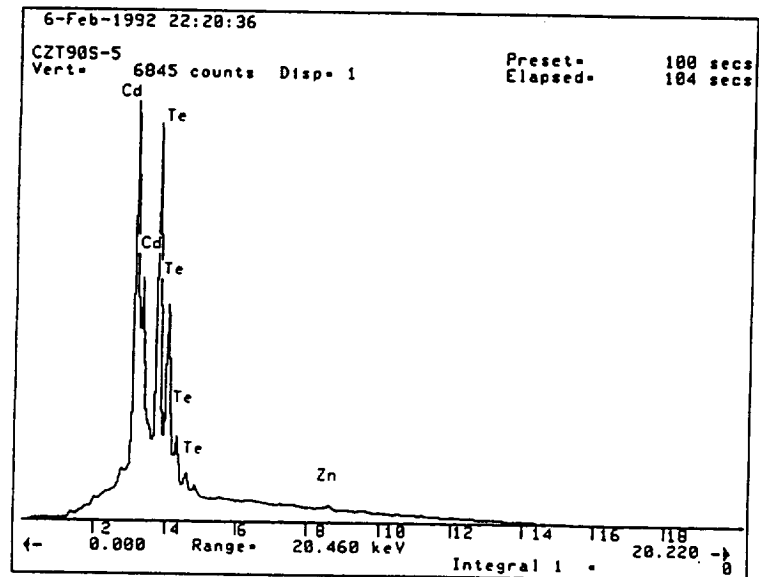
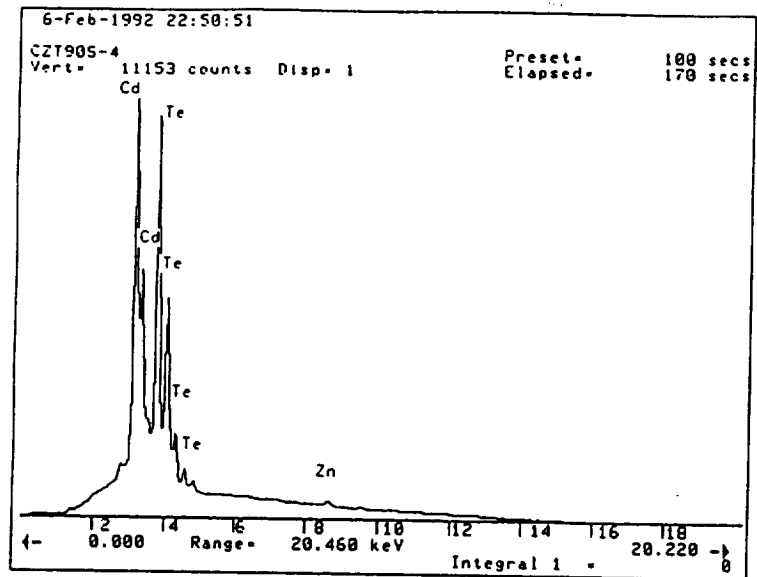
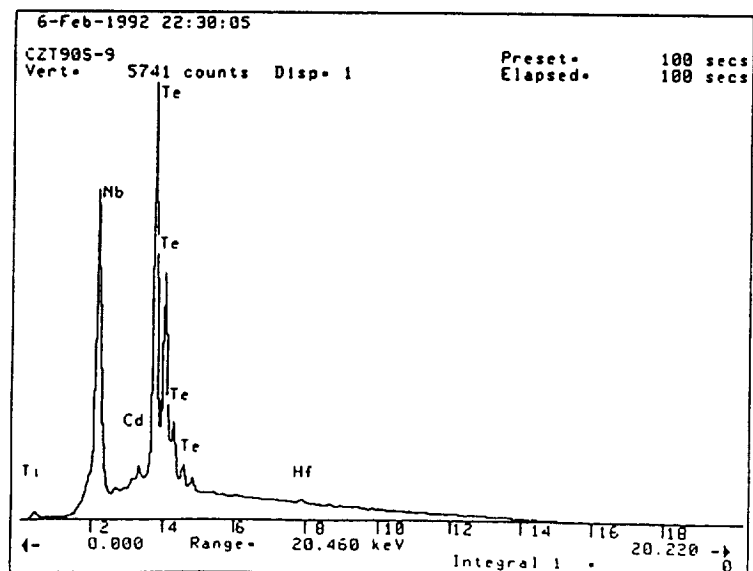
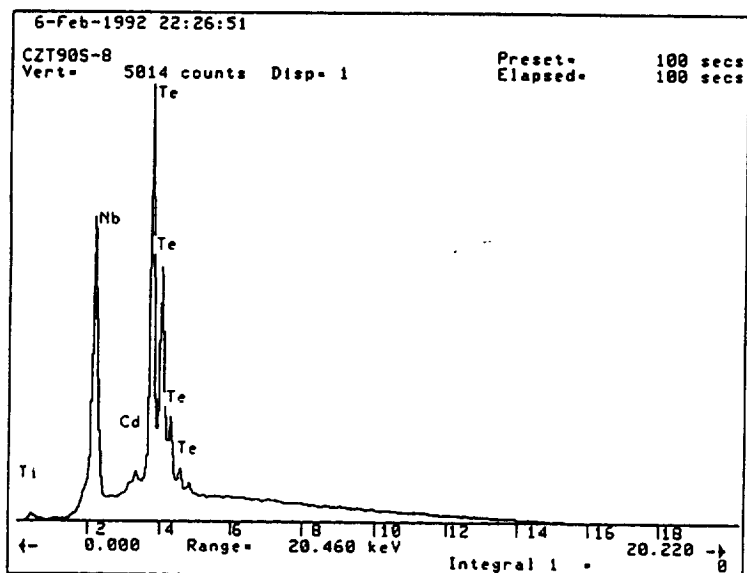
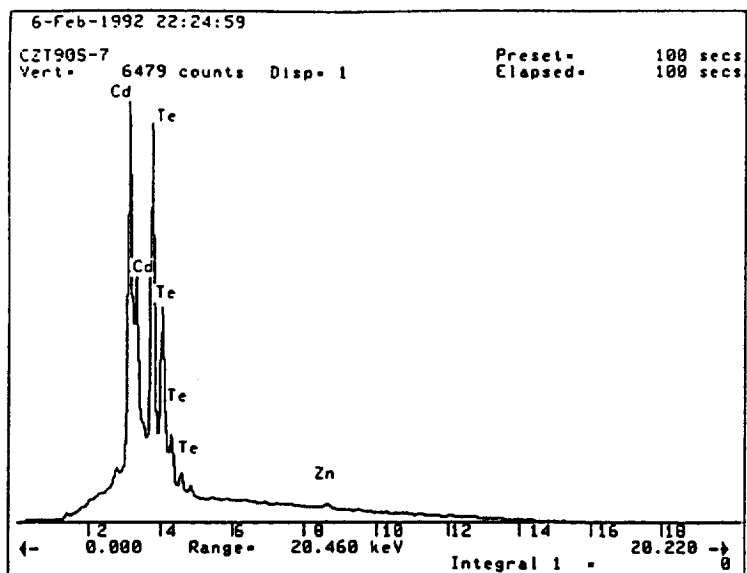


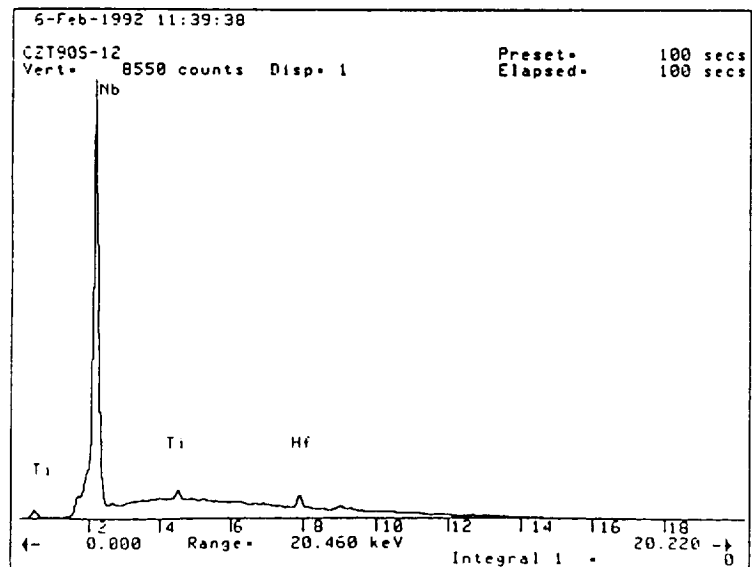
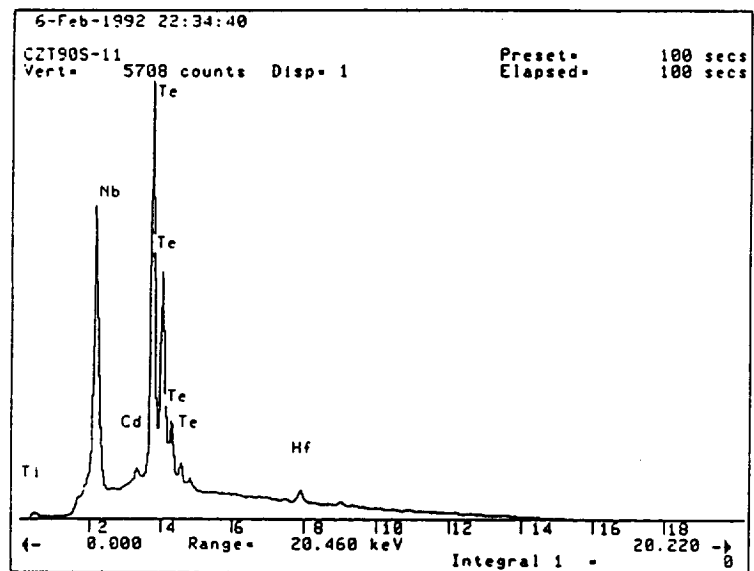
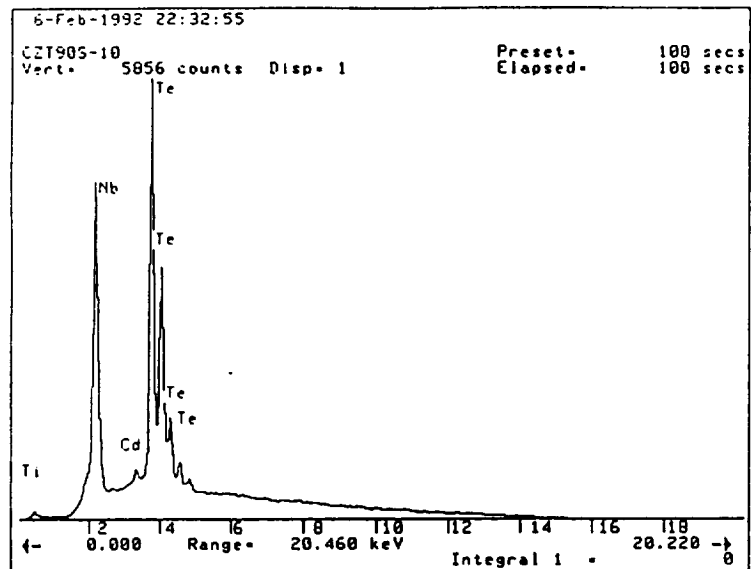
Figure A9. SEM micrograph of CdZnTe/WC-103 couple tested at 1170°C for 90 hours. Numbers indicate points where compositional analysis was performed.

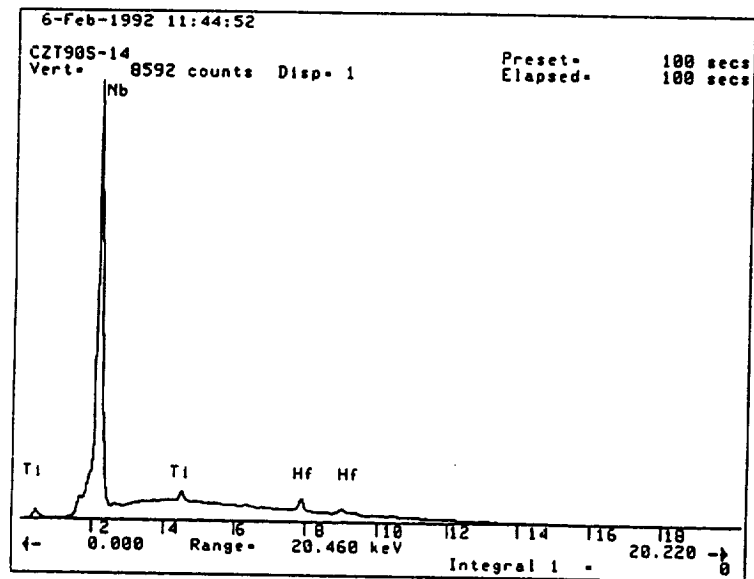
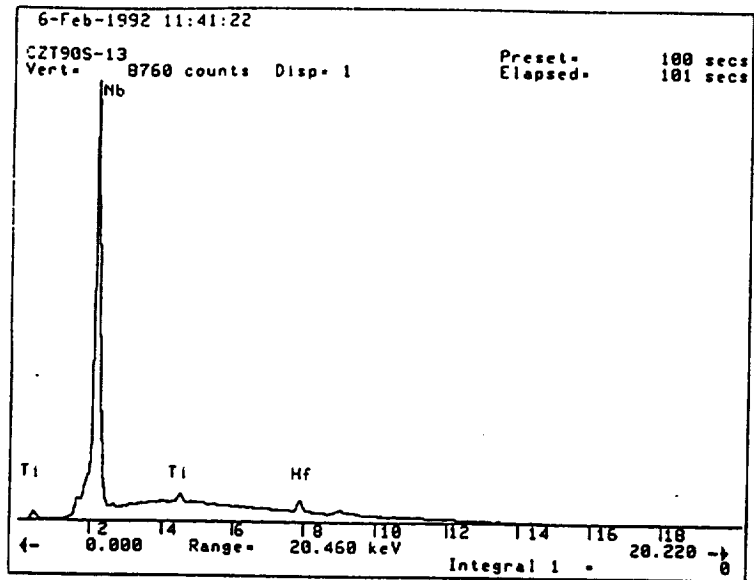
Figure A10. Compositional spectra across the semiconductor/metal interface of a CdZnTe/WC-103 reaction couple tested at 1170°C for 90 hours.











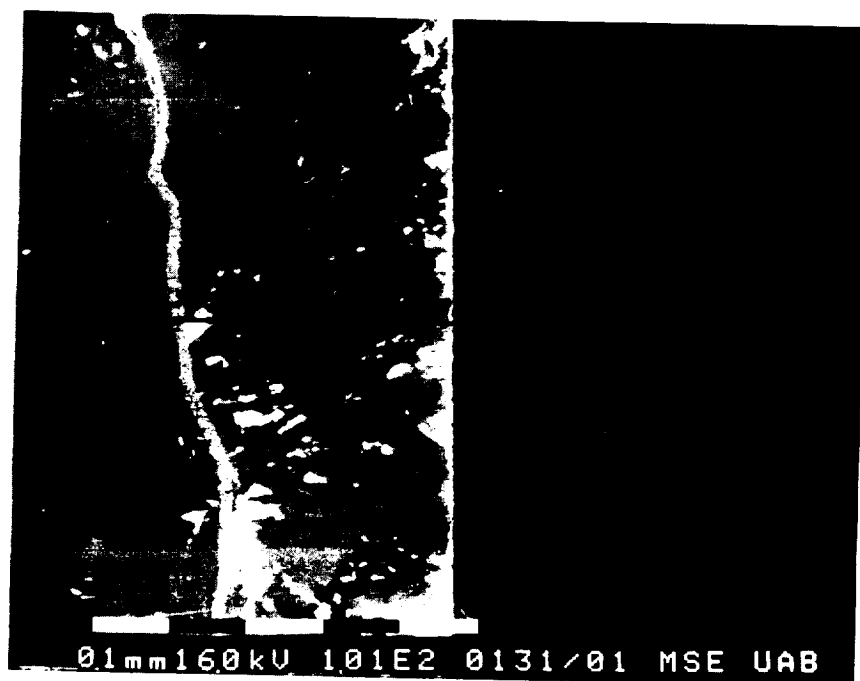
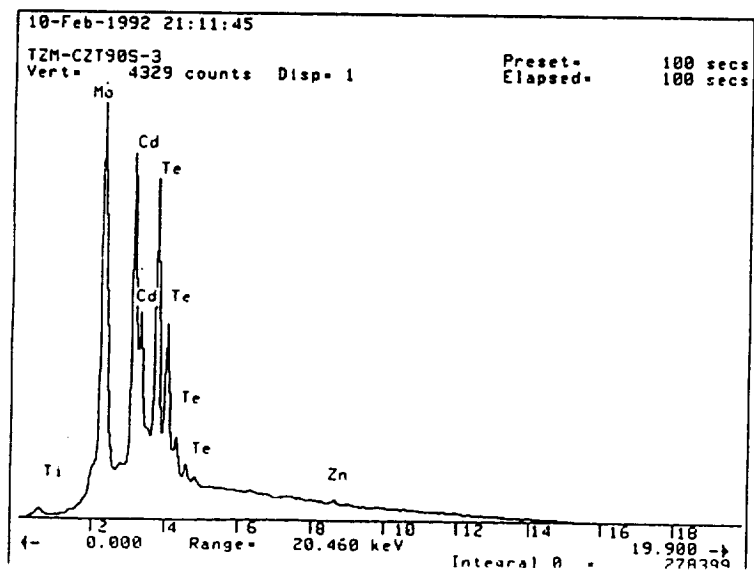
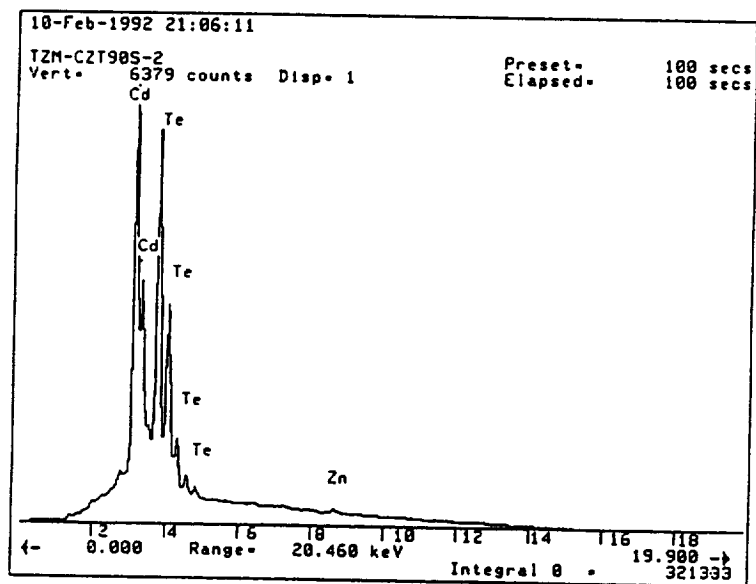
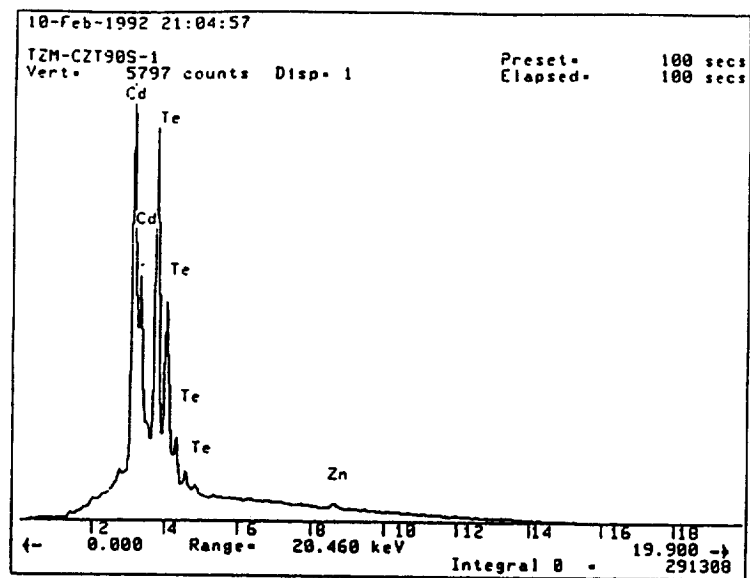
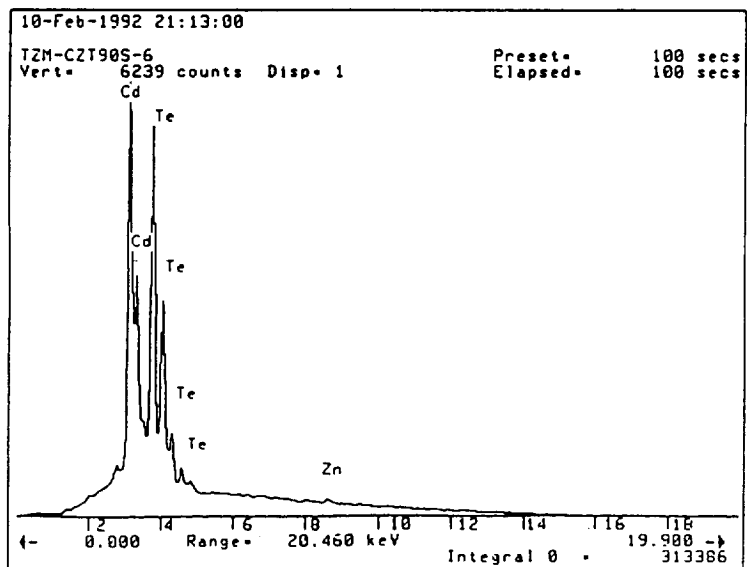
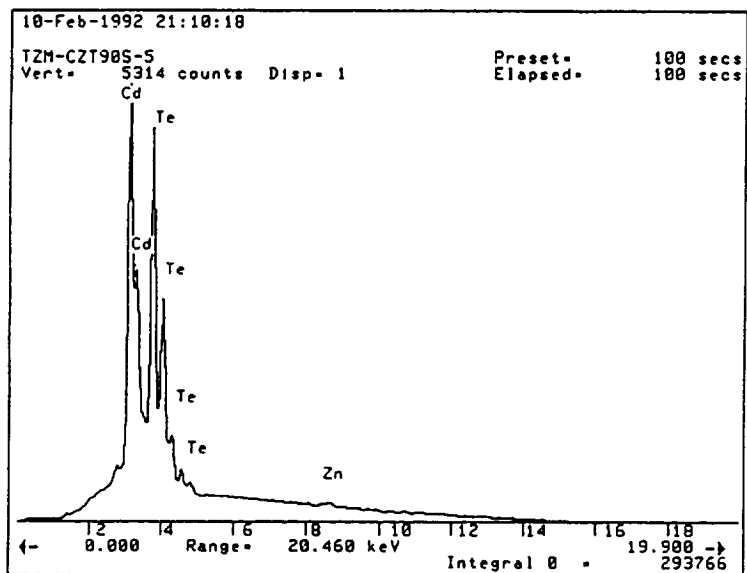
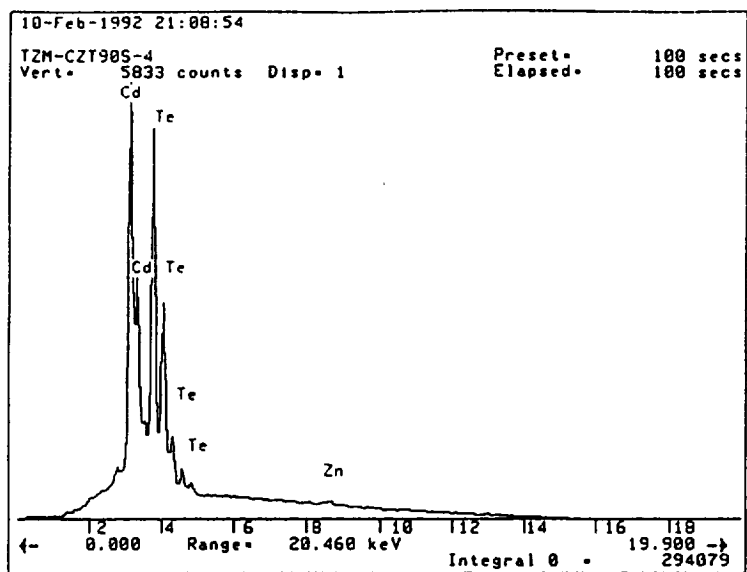
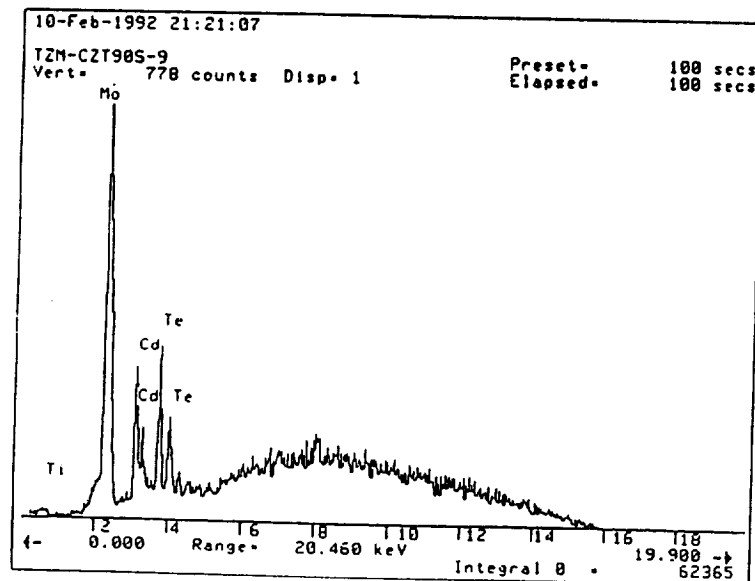
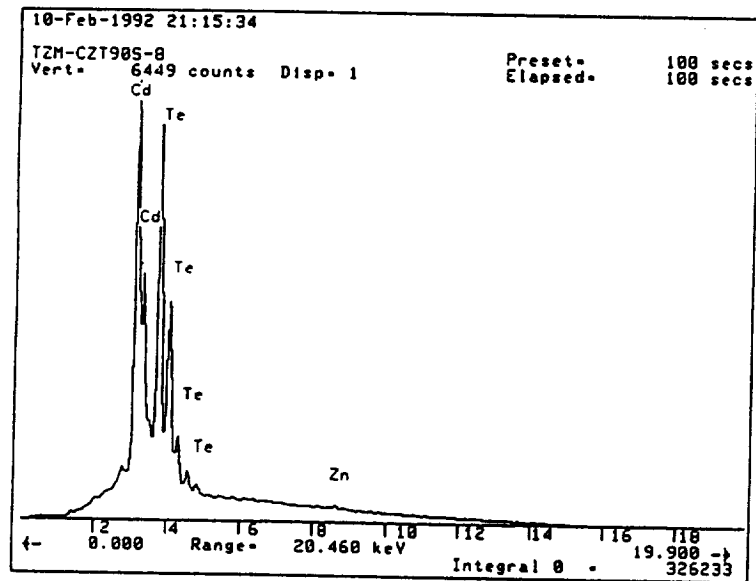
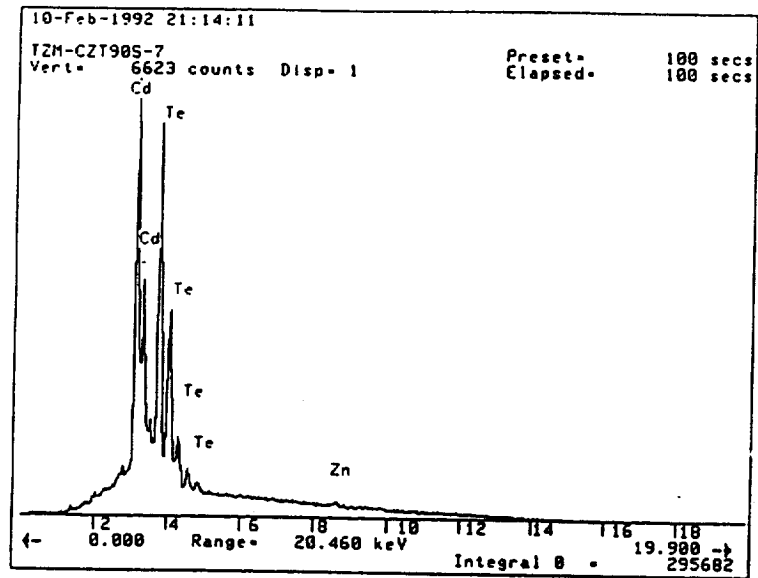


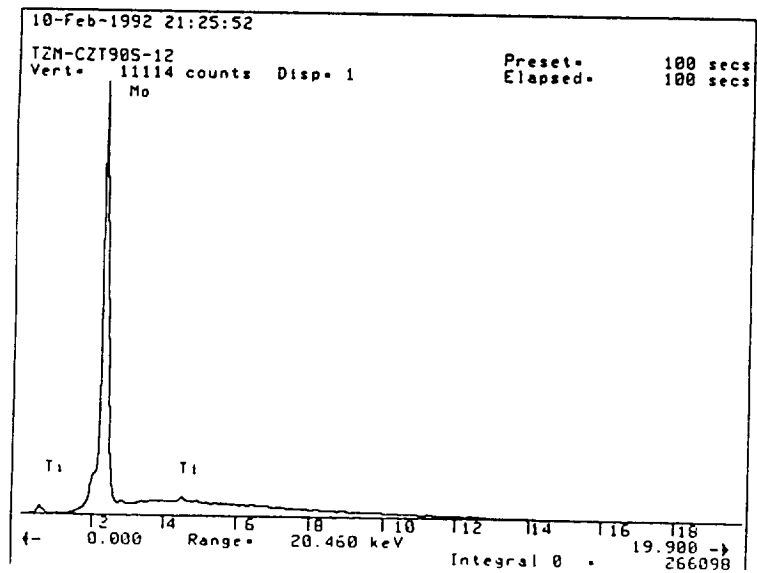
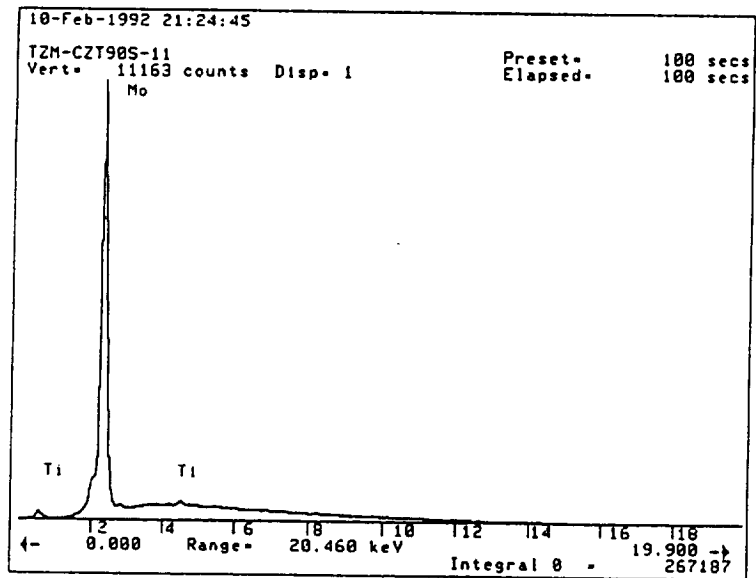
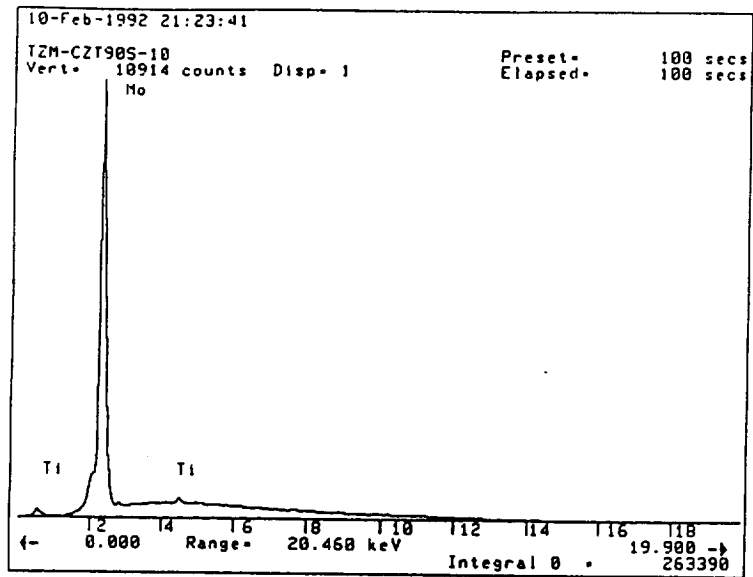
Figure A11. SEM micrograph of CdZnTe/TZM couple tested at 1170°C for 90 hours. Numbers indicate points where compositional analysis was performed.

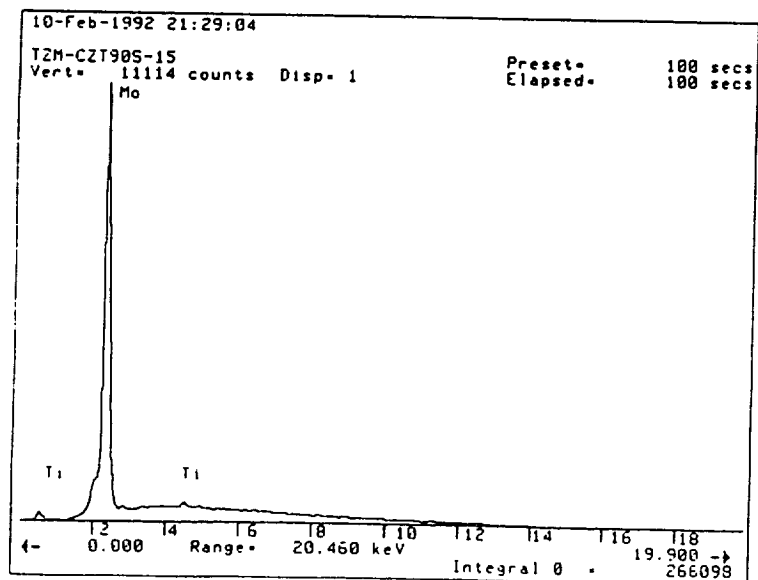
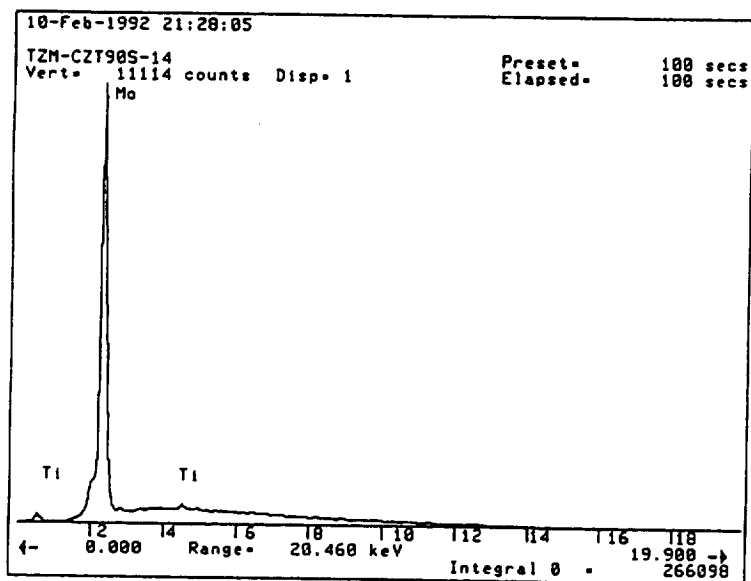
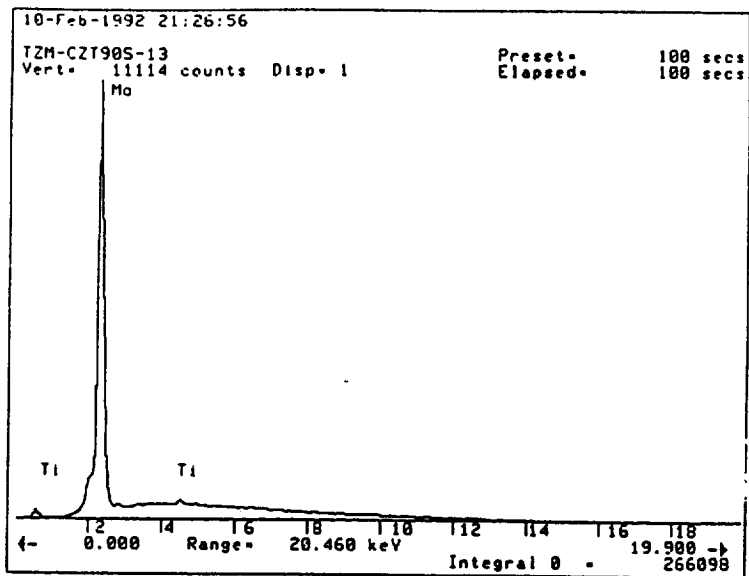
Figure A12. Compositional spectra across the semiconductor/metal interface of a CdZnTe/TZM reaction couple tested at 1170°C for 90 hours.

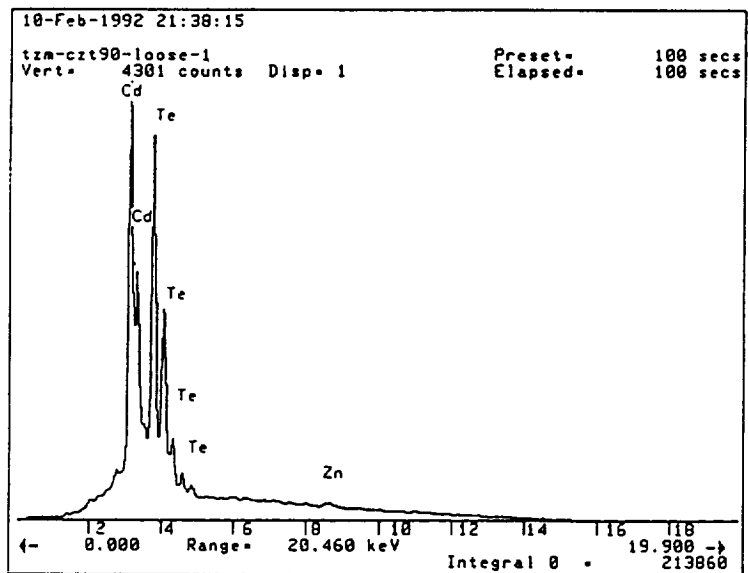
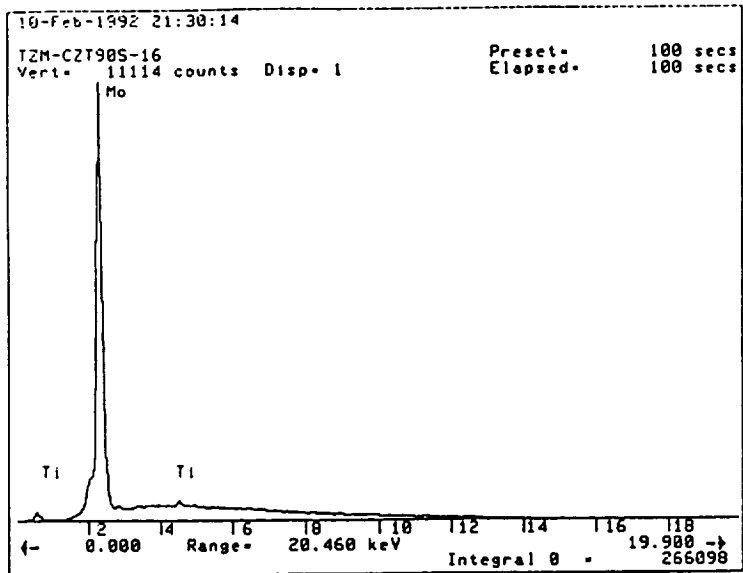












**Chemical Compatibility of
CdZnTe with Silicide Coated WC-103**

Addendum to:

Progress Report

on:

**Chemical Compatibility Studies
of GaAs & CdZnTe
with WC-103 & TZM**

by:

**Rosalia N. Andrews, Ph.D., P.E.
Department of Materials Science and Engineering
University of Alabama at Birmingham
Birmingham, Alabama 35294**

April 20, 1992

**Original Progress Report:
February 10, 1992**

Introduction

The following report summarizes the results obtained for the CdZnTe/ silicide coated WC-103 compatibility test run at 1170°C for 90 hours. WC-103 test coupons of 9.960x9.962x4.978mm were obtained from Southern Research Institute. Two surfaces of these coupons were polished using a procedure identical to that discussed in the initial report submitted on February 10, 1992. This initial report should be referred to for details on procedure. Following surface preparation, test coupons were sent to HITEMCO for silicide coating. Samples were given a heat treatment of one hour at 1566°C (2850° C) after coating to ensure bonding of the silicide coating.

Sample/semiconductor compatibility tests were accomplished by immersion of the test coupons in molten CdZnTe for 90 hours at 1170°C using a procedure identical to that discussed in the report of February 10, 1992.

90 hour CdZnTe/Silicide Coated WC-103 Compatibility Test

An optical micrograph of the reaction zone observed for the 90 hour CdZnTe/silicide coated WC-103 couple is shown in Figure 1. The original thickness of the metal coupon was 4.930 mm. The final thickness of the pure metal was ~ 4.883 mm. However, this reduction in metal thickness did not appear to be due to a reaction between the metal and semiconductor. Apparently the reduction in metal thickness resulted due to interdiffusion between the silicide coating (original thickness 0.056mm or 2.2 mils) and the base metal. The thickness of the initial silicide coating was seen to increase during the compatibility test resulting in a final thickness of 0.079mm or 3.1 mils. After testing, base metal from the coupon was found throughout the silicide coating implying the layer had changed to a mixture of silicide and WC-103. See Figure 2 and EDS plots 1-16.

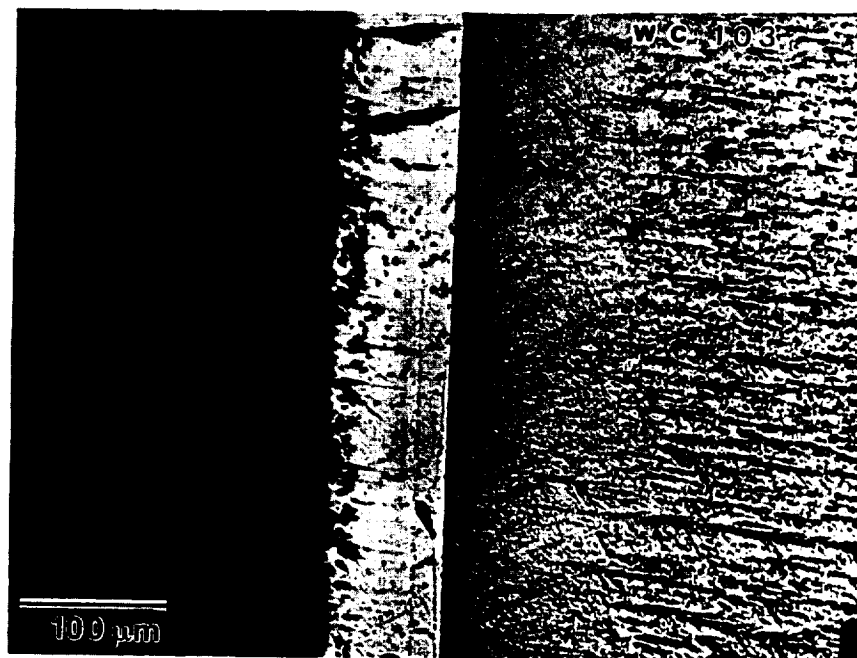


Figure 1. Metal/silicide coating/semiconductor interface in a CdZnTe/silicide coated WC-103 compatibility test carried out for 90 hours at 1170°C.

There does not appear to be any significant reaction between the CdZnTe and the silicide coating. Note also that in those regions where there is a scratch or defect in the silicide coating, the semiconductor has penetrated. Therefore, it is imperative that no defects are present in the coating as applied and that utmost care be taken in the handling of the coated cartridges to prevent damage to the coating. I understand there has been some consideration given to only coating the outside surface of the cartridges. This approach would provide no barrier to the attack of the WC-103 by the CdZnTe semiconductor in the event of an ampoule failure. While the silicide coating would not be chemically attacked in the event the WC-103 was totally consumed by the molten semiconductor, it would not appear that the silicide coating is in, and of itself, sufficiently substantial from a mechanical standpoint to withstand the significant vapor pressure of the semiconductor. In summary, the silicide coating appears to be effective in reducing and/or eliminating WC-103/CdZnTe reaction and if applied to the interior of the cartridge should enhance the ability of the cartridge to function more effectively as a second level of containment.

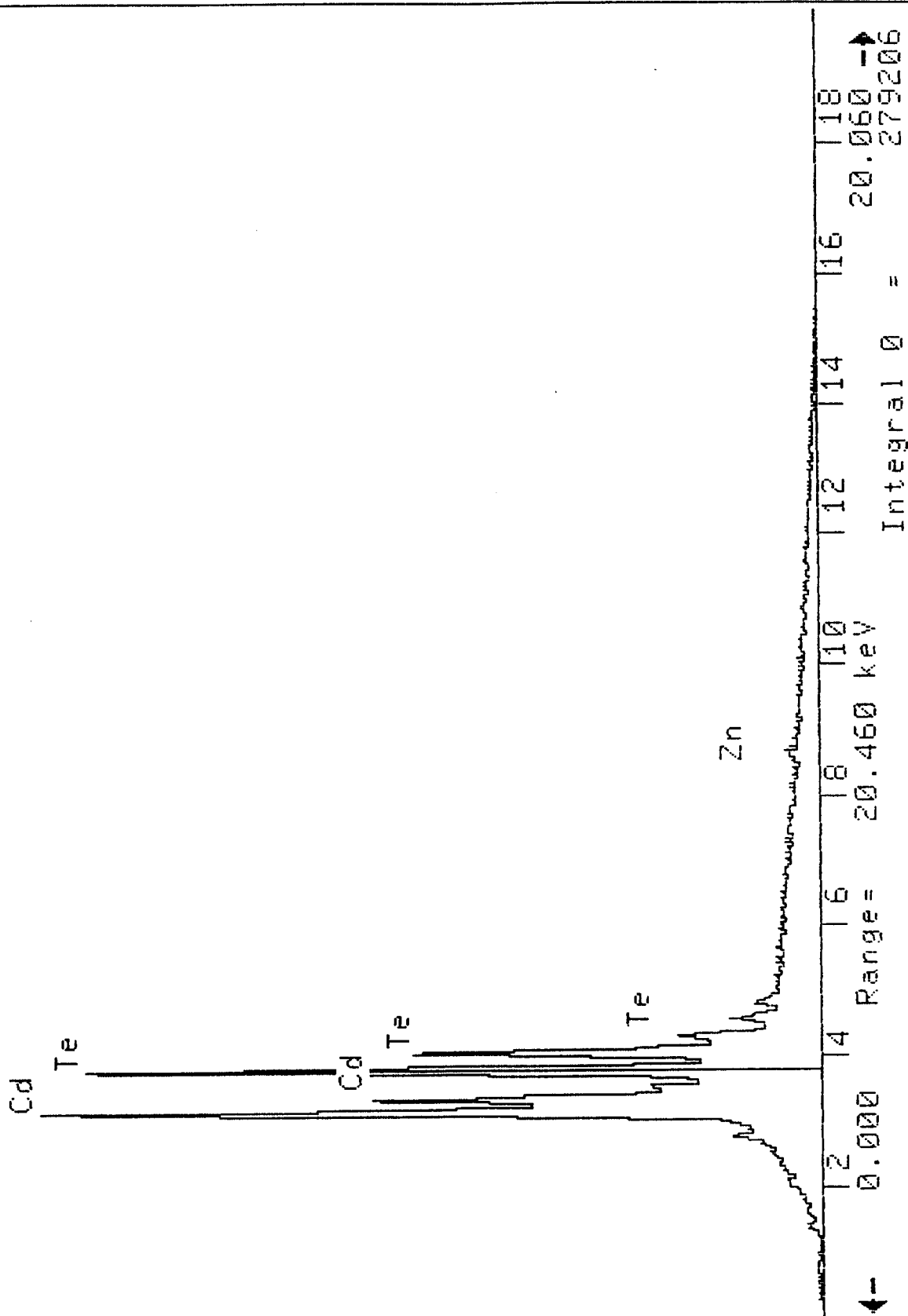


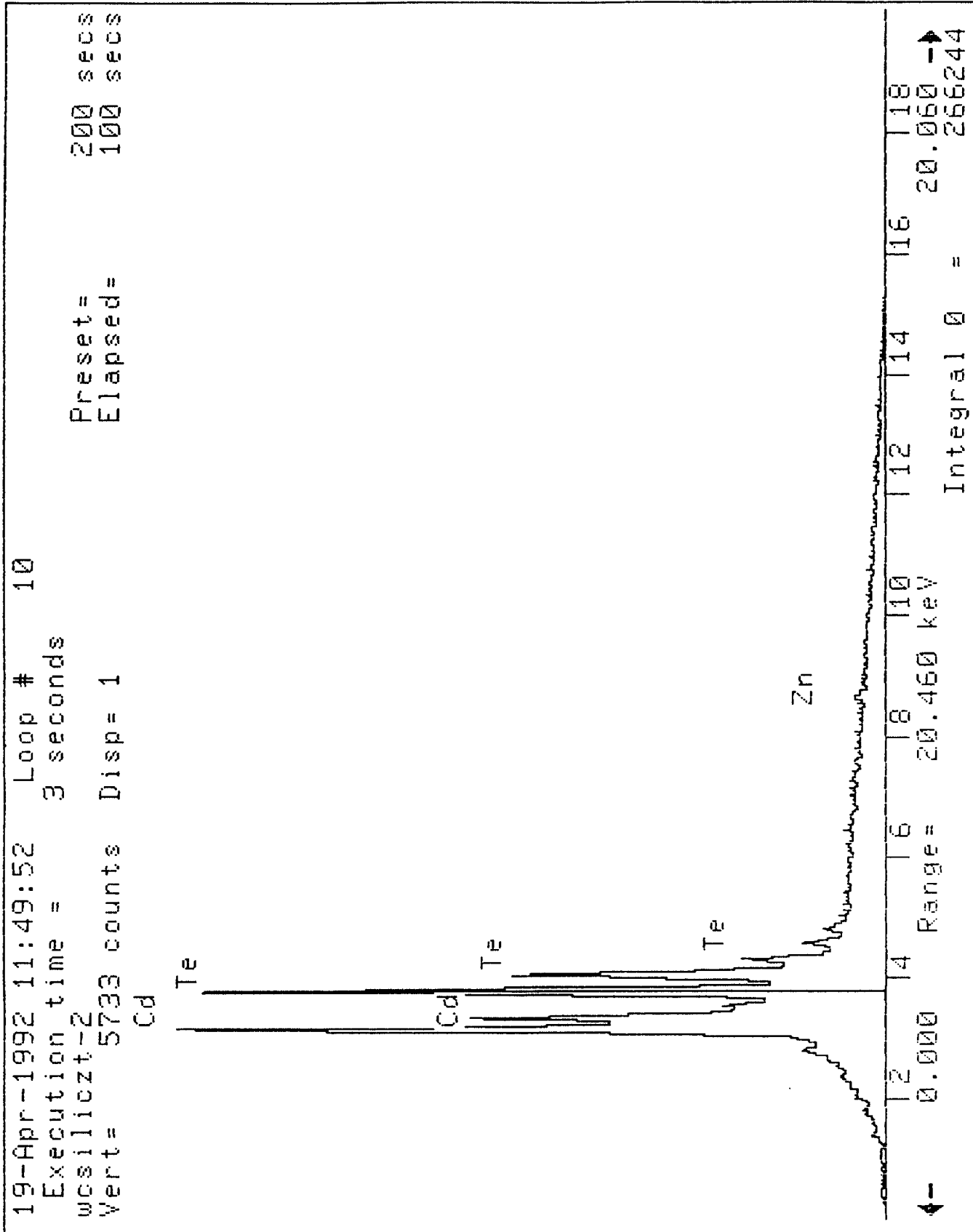
Figure 2. SEM micrograph of CdZnTe/silicide coated WC-103 tested for 90 hours at 1170°C. Numbers indicate where compositional analysis was performed.

Summary of Findings to Date for WC-103 Cartridge Material - Recommendations

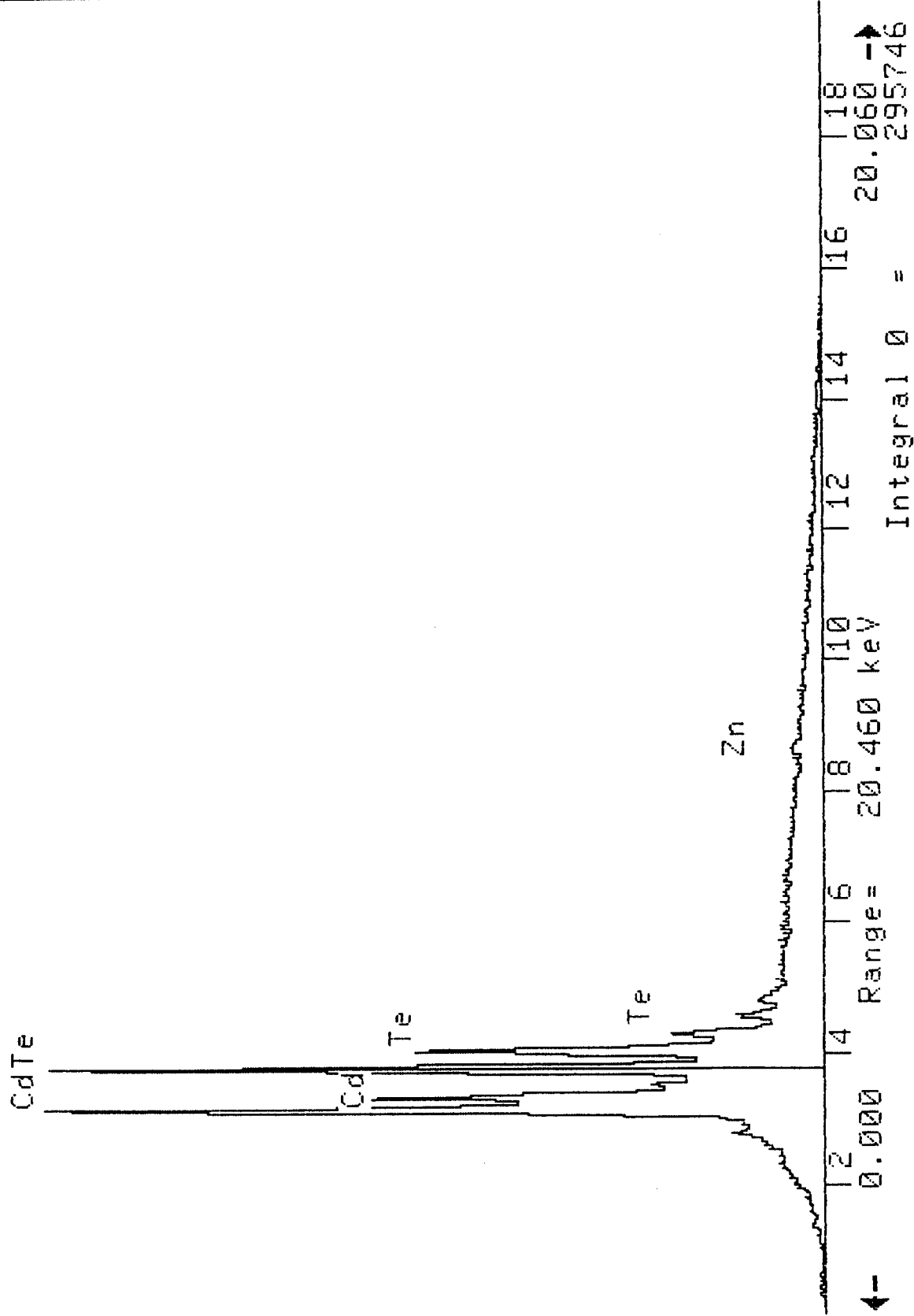
- 1) From a semiconductor/metal compatibility standpoint, the CdZnTe/WC-103 couple appears to be a workable solution to semiconductor containment in the event of an ampoule failure. However, some evidence of a variation in the degree of attack with surface finish was noted during testing. It appears that best results are obtained with a highly polished surface.
- 2) From a compatibility standpoint the CdZnTe/silicide coated WC-103 couple also appears to be a workable solution to the semiconductor containment problem in case of an ampoule failure. It is recommended that the inside of the cartridge be coated with a silicide layer at least 4-5 mils thick. To be effective, this coating must be perfect and care must be taken not to scratch the coating after application.
- 3) Due to the vigorous reaction of GaAs with WC-103, which results in metal reaction products which spall off, I do not recommend that WC-103 be used in combination with GaAs. Optional coatings or cartridge liners should be investigated for this metal/semiconductor combination.

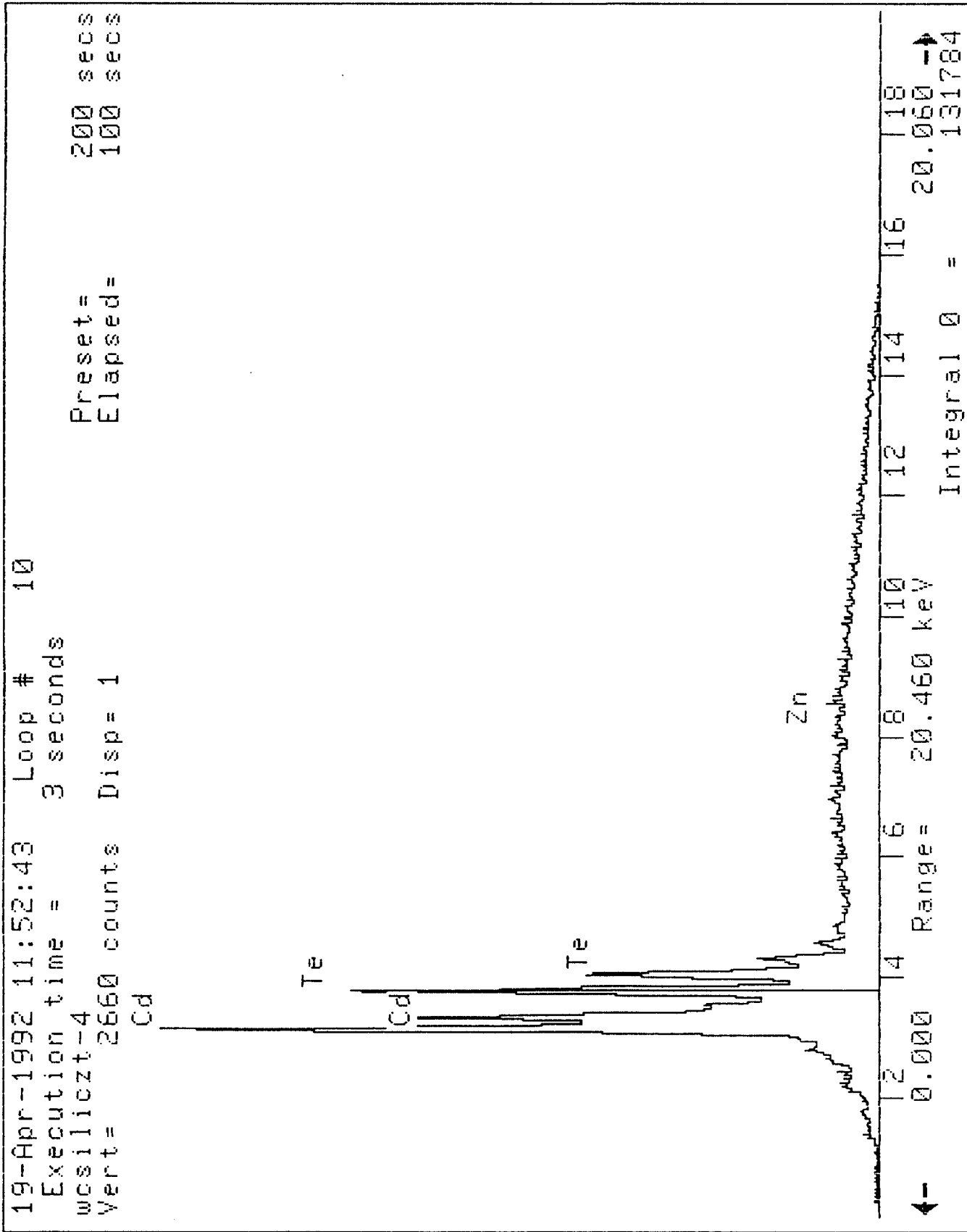
19-Apr-1992 11:48:40 Loop # 10
 Execution time = 2 seconds
 wcsiliczt-1
 Vert= 6023 counts Disp= 1
 Preset= 200 secs
 Elapsed= 100 secs





19-Apr-1992 11:50:56 Loop # 10
 Execution time = 3 seconds
 wcsiliczt-3
 Vert= 6322 counts Disp= 1
 Preset= 200 secs
 Elapsed= 100 secs





19-Apr-1992 11:16:35 Loop # 10
 Execution time = 2 seconds
 wcsiliczt-6
 Vert= 420 counts Disp= 1
 Preset= 200 secs
 Elapsed= 100 secs

Te

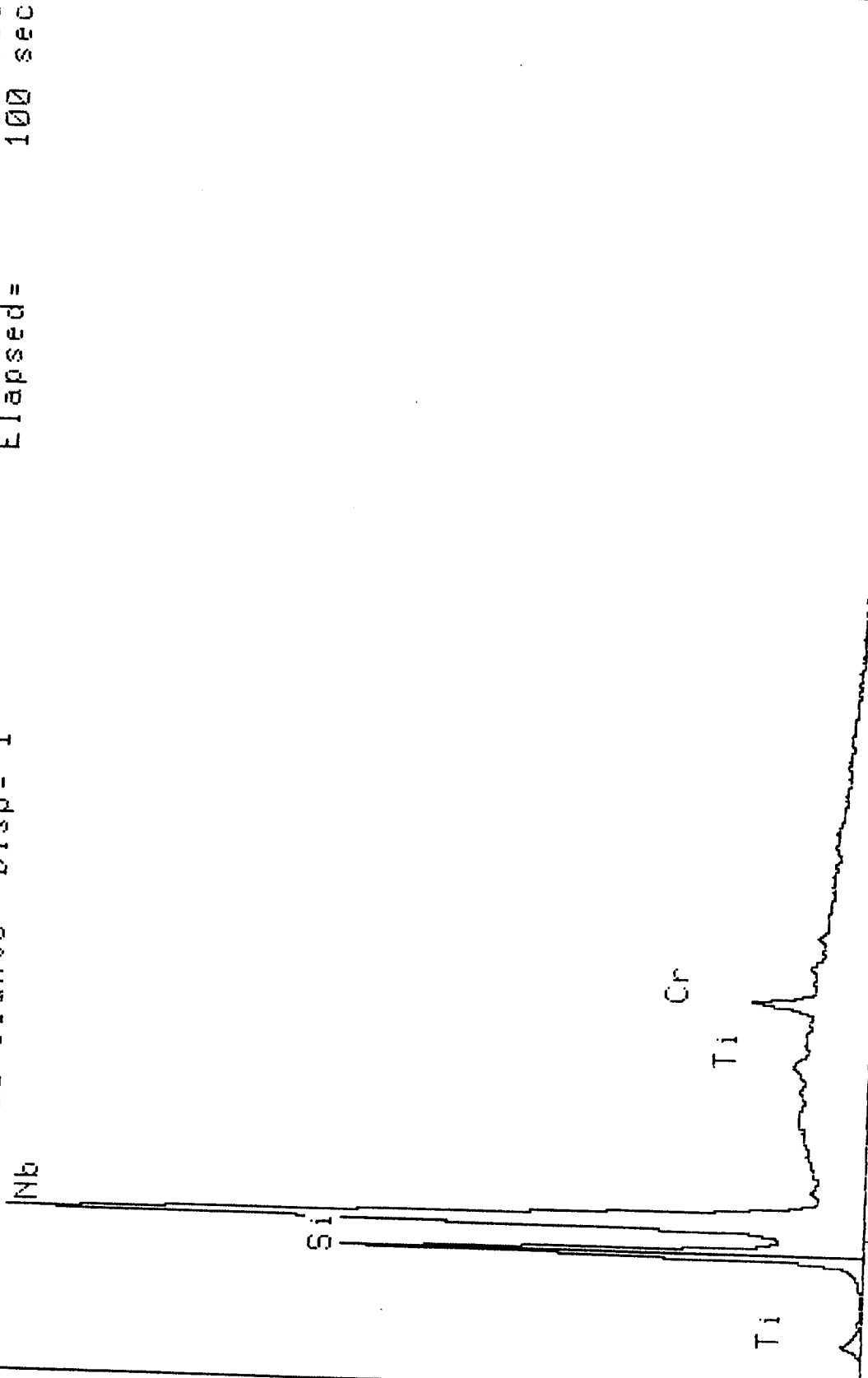
Cd

Nb

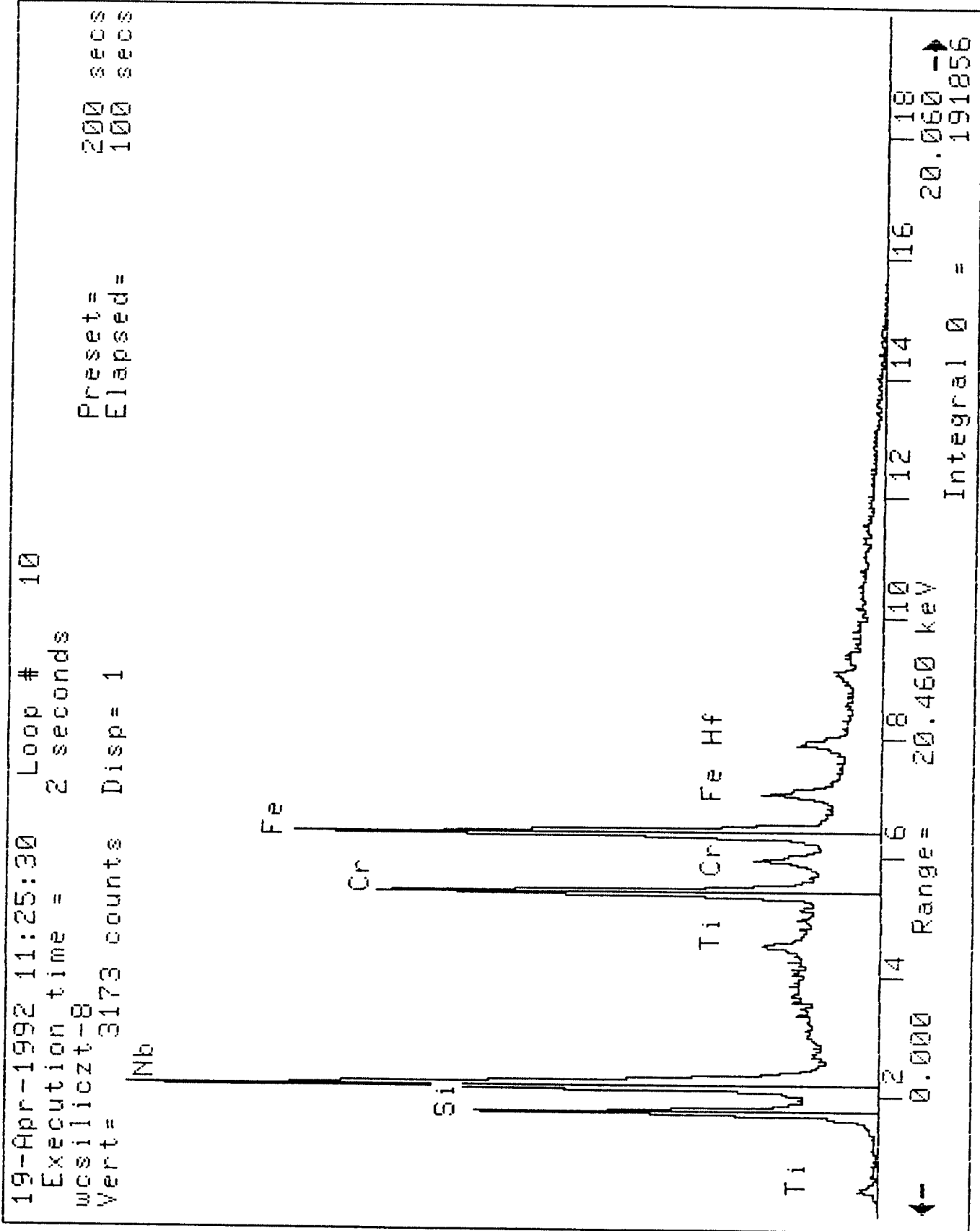
Te

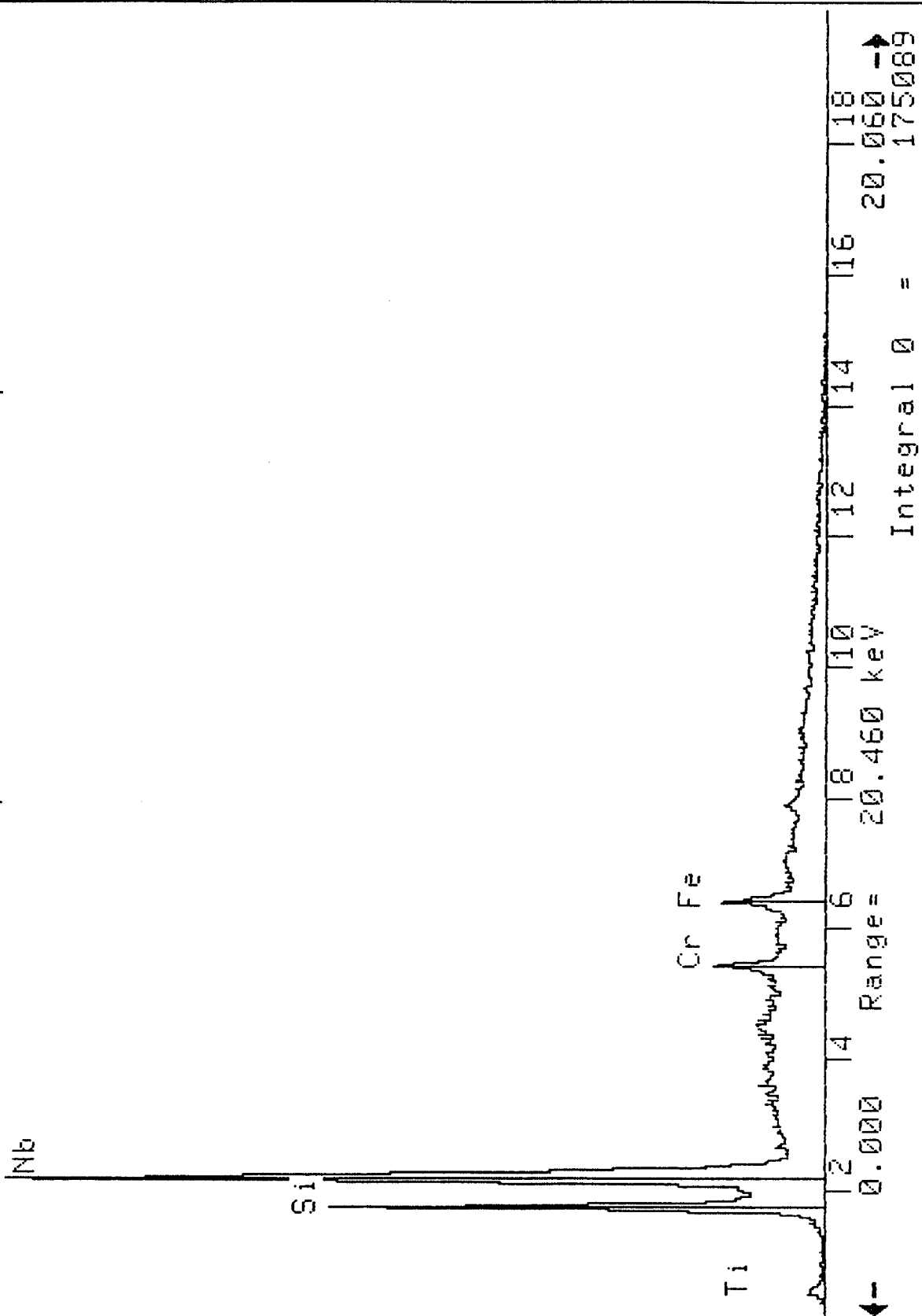
← 12 14 16 18 20.460 keV
 0.000 Range= 20.460 keV
 Integral 0 = 48222

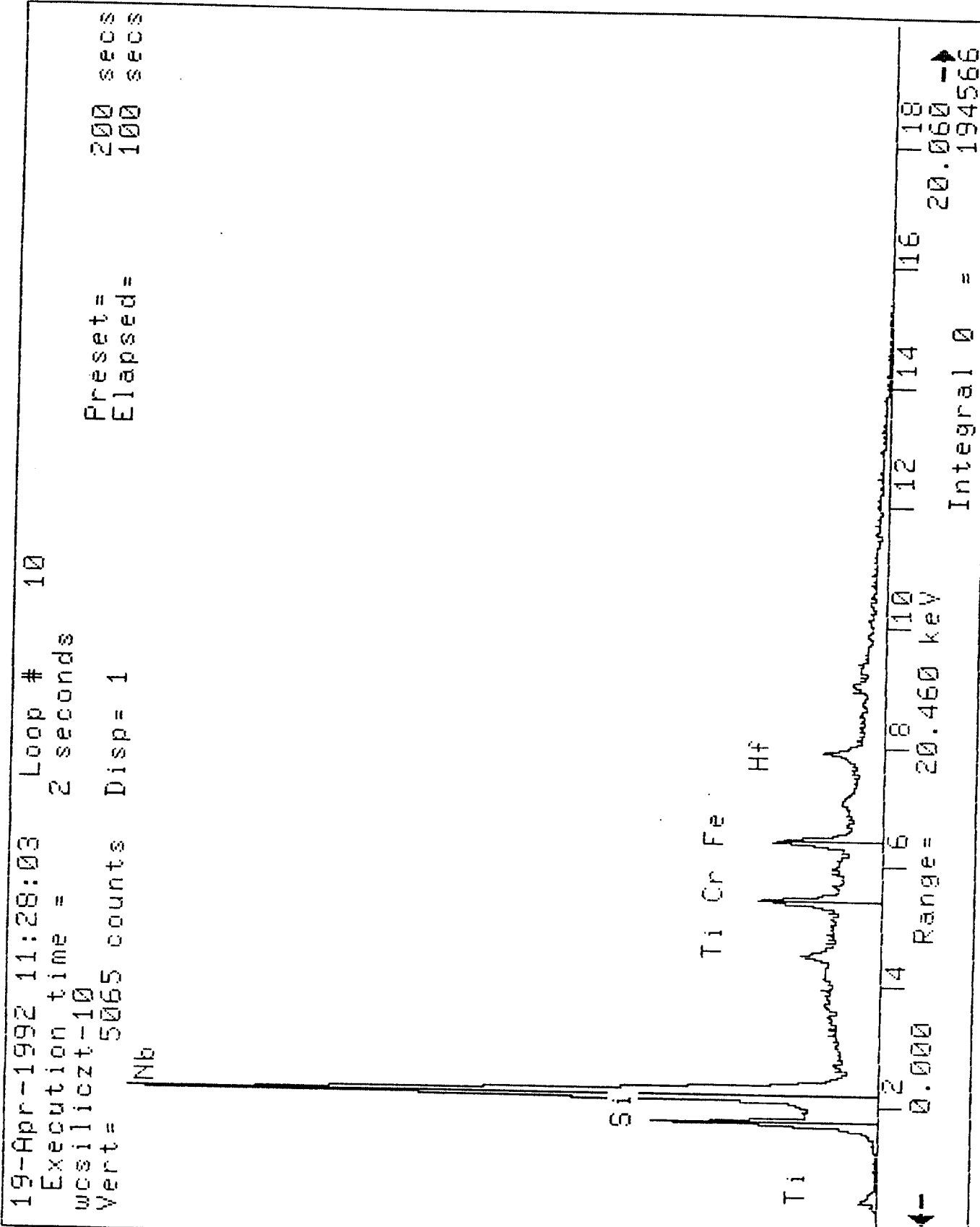
19-Apr-1992 11:21:50 Loop # 10
 Execution time = 2 seconds
 wcsiliczt-7
 Vert= 3501 counts Disp= 1
 Preset= 200 secs
 Elapsed= 100 secs



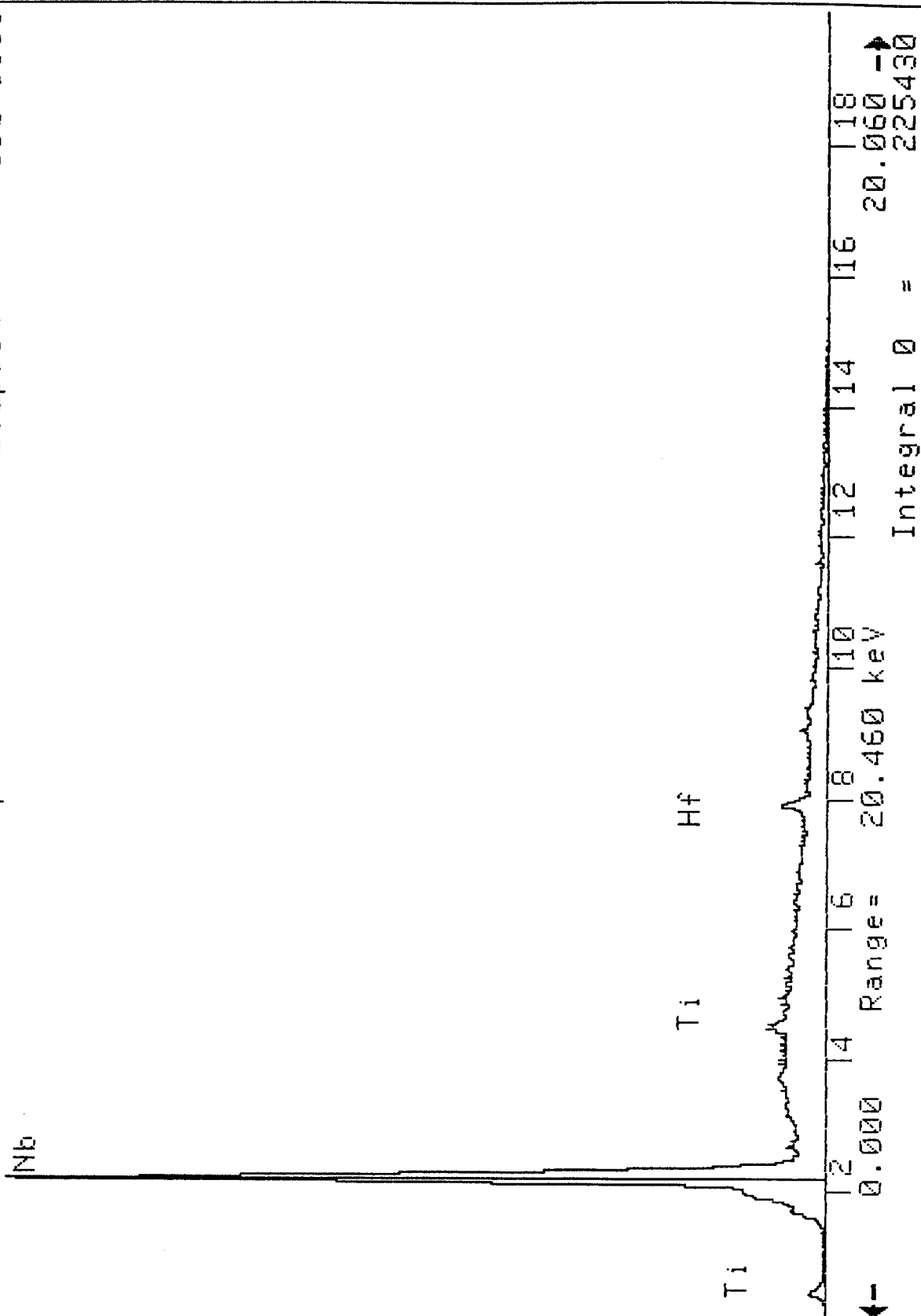
← 0.000 Range= 20.460 keV
 Integral 0 = 148060



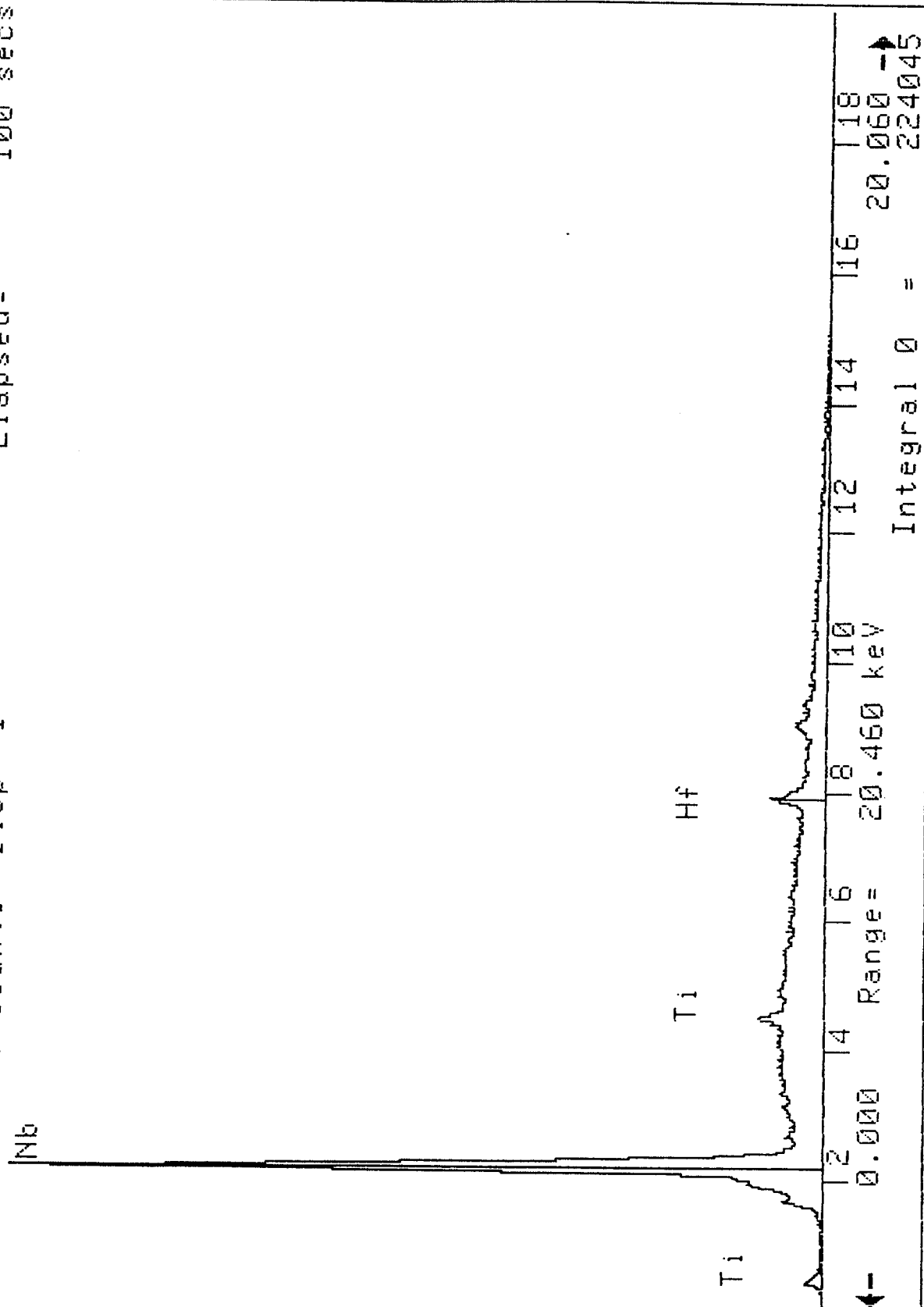
[illegible]



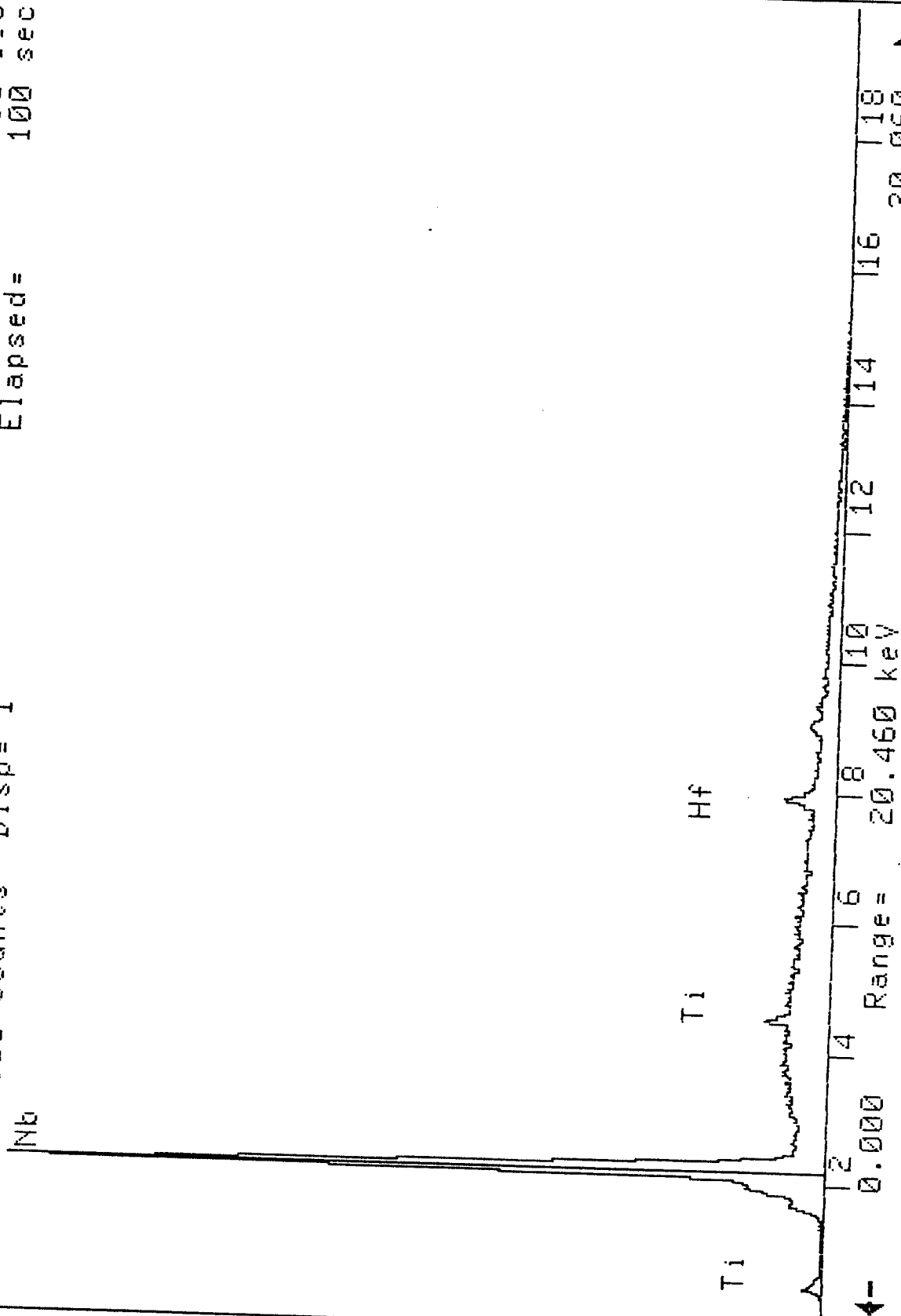
2	1
<input checked="" type="checkbox"/>	<input checked="" type="checkbox"/>
<input checked="" type="checkbox"/>	<input checked="" type="checkbox"/>
<input checked="" type="checkbox"/>	<input checked="" type="checkbox"/>
<input checked="" type="checkbox"/>	<input checked="" type="checkbox"/>
<input checked="" type="checkbox"/>	<input checked="" type="checkbox"/>



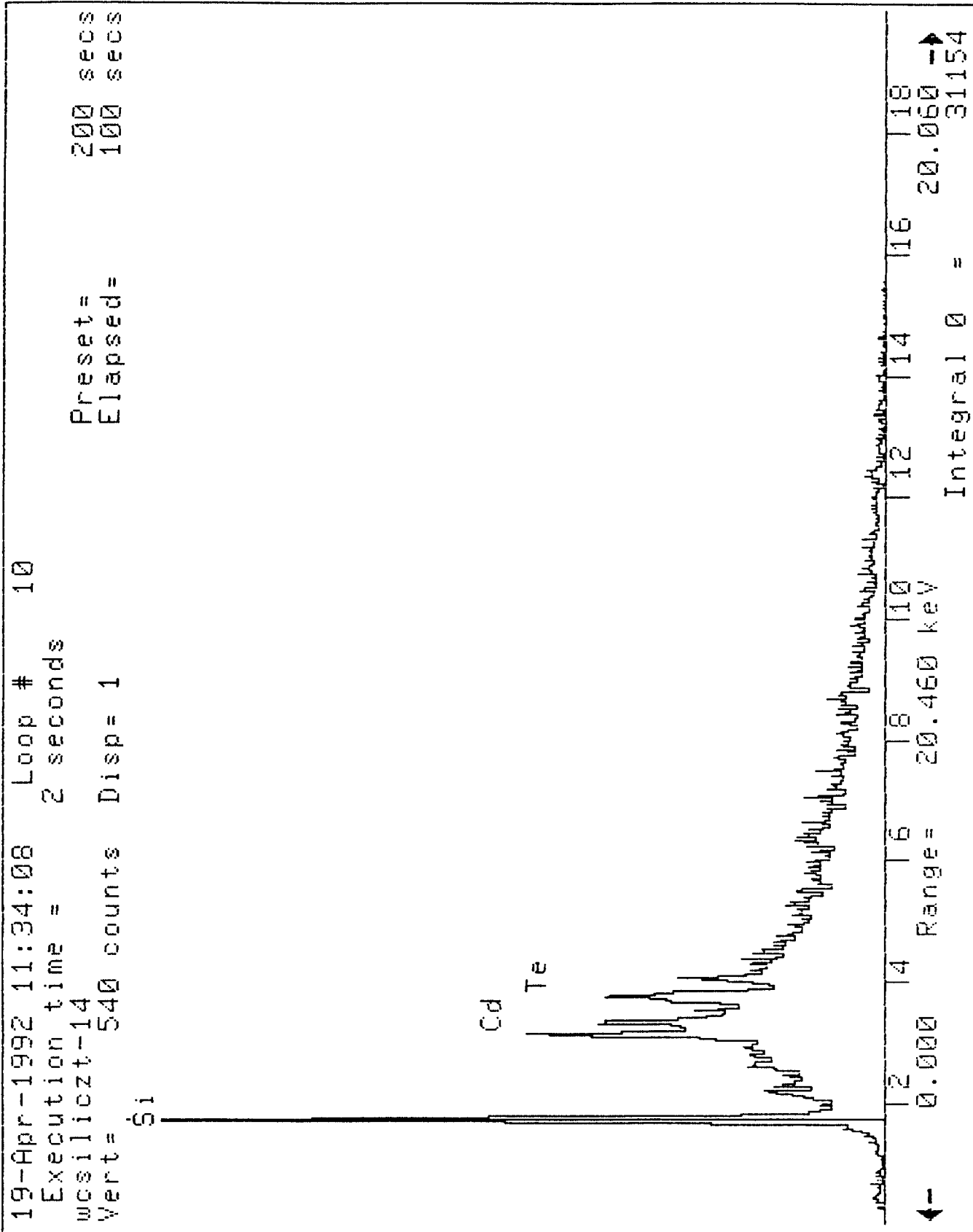
Eligible	100	55
Not eligible	200	55



19-Apr-1992 11:31:16 Loop # 10
 Execution time = 1 seconds
 wcsiliczt-13
 Vert= 7538 counts Disp= 1
 Preset= 200 secs
 Elapsed= 100 secs



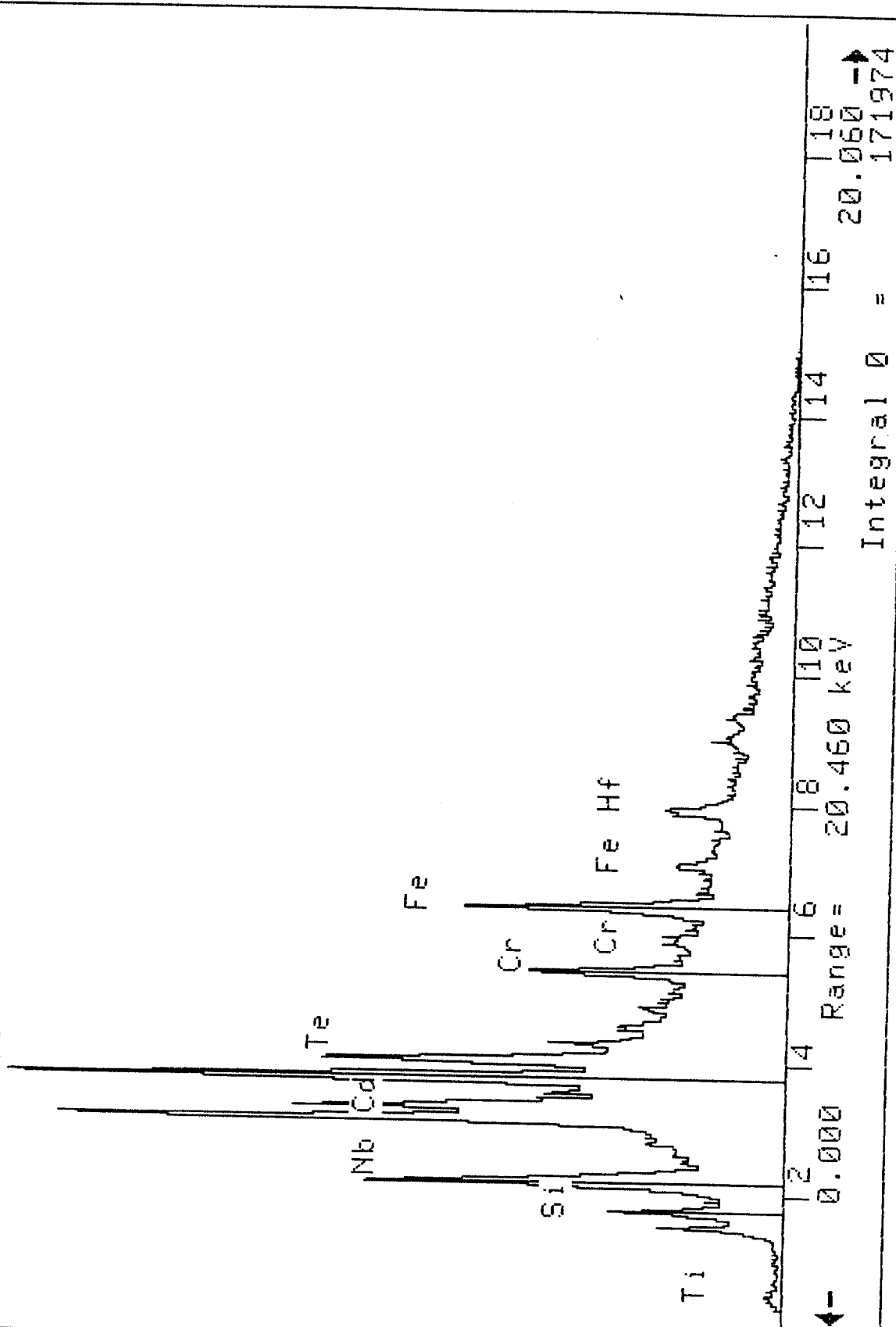
← 0.000 Range= 20.460 keV
 Integral 0 = 220710



```

Presets =
Elapsed =
200s
100s

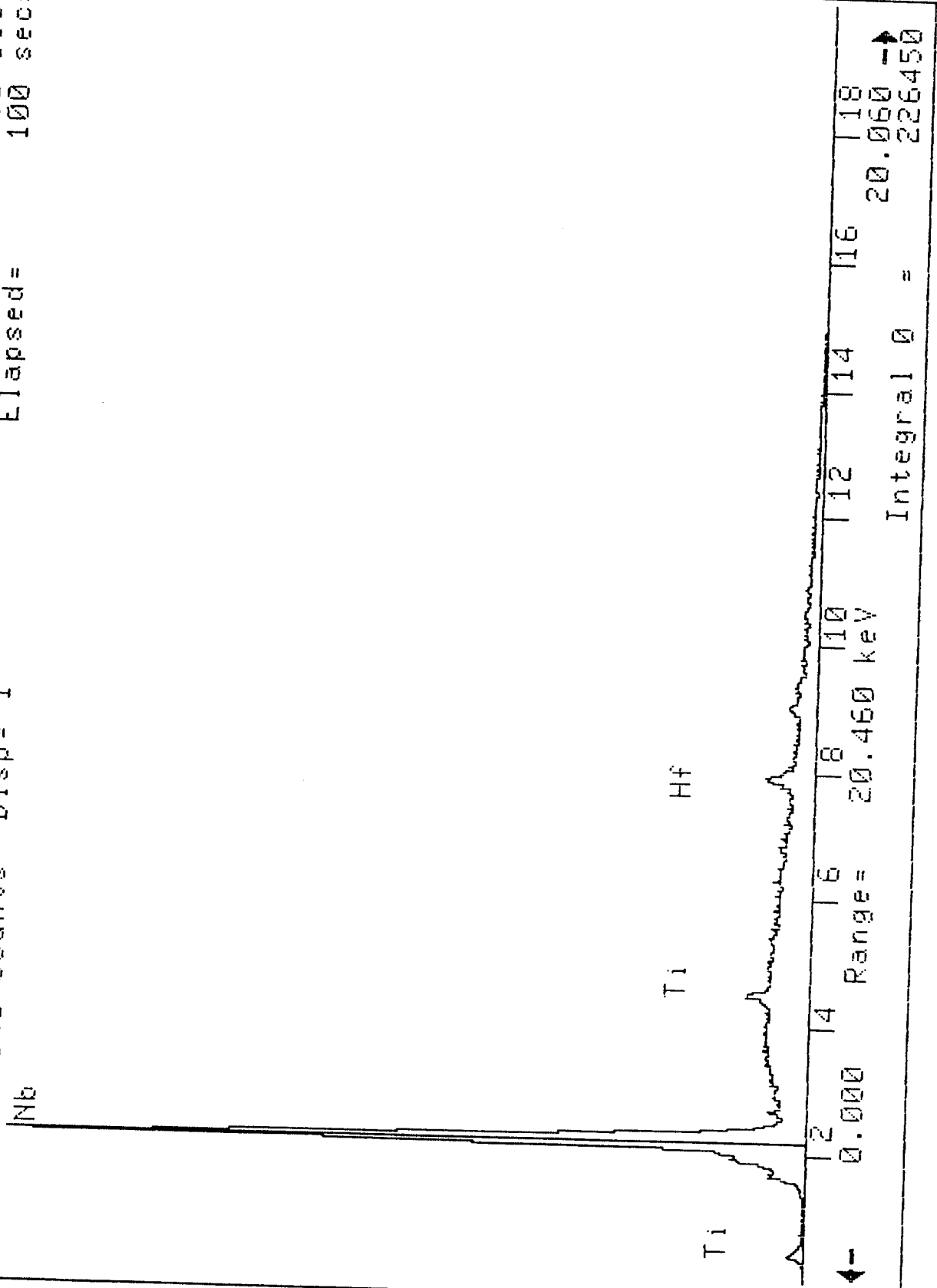
```

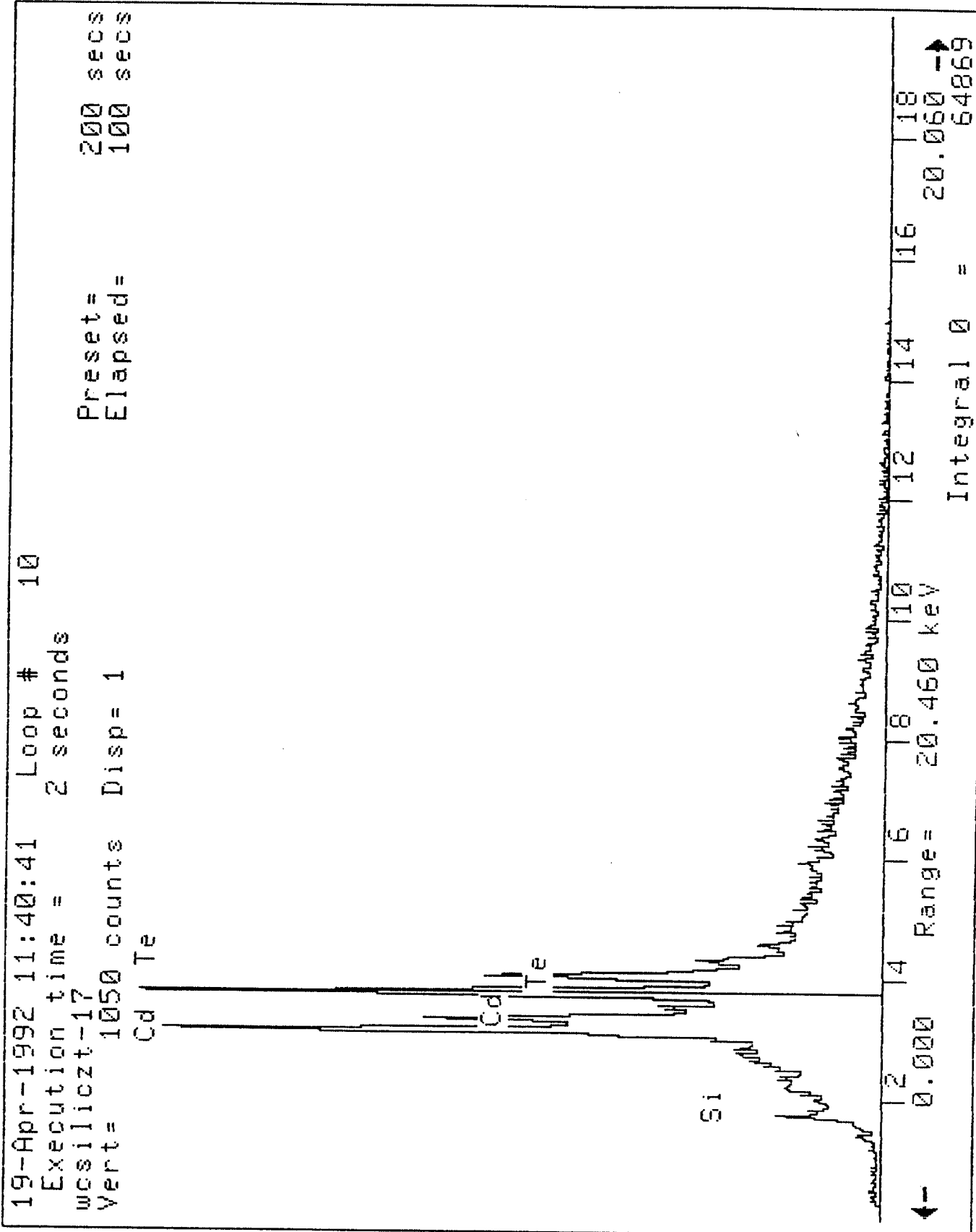


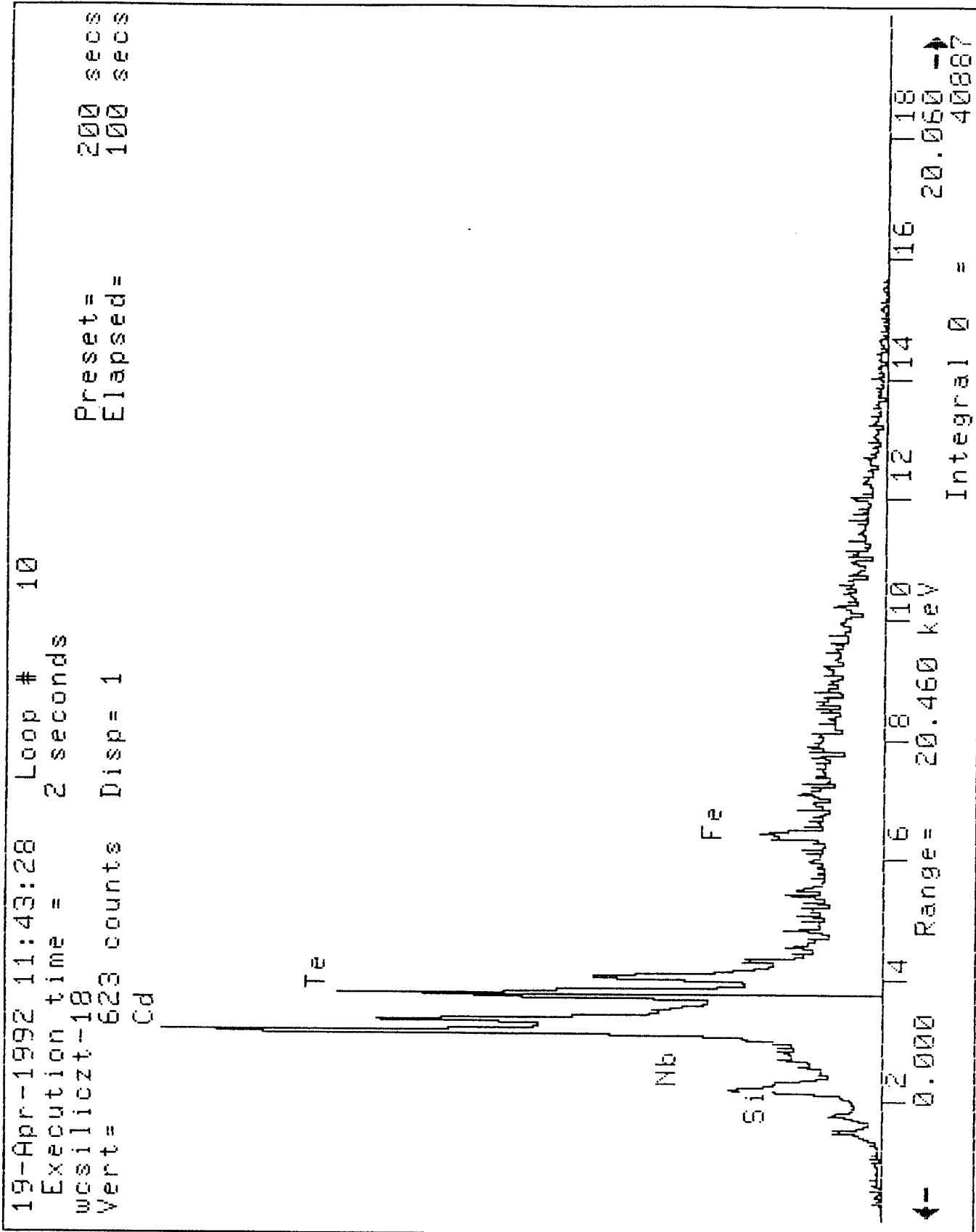
```

Preset =
Elapsed =
200  200  200
sec  sec  sec

```







**Chemical Compatibility of GaAs with Silicide Coated WC-103
and Hot Pressed Boron Nitride**

Addendum to:

Progress Report

on:

**Chemical Compatibility Studies
of GaAs & CdZnTe
with WC-103 & T2M**

by:

**Rosalia N. Andrews, Ph.D., P.E.
Sherrie A. Beske, Research Assistant
Department of Materials Science and Engineering
University of Alabama at Birmingham
Birmingham, Alabama 35294**

April 1, 1993

**Original Progress Report:
February 10, 1992**

Introduction

The following report summarizes the results obtained for the GaAs/silicide coated WC-103 and GaAs/hot pressed boron nitride compatibility tests run at 1260°C for 24 hours. WC-103 test coupons of 10.110 x 10.120 x 5.044 mm and hot pressed BN test coupons of 10.000 x 9.995 x 5.000 mm were obtained from Southern Research Institute. The WC-103 coupon surfaces were polished using a procedure identical to that discussed in the initial report submitted on February 10, 1992. This initial report should be referred to for details on experimental procedure. Following surface preparation of the WC-103, test coupons were sent to HITEMCO for silicide coating. Samples were given a heat treatment by HITEMCO of one hour at 1566°C (2850°F) after coating to ensure bonding of the silicide coating. Two surfaces of the hot pressed BN coupons were abraded with #98 Scotch Brite and rinsed three times with methanol. The coupons were then heated with a heat gun to remove any residual methanol.

Sample/semiconductor compatibility tests were accomplished by immersion of the test coupons in molten GaAs for 24 hours at 1260°C using a procedure identical to that discussed in the report of February 10, 1992.

24 hour GaAs/Silicide Coated WC-103 Compatibility Test

An optical micrograph of the reaction zone observed for the 24 hour GaAs/silicide coated WC-103 couple is shown in Figure 1. The initial thickness of the bare metal was ~4.932 mm. A silicide coating of ~0.056 mm (2.205 mils) was applied to each side of the coupon. The total thickness of the coated metal coupon was thus 5.044 mm. The final thickness of the remaining metal coupon after the compatibility test was ~4.757 mm. The total loss of coupon thickness was 0.287 mm (11.299 mils). Considering attack from one side of the sample, as would be seen in a cartridge assembly, this amounts to a thickness loss of 0.144 mm (5.565 mils).

After completion of the compatibility test, no silicide coating could be found using EDS analysis. Several locations in the pure semiconductor, the reaction product, and in the metal were analyzed. No traces of silicon, iron, or chromium, the principle components of the silicide coating, were found at any of the locations. Traces of arsenic were found in the metal coupon, with the concentration of arsenic becoming negligible at ~ 0.07 mm (2.76 mils) away from the interface. See Figure 2 and EDS plots 1-12.

The silicide coating did not prevent GaAs attack of the WC-103. On exposure to molten GaAs for 24 hours at 1260°C, a 27 mil thick WC-103 cartridge with a 2.205 mil thick silicide coating (total thickness 29.205 mils) would experience approximately a 20% reduction in thickness. Also, there would be arsenic penetration into 0.07 mm (2.76 mils) of the remaining metal thickness.

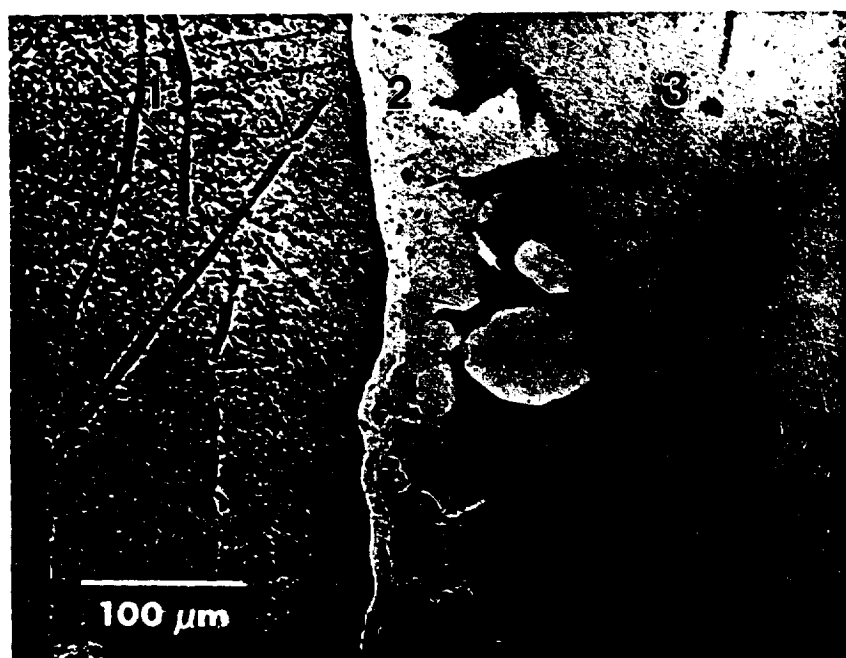


Figure 1. Metal/silicide coating/semiconductor interface in a GaAs/silicide coated WC-103 compatibility test carried out for 24 hours at 1260°C. 1=metal, 2=reaction zone, and 3=semiconductor



Figure 2. SEM micrograph of GaAs/silicide coated WC-103 tested for 24 hours at 1260°C. Numbers indicate where compositional analysis was performed.

24 hour GaAs/Hot Pressed BN Compatibility Test

The GaAs/hot pressed BN couple as removed from the boat after the compatibility test is shown in Figure 3. On initial observation, it did not appear that the ceramic coupon was wet by the GaAs. An optical micrograph of the semiconductor/BN interface for the 24 hour GaAs/hot pressed BN couple is shown in Figure 4. There did not appear to be any visible reaction product. The original thickness of the hot pressed BN coupon was 5.000 mm. The final thickness of the coupon was ~ 5.000 mm. Thus, no loss in material thickness occurred due to exposure to GaAs.

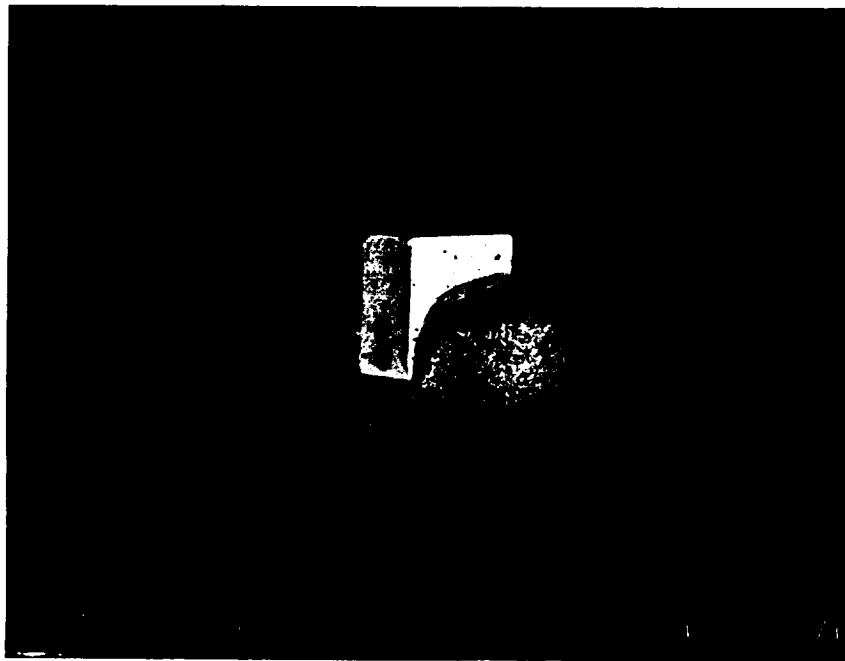


Figure 3. GaAs/hot pressed BN couple after compatibility test carried out for 24 hours at 1260°C.

The semiconductor/BN interface was examined using EDS analysis. Traces of arsenic were found at 0.21 mm into the ceramic coupon, but at 0.30 mm, the traces of arsenic became negligible. Binding elements used in hot pressed BN were also found throughout the ceramic coupon. See Figure 5 and EDS plots 13-22.

There did not appear to be any visible reaction between GaAs and the hot pressed BN. For a 27 mil thick BN cartridge exposed to molten GaAs at 1260°C for 24 hours, there would be no reduction in thickness. There would, however, be traces of arsenic penetration up to 0.30 mm (11.81 mils) into the cartridge.



Figure 4. Semiconductor/ceramic interface in a GaAs/hot pressed BN compatibility test carried out for 24 hours at 1260°C. 1=Hot pressed BN, 3=semiconductor.

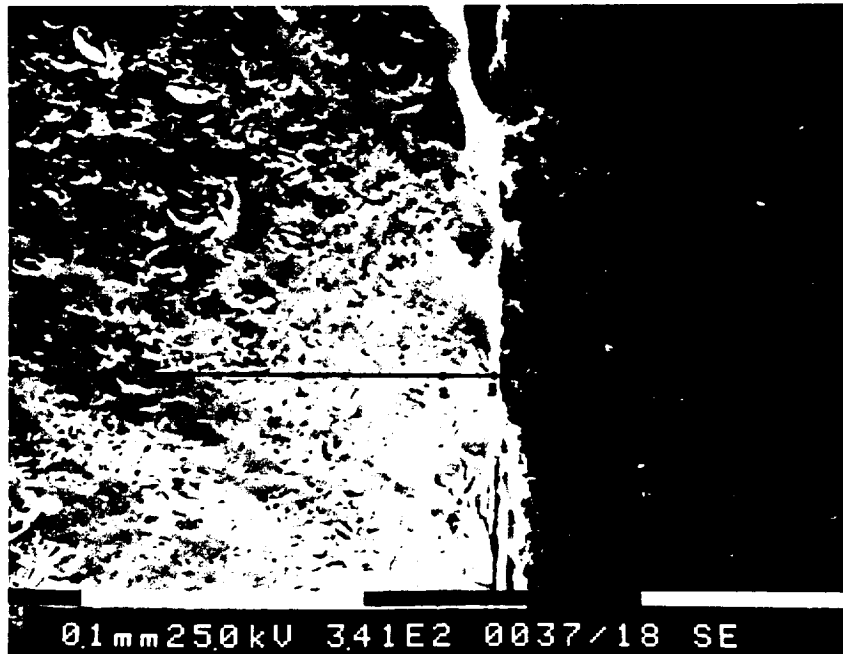


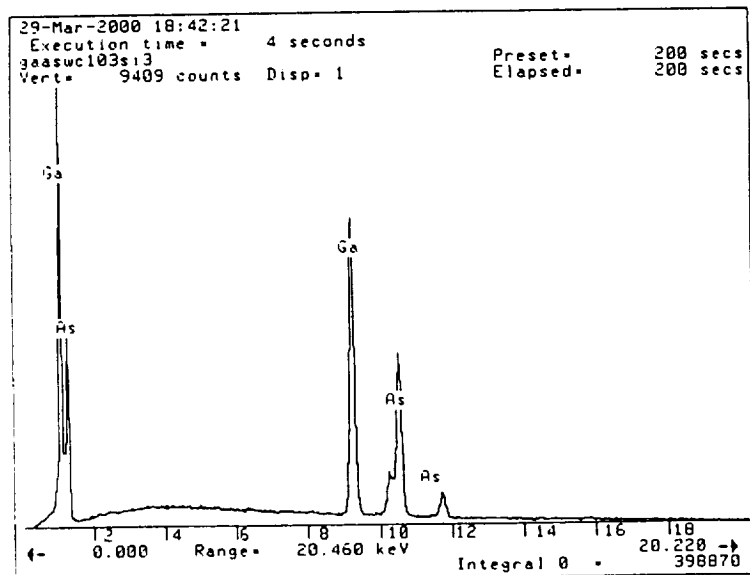
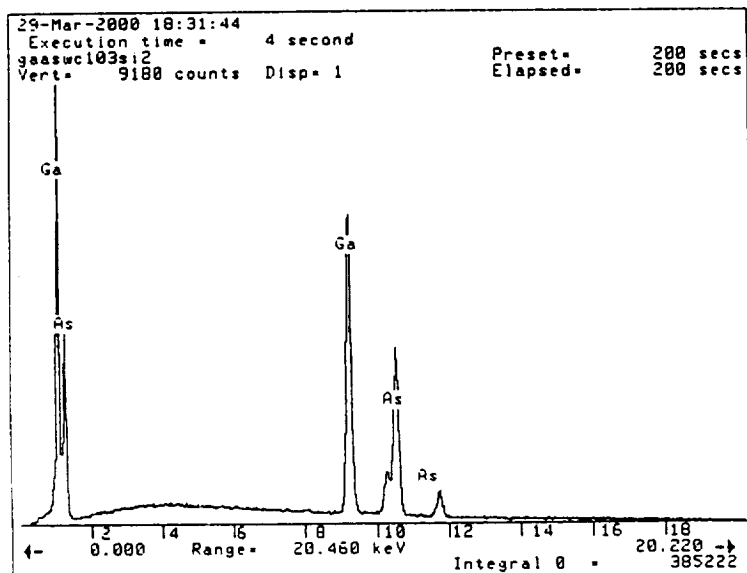
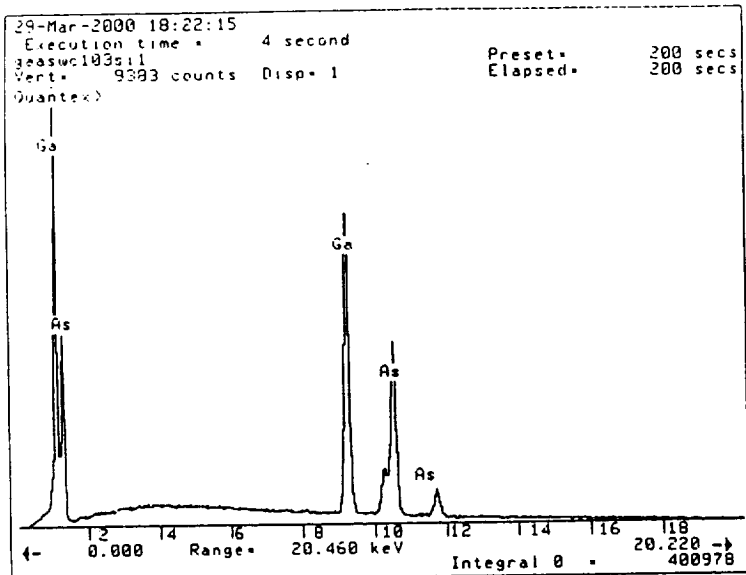
Figure 5. SEM micrograph of GaAs/hot pressed BN tested for 24 hours at 1260°C. Numbers indicate where compositional analysis was performed.

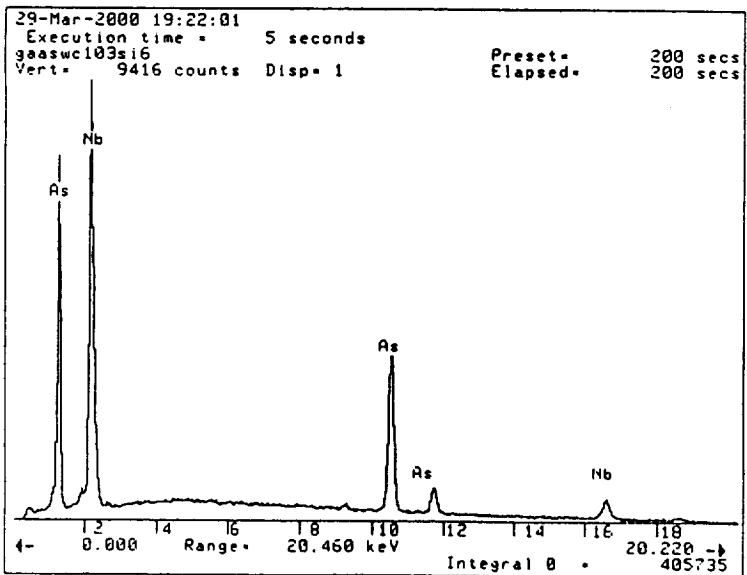
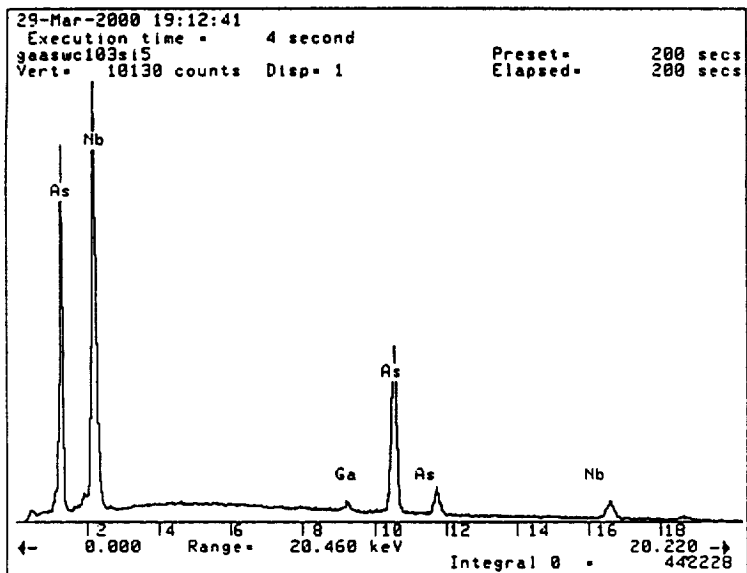
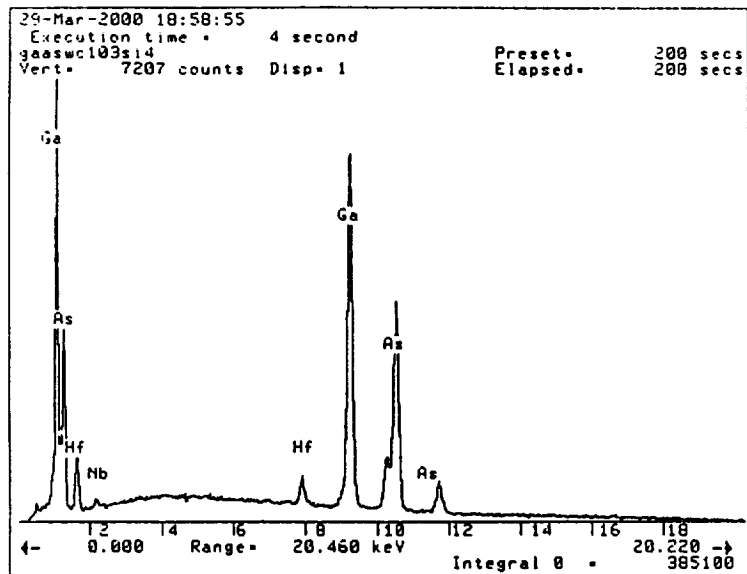
Summary of Findings

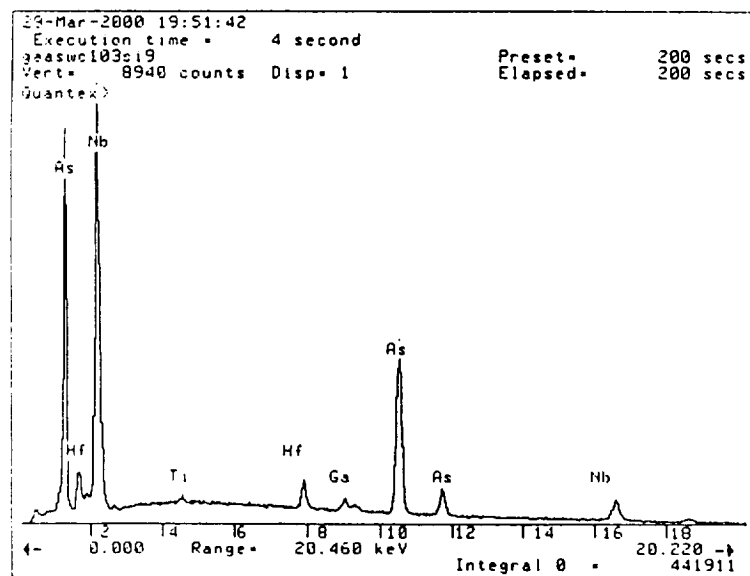
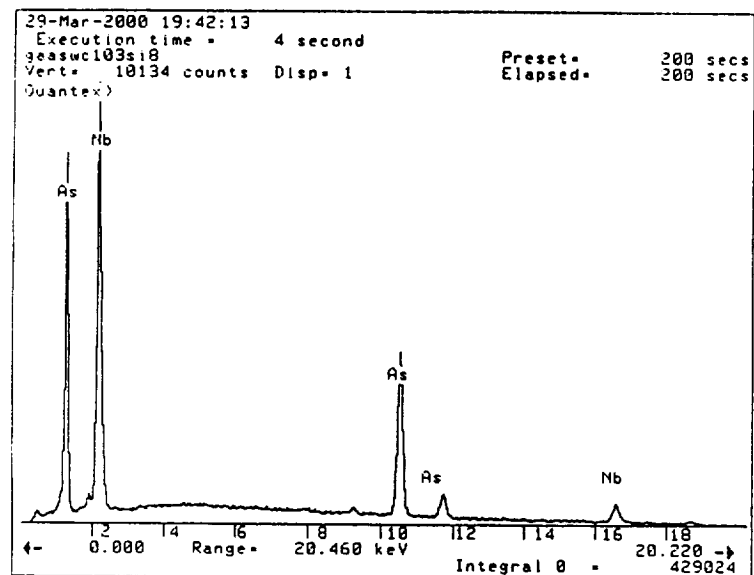
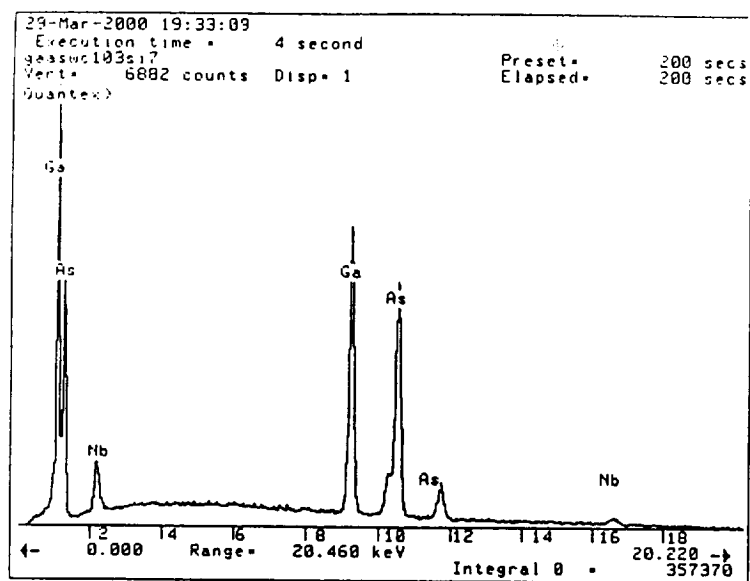
- 1) The silicide coating tested in this study did not prevent GaAs attack of the WC-103. The metal was attacked by the semiconductor and the reaction products were observed to break off and float into the surrounding semiconductor (a result similar that obtained in the uncoated GaAs\WC-103 compatibility tests). On exposure to GaAs for 24 hours at 1260°C, a 27 mil thick WC-103 cartridge with a 2.205 mil thick silicide coating (total thickness of 29.205 mils) would experience approximately a 20% reduction in thickness. Also, there would be arsenic penetration into 0.07 mm (2.76 mils) of the remaining metal thickness.

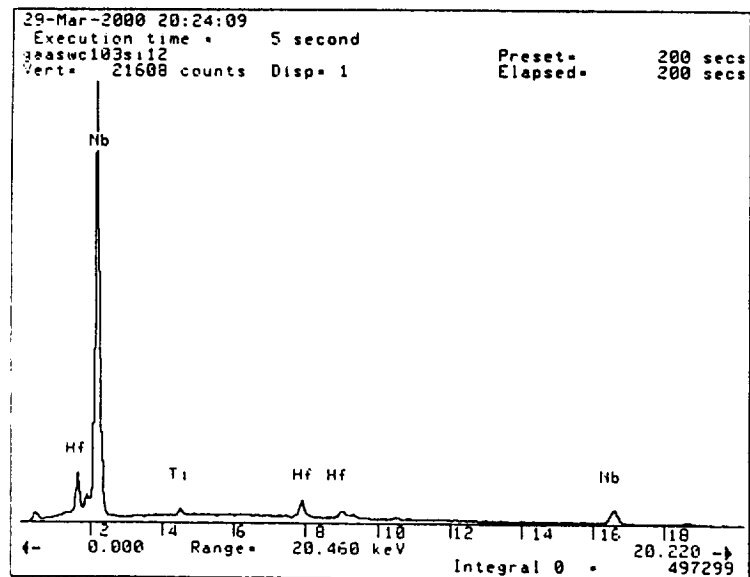
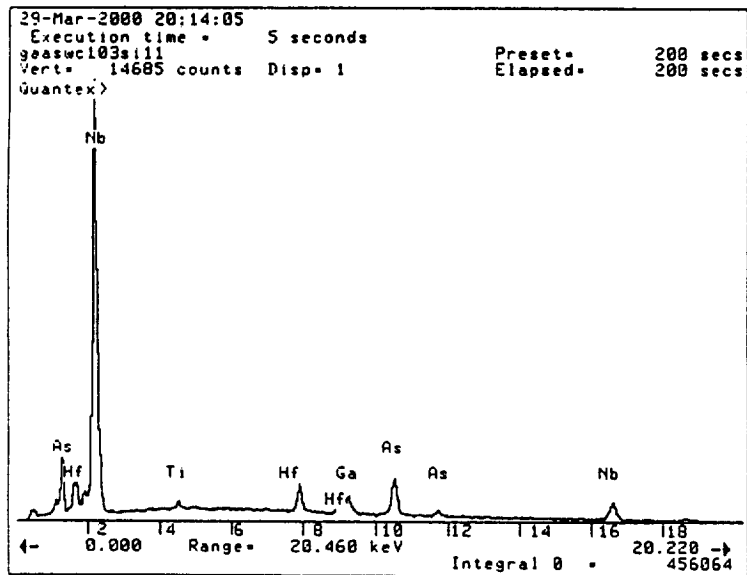
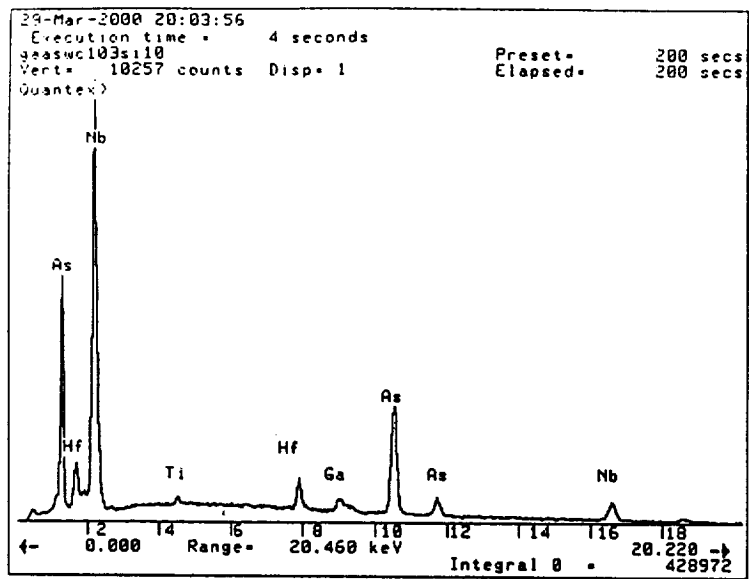
- 2) There did not appear to be any visible reaction between GaAs and the hot pressed BN. For a 27 mil thick BN cartridge exposed to molten GaAs at 1260°C for 24 hours, no reduction in thickness of the BN is expected. There would, however, be traces of arsenic penetration up to 0.30 mm (11.81 mils) into the cartridge.

Plots 1-12. Compositional spectra across the semiconductor/metal interface of a GaAs/silicide coated WC-103 reaction couple tested at 1260°C for 24 hours.

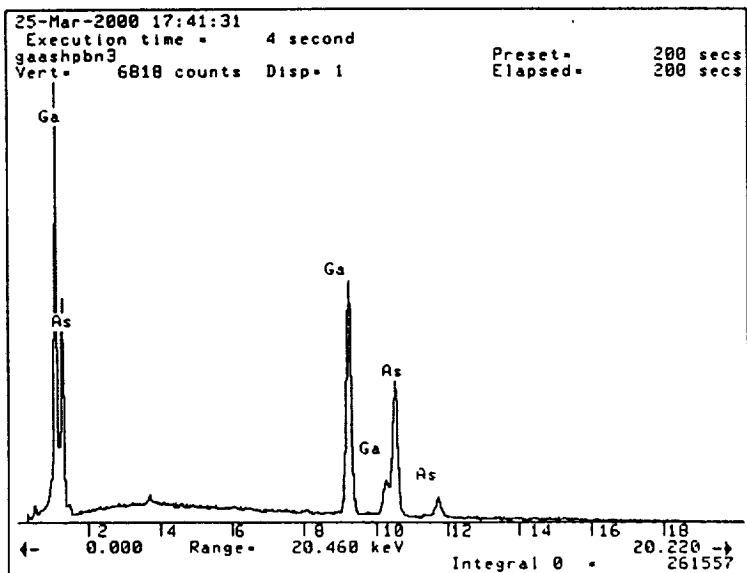
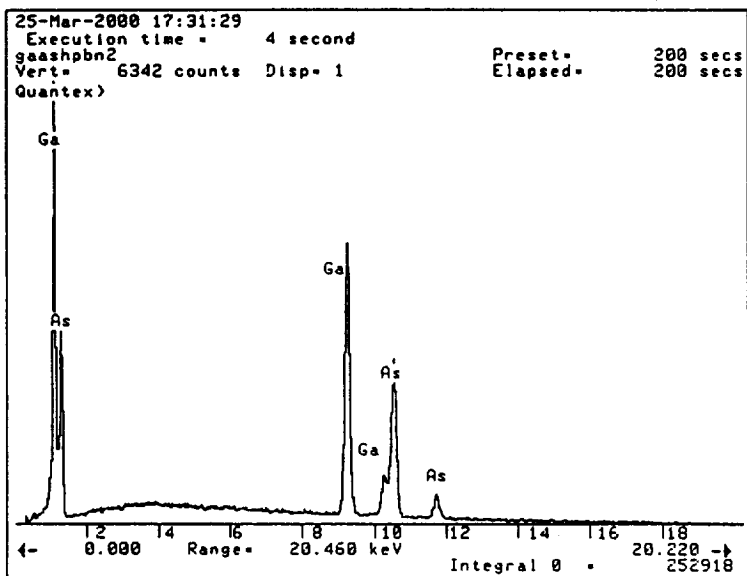
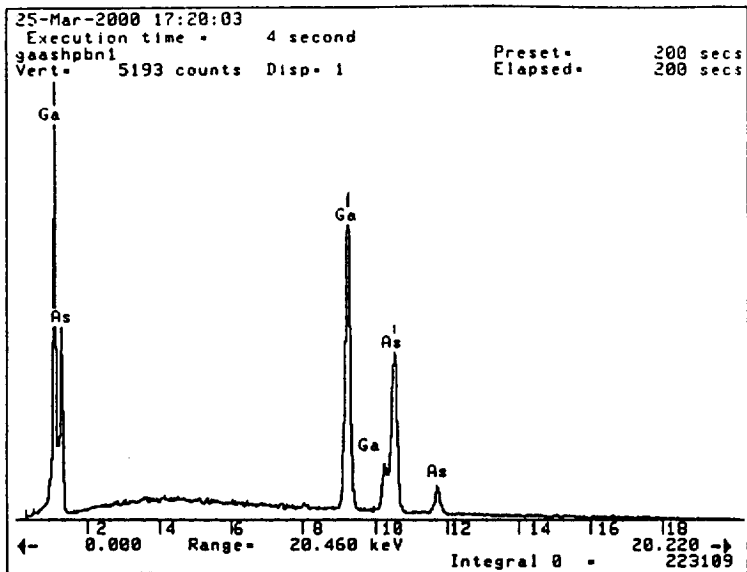


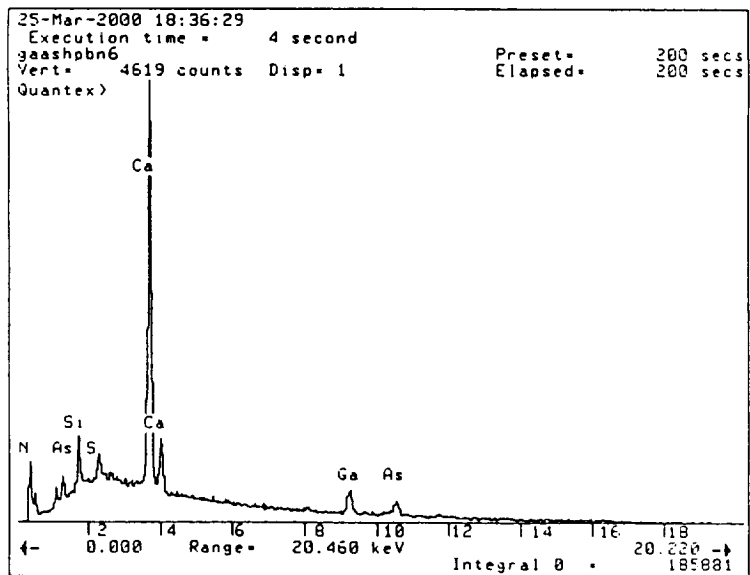
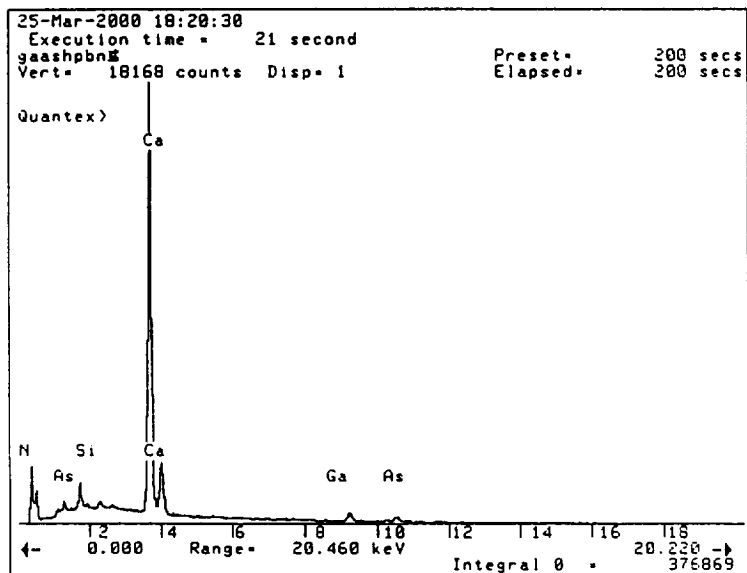
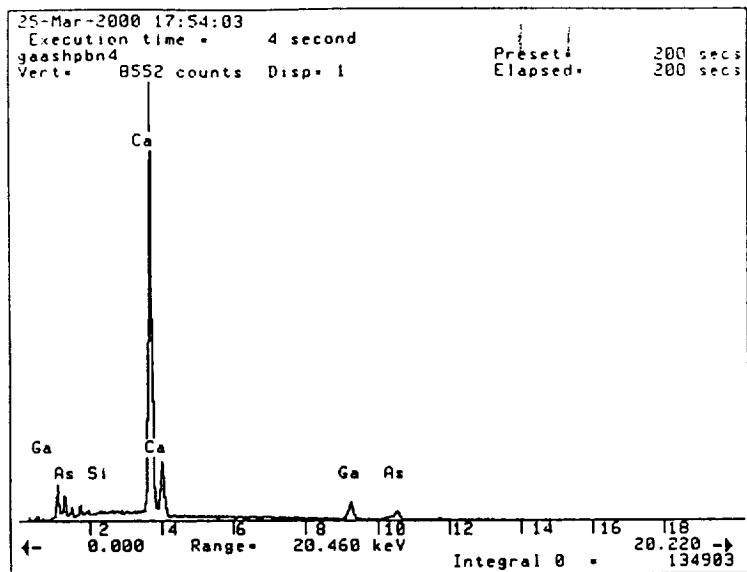


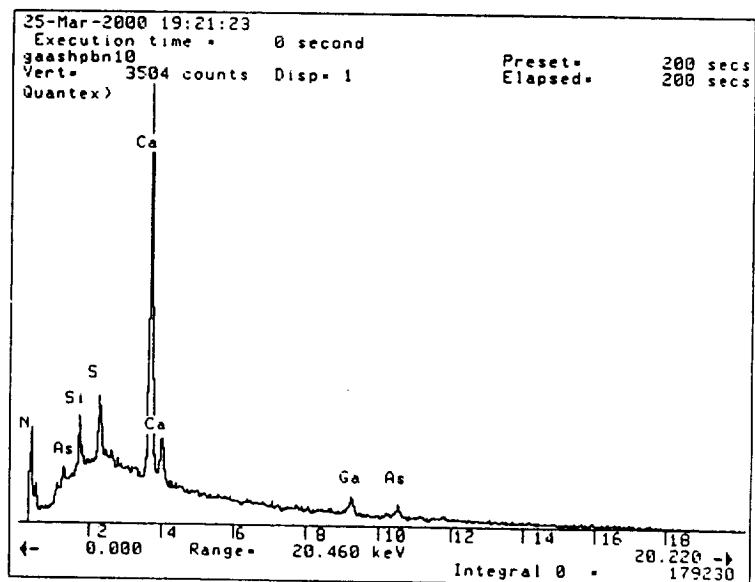
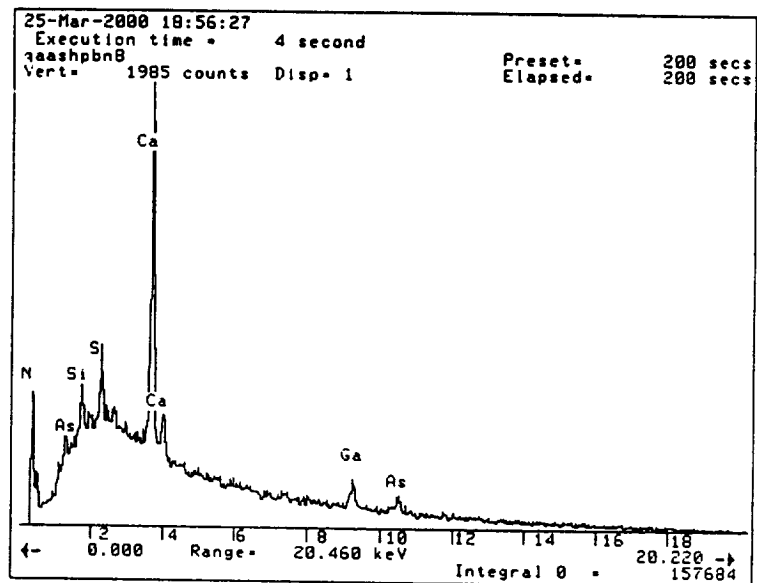
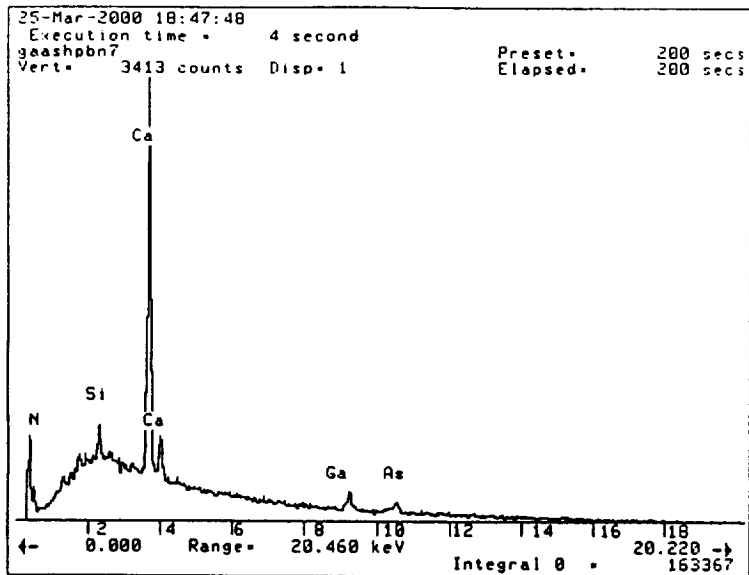


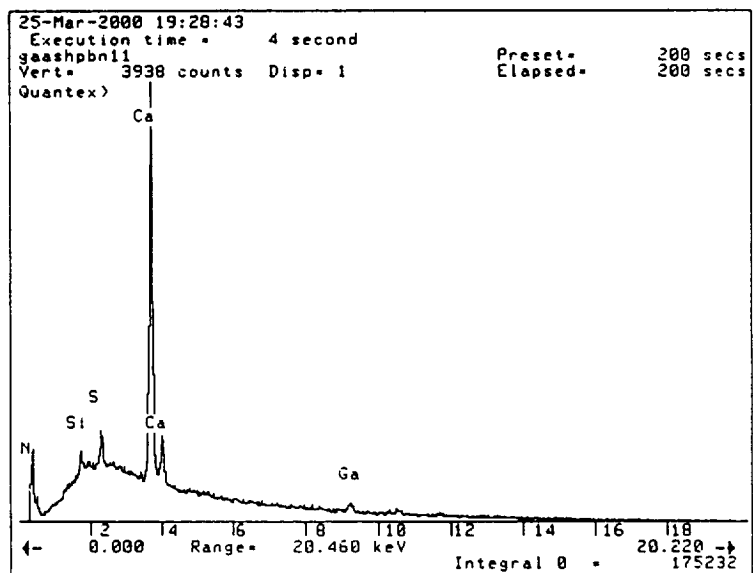


Plots 13-22. Compositional spectra across the semiconductor /ceramic interface of a GaAs/hot pressed boron nitride reaction couple tested at 1260°C for 24 hours.









APPENDIX B

CGF CARTRIDGE CANDIDATE METALS AND METAL ALLOYS

Material ***IRIDIUM***

Density (gm/cm³) 22.50 **Melting Point (°C)** 2410

Hardness (Brinell) 351

Temperature (°C)	RT	100	627	927	1227			
Thermal Conductivity (W / m – °K)	147.1	145.4	128.9	119.9	110.9			

Temperature (°C)	127	727	1327	1927	2227		
Linear Thermal Expansion (10 ⁻³ cm/cm)	0.70	5.35	10.68	17.58	21.78		

Temperature (°C)	RT			
Modulus of Elasticity (x 10 ³ MPa)	544.7			

Temperature (°C)	RT			
Ultimate Tensile Strength (MPa)	1999			

Temperature (°C)	RT			
Yield Strength (MPa)				

NOTES: Most corrosion-resistant element known. Very brittle.

Material**IRIDIUM****Density (lb/in³)**

0.8129

Melting Point (°F)

4370

Hardness (Brinell)

351

Temperature (°F)	RT	212	1161	1701	2241			
Thermal Conductivity (Btu – in / h – ft ² – °F)	1020	1008	894	831	769			

Temperature (°F)	261	1341	2421	3501	4041		
Linear Thermal Expansion (10 ⁻³ in / in)	0.70	5.35	10.68	17.58	21.78		

Temperature (°C)	RT			
Modulus of Elasticity (MSI)	79			

Temperature (°F)	RT			
Ultimate Tensile Strength (10 ³ psi)	290			

Temperature (°F)	RT			
Yield Strength (10 ³ psi)				

NOTES: Most corrosion-resistant element known. Very brittle.

Material

NIOBIUM

Density (gm/cm³)

8.57

Melting Point (°C) 2468

Hardness (Brinell)

114

Temperature (°C)	RT	100	627	927	1227	1627	1927	
Thermal Conductivity (W / m – °K)	53.7	54.5	62.8	67.5	72.2	77.9	81.5	

Temperature (°C)	127	727	1327	1927	2027		
Coefficient of Thermal Expansion (10 ⁻³ cm/cm)	0.78	5.61	11.02	16.87	17.88		

Temperature (°C)	RT			
Modulus of Elasticity (x 10 ³ MPa)	96.5			

Temperature (°C)	RT			
Ultimate Tensile Strength (MPa)	645			

Temperature (°C)	RT			
Yield Strength (MPa)	207			

NOTES: Oxidation above 230°C which causes brittleness.

Material**NIOBIUM****Density (lb/in³)**

0.3096

Melting Point (°F) 4474**Hardness (Brinell)**

114

Temperature (°F)	RT	212	1160	1700	2240	2960	3500	
Thermal Conductivity (Btu-in / h-ft² - °F)	372	378	435	468	501	540	565	

Temperature (°F)	261	1341	2421	3501	3681		
Coefficient of Thermal Expansion (10⁻³ in / in)	0.78	5.61	11.02	16.87	17.88		

Temperature (°F)	RT			
Modulus of Elasticity (Mpsi)	14.0			

Temperature (°F)	RT			
Ultimate Tensile Strength (10³ psi)	93.5			

Temperature (°F)	RT			
Yield Strength (10³ psi)	30			

NOTES: Oxidation above 446°F which causes brittleness.

Material

WC-103 (NIOBIUM ALLOY)

Density (gm/cm³)

8.86

Melting Point (°C) 2350

Hardness (Brinell)

Temperature (°C)	RT	815	954	1093	1232	1304	1371	
Thermal Conductivity (W / m - °K)		38	40	42.4	44.1	44.6	49.3	

Temperature (°C)	127	727	1327	1927	2027		
Linear Thermal Expansion (10 ⁻³ cm/cm)							

Temperature (°C)	RT	982	1093	1482
Modulus of Elasticity (x 10 ³ MPa)	90.3	92.4	84.8	24.8

Temperature (°C)	RT	538	1093	1482
Ultimate Tensile Strength (MPa)	420	310	188	65.5

Temperature (°C)	RT	538	1093	1371
Yield Strength (MPa)	276	176	124	62

NOTES: Extensive oxidation above 230°C.

Material

WC-103 (NIOBIUM ALLOY)

Density (lb/in³)

0.3201

Melting Point (°F) 4262

Hardness (Brinell)

Temperature (°F)	RT	1500	1750	2000	2250	2380	2500
Thermal Conductivity (Btu-in / h-ft ² -°F)		264	277	294	306	309	342

Temperature (°F)	260	1340	2420	3500	3680		
Linear Thermal Expansion (10 ⁻³ in / in)							

Temperature (°F)	RT	1800	2000	2700
Modulus of Elasticity (Mpsi)	13.1	13.4	12.3	3.6

Temperature (°F)	RT	1000	2000	2700
Ultimate Tensile Strength (10 ³ psi)	61	45	27	9.5

Temperature (°F)	RT	1000	2000	2500
Yield Strength (10 ³ psi)	40	26	18	9

NOTES: Extensive oxidation above 446°F.

Material *PLATINUM*

Density (gm/cm³) 21.5 **Melting Point (°C)** 1772

Hardness (Brinell) 106

Temperature (°C)	RT	100	627	927	1227	1527		
Thermal Conductivity (W / m – °K)	71.5	71.5	77.0	82.6	89.7	97.3		

Temperature (°C)	127	727	1327	1627			
Linear Thermal Expansion (10 ⁻³ cm/cm)	0.96	6.99	14.14	18.37			

Temperature (°C)	RT			
Modulus of Elasticity (x 10 ³ MPa)	172.4			

Temperature (°F)	RT			
Ultimate Tensile Strength (MPa)	206.8			

Temperature (°F)	RT			
Yield Strength (MPa)	186.2			

NOTES: High oxidation resistance ; Ductile at room temperature.

Material *PLATINUM*

Density (lb/in³) 0.7767 **Melting Point (°F)** 3222

Hardness (Brinell) 106

Temperature (°F)	RT	212	1160	1700	2240	2780		
Thermal Conductivity (Btu – in / h – ft ² – °F)	496	496	534	573	622	675		

Temperature (°F)	260	1340	2420	2960			
Linear Thermal Expansion (10 ⁻³ in / in)	0.96	6.99	14.14	18.37			

Temperature (°F)	RT			
Modulus of Elasticity (Mpsi)	25.0			

Temperature (°F)	RT			
Ultimate Tensile Strength (10 ³ psi)	30.0			

Temperature (°F)	RT			
Yield Strength (10 ³ psi)	27.0			

NOTES: High oxidation resistance ; Ductile at room temperature.

Material

PLATINUM / 20% IRIDIUM

Density (gm/cm³)

Melting Point (°C)

Hardness (Brinell)

Temperature (°C)	RT							
Thermal Conductivity (W / m – °K)	17.6							

Temperature (°C)	127						
Linear Thermal Expansion (10 ⁻³ cm/cm)							

Temperature (°C)	RT			
Modulus of Elasticity (x 10 ³ MPa)				

Temperature (°C)	RT			
Ultimate Tensile Strength (MPa)	641.2			

Temperature (°C)	RT			
Yield Strength (MPa)				

NOTES: Not commercially available in large quantities.

Material

PLATINUM / 20% IRIDIUM

Density (lb/in³)

Melting Point (°F)

Hardness (Brinell)

Temperature (°F)	RT							
Thermal Conductivity (Btu – in / h – ft ² – °F)	122							

Temperature (°F)	261						
Linear Thermal Expansion (10 ⁻³ in / in)							

Temperature (°F)	RT			
Modulus of Elasticity (Mpsi)				

Temperature (°F)	RT			
Ultimate Tensile Strength (10 ³ psi)	93.0			

Temperature (°F)	RT			
Yield Strength (10 ³ psi)				

NOTES: Not commercially available in large quantities.

Material *PLATINUM / 20% RHODIUM*

Density (gm/cm³) 18.7 **Melting Point (°C)**

Hardness (Brinell)

Temperature (°C)	RT							
Thermal Conductivity (W / m - °K)								

Temperature (°C)	127						
Linear Thermal Expansion (10 ⁻³ cm/cm)							

Temperature (°C)	RT			
Modulus of Elasticity (x 10 ³ MPa)				

Temperature (°C)	RT			
Ultimate Tensile Strength (MPa)	482.6			

Temperature (°C)	RT			
Yield Strength (MPa)				

NOTES: Not commercially available in large quantities.

Material

PLATINUM / 20% RHODIUM

Density (lb/in³)

0.6756

Melting Point (°F)

Hardness (Brinell)

Temperature (°F)	RT							
Thermal Conductivity (Btu – in / h – ft ² – °F)								

Temperature (°F)	261						
Linear Thermal Expansion (10 ⁻³ in / in)							

Temperature (°F)	RT			
Modulus of Elasticity (Mpsi)				

Temperature (°F)	RT			
Ultimate Tensile Strength (10 ³ psi)	70.0			

Temperature (°F)	RT			
Yield Strength (10 ³ psi)				

NOTES: Not commercially available in large quantities.

Material ***RHENIUM*****Density (gm/cm³)** 21.0 **Melting Point (°C)** 3180**Hardness (Brinell)** 555

Temperature (°C)	RT	100	627	927	1227	1627	2327	
Thermal Conductivity (W / m – °K)	48.3	46.7	44.3	45.7	47.8	50.9	59.2	

Temperature (°C)	127	727	1327	1927	2527		
Linear Thermal Expansion (10 ⁻³ cm/cm)	0.67	4.60	8.96	13.86	19.41		

Temperature (°C)	RT	871		
Modulus of Elasticity (x 10 ³ MPa)	468.8	375.8		

Temperature (°C)	RT	871	1316	
Ultimate Tensile Strength (MPa)	1931	924	455	

Temperature (°C)	RT			
Yield Strength (MPa)	1862			

NOTES: Rapid oxidation over 593°C ; High melting point and brittle intermetallic formation make welding dissimilar materials difficult ; Ductile at room temperature ; Accomodates large thermal expansion mismatches ; Can be diffusion bonded, electron-beam welded, brazed and soldered.

Material***RHENIUM*****Density (lb/in³)**

0.7587

Melting Point (°F)

5756

Hardness (Brinell)

555

Temperature (°F)	RT	212	1161	1701	2241	2961	4221	
Thermal Conductivity (Btu – in / h – ft ² – °F)	334.9	323.8	307.1	316.9	331.4	352.9	410.5	

Temperature (°F)	261	1341	2421	3501	4581		
Linear Thermal Expansion (10 ⁻³ in / in)	0.67	4.60	8.96	13.86	19.41		

Temperature (°F)	RT	1600		
Modulus of Elasticity (Mpsi)	68.0	54.4		

Temperature (°F)	RT	1600	2401	
Ultimate Tensile Strength (10 ³ psi)	280	134	66	

Temperature (°F)	RT			
Yield Strength (10 ³ psi)	270			

NOTES: Rapid oxidation over 1099°F ; High melting point and brittle intermetallic formation make welding dissimilar materials difficult ; Ductile at room temperature ; Accomodates large thermal expansion mismatches ; Can be diffusion bonded, electron-beam welded, brazed and soldered.

Material***RHODIUM*****Density (gm/cm³)** 12.4 **Melting Point (°C)** 1966**Hardness (Brinell)** 401

Temperature (°C)	RT	100	627	927	1127			
Thermal Conductivity (W / m – °L)	150.6	148.8	123.9	114.9	110.9			

Temperature (°C)	127	427	727	1327			
Linear Thermal Expansion (10 ⁻³ cm/cm)	0.91	3.78	7.12	15.26			

Temperature (°C)	RT			
Modulus of Elasticity (x 10 ³ MPa)	317.2			

Temperature (°C)	RT			
Ultimate Tensile Strength (MPa)	2068			

Temperature (°C)	RT			
Yield Strength (MPa)				

NOTES: Oxidizes slowly if heated in air.

Material***RHODIUM*****Density (lb/in³)**

0.4480

Melting Point (°F)

3571

Hardness (Brinell)

401

Temperature (°F)	RT	212	1161	1701	2061			
Thermal Conductivity (Btu – in / h – ft² – °F)	1044	1032	859	797	769			

Temperature (°F)	261	801	1341	2421			
Linear Thermal Expansion (10⁻³ in / in)	0.91	3.78	7.12	15.26			

Temperature (°F)	RT			
Modulus of Elasticity (Mpsi)	46.0			

Temperature (°F)	RT			
Ultimate Tensile Strength (10³ psi)	300			

Temperature (°F)	RT			
Yield Strength (10³ psi)				

NOTES: Oxidizes slowly if heated in air.

Material *TANTALUM*

Density (gm/cm³) 16.6 **Melting Point (°C)** 2996

Hardness (Brinell) 237

Temperature (°C)	RT	100	627	927	1227	1627	1927	2727
Thermal Conductivity (W / m – °K)	57.5	54.5	59.9	60.9	62.1	63.7	64.7	66.5

Temperature (°C)	127	727	1327	1927	2527	2927	
Linear Thermal Expansion (10⁻³ cm/cm)	0.69	4.85	9.41	14.88	23.00	31.26	

Temperature (°C)	RT	871		
Modulus of Elasticity (x 10³ MPa)	186.2	179.3		

Temperature (°C)	RT	871	1316	
Ultimate Tensile Strength (MPa)	414	207	90	

Temperature (°C)	RT	871		
Yield Strength (MPa)	331	103		

NOTES: High purity Tantalum is ductile. A stable oxide film is formed below 300°C;
A protective coating is necessary for elevated temperature service in air above 982°C.

Material *TANTALUM*

Density (lb/in³) 0.5997 **Melting Point (°F)** 5425

Hardness (Brinell) 237

Temperature (°F)	RT	212	1161	1701	2241	2961	3501	4941
Thermal Conductivity (Btu-in / h-ft² - °F)	399	378	415	422	431	442	449	461

Temperature (°F)	261	1341	2421	3501	4581	5301	
Linear Thermal Expansion (10⁻³ in / in)	0.69	4.85	9.41	14.88	23.00	31.26	

Temperature (°F)	RT	1600		
Modulus of Elasticity (Mpsi)	27.0	26.0		

Temperature (°F)	RT	1600	2401	
Ultimate Tensile Strength (10³ psi)	60	30	13	

Temperature (°F)	RT	1600		
Yield Strength (10³ psi)	48	15		

NOTES: High purity Tantalum is ductile. A stable oxide film is formed below 572°F;
A protective coating is necessary for elevated temperature service in air above 1800°F.

Material**TANTALUM / 10% TUNGSTEN****Density (gm/cm³)**

16.8

Melting Point (°C)

3047

Hardness (Brinell)

Temperature (°C)	RT	100	1371	1527	1627	1927	2427	2927
Thermal Conductivity (W / m – °K)			56.0	54.0	52.6	48.5	41.5	34.6

Temperature (°C)	127	427	727	1327	1927		
Linear Thermal Expansion (10 ⁻³ cm/cm)	0.64	2.54	4.61	9.30	14.64		

Temperature (°C)	RT	871	1093	1316
Modulus of Elasticity (x 10 ³ MPa)	170.9	127.5	105.5	80.7

Temperature (°C)	RT	871	1093	1316
Ultimate Tensile Strength (MPa)	1130	676	538	398

Temperature (°C)	RT	871	1316	
Yield Strength (MPa)	1089	621	138	

NOTES: Tantalum / 10% Tungsten is attacked rapidly at high temperature by oxidizing environments. The alloy's ductility is relatively high at room temperature.

Material

TANTALUM / 10% TUNGSTEN

Density (lb/in³)

0.6069

Melting Point (°F)

5517

Hardness (Brinell)

Temperature (°F)	RT	212	2500	2781	2961	3501	4401	5301
Thermal Conductivity (Btu - in / h - ft² - °F)			388	374	365	336	288	240

Temperature (°F)	261	801	1341	2421	3501		
Linear Thermal Expansion (10⁻³ in / in)	0.64	2.54	4.61	9.30	14.64		

Temperature (°F)	RT	1600	2000	2401
Modulus of Elasticity (Mpsi)	24.8	18.5	15.3	11.7

Temperature (°F)	RT	1600	2000	2401
Ultimate Tensile Strength (10³ psi)	164	98	78	57.7

Temperature (°F)	RT	1600	2401	
Yield Strength (10³ psi)	158	90	20	

NOTES: Tantalum / 10% Tungsten is attacked rapidly at high temperature by oxidizing environments. The alloy's ductility is relatively high at room temperature.

Material

TANTALUM / RHENIUM

Density (gm/cm³)

Melting Point (°C)

Hardness (Brinell)

Temperature (°C)	RT							
Thermal Conductivity (W / m – °K)								

Temperature (°C)	127						
Linear Thermal Expansion (10 ⁻³ cm/cm)							

Temperature (°C)	RT			
Modulus of Elasticity (x 10 ³ MPa)				

Temperature (°C)	RT			
Ultimate Tensile Strength (MPa)				

Temperature (°C)	RT			
Yield Strength (MPa)				

NOTES: Not commercially available.

Material

TANTALUM / RHENIUM

Density (lb/in³)

Melting Point (°F)

Hardness (Brinell)

Temperature (°F)	RT							
Thermal Conductivity (Btu – in / h – ft ² – °F)								

Temperature (°F)	261						
Linear Thermal Expansion (10 ⁻³ in / in)							

Temperature (°F)	RT			
Modulus of Elasticity (Mpsi)				

Temperature (°F)	RT			
Ultimate Tensile Strength (10 ³ psi)				

Temperature (°F)	RT			
Yield Strength (10 ³ psi)				

NOTES: Not commercially available.

Material

TUNGSTEN

Density (gm/cm³)

19.24

Melting Point (°C) 3410

Hardness (Brinell)

443

Temperature (°C)	RT	100	627	927	1227	1327	1727	2727
Thermal Conductivity (W / m – °K)	178.3	167.2	124.1	114.9	109.0	107.0	100.0	91.4

Temperature (°C)	127	427	727	1327	1927	2527	
Linear Thermal Expansion (10 ⁻³ cm/cm)	0.48	1.88	3.39	6.61	10.20	14.69	

Temperature (°C)	RT	871		
Modulus of Elasticity (x 10 ³ MPa)	406.8	379.2		

Temperature (°C)	RT	871	1316	
Ultimate Tensile Strength (MPa)	1517	455	310	

Temperature (°C)	RT	871		
Yield Strength (MPa)	1517	103		

NOTES: Oxidizes rapidly above 704°C; Extremely brittle at room temperature; welding not recommended because of brittleness.

Material**TUNGSTEN****Density (lb/in³)**

0.6951

Melting Point (°F)

6170

Hardness (Brinell)

443

Temperature (°F)	RT	212	1161	1701	2241	2421	3141	4941
Thermal Conductivity (Btu – in / h – ft² – °F)	1236.2	1159.3	860.4	796.6	755.7	741.9	693.3	633.7

Temperature (°F)	261	801	1341	2421	3501	4581	
Linear Thermal Expansion (10⁻³ in / in)	0.48	1.88	3.39	6.61	10.20	14.69	

Temperature (°F)	RT	1600		
Modulus of Elasticity (Mpsi)	59	55		

Temperature (°F)	RT	1600	2401	
Ultimate Tensile Strength (10³ psi)	220	66	45	

Temperature (°F)	RT	1600		
Yield Strength (10³ psi)	220	15		

NOTES: Oxidizes rapidly above 1299°F ; Extremely brittle at room temperature ; welding not recommended because of brittleness.

Material

TUNGSTEN / 25% RHENIUM

Density (gm/cm³)

19.76

Melting Point (°C)

3121

Hardness (Brinell)

Temperature (°C)	RT	100	627	927	1227	1327	1527	1704
Thermal Conductivity (W / m – °K)		12.8	10.4	10.2	10.0	10.0	10.0	9.9

Temperature (°C)	127	427	727	1327	1927	2427	
Linear Thermal Expansion (10 ⁻³ cm/cm)	0.53	2.05	3.68	7.42	11.96	16.54	

Temperature (°C)	RT			
Modulus of Elasticity (x 10 ³ MPa)	413.7			

Temperature (°C)	RT	871	1316	
Ultimate Tensile Strength (MPa)	1669	1020	689	

Temperature (°C)	RT	871		
Yield Strength (MPa)	1551	965		

NOTES: Oxidizes rapidly above 704°C. The addition of Rhenium improves ductility, bendability, and strength. Room temperature ductility is retained even after recrystallization.

Material**TUNGSTEN / 25% RHENIUM****Density (lb/in³)**

0.7139

Melting Point (°F)

5650

Hardness (Brinell)

Temperature (°F)	RT	212	1161	1701	2241	2421	2781	3099
Thermal Conductivity (Btu-in / h-ft ² -°F)		88.7	72.1	70.7	69.3	69.3	69.3	68.6

Temperature (°F)	261	801	1341	2421	3501	4401	
Linear Thermal Expansion (10 ⁻³ in / in)	0.53	2.05	3.68	7.42	11.96	16.54	

Temperature (°F)	RT			
Modulus of Elasticity (Mpsi)	60.0			

Temperature (°F)	RT	1600	2401	
Ultimate Tensile Strength (10 ³ psi)	242	148	100	

Temperature (°F)	RT	1600		
Yield Strength (10 ³ psi)	1551	965		

NOTES: Oxidizes rapidly above 1299°F. The addition of Rhenium improves ductility, bendability, and strength. Room temperature ductility is retained even after recrystallization.

Material *TZM (Alloyed Molybdenum)*

Density (gm/cm³) 10.24 **Melting Point (°C)** 2610

Hardness (Brinell)

Temperature (°C)	RT	200	500	700	1000	1200	1500	2000
Thermal Conductivity (W / m – °K)	140.2	121.8	115.7	111.1	103.2	97.9	88.9	75.0

Temperature (°C)	100	700	1000	1200	1500	1700	2000
Linear Thermal Expansion (10⁻³ cm/cm)	0.92	3.75	5.83	7.42	9.79	11.67	14.58

Temperature (°C)	RT	871	1093	1316
Modulus of Elasticity (x 10³ MPa)	317.2	234.4	203.4	144.8

Temperature (°C)	RT	871	1316	
Ultimate Tensile Strength (MPa)	862	586	379	

Temperature (°C)	RT	871	1316	
Yield Strength (MPa)	793	379	276	

NOTES: Needs protection against oxidation at temperatures above 538°C.

Material *TZM (Alloyed Molybdenum)*

Density (lb/in³) 0.3699 **Melting Point (°F)** 4730

Hardness (Brinell)

Temperature (°F)	RT	392	932	1292	1832	2192	2732	3632
Thermal Conductivity (Btu – in / h – ft² – °F)	972.1	844.5	802.2	770.3	715.5	678.8	616.4	520.0

Temperature (°F)	212	1291	1832	2192	2732	3092	3632
Linear Thermal Expansion (10⁻³ in / in)	0.92	3.75	5.83	7.42	9.79	11.67	14.58

Temperature (°F)	RT	1600	1999	2401
Modulus of Elasticity (Mpsi)	46.0	34.0	29.5	21.0

Temperature (°F)	RT	1600	2401	
Ultimate Tensile Strength (10³ psi)	125	85	55	

Temperature (°F)	RT	1600	2401	
Yield Strength (10³ psi)	115	55	40	

NOTES: Needs protection against oxidation at temperatures above 1000°F.

APPENDIX C

CGF CARTRIDGE CANDIDATE CERAMIC MATERIALS

Material *ALUMINUM OXIDE (Polycrystalline)*

Density (gm/cm³) 3.98

Maximum Operating Temperature 1950°C

Temperature (°C)	RT	127	327	527	727	927	1227	1727
Thermal Conductivity (W / m – °K)	35.9	26.4	15.8	10.4	7.85	6.55	5.66	6.00

Temperature (°C)	127	227	327	527	727	1227	1727
Linear Thermal Expansion (10⁻³ cm/cm)	0.75	1.48	2.25	3.88	5.65	10.5	14.8

Temperature (°C)	RT	1000	2000			
Modulus of Elasticity (x 10³ MPa)	345	324	290			

Temperature (°C)	RT					
Ultimate Tensile Strength (MPa)	207					

NOTES: Excellent chemical stability in reducing atmosphere.
Cracks very easily with small thermal gradient.

Material *ALUMINUM OXIDE (Polycrystalline)*

Density (lb/in³) 0.1438

Maximum Operating Temperature 3542°F

Temperature (°F)	RT	261	621	981	1341	1701	2241	3141
Thermal Conductivity (Btu – in / h – ft² – °F)	248.9	183.0	109.5	72.1	54.4	45.4	39.2	41.6

Temperature (°F)	261	441	621	981	1341	2241	2961
Linear Thermal Expansion (10⁻³ in / in)	0.75	1.48	2.25	3.88	5.65	10.5	14.8

Temperature (°F)	RT	1832	3632			
Modulus of Elasticity (Mpsi)	50	47	42			

Temperature (°F)	RT					
Ultimate Tensile Strength (10³ psi)	30					

NOTES: Excellent chemical stability in reducing atmosphere.
Cracks very easily with small thermal gradient.

Material

ALUMINUM OXIDE with SiC WHISKERS

Density (gm/cm³)

Maximum Operating Temperature

Temperature (°C)								
Thermal Conductivity (W / m - °K)								

Temperature (°C)							
Linear Thermal Expansion (10 ⁻³ cm/cm)							

Temperature (°C)						
Modulus of Elasticity (x 10 ³ MPa)						

Temperature (°C)						
Ultimate Tensile Strength (MPa)						

NOTES: Material not commercially available.

Material

ALUMINUM OXIDE with SiC WHISKERS

Density (lb/in³)

Maximum Operating Temperature

Temperature (°F)								
Thermal Conductivity (Btu – in / h – ft ² – °F)								

Temperature (°F)							
Linear Thermal Expansion (10 ⁻³ in / in)							

Temperature (°F)						
Modulus of Elasticity (Mpsi)						

Temperature (°F)						
Ultimate Tensile Strength (10 ³ psi)						

NOTES: Material not commercially available.

Material ***BERYLLIUM OXIDE (ISOPRESSED)***

Density (gm/cm³) 2.85

Maximum Operating Temperature 2400°C

Temperature (°C)	RT	100	150	327	527	727	927	1227
Thermal Conductivity (W / m – °K)	251	188	146	111	70	47	33	21.5

Temperature (°C)	127	327	527	727	927	1227	1627
Linear Thermal Expansion (10⁻³ cm/cm)	0.70	2.20	3.93	5.86	7.99	11.5	16.8

Temperature (°C)	RT			
Modulus of Elasticity (x 10³ MPa)	345			

Temperature (°C)	RT	649	982	1093
Ultimate Tensile Strength (MPa)	152	120	89.6	72.3

NOTES: Excellent thermal shock resistance; excellent chemical stability in reducing atmosphere; health hazard to machine.

Material***BERYLLIUM OXIDE (ISOPRESSED)*****Density (lb/in³)** 0.1030**Maximum Operating Temperature** 4352°F

Temperature (°F)	RT	212	302	621	981	1341	1701	2241
Thermal Conductivity (Btu – in / h – ft² – °F)	1740	1303	1012	770	485	326	229	149

Temperature (°F)	261	621	981	1341	1701	2241	2961
Linear Thermal Expansion (10⁻³ in / in)	0.70	2.20	3.93	5.86	7.99	11.5	16.8

Temperature (°F)	RT			
Modulus of Elasticity (Mpsi)	50			

Temperature (°F)	RT	1200	1800	2000
Ultimate Tensile Strength (10³ psi)	22.0	17.4	13.0	10.5

NOTES: Excellent thermal shock resistance; excellent chemical stability in reducing atmosphere; health hazard to machine.

Material ***BORON NITRIDE (HP Grade)***

Density (gm/cm³) 1.90

Maximum Operating Temperature 1200°C

Temperature (°C)	RT	316	437	557	711	978		
Thermal Conductivity (W / m – °K)	31.0	27.2	26.8	26.3	26.0	25.6		

Temperature (°C)	127	327	527	727	927	1027	
Linear Thermal Expansion (10 ⁻³ cm/cm)	0.21	0.80	1.67	2.76	4.03	4.73	

Temperature (°C)	RT			
Modulus of Elasticity (x 10 ³ MPa)	46.8			

Temperature (°C)	RT			
Ultimate Tensile Strength (MPa)				

NOTES: In oxidizing atmospheres the performance at maximum temperatures is between 985°C and 1400°C. Moisture sensitive.

Material *BORON NITRIDE (HP Grade)*

Density (lb/in³) 0.0686

Maximum Operating Temperature 2192°F

Temperature (°F)	RT	601	819	1035	1312	1792		
Thermal Conductivity (Btu – in / h – ft² – °F)	215	188	186	182	180	177		

Temperature (°F)	261	621	981	1341	1701	1881	
Linear Thermal Expansion (10⁻³ in / in)	0.21	0.80	1.67	2.76	4.03	4.73	

Temperature (°F)	RT			
Modulus of Elasticity (Mpsi)	6.79			

Temperature (°F)	RT			
Ultimate Tensile Strength (10³ psi)				

NOTES: In oxidizing atmospheres the performance at maximum temperatures is between 1805°F and 2552°F. Moisture sensitive.

Material

CHROMIUM BONDED ALUMINUM OXIDE

Density (gm/cm³)

Maximum Operating Temperature

1371°C

Temperature (°C)	RT	100	150	327	527	727	927	1227
Thermal Conductivity (W / m – °K)	9.62							

Temperature (°C)	127	727	1327	1927	2027		
Linear Thermal Expansion (10 ⁻³ cm/cm)							

Temperature (°C)	RT			
Modulus of Elasticity (x 10 ³ MPa)	283			

Temperature (°C)	RT			
Ultimate Tensile Strength (MPa)	145			

NOTES: Cracks easily with small thermal gradient.

Material

CHROMIUM BONDED ALUMINUM OXIDE

Density (lb/in³)

Maximum Operating Temperature

2500°F

Temperature (°F)	RT	212	302	621	981	1341	1701	2241
Thermal Conductivity (Btu – in / h – ft ² – °F)	67							

Temperature (°F)	261	1341	2421	3501	3681		
Linear Thermal Expansion (10 ⁻³ in / in)							

Temperature (°F)	RT			
Modulus of Elasticity (Mpsi)	41			

Temperature (°F)	RT			
Ultimate Tensile Strength (10 ³ psi)	21			

NOTES: Cracks easily with small thermal gradient.

Material **QUARTZ (Fused Silica)**

Density (gm/cm³) 2.65

Maximum Operating Temperature 1200°C

Temperature (°C)	100	350	500	700	900	1200	1300	
Thermal Conductivity (W / m – °K)	0.69	1.45	1.62	1.92	2.48	4.00	4.82	

Temperature (°C)	127	527	727	927	1027	1127	
Linear Thermal Expansion (10⁻³ cm/cm)	0.061	0.288	0.371	0.445	0.480	0.520	

Temperature (°C)	RT	500	900	
Modulus of Elasticity (x 10³ MPa)	71.1	74.5	76.7	

Temperature (°C)	RT	500	900	1100
Ultimate Tensile Strength (MPa)	79.3	105	158	113

NOTES:

Material **QUARTZ (Fused Silica)**

Density (lb/in³) 0.0957

Maximum Operating Temperature 2192°F

Temperature (°F)	212	662	932	1292	1652	2192	2372	
Thermal Conductivity (Btu – in / h – ft ² – °F)	4.78	10.0	11.2	13.3	17.2	27.7	33.4	

Temperature (°F)	261	981	1341	1701	1881	2061	
Linear Thermal Expansion (10 ⁻³ in / in)	0.061	0.288	0.371	0.445	0.480	0.520	

Temperature (°F)	RT	932	1652	
Modulus of Elasticity (Mpsi)	10.3	10.8	11.1	

Temperature (°F)	RT	932	1652	2012
Ultimate Tensile Strength (10 ³ psi)	11.5	15.2	22.9	16.4

NOTES:

Material *SILICON CARBIDE (Sintered Alpha)*

Density (gm/cm³) 3.10

Maximum Operating Temperature 1650°C

Temperature (°C)	RT	200	400	927	1227	1627	1927	
Thermal Conductivity (W / m – °K)	126	103	77.5					

Temperature (°C)	127	327	527	727	927	1327	1527
Linear Thermal Expansion (10⁻³ cm/cm)	0.41	1.26	2.19	3.21	4.31	6.68	7.95

Temperature (°C)	RT			
Modulus of Elasticity (x 10³ MPa)	407			

Temperature (°C)	RT			
Ultimate Tensile Strength (MPa)				

NOTES:

Material *SILICON CARBIDE (Sintered Alpha)*

Density (lb/in³) 0.1120

Maximum Operating Temperature 3002°F

Temperature (°F)	RT	392	752	1701	2241	2961	3501	
Thermal Conductivity (Btu – in / h – ft² – °F)	874	714	537					

Temperature (°F)	261	621	981	1341	1701	2421	2781
Linear Thermal Expansion (10⁻³ in / in)	0.41	1.26	2.19	3.21	4.31	6.68	7.95

Temperature (°F)	RT			
Modulus of Elasticity (Mpsi)	59			

Temperature (°F)	RT			
Ultimate Tensile Strength (10³ psi)				

NOTES:

Material *SILICON NITRIDE (Hot Pressed)*

Density (gm/cm³) 3.29

Maximum Operating Temperature 1650°C

Temperature (°C)	RT	100	627	927	1204	1627	1927	
Thermal Conductivity (W / m – °K)	25.0				16.0			

Temperature (°C)	127	327	527	727	927	1227	1327
Linear Thermal Expansion (10⁻³ cm/cm)	0.14	0.64	1.24	1.91	2.63	3.76	4.15

Temperature (°C)	RT			
Modulus of Elasticity (x 10³ MPa)	310			

Temperature (°C)	RT			
Ultimate Tensile Strength (MPa)				

Material *SILICON NITRIDE (Hot Pressed)*

Density (lb/in³) 0.1189

Maximum Operating Temperature 3002°F

Temperature (°F)	RT	212	1161	1701	2199	2961	3501	
Thermal Conductivity (Btu – in / h – ft² – °F)	173.3				110.9			

Temperature (°F)	261	621	981	1341	1701	2241	2421
Linear Thermal Expansion (10⁻³ in / in)	0.14	0.64	1.24	1.91	2.63	3.76	4.15

Temperature (°F)	RT			
Modulus of Elasticity (Mpsi)	45			

Temperature (°F)	RT			
Ultimate Tensile Strength (10³ psi)				

NOTES:

Material **ZIRCONIUM OXIDE (Sintered ; MgO Stabilized)**

Density (gm/cm³) 5.37

Maximum Operating Temperature 2500°C

Temperature (°C)	RT	100	600	900	1200	1627	1927	
Thermal Conductivity (W / m – °K)		1.84	2.05	2.13	2.26			

Temperature (°C)	127	327	527	727	927	1027	1127
Linear Thermal Expansion (10 ⁻³ cm/cm)	0.88	2.29	3.60	4.89	6.40	7.38	8.50

Temperature (°C)	RT			
Modulus of Elasticity (x 10 ³ MPa)	179			

Temperature (°C)	RT			
Ultimate Tensile Strength (MPa)	83			

NOTES: Good chemical stability in reducing atmosphere.
 Cracks easily with small thermal gradient.

Material *ZIRCONIUM OXIDE (Sintered ; MgO Stabilized)*

Density (lb/in³) 0.1940

Maximum Operating Temperature 4532°F

Temperature (°F)	RT	212	1112	1652	2192	2961	3501	
Thermal Conductivity (Btu – in / h – ft² – °F)		12.7	14.2	14.8	15.7			

Temperature (°F)	261	621	981	1341	1701	1881	2061
Linear Thermal Expansion (10⁻³ in / in)	0.88	2.29	3.60	4.89	6.40	7.38	8.50

Temperature (°F)	RT			
Modulus of Elasticity (Mpsi)	26			

Temperature (°F)	RT			
Ultimate Tensile Strength (10³ psi)	12			

NOTES: Good chemical stability in reducing atmosphere.
Cracks easily with small thermal gradient.

APPENDIX D

CANDIDATE CARTRIDGE MATERIALS SUMMARY TABLES

SELECTED PROPERTIES OF CANDIDATE REFRACTORY METALS *

Material	Density (g/cm ³)	Modulus of Elasticity (10 ³ MPa)	Ultimate Tensile Strength (MPa)	Yield Strength (MPa)	Linear Thermal Expansion ** (10 ⁻³ cm / cm)	Thermal Conductivity (W / m-K)	Melting Temp. (°C)
NIOBIUM	8.58	96.5	648	207	0.78 @ 127°C	53.7	2,468
WC-103 (NIOBIUM ALLOY)	8.86	90.3	421	276			2,350
IRIDIUM	22.5	545	1,999		0.70 @ 127°C	147	2,410
PLATINUM	21.5	206	207	186	0.96 @ 127°C	71.5	1,772
PLATINUM / 20% IRIDIUM			641			17.6	
PLATINUM / 20% RHODIUM	18.7		483				
RHENIUM	21.0	469	1,931	1,862	0.67 @ 127°C	48.3	3,180
RHODIUM	12.4	316	2,068	69	0.91 @ 127°C	151	1,966
TANTALUM	16.6	186	414	331	0.69 @ 127°C	57.5	2,996
TANTALUM / 10% TUNGSTEN	16.8	200	1,103	1,089	0.64 @ 127°C		3,047
TANTALUM / RHENIUM							
TUNGSTEN	19.2	407	1,517	1,517	0.48 @ 127°C	178	3,410
TUNGSTEN / 25% RHENIUM	19.8	414	1,669	1,551	0.53 @ 127°C		3,121
TZM	10.2	317	862	793	0.92 @ 100°C	140	2,610

* All values at room temperature unless otherwise noted.

** Referenced at room temperature

SELECTED PROPERTIES OF CANDIDATE REFRACTORY METALS *

Material	Density (lb/in ³)	Modulus of Elasticity (Mpsi)	Ultimate Tensile Strength (10 ³ psi)	Yield Strength (10 ³ psi)	Linear Thermal Expansion ** (10 ⁻³ in / in)	Thermal Conductivity (Btu-in/h-ft ² -°F)	Melting Temp. (°F)
NIOBIUM	0.310	14.0	94	30	0.78 @ 261°F	372.3	4,474
WC-103 (NIOBIUM ALLOY)	0.320	13.1	61	40			4,262
IRIDIUM	0.813	79.0	290		0.70 @ 261°F	1019.9	4,370
PLATINUM	0.775	29.9	30	27	0.96 @ 261°F	495.7	3,222
PLATINUM / 20% IRIDIUM			93			122.0	
PLATINUM / 20% RHODIUM	0.676		70				
RHENIUM	0.760	68.0	280	270	0.67 @ 261°F	334.9	5,756
RHODIUM	0.447	45.9	300	10	0.91 @ 261°F	1044.2	3,571
TANTALUM	0.600	27.0	60	48	0.69 @ 261°F	398.7	5,425
TANTALUM / 10% TUNGSTEN	0.608	29.0	160	158	0.64 @ 261°F		5,517
TANTALUM / RHENIUM							
TUNGSTEN	0.695	59.0	220	220	0.48 @ 261°F	1236.2	6,170
TUNGSTEN / 25% RHENIUM	0.714	60.0	242	225	0.53 @ 261°F		5,650
TZM	0.370	46.0	125	115	0.92 @ 212°F	972.1	4,730

* All values at room temperature unless otherwise noted.

** Referenced at room temperature

SELECTED PROPERTIES OF CANDIDATE CERAMIC MATERIALS *

Material	Density (g/cm ³)	Modulus of Elasticity (10 ³ MPa)	Ultimate Tensile Strength (MPa)	Linear Thermal Expansion ** (10 ⁻³ cm/cm)	Thermal Conductivity (W / m - K)	Maximum Service Temp. (°C)
ALUMINUM OXIDE	3.98	345	207	0.75 @ 127°C	35.9	1,950
ALUMINUM OXIDE WITH SiC FIBERS	3.77	417	323	0.50 @ 127°C		
BERYLLIUM OXIDE (ISOPRESSED)	2.85	345	152	0.70 @ 127°C	251	2,400
BORON NITRIDE (HP GRADE)	1.90	75.2		0.21 @ 127°C	31	1,200
CHROMIUM BONDED ALUMINUM OXIDE		283	145		9.62	1,371
QUARTZ (FUSED SILICA)	2.20	72.4		0.061 @ 127°C	1.53	1,200
SILICON CARBIDE (SINTERED ALPHA)	3.10	407		0.41 @ 127°C	126	1,650
SILICON NITRIDE (HOT PRESSED)	3.29	310		0.14 @ 127°C	25	1,650
ZIRCONIUM OXIDE (SINTERED ; MgO)	5.37	179	83	0.88 @ 127°C		2,500

* All properties at room temperature unless otherwise noted.

** Referenced at room temperature

SELECTED PROPERTIES OF CANDIDATE CERAMIC MATERIALS *

Material	Density (lb/in ³)	Modulus of Elasticity (Mpsi)	Ultimate Tensile Strength (10 ³ psi)	Linear Thermal Expansion ** (10 ⁻³ in/in)	Thermal Conductivity (Btu-in / h-ft ² -°F)	Maximum Service Temp. (°F)
ALUMINUM OXIDE	0.1438	50	30	0.75 @ 261°F	249	3,542
ALUMINUM OXIDE WITH SiC FIBERS	0.1362	60	47	0.50 @ 261°F		
BERYLLIUM OXIDE (ISOPRESSED)	0.1030	50	22	0.70 @ 261°F	1740	4,352
BORON NITRIDE (HP GRADE)	0.0686	11		0.21 @ 261°F	215	2,192
CHROMIUM BONDED ALUMINUM OXIDE		41	21		67	2,500
QUARTZ (FUSED SILICA)	0.0795	10.5		0.061 @ 261°F	11	2,192
SILICON CARBIDE (SINTERED ALPHA)	0.1120	59		0.41 @ 261°F	874	3,002
SILICON NITRIDE (HOT PRESSED)	0.1189	45		0.14 @ 261°F	173	3,002
ZIRCONIUM OXIDE (SINTERED ; MgO)	0.1940	26	12	0.88 @ 261°F		4,532

* All properties at room temperature unless otherwise noted.

** Referenced at room temperature

SELECTED PROPERTIES OF CANDIDATE REFRACTORY METALS AT ELEVATED TEMPERATURES

Material	Modulus of Elasticity @ 871°C (10 ³ MPa)	Ultimate Tensile Strength @ 1316°C (MPa)	Yield Strength @ 871°C (MPa)	Linear Thermal Expansion ** @ 1327°C (10 ⁻³ cm / cm)	Thermal Conductivity @ 1227°C (W / m-K)
NIOBIUM				11.02	72.3
WC – 103 (NIOBIUM ALLOY)	91.0	93.1	131		44.0
IRIDIUM				10.68	111
PLATINUM				14.14	89.7
PLATINUM / 20% IRIDIUM					
PLATINUM / 20% RHODIUM					
RHENIUM	376	455		8.96	47.7
RHODIUM				15.26	
TANTALUM	179	89.6	103	9.41	62.2
TANTALUM / 10% TUNGSTEN	128	400	621	9.30	
TANTALUM / RHENIUM					
TUNGSTEN	379	310	103	6.61	109
TUNGSTEN / 25% RHENIUM		689	965	7.42	9.95
TZM	234	379	379	8.20	97.5

** Referenced at room temperature

SELECTED PROPERTIES OF CANDIDATE REFRACTORY METALS AT ELEVATED TEMPERATURES

Material	Modulus of Elasticity @ 1600°F (Mpsi)	Ultimate Tensile Strength @ 2400°F (10 ³ psi)	Yield Strength @ 1600°F (10 ³ psi)	Linear Thermal Expansion ** @ 2421°F (10 ⁻³ in / in)	Thermal Conductivity @ 2240°F (Btu-in / h-ft ² -°F)
NIOBIUM				11.02	501
WC-103 (NIOBIUM ALLOY)	13.2	13.5	19		305
IRIDIUM				10.68	769
PLATINUM				14.14	622
PLATINUM / 20% IRIDIUM					
PLATINUM / 20% RHODIUM					
RHENIUM	54.5	66		8.96	331
RHODIUM				15.26	
TANTALUM	26.0	13	15	9.41	431
TANTALUM / 10% TUNGSTEN	18.5	58	90	9.30	
TANTALUM / RHENIUM					
TUNGSTEN	55.0	45	15	6.61	756
TUNGSTEN / 25% RHENIUM		100	140	7.42	69
TZM	34.0	55	55	8.20	676

** Referenced at room temperature

SELECTED PROPERTIES OF CANDIDATE CERAMIC MATERIALS AT ELEVATED TEMPERATURES

Material	Modulus of Elasticity @ 1093°C (10 ³ MPa)	Ultimate Tensile Strength @ 1093°C (MPa)	Linear Thermal Expansion ** @ 1327°C (10 ⁻³ cm/cm)	Thermal Conductivity @ 1227°C (W / m-K)
ALUMINUM OXIDE	324 @ 1000°C		11.58	5.66
ALUMINUM OXIDE WITH SiC FIBERS	344	183	10.70	
BERYLLIUM OXIDE (ISOPRESSED)		72.3	12.78	21.5
BORON NITRIDE (HP GRADE)				
CHROMIUM BONDED ALUMINUM OXIDE				
QUARTZ (FUSED SILICA)		113		4.00 @ 1200°C
SILICON CARBIDE (SINTERED ALPHA)			6.68	
SILICON NITRIDE (HOT PRESSED)			4.15	16.0 @ 1204°C
ZIRCONIUM OXIDE (SINTERED ; MgO)				2.26 @ 1200°C

** Referenced at room temperature

SELECTED PROPERTIES OF CANDIDATE CERAMIC MATERIALS AT ELEVATED TEMPERATURES

Material	Modulus of Elasticity @ 2000°F (Mpsi)	Ultimate Tensile Strength @ 2000°F (10 ³ psi)	Linear Thermal Expansion ** @ 2420°F (10 ⁻³ in/in)	Thermal Conductivity @ 2240°F (Btu-in / h-ft ² -°F)
ALUMINUM OXIDE	47 @ 1832°F		11.58	39.2
ALUMINUM OXIDE WITH SiC FIBERS	50	27	10.70	
BERYLLIUM OXIDE (ISOPRESSED)		10.5	12.78	149.1
BORON NITRIDE (HP GRADE)				
CHROMIUM BONDED ALUMINUM OXIDE				
QUARTZ (FUSED SILICA)		16		27.73 @ 2192°F
SILICON CARBIDE (SINTERED ALPHA)			6.68	
SILICON NITRIDE (HOT PRESSED)			4.15	110.9 @ 2200°F
ZIRCONIUM OXIDE (SINTERED ; MgO)				15.67 @ 2192°F

** Referenced at room temperature

APPENDIX E

LITERATURE SEARCH REFERENCES

REFERENCES

1. Aerospace Structural Metals Handbook, 1988.
2. Frank P. Incropera and David P. DeWitt, Fundamentals of Heat and Mass Transfer, 2nd Edition, John Wiley & Sons, New York, 1985.
3. Materials Engineering Materials Selector 1991.
4. Rockwell International Materials Properties Manual, Tantalum-10W, UNS R05255, 1987.
5. Nerva Program Materials Data Book, Refractory Metals and Alloys, 1967.
6. Charles L. Mantell, Engineering Materials Handbook, McGraw-Hill Book Company, Inc., New York, 1958.
7. Clifford A. Hampel, Rare Metals Handbook, Reinhold Publishing Corporation, 1961.
8. Brush Wellman Engineered Materials, Beryllium Oxide Brochure.
9. Ceradyne, Inc., Silicon Nitride Brochure.
10. The Carborundum Company, Combat Boron Nitride Brochure.
11. The Carborundum Company, Hexoloy Silicon Carbide Materials Brochure.
12. The TPRC Data Series, Thermophysical Properties of Matter, Volume 1, Thermal Conductivity, Metallic Elements and Alloys, IFI/Plenum, New York, 1970.
13. The TPRC Data Series, Thermophysical Properties of Matter, Volume 2, Thermal Conductivity, Nonmetallic Solids, IFI/Plenum, New York, 1970.
14. The TPRC Data Series, Thermophysical Properties of Matter, Volume 12, Thermal Expansion, Metallic Elements and Alloys, IFI/Plenum, New York, 1970.
15. The TPRC Data Series, Thermophysical Properties of Matter, Volume 13, Thermal Expansion, Nonmetallic Solids, IFI/Plenum, New York, 1970.
16. Wah Chang Albany, WC-103 Report.



Report Documentation Page

1. Report No.		2. Government Accession No.		3. Recipient's Catalog No. SRI-MME-93-261-7244.02	
4. Title and Subtitle CGF Cartridge Development, Volume I				5. Report Date March 1993	
				6. Performing Organization Code	
7. Author(s) Carl A. Dixon				8. Performing Organization Report No.	
				10. Work Unit No.	
9. Performing Organization Name and Address Southern Research Institute 2000 Ninth Avenue South Birmingham, Alabama 35255				11. Contract or Grant No. NAS8-39026	
				13. Type of Report and Period Covered Final Nov 90 - Dec 92	
12. Sponsoring Agency Name and Address National Aeronautics and Space Administration Washington, D.C. 20546-0001 NASA Marshall Space Flight Center				14. Sponsoring Agency Code	
15. Supplementary Notes					
16. Abstract Summary of SRI's efforts in Crystal Growth Furnace cartridge developments. Includes evaluation of molybdenum, TZM, and WC-103 as cartridge materials, survey of oxidation resistant coatings, chemical compatibility studies of cadmium-zinc-telluride and gallium-arsenide with TZM and WC-103, survey of future cartridge materials, and suggested improvements in ampoule design.					
17. Key Words (Suggested by Author(s)) CGF Ampoule Ceramics Cartridge Molybdenum Refractory Compatibility WC-103 Metals Oxidation TZM			18. Distribution Statement		
19. Security Classif. (of this report) Unclassified		20. Security Classif. (of this page) Unclassified		21. No. of pages	
				22. Price	

